The development of an endoprosthesis for the metacarpophalangeal joint

Joyce, Thomas J

THE DEVELOPMENT OF AN ENDOPROSTHESIS FOR THE METACARPOPHALANGEAL JOINT

By

Thomas J Joyce BEng MSc

Thesis submitted for the degree of
Doctor of Philosophy
at the
University of Durham

School of Engineering
University of Durham
South Road
Durham
DH1 3LE

August 1997

ABSTRACT

The Development of an Endoprosthesis for the Metacarpophalangeal Joint

Thomas Jonathan Joyce

Doctor of Philosophy
1997

Rheumatoid arthritis is a painful and debilitating disease which often afflicts the key joint of the hand, the metacarpophalangeal joint. In the worst cases the diseased joint has to be replaced with an artificial joint or prosthesis. The development of the Durham metacarpophalangeal prosthesis as it was taken from prototypes through to production samples, is described in this thesis. Testing of several Durham prostheses to over 70 million cycles has been carried out on a finger function simulator and consistent wear factors of the order of $0.4 \times 10^{-6} mm^3/Nm$ have been measured. These wear factors for the prosthesis were also significantly lower than any found previously. Production samples of the prosthesis have been manufactured together with appropriate surgical instrumentation. Tests of the prosthesis material, cross-linked polyethylene, rubbing against itself, have been undertaken on reciprocating pin on plate rigs and again show total wear factors of the order of $0.4 \times 10^{-6} mm^3/Nm$. Interestingly, it was found that pin wear was very much less than plate wear. The pin on plate tests were extended to include ultra-high molecular weight polyethylene (UHMWPE) rubbing against UHMWPE, as well as both polyethylenes against hard counterfaces and the results are reported. A new finger function simulator has been designed, manufactured and a validation test undertaken. Having written the necessary protocol, in conjunction with clinicians and the prosthesis manufacturer, ethical approval was obtained from the local research ethics committee and the Medical Devices Agency, to permit implantation of the prosthesis in human subjects. Lastly a hand strength measurement device for pre and post operation assessment of patients has been developed and manufactured.

DECLARATION

The work presented in this thesis was carried out in the School of Engineering at the University of Durham. This material has not been submitted previously for any degree in this or any other university.

No claim of originality is made for chapter 1, but the remaining chapters are claimed as original, except where authors have been specifically acknowledged in the text. Material from Chapters 3 and 4 has been published in the Journal of Engineering in Medicine, part H of the Proceedings of the Institution of Mechanical Engineers.

ACKNOWLEDGEMENTS

I would like to thank the technical staff of the School of Engineering, specifically the staff of the mechanical, electronic and electrical workshops. Brian Blackburn, Harry Kelly, Roger Little, Michael Wilson and Ian Garrett have all, at times, provided much assistance. In particular, the craftsmanship of Mr George Turnbull is appreciated. George was responsible for the manufacture of the mechanical components used in the simulator described in Chapter 5. Also thanks are due to Ms Julie Morgan who supplied many of the photographs included in this thesis.

De Puy International Limited supplied the test prostheses and the bulk of the test material.

None of my work would have been possible without the support of Action Research (Grant Ref. A/F/0475) and I thank the charity for this fellowship, and its belief in me.

Finally, thanks are due to my family; my supervisor, Professor Tony Unsworth; and especially my partner Ms Pauline McCormack. Their contribution, advice and comments have helped my work greatly.

This thesis is dedicated to my dearest friend, Ben Brown, killed by a drunk driver 30th July 1997. Ben's two sons are too young to remember him, but I'll never forget him.

CONTENTS

List of Figures

Figures in appendices

List of Tables

Tables in Appendices

Notation

a	Major axis length of phalangeal prosthetic component
A-D	Analogue to digital
b	Minor axis length of phalangeal prosthetic component
CIT	Crossed intrinsic transfer
Co	Control
cpm	cycles per minute
D	Distance
ED	Extensor Digitorum
F	Female
I	Index finger
k	Wear factor
L	Load, little finger, longitudinal
M	Middle finger, male
MCP	Metacarpophalangeal
P	External load at finger tip
PE	Polyethylene
PMMA	Polymethylmethacrylate
r	Radius on head of metacarpal bone
R	Ring finger, radius, Durham prosthesis size (radius)
Ra	Roughness average
RA	Rheumatoid Arthritis
s	Distal radius of phalangeal prosthetic component
t	Thickness of metacarpal lip
T	Tangential
THR	Total hip replacement
TKR	Total knee replacement
UHMWPE	Ultra high molecular weight polyethylene
UH	Ultra high molecular weight polyethylene test component
UC	Ultra high molecular weight polyethylene control component
V	Volume
w	Width of metacarpal component
W	Weight
Wt	Weight
WI	Weight increase
XLPE	Cross-linked polyethylene
XL	Cross-linked polyethylene test component
XC	Cross-linked polyethylene control component

CHAPTER ONE

Introduction and Literature Review

1.1 Introduction

Arthritis, the single biggest cause of disability in the UK, is just one of over 200 rheumatic diseases, severely affecting between seven and eight million people in Britain. Rheumatism accounts for 88 million working days lost per year, at a cost of approximately £1200 million in medical bills and loss of earnings (Arthritis and Rheumatism Council, 1992).

Hands are so vital to everyday life that the loss of strength and mobility, together with the pain due to arthritis, can lead to loss of independence. The crucial joint of the hand is the metacarpophalangeal (MCP) joint as all precision movements of the fingers are based on its correct initial position. It is this joint that is frequently affected by rheumatoid arthritis, one of the most common and debilitating types of arthritis.

When therapy, drugs and arrestive surgery have all been tried and found unsuccessful, prosthetic replacement of the MCP joint is the final option. That is, an artificial joint is implanted. At the moment this usually entails the diseased bones being cut and a silicone spacer, known as the Swanson prosthesis, inserted. Following surgery, pain is absent and the hands are cosmetically much improved, but mobility is unchanged and grip strength shows no improvement (Blair et al, 1984 a). Additionally, the prostheses can break (Kay et al, 1978) deformity may return (Wilson et al, 1993) and there are fears that the silicone material can cause cancer (Khoo, 1993).

For these reasons a new two piece finger prosthesis, the 'Durham' prosthesis, had been conceived and prototypes tested by Stokoe (1990) and Sibly and Unsworth (1991). The aim of the work described in this thesis was to complete the design of the Durham prosthesis, exhaustively test it and its material, and in doing so taking the Durham prosthesis forward to the point where clinical implantation could be considered.

Chapter 1 of this thesis therefore reviews finger joint replacement and related fields of interest. Beginning with a consideration of the natural finger joint and the ailments which may cause its need for replacement, this chapter goes on to survey the history of finger prostheses, assess the materials from which they may be manufactured and consider the tribology of natural and artificial joints.

On this foundation, the development of the Durham prosthesis from the prototypes outlined by Stokoe (1990) is described in chapter 2. This chapter includes a full review of the available anatomical data and ends with a finished design of the metacarpal and phalangeal components which together comprise the production prostheses.

As the Durham prosthesis is intended to replace only the diseased articular cartilage found on the ends of the finger bones, so the wear of the two components against each other becomes critical. Therefore chapter 3 describes a number of wear tests undertaken on Durham prostheses and analyses the findings.

In turn the results of chapter 3 are augmented by wear testing of the cross-linked polyethylene (XLPE) material from which the Durham prosthesis is manufactured. As well as tests of XLPE rubbing against XLPE, chapter 4 also provides comparative information by measuring the wear of UHMWPE against itself. The chapter concludes with wear tests of the two polyethylenes against stainless steel and zirconia counterfaces.

In chapter 5 the design of a new finger function simulator for the testing of finger prostheses is described, together with the results of a commissioning test. Based on the laboratory results provided by earlier chapters, chapter 6 outlines the work towards implantation of the Durham prosthesis in human subjects. In particular the 'protocol' required for statutory approval, the surgical tools, and hand assessment equipment necessary for patient assessment are all discussed.

Finally, chapter 7 summarises the main results of this thesis and suggests directions in which the work could be further developed.

1.2 Anatomy and Physiology of the Hand

Anatomy is the science of bodily structure and a description of the arrangement of bodily parts. Physiology deals with how these body parts work. The various parts of the body can be described relative to imaginary planes passing through the body. The transverse plane separates an organ or the body into superior (top) and inferior (bottom) portions, the frontal plane divides an organ or the body into anterior (front) and posterior (back) portions and the sagittal plane is a vertical plane separating an organ or the body into right and left sides. Other reference terms include distal, referring to a position further from the point of origin, while proximal refers to a position nearer to the point of origin.

1.2.1 Osteology

The carpals, metacarpals and phalanges (Figure 1.1) comprise the bones of the hand. The wrist or carpus consists of eight small bones arranged in two transverse rows and joined to one another by ligaments. The proximal row consists of the scaphoid, lunate, triquetrum and pisiform. The distal row consists of the trapezium, trapezoid, capitate and hamate. The five bones of the palm are called metacarpals and are numbered I to V, I being at the thumb. The base of each metacarpal is irregular in shape, while the head is rounded and articulates with the proximal phalanx of the corresponding digit. The heads of the metacarpals, which become prominent if the fist is clinched, are often called the 'knuckles'. Each of the bones in the finger is called a phalanx and, like each metacarpal, consists of a proximal base, an intermediate shaft and a distal head. The base of each proximal phalanx is concave to receive the head of the metacarpal. There are 14 phalanges in each hand, named either proximal, middle or distal, and there is no middle phalanx in the thumb. The anatomy of bones can be described further. The hard external layer of bone tissue is known as cortical bone, while the inner section is known as cancellous bone, as it has a honeycomb like structure. The medullary canal refers to the space within the shaft of the bone that contains bone marrow.

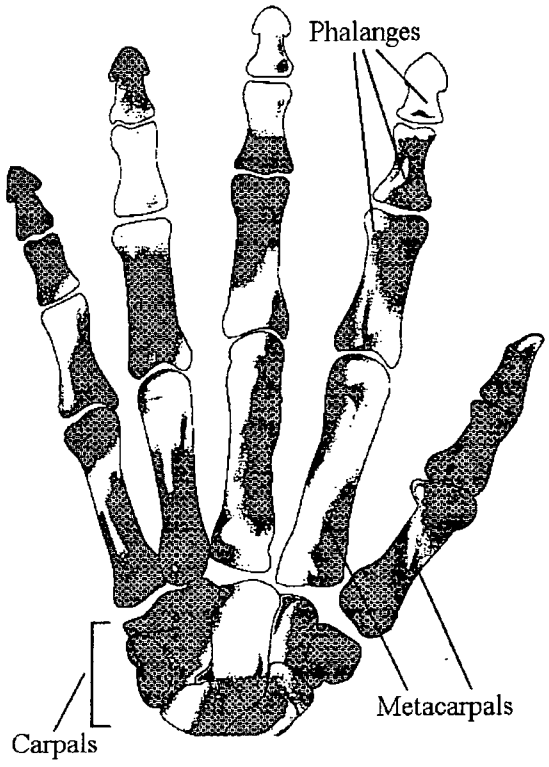

Figure 1.1 - The bones of the hand

1.2.2 Synovial Joints

The finger joints are all synovial joints, so named as there is a space or synovial cavity which separates the articulating bones. These joints are also known as diarthroses, or freely movable joints. Such a joint is enclosed by a sleeve like articular capsule which, by being attached to the periosteum, unites the articulating bones. This capsule consists of an outer layer known as the fibrous capsule, and an inner layer called the synovial membrane or synovium (Figure 1.2). The fibrous capsule has flexibility to allow movement of the joint as well as high tensile strength to resist dislocation. Additionally, the fibres of some fibrous capsules are arranged in parallel bundles called ligaments. They therefore keep the articular surfaces together and limit the range of motion of the joint. The inner layer of the articular capsule secretes synovial fluid, which acts as a lubricant to the joint, as well as nourishing and removing waste from the hyaline cartilage which covers the ends of each finger bone. The synovial fluid consists of hyaluronic acid together with an interstitial fluid formed from blood plasma, and it forms a thin, viscous film over the surfaces within the articular capsule. The

cartilage, which consists of a dense network of collagen fibres, acts as a bearing material.

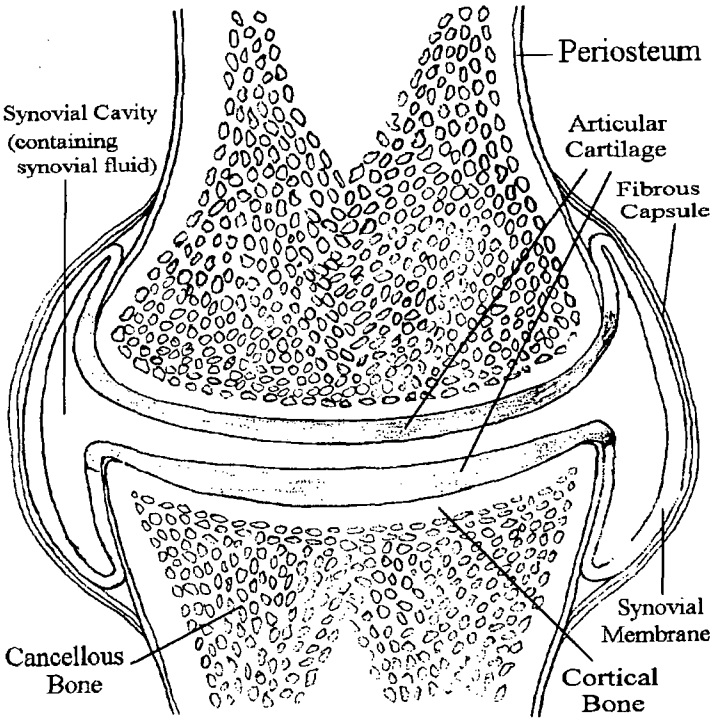

Figure 1.2 - Section through a generalised synovial joint

1.2.3 Skeletal Muscle Tissue

Skeletal muscle tissue functions to move bones, and is attached primarily to bones. The muscle tissues relevant to the fingers include a number of tendons, cords of dense connective tissue which attach a muscle to the periosteum of a bone, and the intrinsic muscles of the hand. The latter are called intrinsic muscles as their origins and insertions are both within the hand. The tendons are enclosed by tubes known as tendon sheathes and as these sheathes contain a film of synovial fluid, their task is to reduce friction as the tendons slide back and forth. The tendons of the hand serve to produce flexion, where the angle between the articulating bones is decreased, and extension, where this angle is increased.

1.2.3.1 Flexor Tendons

There are two main flexors of the fingers, the flexor digitorum sublimis and the flexor digitorum profundus (Figure 1.3). The flexor digitorum sublimis has its insertion on the middle phalanx, therefore it flexes the proximal interphalangeal joint. The flexor digitorum profundus has its insertion on the base of the distal

phalanx therefore it flexes the distal interphalangeal and proximal interphalangeal joints. The flexor digitorum profundus passes through a slot in the flexor digitorum sublimis.

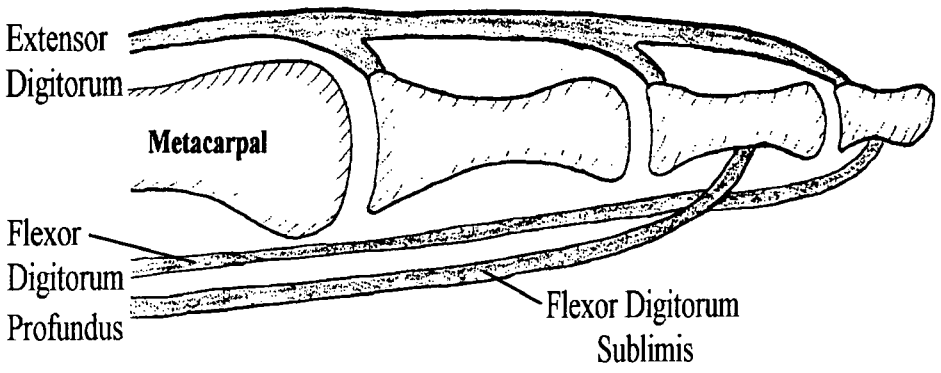

Figure 1.3 - Tendons of the finger

1.2.3.2 Extensor Tendons

The extensor tendons pass on the dorsal side of the wrist to the fingers. Dorsal refers to the back or posterior of the hand, whereas palmar refers to the palm side of the hand. The most important extensors are four extensor digitorum (ED) tendons (Figure 1.3). Each is dedicated to one of the fingers and each has an insertion into the proximal phalanx, middle phalanx and the distal phalanx. There are also the extensor digiti minimi and the extensor indicis tendons. The extensor digiti minimi aids extension of the little finger, and is connected with the ED of the little finger in the forearm. Similarly, there is the extensor indicis, which joins the ED for the index finger.

1.2.3.3 Intrinsic Muscles of the Hand

The muscles of the palm of the hand include the interosseous muscles and the lumbrical muscles. They act to enhance or oppose the action of the flexor and extensor tendons, and therefore permit precise, stabilised motion of the fingers. They also permit abduction and adduction of the fingers. Abduction refers to a movement of a bone away from the midline of the body while adduction refers to a movement towards the midline. The interossei occupy the intervals between the metacarpal bones, and are divided into a dorsal and a palmar set. There are four dorsal interossei. Each arises from the adjacent sides of two metacarpal bones, and each is attached to the bases of the proximal phalanges. The palmar interossei are larger and more powerful than the dorsal interossei and are joined to the metacarpals. The lumbricals are four small muscles which arise from the flexor

digitorum profundus tendons. Each passes to the radial side of the corresponding finger, radial referring to the thumb side of the hand. In contrast, ulnar refers to the little finger side of the hand.

1.2.4 Metacarpophalangeal (MCP) Joint Anatomy

The MCP joint is a complex joint, with local soft tissue structures giving important contributions to both joint function and stability. The MCP joint (Figure 1.4) is a partial ball and socket joint, consisting of an approximately spherical metacarpal head articulating with the concave base of the proximal phalanx (Unsworth and Alexander, 1979). The two bones are joined by the collateral and metacarpoglenoidal ligaments, as well as the joint capsule.

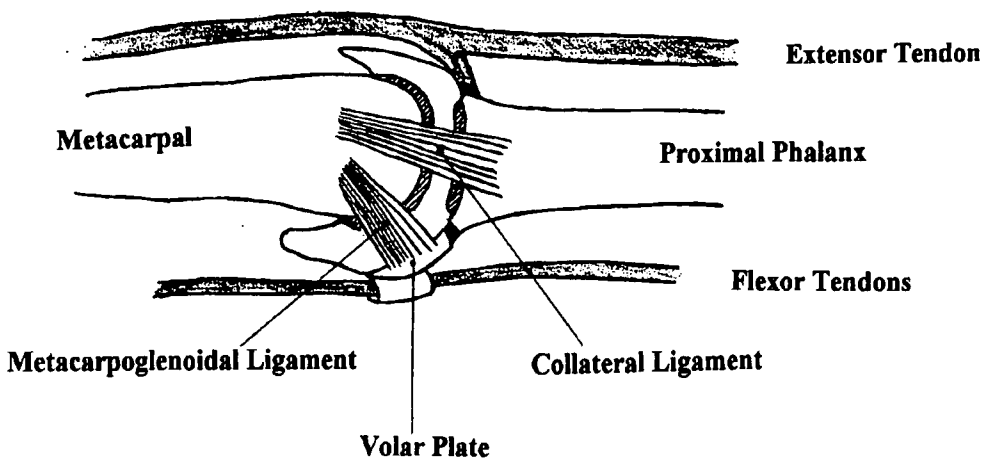

Figure 1.4 - Metacarpophalangeal joint anatomy (sagittal plane)

The collateral ligaments arise from each side of the metacarpal head, called radial and ulnar, depending from which side they originate. The insertion of the ligaments in the metacarpal head is slightly dorsal to the centre of rotation of the head. These ligaments also run obliquely, so that laxity is taken up as the joint moves from extension to flexion, and Minami et al (1985) gave quantitative results showing that the collateral ligaments are the primary means of stabilising the MCP joint. The metacarpoglenoidal ligament joins the metacarpal head to the volar plate, beneath which is affixed the flexor tendon sheath. The volar plate is also attached to the proximal phalanx by a small, hinge-like fibrous band called the incisura.

There are six muscles which actively control movement of the MCP joint. Three are extrinsic muscles and three are intrinsic muscles. The extrinsic muscles are so named as the muscles are not in the hand, but in the forearm. The extrinsic muscles are those connected to the extensor digitorum, the flexor digitorum sublimis and the flexor digitorum profundus. These are the primary movers of the MCP joint in a flexion-extension axis. The intrinsic muscles, ulnar and radial interossei and lumbrical, act to permit abduction-adduction and also contribute to MCP flexion (Youm et al, 1978).

1.3 Rheumatism and Arthritis

1.3.1 Significance

There are over 200 rheumatic diseases, severely affecting between seven and eight million people in Britain. Rheumatism accounts for 88 million working days lost per year, at a cost of £1,200 million in medical bills and loss of earnings (Arthritis and Rheumatism Council, 1992). Rheumatism refers to any joint or muscle pain not caused by infection or injury. Arthritis is again a general term referring to the inflammation of a joint and a sufferer encounters pain, loss of strength and loss of mobility. The two most common and important types of arthritis are rheumatoid arthritis and osteoarthritis.

1.3.2 Rheumatoid Arthritis

Rheumatoid arthritis is the most common inflammatory disease of the joints in the UK, with a prevalence of approximately 1% (Sturrock, 1992). Its cause is unknown, but an immunological basis seems likely. It can result in severe physical, psychological, economic and social handicap. Indeed, rheumatoid arthritis may threaten the whole lifestyle of the sufferer. A sufferer may lose his or her job because of arthritis, leading to a loss of earnings and a subsequent decline in their standard of living. At home, aspects of daily life such as feeding and toileting may become impossible for the individual to accomplish alone. In turn depression is commonly associated with arthritis, and can be exacerbated when the sufferer feels resentment at their loss of independence. Additionally the

disease can become cosmetically upsetting. Women are more commonly affected than men in a ratio of three to one. The disease usually strikes between the age of forty and sixty, although it can develop at any age. In detail, the synovium becomes chronically inflamed, the synovial membrane thickens and synovial fluid accumulates. The resulting pressure leads to swelling, pain and the restriction of movement. In the worst cases, the inflamed synovial membrane produces abnormal granulation tissue called pannus which causes roughening and thinning of the cartilage, as well as erosion of the bone (Figure 1.5). The swelling can also lead to stretching of the ligaments and damage to the tendons sheathes together with the tendons within them.

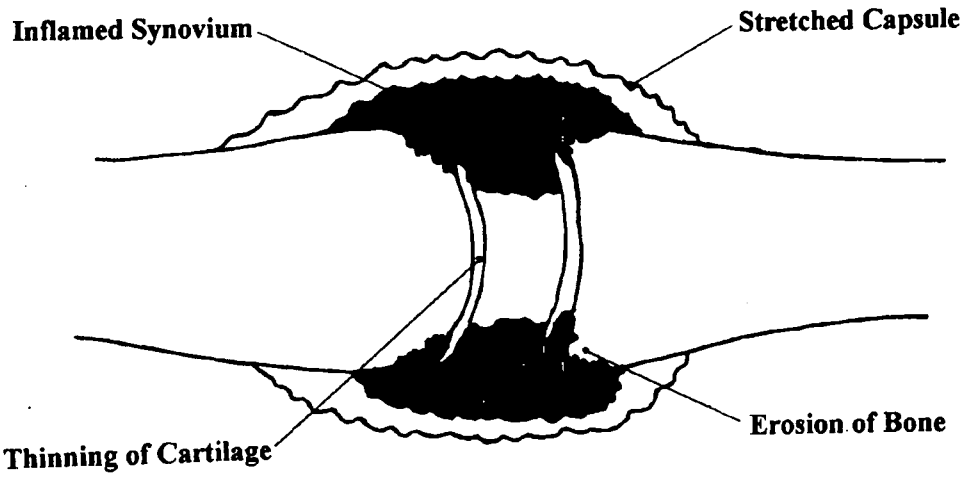

Figure 1.5 - Joint affected by rheumatoid arthritis

Any synovial joint may be involved, but the hands are very commonly affected, and most affected of all is MCP joint, in 87% of cases (Sturrock, 1992). Unfortunately, the MCP joint is the crucial joint of the hand as all precision movements of the fingers are based on its correct initial position. Indeed Smith and Kaplan (1967) described the MCP joint as the 'keystone of the hand', while McMaster (1972) described it as 'the key element in the normally functioning hand'. Typically rheumatoid arthritis of the hands includes symmetrical joint involvement and the development of characteristic changes such as swan necking and boutonniere deformities (McMaster, 1972; Backhouse, 1968; Hakstain and Tubiana, 1967; and Smith and Kaplan, 1967). At the MCP joint itself, once the ligaments become stretched, the joint loses its natural balance and the forces from the flexor tendons dominate, leading to ulnar drift and volar subluxation (Figure 1.6). Subluxation refers to a partial or incomplete dislocation.

Figure 1.6 - Rheumatoid arthritis of the hands

It must be remembered that the MCP joint is only one of a system of joints in the upper limb that may be affected by rheumatoid arthritis, from the shoulder to the distal interphalangeal joint, and despite the importance of the MCP joint it is only one link in this chain. Sturrock (1992) states that in 82% of cases the wrist will be affected by rheumatoid arthritis, and in 63% of cases the proximal interphalangeal joints will be involved. Therefore the condition of surrounding joints and tendons is critical and can lead to a variety of results following MCP joint treatment.

Indeed, a wide range of treatments is available to patients with rheumatoid arthritis; from rest, exercise, advice, aids and appliances, physiotherapy and drugs, through to surgery. Drug treatments include non-steroidal anti-inflammatory drugs (NSAIDs). Their prime effect is to relieve pain and stiffness, and to reduce joint swelling, although side effects can be a problem. More powerful, slow acting anti-rheumatic drugs or 'second line agents' are given for the active disease. Again side effects can result. Patients themselves can also help in several ways. This can be through psychological factors, positive thought and attitude; physical factors, achieving the correct balance of rest and activity; and a healthy diet. Interestingly, it has been found that a vegetarian diet can ameliorate symptoms, plus there is the added benefit of no side effects (Kjeldsen-Kragh et al, 1991).

Surgery is obviously one of the last treatments undertaken due to its cost and complexity, but where appropriate it can be very successful. Arrestive surgical treatments include synovectomy, in which the inflamed synovium is removed; tenosynovectomy, removing nodules from the tendons; and tendon transfer, relocation of the tendon from one side of the joint to the other. The final surgical options are those which remove the pain by either fusing the joint - arthrodesis, although this is rarely performed at the metacarpophalangeal joint because it is so functionally limiting, and arthroplasty which replaces the joint with an artificial one, and it is the latter with which this thesis is concerned.

1.3.3 Osteoarthritis

Osteoarthritis is the most common form of arthritis affecting 5 million people in the UK (Dieppe, 1994) and particularly affects the weight bearing joints. There is no primary inflammation, so osteoarthrosis is perhaps a more appropriate term for this disease (arthrosis is the degeneration of a joint). Damage to joints appears to be due to the wear and tear of ageing, as the disease becomes more common with increasing age, resulting in a roughening and thinning of cartilage, in turn leading to stiffness and diminished motion. Osteoarthritis usually only affects the articular cartilage, unlike rheumatoid arthritis where various tissues are involved. Both osteoarthritis and traumatic arthritis, that due to injury, rarely affect the MCP joints to a sufficient degree to entail joint replacement (Beckenbaugh et al, 1976). Instead, the finger joints most commonly affected by osteoarthritis are the distal interphalangeal joints, where the characteristic joint swelling, due to osteophytes, has been named as Heberden's nodes. Similar swellings at the proximal interphalangeal joint are known as Bouchard's nodes.

1.4 Biomechanics

1.4.1 Introduction

The hand is not only a crucial tool for everyday life and work, but a means of conveying and receiving information. It is a mechanism of great complexity and intricacy. Arguably the key joint of this valuable instrument is the metacarpophalangeal (MCP) joint (McMaster 1972, Smith and Kaplan, 1967). An understanding of the forces and motions affecting this joint is essential to developing a successful MCP prosthesis.

1.4.2 Forces Across the MCP Joint

1.4.2.1 Introduction

In-vivo joint, tendon and muscle forces of the hand are difficult to measure directly. Therefore models of these forces have been devised, to which known external forces can be input to give an estimation of MCP joint forces. However, due to the large number of muscles and ligaments which are in the hand, the task of modelling and then calculating the forces across a particular joint is difficult. Due to this complexity, models which try to predict such forces are often simplified. Further, the position of the joint and its surrounding joints must be specified as these positions will directly affect the forces acting on the MCP joint.

1.4.2.2 Experimental Measurements of Forces

The clinical measurement of hand strength allows pathological conditions and their response to treatments to be assessed, feasible treatment goals to be set and the effectiveness of different surgical procedures to be compared (Mathiowetz et al, 1985). Measurement must be reliable and valid, necessitating the use of standardised equipment, procedures and positioning of the hand. A popular method of measuring grip strength is to squeeze an inflated bag connected to a manometer and to note the increase in pressure. However, different techniques of squeezing will give different results, as indeed will different original bag volumes or pressures (Unsworth et al, 1990). Additionally, the contribution of individual fingers cannot be determined (Jones et al, 1985). Instead strain-gauged devices offer the ability to measure the force of a grip, rather than the pressure indicated by an inflated bag. Further, with certain strain-gauged devices, the magnitude and

contribution of the individual fingers, and finger segments, to the overall grip strength can also be determined.

1.4.2.3 Other Influential Factors

It has been found that the forces acting on the joints of the hand depend on many factors. From past investigations it can been seen that these factors include age, sex, illness, exercise, measuring device, technique of grasp, and temperature. In addition to these, psychological attitude and the orientation of other joints in the upper limb may well influence joint forces. This range of factors should be borne in mind when comparing the various results of hand and finger strength reported in the literature.

1.4.2.4 Definitions of Hand and Finger Strength

Tip, pulp, lateral and three point pinch, as well as grip strength have all been experimentally measured extensively in the past. However, the definitions of the type of pinch and grip being measured have often been contradictory and vague. Therefore the following pinches and grips are defined in Figure 1.7 in order firstly, to compare the various reported experimental measurements of hand and finger strength and secondly to apply this information to the various theoretical models reviewed.

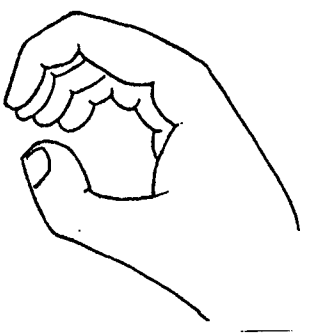

Grip strength/Power grip - all of the fingers together with the thumb gripping an object, producing maximum hand grip strength.

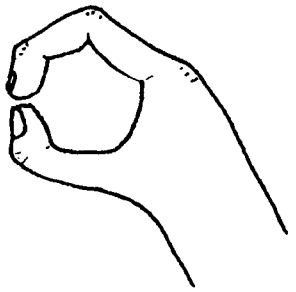

Tip pinch - tip of index, middle, ring or little finger against the tip of the thumb, with the interphalangeal joints flexed.

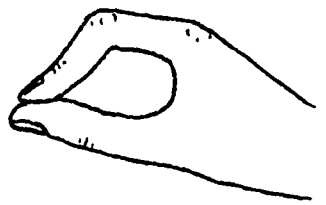

Pulp pinch - distal phalangeal pad of index, middle, ring or little finger against the distal phalangeal pad of the thumb. Interphalangeal joints more extended than in tip pinch.

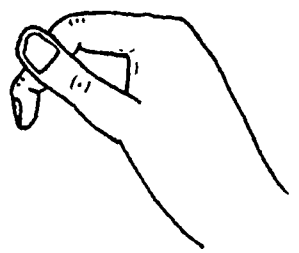

Lateral/Radial pinch - distal phalangeal pad of the thumb against the radial or lateral side of the index finger middle phalanx, other fingers clenched in support. This pinch is sometimes called key pinch.

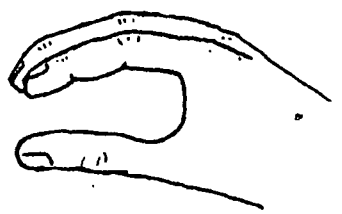

Three point/Palmar pinch - Index and middle fingers against thumb. This pinch is sometimes called chuck pinch.

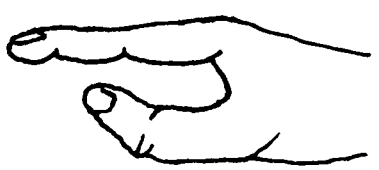

Long finger flexion - pad of the distal phalanx of the finger exerting a force, with the finger in a cantilever position.

Figure 1.7 - Definitions of hand and finger strength

1.4.2.5 Reported Values of Hand and Finger Strength

(all results were obtained using strain gauged devices.)

Table 1.1 Grip Strength Data for Normals

Reference		Male/ Female	No. of Subjects	Max. Force (N)
An et al (1978)	Hand	M	18	368
		F	22	219
Cutts and Bollen (1993)	Hand	M	12	428
		M	13	520
Helliwell et al (1988)	Hand	--	30	238
Amis (1987)	Hand	14M/3F	17	200 - 540
Walker et al (1978)	Hand	M	65	153
		F	80	79
Jones et al (1985)	Hand	--	20	345
	I	--	20	75
	M	--	20	125
	R	--	20	90
	L	--	20	60
Mathiowetz et al (1985)	Hand	M	310	439
		F	318	260

Table 1.2 Grip Strength Data for Rheumatoid Arthritis Patients

Reference	Comment	Male/ Female	No. of Subjects	Max. Force (N)
Pearson et al (1982)	-----	----	11	18
Walker et al (1978)	-----	Mostly F	30	9
Blair et al (1984 a)	Pre op RA	Mostly F	24	74
	Post op RA	Mostly F	34	62
Helliwell et al (1988)	Inactive RA	----	32	87
	Active RA	----	66	58
	Subluxed MCP	----	32	44
	Pre op RA	----	3	19
	Post op RA	----	3	19
	Osteoarthritis	----	6	102
Jones et al (1985)	Outpatients and Inpatients	----	38	110
		----		I 25
		----		M 38
		----		R 33
		----		L 24

Table 1.3 Pinch Strength Data for Normals

Reference	Type of Pinch	Finger	Male/ Female	No. of Subjects	Av. Max. Force (N)
Walker et al (1978)	Pulp	I	M	65	74
		M	M	65	65
		R	M	65	47
		L	M	65	37
		I	F	80	56
		M	F	80	49
		R	F	80	34
		L	F	80	25
	Three	-	M	65	91
	Point	-	F	80	73
Berme et al (1977)	Pulp	I	F	4	19
An et al (1978)	Tip	I	M	18	63
			F	22	47
		M	M	18	63
			F	22	46
	Pulp	I	M	18	66
			F	22	45
		M	M	18	62
			F	22	45
	Lateral	I	M	18	75
			F	20	59
		M	M	18	68
			F	20	51
Weightman and Amis (1982)	Pulp	I	F	11	34
	Tip	I	F	11	36
Jones et al (1985)	Pulp	I	--	20	57
		M	--	20	54
		R	--	20	40
		L	--	20	31
	Lateral	---	--	20	92
Mathiowetz et al (1985)	Tip	I	M	310	74
		I	F	318	49

I = Index Finger M = Middle Finger R = Ring Finger L = Little Finger

Table 1.4 Pinch Strength Data for Rheumatoid Arthritis Patients

Reference	Type of Pinch	Finger	Male/ Female	No. of Subjects	Av. Max. Force (N)
Jones et al (1985)	Pulp	I	-----	38	19
		M			18
		R			13
		L			11
Walker et al (1978)	Pulp	I	Mostly F	30	13
		M			11
		R			10
		L			7
	Lateral*	I			12
		L			9
	Three Point	---			19
Blair et al (1984 a)	Lateral	---	26F/2M	28	28

* Other fingers not in support.

I = Index Finger M = Middle Finger R = Ring Finger L = Little Finger

1.4.2.6 Discussion of Grip Strength Data

Tests conducted by Walker et al (1978) found males to be approximately twice as strong as females in terms of grip strength. Mathiowetz et al (1985) found a high correlation between grip strength and age. Pathological conditions such as rheumatoid arthritis and osteoarthritis severely reduce grip strength, rheumatoid patients only being one third as strong (Jones et al, 1985) or one tenth as strong (Walker et al, 1978) as normals. Helliwell et al (1988) further subdivided the patients they studied who suffered from rheumatoid arthritis. This division ranged from those with rheumatoid arthritis severe enough to need arthroplasty to those with inactive disease. The values of grip strength they measured across this spectrum was from 19N to 87N respectively. Therefore, a factor of 4 separated the grip strength of 'rheumatoid arthritis' patients. Two other interesting points to note from the results of Helliwell et al (1988) are that Swanson's arthroplasty gave no increase in grip strength, and that osteoarthritis suffers had a greater grip strength than those suffering from rheumatoid arthritis. The former result was confirmed by the results of Blair et al (1984 a) which reported a reduction in grip strength. The results of Jones et al (1985) indicate that for rheumatoid arthritis

patients, the percentage contribution of each of the fingers towards the total grip strength is far more even than in 'normals'.

Amis (1987) considering grip strengths on a range of cylinder diameters found that strengths decreased as diameters increased. From approximately 540N to 200N as the cylinder diameter was increased from 31 to 116mm. Such data proves that grip strength values are machine sensitive. Therefore, it can be seen that the position of the individual fingers and their joints is crucial to the magnitude of the forces which can be measured. This conclusion is also supported by the variety of grip strength measurements obtained by the various researchers. For example, 'normal' females have a reported mean grip strength from 79 to 260N, while that of 'normal' males ranges from 153 to 540N.

Amis (1987) also showed that the distal phalangeal force component of the total grip strength was the largest, followed by that of the proximal, then that of the middle phalanx. The mean contributions of the fingers to grip strength were found to be 30% index, 30% middle, 22% ring and 18% little. These figures closely match those of An et al (1978) who give 32, 33, 21 and 14%, although no cylinder size was specified. Therefore, the percentage contribution of individual fingers to the total grip force appears to be roughly constant. This was also shown separately by both Jones et al (1985) and Ohtsuki (1981) who gave figures of 22, 36, 26 and 17% respectively. Unlike Amis (1987) and An et al (1978), they did not use cylinders which forced the individual fingers into a set position, but devices which permitted the fingers to adopt a more natural grip position.

Grip strength values are obviously greater than those for tip/pinch as the whole hand is employed. However, it will be seen that this fact does not necessarily mean that joint forces due to grip are greater than those from pinch situations.

1.4.2.7 Discussion of Pinch Strength Data

The experimental data show that males have greater pinch strength than females, males having a maximum mean pinch strength of approximately 70N, and females of approximately 50N. Tip, pulp and long finger flexion all seem to produce similar force ranges. Lateral and three point pinch in general have a greater upper value of force than tip or pulp, probably because more than one finger is involved. For tip and pulp pinch, the index finger is approximately equal in strength to the middle finger, with the ring finger next and finally the little finger. Mathiowetz et

al (1985) found a low to moderate correlation between pinch strength and age. Weightman and Amis (1982) and Walker et al (1978) commented on the wide variety of their results, reporting a standard deviation of approximately 30%.

Regarding patients with rheumatoid arthritis, Jones et al (1985) measured a pinch strength range from index to little finger, of 19N to 11N. Similarly, Walker et al (1978) measured the range from 13N to 7N. Finally, Linscheid and Dobyns (1979) stated that rheumatoid arthritis patients had a pinch strength between 5 and 20N, but did not state to which particular finger or fingers these values applied. Walker et al (1978) measured the pinch strength of rheumatoid arthritis patients to be a quarter that of 'normals', while Jones et al (1985) measured this difference to be one third. These results also showed that for pulp pinch, the index finger is approximately equal in strength to the middle finger, with the ring finger next and finally the little finger.

1.4.3 Models of MCP Joint Forces

1.4.3.1 Overview

Most of the theoretical models to predict the loads across the MCP joint have been based on the two dimensional action of the index finger, in a pinch grip situation. The general strategy has been to produce equilibrium moment equations and apply known external forces; it is these external actions which produce the large internal forces on the MCP joint. For these moment equations, the necessary dimensions and locations of the various anatomical bodies have been obtained from cadaveric specimens. Next, any indeterminate models were solved using simplifying assumptions. As hand action is elaborate, and complicated further by the involvement of many tendons, muscles and soft tissue structures, several assumptions are often required to permit answers to be obtained. Examples of these assumptions have included neglecting the frictional, inertial and viscoelastic effects of soft tissues, and tendons and tendon sheaths have been modelled as frictionless. Joint contact forces have been required to act through the bearing surfaces, and extensor action has been neglected as electromyography (the study of nerve impulses to muscles and the response of the muscle) has shown it to be inactive (Long et al, 1970). Despite such assumptions, the various papers give widely different results. The reason for these differences is essentially that disparate simplifications and assumptions have been made to the various models. For example, some researchers have ignored the effects of the

collateral ligaments on joint loading (Chao et al, 1976) although such tissues are crucial to joint function.

Additionally, it must be remembered that a particular finger posture produces a unique loading at the MCP joint, and the various papers have not always stated the exact posture of the joints used in the different experiments. A final point to note is that some researchers have quoted an overall joint force, whereas others have offered two or three components, dependent on whether a two or three dimensional model was presented. Three dimensional models have, however, indicated that the third component, the radial shear force, is relatively insignificant.

1.4.3.2 The Models

The earliest model presented was that of Smith et al (1964) who offered a two dimensional model of joint forces during tip pinch. A force polygon produced a value of 7.5P for the MCP joint force, where P was the external force applied at the finger tip. However, the intrinsic muscles were modelled in a simplified form, the exact index finger position was not defined and the capsulo-ligamentous structures surrounding the joint were ignored altogether.

Chao et al (1976) presented a three dimensional model to analyse joint forces during tip, lateral, and ulnar pinch; as well as during grip. They used cadavers to find the geometric positions of the relevant muscles and tendons after which free body analyses were performed. This method produced 19 equations with 23 unknowns. Being indeterminate, 4 of the 9 tendon forces were assumed to be zero to give 126 possible solutions. Therefore certain solutions were made inadmissible. The results presented for 'pinch' were averages of the three different types of pinch action considered, i.e. tip, lateral, and ulnar. In conclusion, a MCP joint load for the index finger of 8.8P was given. These authors saw some faults in their own work, namely that the lumbricals carried too much force, the ligaments were ignored and that cadavers were used.

Later work by the same authors was based on their 1976 model but considered only tip pinch action. Chao and An (1978) with a different method of solution obtained a MCP joint force of 8.6P. Next, An et al (1985) found MCP joint forces for tip pinch in the range of 4.1 to 4.5P. Further, results from the models of Chao and An (1978) and Chao et al (1976) showed joint force during pinch to be greater than during grip. In contrast results from An et al (1985) concluded

the opposite. As the same model gives such widely different results, its validity ought to be treated with caution.

Berme et al (1977) produced a three dimensional model of index finger MCP joint forces during pinch and tap turning actions, and then measured the external finger forces occurring during these actions. From these measured values, compressive forces across the joint of up to 190N were calculated. Interestingly, the tap turning mean compressive joint force was determined to be 170N, whereas that occurring during pinching was only 102N. These figures therefore indicated that the joint load during tap turning would be greater than that occurring during pinch action. However, the normal female subjects who were used in the measurements gave pulp pinch values of only 19N, much less than that the values reported by other researchers.

Weightman and Amis (1982) reviewed previous finger joint models and, based on this research, produced a two dimensional, pin-jointed model for several pinch postures. The relationships between muscle forces were taken to be the same as those of Chao and An (1978), except that the extensor tendons were assumed to be relaxed. Further, it was assumed that tensions in the intrinsic muscles were in proportion to their physiological cross-sectional area. Interestingly, Chao et al (1976) noted discrepancies in their model because their calculated forces were not proportional to the physiological cross-sectional area. Tendon positions were determined from information given by Chao and An (1978) with fixed distances between the centres of rotation of the three joints of the finger. Importantly, the model included the effects of the collateral ligaments of the MCP joint. The analysis of Weightman and Amis gave a statically determinate model, from which the magnitude and direction of the resultant joint forces was obtained. Results showed that joint forces increased during pinch grip as the finger extended towards a cantilever position. Also, that the magnitude and direction of the force on each of the three finger joints varied progressively with the flexion of each joint. In the range of postures considered, MCP joint forces were predicted to lie between 3.6 and 5.6P. Again, where P is the external force applied at the finger tip.

More recently, Tamai et al (1988) offered values for MCP joint forces. Though not providing a model, they calculated forces based on contact area and contact pressure. Such a method gave a force of 14N across the MCP joint at the 'neutral' position due to the balance of muscle forces alone.

1.4.4 MCP Joint Range of Motion

The MCP joint allows active flexion-extension, adduction and abduction. The MCP joint has a range of motion from 30° extension to 90° flexion. Youm et al (1978) stated that the range of abduction-adduction decreases from 40° to 0° with increasing flexion of the MCP joint from 0° to 90°. Both Walker et al (1978) and Youm et al (1978) have shown that passive movement is greater than active in both the flexion-extension plane and the abduction-adduction plane. Walker et al (1978) found that there was little difference in motion between men and women and between different age groups. However, in manipulative ability these researchers also found there to be a decline with age.

1.5 Biomaterials

1.5.1 Introduction

When discussing prosthetic materials, the implantation of a foreign device to replace or otherwise assist certain tissues of the body has to be considered. However, the tissues being replaced are living, capable of self repair and adaptation. They are viscoelastic, anisotropic and piezoelectric (Williams, 1990). In contrast, the materials that are currently available to replace them are monolithic, isotropic and synthetic. Until materials with similar functional characteristics to tissues can be manufactured, or grown, this will always be the case. Currently, the engineering materials available for prostheses can only offer a compromise in trying to match the physical properties of tissues, and therefore the choice of materials for implantation is limited from the beginning.

At the same time, the body is an extremely delicate yet aggressive environment for any foreign object. While this balance generally helps to resist infection, it greatly reduces the range of materials available for use in potential prostheses. Such materials have to be inert and non-toxic, as do any wear products that may originate from them over their desired life span of up to several decades. Therefore a material can be said to be biocompatible if it produces an acceptable and predictable response from the host environment (Profio, 1993).

After producing a list of materials having both biocompatibility and the requisite mechanical properties, more specific demands can be investigated and a final choice made. Such demands include wear resistance and the capability of being sterilised.

In conclusion, compared with the tissues they are replacing, the biomaterials currently available lack both performance and sophistication. While efforts continue to be made to improve this situation, the task of making the best of the materials currently on offer remains. These available materials can be divided into several groups.

1.5.2 Metals

Stainless steel, titanium alloy and cobalt chromium molybdenum alloy are the metals currently used in prostheses. All three metals are expensive, and their method of manufacture into prostheses is complex. Corrosion resistance can be a problem, hence the use of the three metals listed above, all of which naturally form a protective oxide layer which inhibits corrosion. In general, metals offer strength, ductility, hardness and low wear. However, this hardness can cause problems. It is recognised that bone which is loaded maintains or increases its mineral content, while the opposite occurs in bone that is not loaded. Arthroplasty may disrupt limb loading so that loads normally carried by the bone would be carried by the prosthesis. Such a situation would cause the loss of bone in the unloaded bony area and this phenomenon is known as stress shielding. Furthermore, work by Szivek et al (1981) demonstrated that more mineral bone was lost under a stiffer implant material. Therefore, as all metals have a stiffness very much greater than that of bone, stress shielding can occur. Also, if not fixed in place, metallic prostheses can also penetrate the softer surrounding bone.

Of the three metals, stainless steel offers a compromise between wear properties and machinability as well as having excellent ductility to cope with the cyclic loading occurring across artificial joints in vivo. Although it is the least inert of the three metals, its corrosion resistance can be much improved by the process of 'passivation'. Here the material is immersed in an oxidising agent such as nitric acid, which thickens the oxide layer on the surface of the metal (Dowson and Wright, 1981). Cobalt chromium molybdenum alloys are extremely hard and wear resistant but difficult to fabricate except through precision casting, and they

have poor ductility. Titanium is the lightest and least inert of the metals, and it can also provoke a favourable bone response through osseointegration. However, it is also the least wear resistant of the three metals, a concern which has recently been highlighted (Drabu et al, 1994).

With reference to the various MCP prostheses, the Flatt prosthesis used 316 stainless steel throughout and perforation of the cortical bone of both the metacarpal and phalanx was noted (Blair et al, 1984 b). The Welsh prosthesis also used stainless steel for both components, but with a polyethylene button inset (Welsh et al, 1982). In a similar fashion, the Griffiths-Nicolle prosthesis used a stainless steel cylinder inset into a plastic stem. Cobalt chromium molybdenum was used throughout in the Link design, and for one half of both the Steffee implant and the prosthesis described by Weightman et al. This mixing of polymers and metals is the norm in the majority of all prostheses used in the body. Other examples in MCP joint replacement include the prosthesis of Walker and Erkman, and the St Georg and Steffee prostheses (Gillespie et al, 1979). Titanium was used throughout for the original Brannon-Klein prosthesis, while the prostheses described by Hagert et al and by Lundborg used titanium stems to encourage fixation by osseointegration. Titanium grommets are used to protect Swanson prostheses from tearing by bone.

1.5.3 Polymers

Polymers have the advantages of low cost, low friction against metal, ease of manufacture and chemical inertness. Compared with metals, polymers more evenly distribute the stresses to the bone (Walker et al, 1983) when used as a prosthetic material. However, they lack the strength and hardness of metals. The most commonly used polymeric biomaterial is UHMWPE which is successfully used in many joint replacement implants.

With reference to the various finger prostheses, UHMWPE has often been used as a bearing component in several designs, for example those of Weightman et al, Steffee, Welsh and the alumina ceramic prostheses. Silicone is the basis of the Kessler, Niebauer, and Swanson prostheses, as well as the more recent Sutter implant. Having a lower value of elastic modulus than polyethylene, the use of silicone permits a flexible, single piece implant to be manufactured. However, there are fears that silicone can cause cancer (Gordon and Bullough, 1982; Khoo,

1993). Polypropylene was used in the prostheses of Calnan and Reis (1969), Nicolle and Calnan (1972), and Schetrumpf (1975), the latter design also employing polyacetal. However, polypropylene shows high wear (Dowson and Wright, 1981).

1.5.4 Ceramics

As inorganic materials, ceramics remain chemically stable and inert when used in the body. Further, lower values of wear are achieved by ceramics than metals when used against UHMWPE, and porous ceramics can encourage bony ingrowth and therefore promote strong fixation (Black, 1988). Ceramics are also extremely hard though lacking in toughness, and this hardness has led to bone resorption and implant migration in the case of a ceramic MCP prosthesis (Minami et al, 1988). Finally, ceramics are extremely expensive and quality control is crucial to obtain a material without impurities or defects. The ceramics used for prostheses currently include alumina and zirconia, although the only example of a ceramic used in a finger prosthesis is that of alumina (Minami et al, 1988; Doi et al, 1984).

1.5.5 Other Materials

In an attempt to match more closely the properties of bone, and therefore increase implant acceptance, a number of other materials have been suggested. Such materials include carbon fibre, carbon and composites of hydroxyapatite. Hydroxyapatite being a natural mineral found in human bones. However, all such materials currently lack long term clinical success. Pyrolytic (processed) carbon has been used in a surface replacement MCP prosthetic design described by Beckenbaugh & Linscheid (1989).

1.5.6 Cross-Linked Polyethylene (XLPE)

The cross-linking of polyethylene has significantly improved its engineering properties. Being a polymer, it has a stiffness approaching that of bone therefore stresses are more evenly distributed to the host bone so that the chances of acceptance by the host ought to be increased. Work has also shown that XLPE

is biocompatible (Rae et al, 1988), and a clinical trial of XLPE acetabular cups, with an average follow up of 77 months, has shown positive results (Wroblewski et al, 1996). Cross-linking has the additional advantage of permitting a lower molecular weight base material to be used, so that components can be injection moulded rather than machined. Injection moulding offers the opportunity of mass producing complex three dimensional components to repeatable, close tolerances. Generally, the use of a material against itself in a bearing is to be avoided, particularly in the case of materials as soft as polymers. However, work has indicated a wear factor of XLPE against itself of the order of $1.8 \times 10^{-6} mm^3/Nm$ together with a coefficient of friction of 0.14 (Sibly and Unsworth, 1991). Therefore, due to its blend of biocompatibility, low cost, ease of manufacture, appropriate mechanical properties and high wear resistance, XLPE was chosen as the optimum material for use as a surface replacement prosthesis for the metacarpophalangeal joint.

There are a number of methods by which polyethylene can be cross-linked and the method employed by De Puy International for the Durham prosthesis is the silane method. In this process, the XLPE test samples were manufactured from powdered polyethylene which was mixed with liquid silane. This mixture was then extrusion injection moulded. The cross-linking process between the polyethylene molecules occurred by placing the samples in a steam autoclave. Finally, the samples were sterilised by irradiation. The degree of cross-linking was measured from a number of sacrificial samples by boiling away in xylene the non cross-linked material. Therefore the weight of the material remaining after this process, divided by the original weight, gave the percentage of cross-linking. In such a sacrificial process the measurement error was within ±2%.

1.6 Metacarpophalangeal Prostheses

1.6.1 Introduction

The development of MCP prostheses can be divided into four categories. The earliest prostheses were the metallic, rigid single hinge implants. These designs of Brannon and Klein, and Flatt are no longer in use. Next came the flexible, one piece silicone rubber implants, such as those of Swanson and Niebauer. Of these, the Swanson is still in use and currently the most successful and commonly

employed MCP prosthesis. In an attempt to follow from the success of hip and knee prostheses came the next group of prostheses, those of articulated joints made of dissimilar materials. They are fixed or snap together to make a single unit and usually require cement fixation of the stems. Despite a myriad of designs they have failed to match the success of the flexible one piece implants. This failure has been due to a number of reasons, including the need for cement fixation, high cost and surgical difficulties. In turn, this failure has led to a new concept in MCP prostheses, that of surface replacement, of which the Durham prosthesis is an example. These surface replacement prostheses follow the natural contours of the joint, are two piece and un-cemented. They aim to supplement the joint rather than replace it, and rely on surgical technique to re-balance the joint rather than any restrictions imposed by the prosthesis itself. As such, their use should be in cases where soft tissue rebalancing can be achieved.

1.6.2 First Generation Prostheses

The first reported MCP prosthesis to be implanted was that of Brannon and Klein in 1953 (Brannon and Klein, 1959). Manufactured entirely from titanium, the metacarpal and phalangeal components were joined together by a screw which formed a hinge (Figure 1.8). To prevent rotation, the stems were manufactured with a triangular cross section, and two staples were used to prevent the prosthesis from sinking into the bones. However, the design gave no allowance for abduction-adduction, and the axis of the stems was placed in line with each other, unlike in the natural joint.

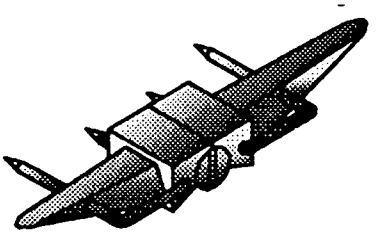

Figure 1.8 - Brannon and Klein Prosthesis

Introduced in 1963, and now no longer in use, the Flatt prosthesis was essentially a modified Brannon and Klein prosthesis. Manufactured from three stainless steel components, later versions had the centre of rotation of the prosthesis offset from the centreline of the metacarpal shaft to match that of the natural joint. Each

stem consisted of two prongs, which were intended to provide rotational stability. Again, this was a hinge type prosthesis, with no allowance for adduction-abduction. The two pieces were linked by a screw around which flexion-extension could take place. Unfortunately, surgical technique included excision of the collateral ligaments. Blair et al (1984b) in a comprehensive follow up (average 138 months) to Flatt arthroplasty, found a 47% failure rate together with poor host bone response in 87% of cases and, with bone resorption leading to prosthesis migration, perforation of the cortex of the metacarpal and the proximal phalanx in 44% and 59% of cases respectively. Recurrent ulnar deviation was found in 58% of patients. Despite these findings, patient satisfaction remained high, due to pain relief and aesthetic improvements.

1.6.3 Second Generation Prostheses

The availability of silicone permitted a range of prostheses to be developed in an attempt to overcome the inadequacies of the first MCP prostheses. The most important of the second generation prostheses is the Swanson, a flexible, single piece of silicone, simple in design and acting as a spacer to encourage encapsulation (Figure 1.9). The inherent flexibility of the silicone used for the prosthesis permitted some abduction-adduction. Benefits of the Swanson prosthesis are recognised as alleviation of pain, improved cosmetic appearance and a more functional arc of movement; together leading to contented patients. Thousands of these prostheses have been fitted since 1968, surgery is straightforward and results are well documented, with surgeons recognising the prosthesis as the best currently available (Nalebuff, 1984; Fleming and Hay, 1984; and Wilson et al, 1993).

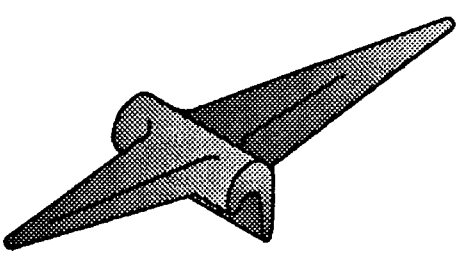

Figure 1.9 - Swanson Prosthesis

Disadvantages include no significant increase in grip strength (Blair et al, 1984a), worries over a link between the silicone material and cancer (Gordon and

Bullough, 1982; Khoo, 1993), and breakages at a rate of up to 26% after 2.7 years (Beckenbaugh et al, 1976) and 82% after 5 years (Kay et al, 1978). Fracture of the prosthesis is thought to be due to small cuts produced by sharp spurs of the bones, therefore titanium grommets have been introduced to combat this problem. Another contributory cause of fracture could be that the prosthesis flexes at the stem rather than the hinge. In turn, flexion at the stem could be due to either the fact that the stems are in line or because the hinge is positioned dorsally. However, in about 50% of cases, breakage does not mean loss of function, due to the fact that encapsulation around the prosthesis has already occurred (Beckenbaugh et al, 1976). To reduce the cases of breakage, the silicone material was significantly strengthened in 1974 (Swanson and de Groot Swanson, 1984) although this means that any debris is more likely to be of a particulate nature. While the arc of motion of the MCP joint is improved following surgery, the range of motion is not increased and can even be reduced (Blair et al, 1984a). A recurrence of ulnar drift is often noted too (Kay et al, 1978; Wilson et al, 1993). A further concern is that a substantial amount of bone has to be removed when a Swanson prosthesis is implanted, whether the bone is diseased or not, limiting future surgery. In the process of surgery, the ligaments are often excised too. Another point to note is that the stems tend to piston in the medullary canals. Some commentators view this as a significant disadvantage as it causes cortical erosion (Levack et al, 1987), however Swanson considers that this movement produces a favourable biological effect at the bone interface, as well as reducing the stresses on the prosthesis itself (Swanson et al, 1986). Additionally he states that the silicone material, having a significantly lower modulus than bone, has force dampening characteristics that further protect the bone and soft tissues (Swanson and de Groot Swanson, 1984). Unfortunately, this softness makes the prosthesis open to damage from cuts occurring during fitting.

First implanted in 1966, the Niebauer prosthesis was also a single piece silicone prosthesis, but reinforced with Dacron at the hinge (Figure 1.10). It was initially fixed to the intramedullary canals using Dacron ties and had a dacron sleeve sown around each stem to encourage bone ingrowth (Niebauer et al, 1969). Unfortunately, the dacron sleeves did not fulfil their purpose, instead the rough dacron caused erosion within the medullary canals (Hagert, 1975). Clinical results showed the Niebauer to be inferior to the Swanson. Hagert (1975) showed a 54% fracture rate, Beckenbaugh et al (1976) stated that clinical deformity returned in 44% of cases, and Derkash et al (1986) reported a 87%

fracture rate together with recurrence of deformity in 58% of cases. Fracture was thought to be due to the inherent weakness of the silicone material, in tandem with the fact that, unlike the Swanson, the prosthesis was not free to move and therefore had to flex at the hinge. Recurrent deformity was due to the removal of the collateral ligaments during surgery, combined with the inherent lack of strength of the silicone material.

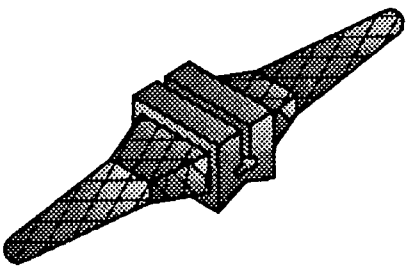

Figure 1.10 - Niebauer Prosthesis

Calnan and Reis (1969) presented a single piece polypropylene prosthesis, which had its stems cemented in place. Lacking shoulders, the bone ends telescoped over the implant and joined together (Dowson and Wright, 1981). Therefore Nicolle and Calnan (1972) introduced a hollow silicone sphere over the hinge and ceased to use cement. However, the sphere produced prominent knuckles in patients and the prosthesis had a high fracture rate (Dowson and Wright, 1981).

Introduced in 1987, the Sutter prosthesis can be thought of as an modified version of the Swanson, with a hinge offset palmarly, and the stems in-line with the medullary canals rather than each other. However, no clinical trials of this prosthesis have been reported yet. Other examples of second generation MCP prostheses include the Helal flap (Levack et al, 1987) and the Kessler (Kessler, 1974) (Figure 1.11).

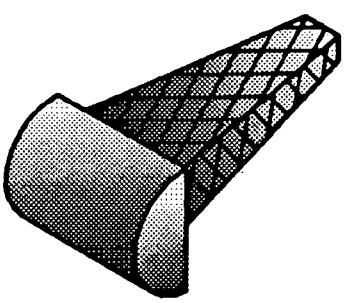

Figure 1.11 - Kessler Prosthesis

1.6.4 Third Generation Prostheses

Schetrumpf (1975) designed a two piece plastic prosthesis having components which snapped together (Figure 1.12). The prosthesis was a cementless design, inexpensive and simple, but this simplicity of design also meant that it functioned as a one dimensional hinge with the inherent limitations of such a design. A small clinical trial has been described (Schetrumpf, 1975) but no independent follow ups have been reported. Similar to the Schetrumpf design was the Griffiths-Nicolle prosthesis (Varma and Milward, 1991) (Figure 1.13) and the Link prosthesis (Devas and Shah, 1975).

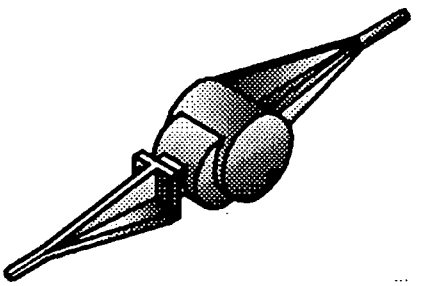

Figure 1.12 - Schetrumpf Prosthesis

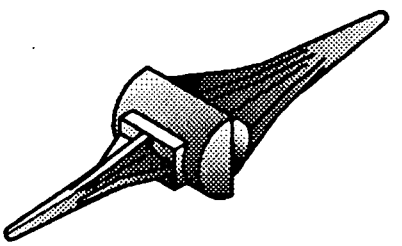

Figure 1.13 - Griffiths Nicolle Prosthesis

Weightman et al (1983) produced an interesting design, including some novel features, such as a common hinge pin for adjacent pairs of fingers and UHMWPE bearing sleeves inserted in proximal phalanges to permit rotation (Figure 1.14). However, the design was complex, expensive and no clinical trials have ever been reported.

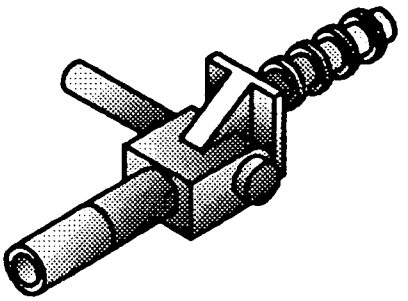

Figure 1.14 - Weightman et al Prosthesis

The prostheses described by Doi et al (1984) and Minami et al (1988) were each composed of two alumina ceramic components together with a HDPE bearing (Figures 1.15 and 1.16). Each design employed cementless fixation and concentrated on overcoming the problems of prosthesis fracture, while at the same time achieving low wear. These aspects it succeeded in doing, although employing a material such as alumina ceramic created its own set of problems. The first of these is the expense of top quality alumina ceramic. The second was shown by X-rays of one case which showed implant migration and perforation of the cortex, indicating the unsuitability of such a hard material moving against much softer bone (Minami et al, 1988). The designers also forgot about the centre of rotation of the MCP joint being offset relative to the medullary canal of the metacarpal. Again collateral ligaments were incised during surgery. Doi et al (1984) reported the clinical results of only two implants, with only a one year follow up. Minami et al (1988) reported the results from 21 implants, with a mean follow up of 3.2 years. In both cases no independent long term trials have ever been reported.

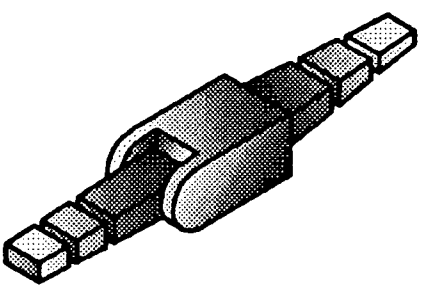

Figure 1.15 - Doi et al Prosthesis

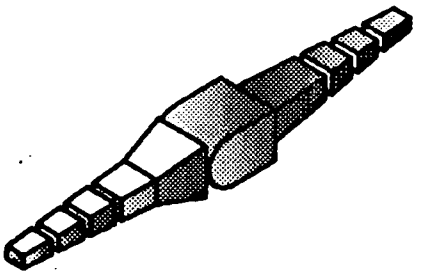

Figure 1.16 - Minami et al Prosthesis

The Schultz prosthesis (Figure 1.17) consisted of a metal phalangeal component which fitted inside a plastic metacarpal component, the stems being cemented in place (Adams et al, 1990). Flexion, extension, abduction and adduction were all allowed for. However, costs were high, and the use of cement introduced additional problems. In a study with an average follow up of 10.9 years, Adams et al (1990) found fracture of the phalangeal component in 39% of cases and the recurrence of ulnar drift in all joints. Similar designs to the Schultz include the Steffee (Figure 1.18), St Georg (Figure 1.19) and Strickland prostheses (Gillespie et al, 1979). Walker and Straub (1977) developed a two-piece, cemented MCP prosthesis and had some inserted but no results of the clinical trial have ever been published.

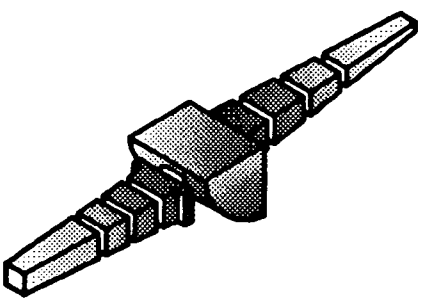

Figure 1.17 - Schultz Prosthesis

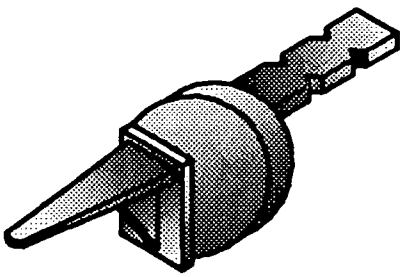

Figure 1.18 - Steffee Prosthesis

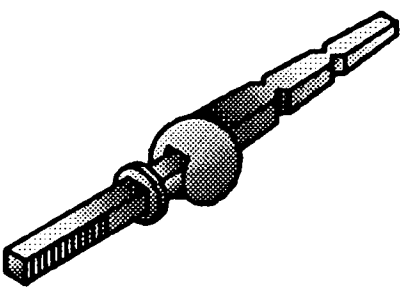

Figure 1.19 - St Georg Prosthesis

The Hagert (Figure 1.20) (Hagert et al, 1986) and Lundborg (Lundborg et al, 1993) prostheses were similar in that each had two titanium, threaded stems, designed to encourage fixation by osseointegration. In a small clinical trial of five Hagert prostheses, it was found that one fractured. The Lundborg prosthesis has fared better (Lundborg et al, 1993). However, as it employs a silastic hinge, a long term follow up is required to determine whether the fractures seen in other silastic prostheses will occur in it too.

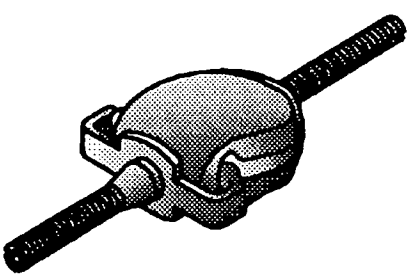

Figure 1.20 - Hagert Prosthesis

1.6.5 Fourth Generation Prostheses

Welsh et al (1982) offered a prosthesis consisting of two stainless steel uncemented components, the phalangeal part having a HDPE 'button' inserted as a bearing. No laboratory tests were described and only one in-vivo case was reported. When compared with the Durham design (Figure 1.21) extra bone resection of the metacarpal head would be required, the metallic components will be more expensive and there may be problems due to the difference in modulus between stainless steel and bone.

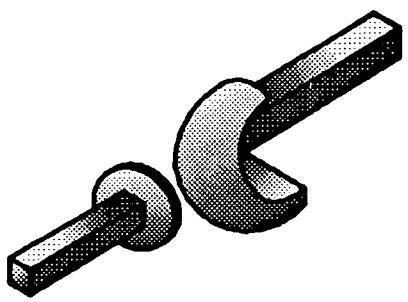

Figure 1.21 - Durham Prosthesis

Cook et al (1983) undertook implantation of a cementless, two part prosthesis made of processed carbon, in baboons. The metacarpal component had a spherical head and the phalangeal component had a deep matched concave surface. Both components were a press fit and achieved stability through 'appositional bone growth'. The friction and wear characteristics of the carbon material were not described. Clinical results from human subjects were reported by Beckenbaugh (1983). These results concerned a clinical trial with a one year follow up, but no long term or independent results have since been reported.

Another fourth generation design of MCP prosthesis is the Landos design, which is two piece having a stainless steel metacarpal component articulating against a UHMWPE phalangeal component. The metacarpal component fits within a polyethylene stem, and both stems have circumferential fins to permit fixation by bone ingrowth. Although intended as a PIP replacement joint, it has also been applied to MCP joints. Condamine et al (1988) have reported clinical results of the Landos design after a minimum of one year. Not surprisingly, results from the replacement of rheumatoid MCP joints were inferior to those of PIP replacement in post-traumatic cases.

1.7 Tribology of Natural and Artificial Joints

1.7.1 Introduction

Tribology is defined as the science of interacting surfaces in relative motion. As such, it is concerned with the often synergistic effects of wear, lubrication and friction. Of these three parameters, wear is perhaps the most important with respect to artificial joints. Currently, the wear of UHMWPE is attracting a great deal of attention, particularly in terms of the causes of such wear and the effects it produces. Indeed, concern about polyethylene wear is so great that metal against metal hip replacements have been recently re-introduced. What is agreed is that, in the human body, polyethylene wear debris is to be avoided as it can become deposited in surrounding tissues (Malcolm, 1988), leading to inflammation and the activation of macrophages (scavenging cells). In turn these macrophages can stimulate bone eating cells (osteoclasts) which may lead to bone resorption (Howie et al, 1988), causing eventual loosening of the prosthesis together with pain for the patient (Mirra et al, 1982). Although biomaterials may be tolerated in bulk in the body, small wear particles may produce adverse reactions (Saikko, 1993). Further, these reactions depend on both the volume and the morphology of the wear debris, hence the importance of wear studies.

It is obvious that any material which is to be implanted into the human body for any length of time should have its properties fully understood. Such understanding can only be achieved by thorough testing. XLPE has been used in implants for several years and has produced no adverse reaction in the body. This use has primarily been in the non-rubbing situation, of the De Puy Ogee flange on the acetabular component of a total hip replacement. However, trial XLPE acetabular cups have been implanted for a number of years and have shown low wear and no adverse reaction (Wroblewski et al, 1996). Further, XLPE debris has been shown to be no worse in the body than UHMWPE debris (Rae et al, 1988). In support of this clinical information, there is only one set of wear test data published in a peer reviewed journal (Sibly and Unsworth, 1991). Therefore comprehensive wear testing of XLPE was undertaken and the results are described later in chapters three and four of this thesis. First, however, the tribological aspects of natural and artificial joints need to be considered.

1.7.2 Wear Regimes

Wear contributes to the decreased usefulness of an item through loss of dimension. The various wear regimes rarely exist in isolation, but are often synergistic. There are several wear regimes, but the three most important to biotribologists are abrasive, adhesive and fatigue wear (Dowson, 1994).

Abrasive wear is that due to hard particles or protuberances forced against and moving along a solid surface. Abrasive wear can be further sub-divided into two types. . One involving small abrasive particles interposed between two moving surfaces (three body abrasion), and the other, where a single surface contacts the abrading medium (two body abrasion). Abrasive wear has its own nomenclature, for example scratching, abrasion, gouging, and these terms give an indication of the visual appearance of a surface affected by abrasive wear.

Adhesive wear occurs when the contact stresses during sliding are sufficient to produce local plastic deformation and 'welding' between the two surfaces in relative motion. Similar materials articulating together are particularly prone to this type of wear, but so too are clean surfaces and those where an oxide film cannot form. Therefore the presence of an intermediate material, such as a lubricant, will have a dramatic effect on whether adhesive wear occurs or not. A transfer film is an example of adhesive wear.

Fatigue wear results from repeated cyclic loading. The worst cases of fatigue wear in prostheses are those seen in the tibial components of some total knee replacements. Here, due to high contact stresses and low conformance, the same type of failure that occurs in metallic engineering components can be seen. Hertzian shear stresses some millimetres below the surface produce pits on the surface which measure up to 3mm across and 2mm deep. Worse still is 'delamination', in which a sheet of polyethylene is removed, and this can occur due to the same fatigue mechanism. In those prosthetic components where stresses are lower and conformity greater, such as the acetabular component of total hip replacements, fatigue wear exhibits a different form. Here, it is surface failure associated with the scale of the irregularities on the polymer surface (Dowson, 1994). Fatigue wear can, under a powerful microscope, be identified as small, wavy tears perpendicular to the direction of motion.

1.7.3 Wear Testing Machines

The results of wear tests tend to give a large degree of scatter (Wallbridge and Dowson, 1987) therefore, for accuracy, a large number of tests have to be undertaken. Further, to establish fully the wear properties of a particular material combination, a large number of test cycles also have to be carried out, often greater than one million. These two points, the scatter in results and the long test duration, mean that comprehensive testing is a laborious process.

Wear test machines can be divided into three categories. Pin on disc machines fall into the first category. These tend to be high speed, and are widely used by tribologists. However, they employ unidirectional motion which is not appropriate as an approximation to the motion of natural joints. Instead, the reciprocating motion of pin on plate machines is similar to that found in many natural joints, and therefore these machines are widely used as screening devices in wear studies of biomaterials (Saikko 1993, Dowson, 1994). These devices form the second category of wear testing machines. Although pin on plate machines do not employ dynamic loading or mimic the geometry of a joint, such simplifications ensure that these machines are reliable and consistent. They also mean that basic wear mechanisms can be determined and understood. When appropriate levels of load, speed and contact stress are employed, then the results of wear studies on various combinations of materials can be compared with those of other researchers. The final category of wear test machines are joint simulators. These machines test the actual prostheses, and attempt to imitate the loads and motions found in vivo. However, this aim makes such machines both complex and expensive.

1.7.4 Measurement of Wear

An assessment of wear is often undertaken by gravimetric measurement of the test specimens, by the collection and weighing of debris or from dimensional changes. Dimensional changes are usually measured using displacement probes (Kumar et al, 1991). This method, which has the advantage of not necessitating the removal of the test specimen, assumes that no creep of the specimen occurs and that wear is equally distributed across it. The collection and weighing of debris also shows significant problems. Such debris, for example third body wear particles, may play an important role in the wear process itself. Additionally, the

separation of debris from a lubricant can be an involved procedure (Rose et al, 1978). For these reasons, gravimetric measurement is the technique most often used for the measurement of the wear of biomaterials. Any weight changes due to the absorption of lubricant can be compensated, either through the use of a control specimen, or by the pre-soaking of the test specimens.

1.7.5 Reporting of Wear Results

Wear results are often reported in terms of the wear factor k (units mm^3/Nm) which is defined as:

$$k = \frac{V}{LD} \qquad \text{Equation 1.1}$$

where V = Volume loss (mm^3)
L = Load (N)
D = Sliding distance (m)

but volume = mass (m)/density (ρ)

$$\therefore k = \frac{m}{\rho LD}$$

Usually, k is calculated from the gradient of a best fit line on a volume against sliding distance plot. Volume losses can be calculated from weight losses, by knowing the density of the test material. However, if different wear regimes are seen to have occurred then more than one wear factor may be reported. A similar consideration applies if wear is reported in terms of mm^3 per million cycles. It is also possible to report wear in terms of mm per year, and this is often used for the acetabular cups of total hip replacements. While appropriate in this instance, it is less so for reporting laboratory results.

1.7.6 Test Duration

As a typical joint replacement has an average lifetime of 10 years then, at an average of one million cycles per annum, 10 million cycles are required. Due to

such a long test duration, there is a general requirement for multi-station test rigs. Further, an increase in test speed can result in significant changes in tribological conditions, such as a shift from boundary to hydrodynamic lubrication. Therefore, for accuracy, wear tests are normally undertaken at speeds comparable with those in vivo (30mm/s and 1Hz). Additionally, different wear mechanisms can occur at different sliding distances (Stokoe, 1990, Cooper et al, 1993, a) so it is important that tests have sufficient duration.

1.7.7 Lubricants

The ideal lubricant to be used in the wear test of a biomaterial combination would be human synovial fluid. However, there are difficulties in obtaining sufficient quantities of this liquid, it has highly variable rheological properties, and the viscosity of synovial fluid from a rheumatoid joint is much lower than the equivalent fluid from a normal joint (Geborek and Wollheim, 1993).

As synovial fluid is mainly a filtrate of plasma plus hyaluronic acid (Geborek and Wollheim, 1993) so bovine serum is commonly used as a lubricant in wear tests. Plasma is one of the three major constituents of blood, the other two being white cells and red cells. Plasma is the liquid portion of blood and is a solution in water of approximately 7% proteins. These plasma proteins are albumin, globulin and fibrinogen. Serum is not quite the same as plasma. It is the fluid which separates from clotted blood, namely plasma without fibrinogen and other components of clot.

The proteins within bovine serum act as boundary lubricants and have therefore been shown to prevent the formation of a transfer film in wear tests between polyethylene and hard counterfaces, such as metals and ceramics, and no transfer film is seen on explanted joints (Cooper et al, 1993, a). In contrast, when distilled water has been used as a lubricant for such polyethylene against hard counterface wear tests, then a transfer film has often been found (Cooper et al, 1993, a). In turn the transfer film created has been blamed for a range of tribological effects, from reduced wear to increased wear (Brown et al, 1976). However, Kumar et al (1991) conducted tests using serum which resulted in the formation of a transfer film. This may be explained by the degradation of the serum, so that it's boundary lubricating properties were lost. To prevent such degradation, a chemical such as sodium azide or phenoxetol may be added.

However, such a chemical may, in turn, affect the rheological properties of the lubricant. Despite this addition, the serum still has to be changed on a regular basis, and this regime will result in the removal of third body particles which might otherwise have influenced the wear process.

Due to such problems, distilled water has frequently been used as a lubricant as it is safe and inexpensive. Also, the viscosity of water approaches that of rheumatoid synovial fluid. Indeed, Davidson and Lynch (1988) compared the lubrication properties of distilled water with those of synovial fluid taken from patients with total replacement hip joints and, using a hip simulator, found no major differences between lubricating properties. This combination of reasons has meant that a great deal of biomaterial wear data employing distilled water as a lubricant have been published. Indeed, distilled water is still widely used as a lubricant for testing biomaterials. Brummitt and Hardaker (1996) used distilled water in a ten station hip simulator and found wear results comparable with surgical data.

It has been suggested that Ringers solution would be a more appropriate lubricant than distilled water as it contains salts equivalent to those in the body, whereas distilled water does not. However, relatively little work has been done using saline or Ringers solution as a lubricant in pin on plate tests. McKellop (1981) and Kumar et al (1991) used saline and Ringers solution as alternative lubricants. Heavy transfer films were recorded with the saline solution and the wear rate was twice as high as that found in distilled water.

1.7.8 Lubrication Regimes

There are several lubrication regimes relevant to the tribology of natural and artificial joints. The longevity and success of natural joints is largely based on their functioning with a film of synovial fluid separating the two cartilage surfaces. As such, full fluid film, squeeze film, and elastohydrodynamic modes of lubrication are all considered to be important in natural joints (Unsworth, 1993). Which of these modes of lubrication is in operation at any one time depends on a complex inter-relationship between the load across the joint, the immediate and recent velocity of the joint, the viscosity of the synovial fluid and the condition of the articular cartilage. What is important is that, as no surface contact occurs, therefore negligible wear takes place.

When a person is stationary, then the situation is more complex. After squeeze film effects have disappeared, then cartilage to cartilage contact will occur, with the potential for increased friction and wear Such a situation is defined as boundary lubrication, where the combined roughness of the two surfaces is greater than the depth of any fluid film between them. However, even when this occurs in the natural joint, proteins in the synovial fluid maintain the friction at a low level and in doing so minimise the potential for wear (Unsworth, 1993).

As current artificial joints are manufactured from engineering materials which lack the ability of cartilage to deform readily, then such joints normally operate with mixed lubrication, a combination of boundary and fluid film lubrication regimes (Unsworth, 1993). Consequently, as surface to surface contact happens, so too does wear. It is this wear of artificial joints, usually of the softer polymeric material, which eventually leads to 'failure' of the artificial joint.

In an attempt to mimic the ability of cartilage to deform, 'soft layer joints' have recently been suggested (Unsworth, 1993, Dowson, 1989). By employing one surface coated with a pliant material such as polyurethane, these artificial joints are designed to encourage fluid film lubrication and therefore prevent any wear from occurring. However, their development is still at an early stage as material problems exist, as do concerns over the high coefficients of friction at 'start up', i.e. before a lubricating film can be formed.

1.7.9 Friction

Human synovial joints are so beautifully engineered that, when they maintain a full film of synovial fluid between the cartilage surfaces, they have a coefficient of friction of the order of 0.01. Furthermore they can retain this capacity for tens of years. In comparison artificial joints, operating with mixed lubrication, tend to have a coefficient of friction of the order of 0.1 (Unsworth, 1993).

CHAPTER TWO

Design of Durham Metacarpophalangeal Prosthesis

2.1 Introduction

2.1.1 Concept

The aim of this procedure is to re-surface a diseased MCP joint, to replace only the articular cartilage that is damaged by rheumatoid arthritis, and to rely once again on the soft tissues to control and move the joint.

2.1.2 Surgical Justification for Durham MCP Prosthesis

That such a concept of utilising the damaged soft tissue structures can work, has been shown by a clinical trial in which a quarter of the rheumatoid patients presented for MCP surgery had sufficient articular cartilage remaining to allow soft tissue reconstruction to be as successful as replacement of the joint by a Swanson prosthesis (Wood et al, 1989). Therefore, even in such late cases as those presented for surgery, the natural joint can still be rectified rather than removed. If surgery were to be attempted earlier, then the soft tissues would be in even better condition (Flatt, 1983). Further, work by El-Gammal and Blair (1993) showed that crossed intrinsic transfer (CIT) maintained MCP range of motion for 5 years and increased both distal and proximal interphalangeal joint range of motion for 5 years, and therefore gave superior results to those measured when using the Swanson prosthesis alone.

2.1.3 Advantages of Durham Prosthesis Design

The Durham prosthesis is designed to replace the damaged articular cartilage of the MCP joint and in addition to act as a low friction shield to the undamaged bone beneath. As such, the shape and dimensions of the prosthesis are closely related to those of the natural joint, imitating them as closely as possible, and therefore permitting the same range of motion. In turn, loads and stresses will be

transmitted to the bone ends, as in the natural joint, rather than to the medullary canals. The prosthesis is therefore two piece, having a metacarpal and a phalangeal component. Being in two pieces, the problem of fracture associated with the Swanson prosthesis is eliminated. Instead, wear of the prosthetic components against each other assumes importance and will be discussed in a later chapter.

Torsion and shear forces across the MCP joint are allowed for by conformance of spherical surfaces of the metacarpal and phalangeal prosthetic components. Torsion is important as cases of Swanson prostheses rotating through 90° have been noted in MCP joints (Sibly and Unsworth, 1991). Another advantage of the Durham design is that bone removal is minimised. Then, since bone stock is preserved, future surgery is still feasible. The Durham prosthesis is designed to be slightly thicker than the natural articular cartilage it replaces, to re-tension the ligaments which become lax in rheumatoid cases (Harrison, 1978). For more significant adjustment, the ligaments can be re-tensioned or released by the surgeon. Finally, the best aspects of the Swanson; low cost, ease of fitting, minimal operating time and ease of removal; also apply to the Durham prosthesis.

2.1.4 Discrepancies with Earlier Design Work

Stokoe (1990) had done some preliminary work on the Durham prosthesis. She had measured a number of metacarpal bones and found metacarpal head radii in the range from 4.65mm to 7.70mm. However, the prostheses she recommended to cover this range were of internal radius from 6.0mm to 9.0mm. Therefore prosthesis size did not match anatomical dimensions. This discrepancy meant that the range of prosthesis sizes recommended by Stokoe (1990) had to be re-evaluated. Stokoe (1990) also gave no justification for the choice of 1mm prosthesis thickness or of the 0.5mm steps in her range of 7 sizes. Further, Stokoe (1990) obtained a relationship between metacarpal head radius (r) and head width (w) of $w/r = 1.75$. However, the final prosthetic dimensions she specified did not match this relationship. Finally, Stokoe (1990) had produced no engineering drawings of the prosthesis, and there was no indication of the need for a lip to counter any coronal plane rotation. This requirement had been identified by Sibly and Unsworth (1991) but no precise dimensions given. In summary, MCP joint dimensions had to be obtained, prostheses based on these sizes designed, and drawn up to permit manufacture.

2.2 Survey of Research

2.2.1 Centre of Rotation of MCP Joint

The centre of rotation of the MCP joint lies within the head of the metacarpal, although its exact location is open to debate.

Flatt and Fischer (1969) found that, in the sagittal plane, the MCP joint had a fixed centre of rotation. Their work was done with living hands rather than cadavers and joint motion was studied rather than simply the joint itself. This is important because the centre of rotation depends not only on the geometry of the joint surfaces, but on the ligaments too, which have an offset attachment relative to any centre of the metacarpal head. Other work examining only the dimensions of the MCP joint has of necessity involved the removal of the ligaments surrounding these joints, but has agreed with their findings (Unsworth and Alexander, 1979).

Youm et al (1978) using an X-ray technique, also found the centre of rotation of the MCP joint to be constant in both the sagittal and transverse planes. Additionally, using an analytical method, and taking into account possible errors, they concluded that the centre of rotation was fixed within a 1.5mm sphere. This result was also found by Unsworth and Alexander (1979) who showed that the MCP joint had a single centre of rotation in both sagittal and transverse planes.

However, other researchers disagree with the concept of a fixed centre of rotation. Pagowski and Piekarski (1977) using measurements from cadavers, calculated the centre of rotation of the MCP joint to travel on an arc of radius 1.5mm. One aspect of their argument against a fixed centre of rotation was that a point load would result, and that this would lead to localised wear. Obviously, this local wear does not occur. In reality, the lack of wear is likely to be due to the cartilage forming a compliant surface, and has little to do with the position of the centre of rotation. An additional assumption was that the collateral ligaments are always taught. However, the collateral ligaments are slack when the joint is in extension, and they tighten as the joint is flexed (Flatt, 1983).

Again using cadavers, Walker and Erkman (1975), fixed the phalanx and moved the metacarpal bones, while graphically determining the position of the centre of rotation. Results gave its position as within 3mm of the centre of the metacarpal head; much greater than that found by any other researchers. Tamai et al (1988) attached springs to the tendons and muscles of cadavers to simulate normal loading, then analysed the MCP joint. They concluded that a fixed centre of rotation did not exist but did not give the dimensional variance.

2.2.2 Conformance Between Metacarpal Head and Phalangeal Base

Crucially, the argument concerning a fixed centre of rotation for the MCP joint is directly linked to that of the degree of similarity between the radius of curvature of the metacarpal head and that of the proximal phalanx. If the radius of the proximal phalanx base is greater than that of the metacarpal head, then a changing centre of rotation could exist.

In natural MCP joints, Unsworth et al (1971) and Walker and Erkman (1975) found the radius of the metacarpal to be very close to that of the proximal phalanx, in both the sagittal and transverse planes. Unsworth and Alexander (1979) measured the articular cartilage surface to be approximately spherical in both the sagittal and transverse planes. In support of these results, Lazar and Schulter-Ellis (1980) reported very close agreement between measurements of the metacarpal head in both the sagittal and transverse planes, again indicating sphericity. In contrast, Pagowski and Piekarski (1977) found the radius of the concave surface of the proximal phalanx to be much greater than that of the convex portion of the metacarpal. This conclusion was repeated by Tamai et al (1988) who measured the difference in radii to be almost double. Further, Tamai et al (1988) described both the cartilage surface of the metacarpal head as well as the bone beneath as resembling an ellipse, though of different sizes. This latter conclusion is in disagreement with Stokoe (1990) who found the bone surfaces to be spherical.

2.2.3 Conclusion

The Durham prosthesis was designed with a fixed centre of rotation, and with conforming spherical surfaces. These decisions were based on much of the anatomical data as well as manufacturing and engineering constraints.

To obtain maximum prosthesis life, contact stresses should be minimised therefore the maximum possible contact area should be created. To achieve maximum contact area, the surfaces must be conforming, which in turn necessitates making the radii of the bearing surfaces; the metacarpal and phalangeal components; equal. Therefore the Durham prosthesis has a fixed centre of rotation. Additionally, a sphere is a relatively easy shape to manufacture, as is producing the requisite spherical form on the head of the metacarpal bone during surgery.

An identical centre of rotation for both cartilage and bone was assumed, giving a constant thickness of prosthetic material over the metacarpal head. Constant thickness means uniform cooling during the production process which leads to consistent and expected material properties. For this reason, the idea of different centres for the articulating surface and the inner surface of the prosthesis was rejected.

2.3 Cartilage Details

Unsworth et al (1971) found the phalangeal and metacarpal cartilage of the MCP joint to have a total thickness of between 0.98 and 1.94mm for 11 healthy middle fingers. A difference of up to 100% was noted between individuals. Lazar and Schulter-Ellis (1980) reported a mean metacarpal head cartilage thickness from 60 joints of 0.75mm. Tamai et al (1988) from 24 metacarpals, measured the mean cartilage thickness to be thinner still at 0.46mm. Tamai et al (1988) also found that the thickness of the cartilage varied along the surface of the joint. This is to be expected from an engineering point of view, as the greatest amount of bearing material should be located where it is required.

Notwithstanding these clinical measurements, the final prosthesis thickness was a size dictated by engineering constraints. From a prosthesis wear life point of view maximum thickness is desired. Unfortunately, prototype prostheses of 2mm thickness showed heat sinks opposite the stem, which were aesthetically unacceptable. These heat sinks disappeared on 1.5mm thick components. The prototype prostheses used by Stokoe were 1mm thick, but increasing the thickness provided a simple way of increasing the wear life of the prostheses.

Therefore, 1.5mm was selected as the optimum prosthesis thickness. A constant thickness was chosen as this gave uniform and predictable material properties.

2.4 Metacarpal Anatomical and Prosthetic Component Details

2.4.1 Radius of Metacarpal Head

2.4.1.1 With Cartilage

Table 2.1 Average Metacarpal Head Radii (mm) in the Sagittal Plane by Finger.

Finger	Alexander (1972)	Lazar & Schulter -Ellis (1980)	Tamai et al (1988)	Unsworth et al (1971)
Index	7.96	7.63	6.91	-
Middle	7.49	7.58	6.66	7.69
Ring	7.10	6.59	-	-
Little	6.60	6.22	-	-
Range	5.08 - 9.65	-	-	6.4 - 9.1
No. off	60	100	20	8

Table 2.2 Metacarpal Head Radii (mm) Against Frequency

Radius	5.5	6.5	7.5	8.5	9.5
Range	5.01-6	6.01-7	7.01-8	8.01-9	9.01-10
Frequency	5	15	24	14	2
Percentage	8.3	25.0	40.0	23.3	3.3

From Alexander (1972): 60 MCP joints from 9 men and 6 women, aged 50-88.
These values are shown in graphical form in figure 2.1.

Figure 2.1 - Frequency of Metacarpal Head Radii Based On 60 Samples

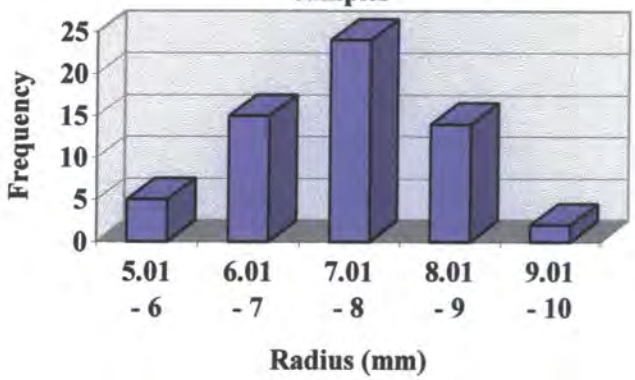

2.4.1.2 Without Cartilage

Table 2.3 Mean Metacarpal Bone Radius (mm)

Finger	Stokoe (1990)	Lazar & Schulter-Ellis (1980)	Tamai et al (1988)
Index	6.46	6.86	6.42
Middle	6.86	6.82	6.44
Ring	6.19	6.06	-
Little	5.47	5.45	-
Range	4.65 - 7.70	--	--
No. off	20	100	20

2.4.1.3 Discussion of Metacarpal Head Sizes

Measurements show that one person's little finger can have a larger metacarpal head radius than another's middle or index finger (Stokoe, 1990). Therefore to differentiate by 'finger' is inappropriate and the data of Alexander (1972), which is based on metacarpal head radius, has formed the basis of the prosthesis sizes chosen.

The sagittal (longitudinal) plane is considered the most important because it is the plane that will be measured by the surgeon during the operation, and this plane has a larger circumference compared with the transverse plane, therefore measurements in this plane will have greater accuracy.

2.4.1.4 Conclusion Regarding Metacarpal Head Radius

A range of five sizes of metacarpal prosthesis was selected, in 1mm steps, having external radii from 5.5 to 9.5mm. This range covers all of the sources listed above (Alexander, 1972; Lazar and Schulter-Ellis, 1980; Tamai et al, 1988; and Unsworth et al, 1971). Each prosthesis size covers a step given by its radius ± 0.5mm. Then allowing 1.5mm for prosthesis thickness, gives a bone radii range of 4 to 8mm which covers all of the sizes given by Stokoe (1990), Tamai et al (1988), and Lazar and Schulter-Ellis (1980). A 1mm step between each size of prosthesis was selected to minimise the inventory and so reduce costs, and it was felt that no benefit would be achieved by having smaller steps between sizes.

2.4.2 Width of Metacarpal Component

Stokoe (1990) produced a model which simplified the frontal shape of the metacarpal bone to that of a trapezium, having equal sides of angle 13°. By making the sides equal, prostheses for the fingers of the right and left hands become identical, thus reducing the inventory by half together with a proportionate reduction in costs. From this trapezium model a value of maximum bone width was obtained, using the formula $w/r = 1.75$, where r is bone radius and w is maximum bone width. The maximum width of the Durham prosthesis was made identical to w, as it is vital that the prosthesis will not interfere with the capsulo-ligamentous structures in any way.

2.4.3 Other Features of the Metacarpal Component

The degree of coverage of the metacarpal head by the prosthesis was chosen to be 200°, as this figure offers the potential for restoration of the complete range of motion of a MCP joint.

At the bottom of the prosthesis a lip was included to counter any coronal plane rotation which may affect the prosthesis, based on the work of Sibly and Unsworth (1991). A corresponding flat will have to be added to the volar aspect of the bone. This flat will be added here, where the bone is at its widest, to maximise the resisting moment. Rotation is to be avoided as it will cause wear leading to debris, inflammation and finally pain (Howie et al, 1988). It was necessary to strike a balance between minimum bone stock removal, and sufficient area of flat to prevent rotation of the prosthesis. Sibly and Unsworth (1991) state that 2mm of bone should be resected from a 15mm diameter metacarpal head, to leave a flat volar surface. Using this figure as a guide, together with superimposing sketches of prosthesis lips on 10x scale drawings of actual bones, a

range of lip dimensions was obtained which achieved the necessary balance. The two smallest sizes, R5.5 and 6.5 were based on the minimum possible thickness needed to give the 20° additional lip which provides the 200° of coverage of the metacarpal head. Above R6.5, the lip thickness was made to equal a proportion of R (25%). It also became evident that the flat had to be parallel with the central hole for the stem otherwise too much bone stock could be cut away.

2.5 Phalangeal Base Details

2.5.1 Radius of Phalangeal Component

As the metacarpal and phalangeal components must conform, the outer articulating surface radii of both were therefore made identical. The inner radius of the phalangeal component was simply determined by allowing a thickness of 1.5mm.

2.5.2 Shape of Phalangeal Component

The phalangeal component was made elliptical to match the natural ellipsoidal recess of the phalangeal articulating surface. Stokoe (1990) obtained a relationship for each of the major and minor axis dimensions of this ellipse, and this relationship was accepted. Rotation of the phalangeal component should be prevented by the square section stem, and by the component lodging within the concavity of the base of the phalanx.

2.6 Stem Details

2.6.1 Stem Section

A 3mm square section stem was chosen for all components. A square section should help to prevent rotation. From scale drawings it became obvious that to increase the 3mm dimension would cause problems with the smaller finger bones

due to excessive bone stock removal, while to reduce it would bring into question the strength of the stem.

2.6.2 Stem Length.

During surgery there was expected to be limited room to fit the prostheses, especially the phalangeal component. Therefore a short stem length of 12mm was chosen for each component. Such a dimension will not foul the stem of any proximal interphalangeal joint prosthesis which may be fitted.

2.6.3 Metacarpal Stem Offset

Unsworth and Alexander (1979) showed that an offset of 2.6mm in the sagittal plane was required to position the stem of any prosthesis in the centre of the medullary canal. This offset has also been described by Walker and Erkman (1975). Such an offset is crucial, as neglecting it has led to failures of the Flatt prosthesis (Flatt and Fischer, 1969, Blair et al, 1984 b). More recently, the same neglect of the offset was noted in the alumina ceramic prosthesis of Minami et al (1988). Although the Durham prosthesis will not rely on fixation based within the medullary canal, this 2.6mm offset was retained to help prevent rotation of the prosthesis (Sibly and Unsworth, 1991). In the transverse plane, the offset was found to be more variable, but generally so small on average that it could be neglected (Unsworth and Alexander, 1979).

2.6.4 Phalangeal Stem Offset.

Work by Unsworth and Alexander (1979) indicated that a wide range of offsets of the medullary canal existed. However, as fixation is to be based within the head of the proximal phalanx, the details of the medullary canal did not affect the design of the prosthesis. Therefore the phalangeal component had no stem offset.

2.7 Fixation

2.7.1 Background

Without fixation it has, as a general rule, been found that prostheses can cause bone resorption, inflammation and pain (Phillips and Messieh, 1988; Dickob and Martini, 1996).

The most common option in prosthetic fixation is to use cement, polymethylmethacrylate (PMMA) having been used successfully in many thousands of hip and knee replacements. Despite this achievement, problems exist which are peculiar to fingers. It is extremely difficult to cement implants into small bones without either damaging the bone (necrosis) or failing to get an adequate permanent fixation. Necrosis is thought to occur at around 50°C, and the temperature of the exothermic polymerisation reaction of the cement is also around 50°C (Schultz et al, 1987). Further, necrosis occurs at a depth of up to 1mm, yet many rheumatoid patients have a thickness of cortical bone of less than 1mm (Lazar and Schulter-Ellis, 1980; Swanson et al, 1986). Moreover the amount of bone resected could limit the range of revision procedures available. Additionally, the time taken by cement to set lengthens the operating time. PMMA debris can cause increased problems of wear (Caravia et al, 1990) and loosening that it was designed to prevent. It can be unforgiving for a two part prosthesis as exact alignment will be required, and it is not good at resisting torsional moments (Weightman et al, 1983). For these reasons, all cemented MCP prostheses have failed. Finally, if the cement does produce adequate fixation, but the prosthesis fails for some other reason, the removal of the prosthesis and cement becomes difficult.

The ideal form of fixation is that which stimulates bone ingrowth and relies on the body itself. Such methods currently available which attempt to achieve this aim include porous surfaces and hydroxyapatite coatings. Hydroxyapatite coatings have given some good results (Geesink and Hoefnagels, 1995). However, a hydroxyapatite coating entails plasma spraying, a post manufacture process which is not applicable to polymers due to the very high temperatures involved. Porous surfaces are usually created on hip or knee prostheses by affixing metal beads, but again, their method of attachment is unsuitable for use with polymers. Therefore hydroxyapatite and porous coatings are were felt not to be applicable to the Durham MCP prosthesis.

Although different to bone ingrowth, it is also usual to find a fibrous membrane surrounding an implant material. Such ingrowth of fibrous tissue was the basis of fixation of the Niebauer prosthesis (Niebauer et al, 1969). Further, Walker et al

(1983) found that fibrous encapsulation of a polymeric prosthetic component could provide adequate fixation.

Supportive features can be built into the prosthesis design to encourage acceptance by the body. Material properties of the prosthesis similar to those of bone help to ensure that bone ingrowth is successful; a further reason for the interest in materials such as hydroxyapatite. Swanson et al (1986) and Walker et al (1983) both consider that a polymeric prosthesis more evenly distributes the stresses imposed upon it, which in turn helps to prevent bone resorption. Additionally, a non-constrained prosthesis design helps to minimise potential forces, in that one part of the prosthesis will not pull on the other part. Yet, in contrast it is also recognised that to encourage bone ingrowth no movement of the prosthesis should be allowed.

2.7.2 Survey of MCP Prosthesis Fixation

All of the uncemented MCP prostheses made from materials much harder than bone have cut into either or both of the phalangeal or metacarpal bones. These have included the stainless steel Flatt prosthesis (Blair et al, 1984 b) and the alumina ceramic prosthesis (Minami et al, 1988). Also unsuccessful were those designs which relied on cemented fixation, and prosthesis failure was generally tied in with a deficiency of fixation (Adams et al, 1990; Beevers and Seedhom, 1993). Therefore the idea of fixation of the Durham MCP prosthesis using cement was rejected.

A plethora of prosthetic MCP designs, based on mechanical fixation, have been tried. Such ideas have included a hollow screw (Walker et al, 1983; and Hagert et al, 1986) circumferential fins (Condamine et al, 1988; and Weightman et al, 1983) appropriate surface texture (Walker et al, 1983) and an interference fit (Beckenbaugh and Linscheid, 1989). All have yet to report long term clinical success. Furthermore, as will be discussed in section 2.7.3, the application of any of the above mechanical modes of fixation to the Durham MCP prosthesis would cause major manufacturing difficulties. Some designs were too complex to be manufactured, others increased the number of pieces needed for the injection moulding tool, and therefore significantly inflated the final cost of manufacture. Additionally, the original design concept envisaged a prosthesis that was easy to fit, and which required minimal bone resection. Both aims could not be reconciled with mechanical fixation.

Interestingly, perhaps the most successful finger prosthesis, the Swanson, and a modern competitor the Sutter prosthesis, have no inherent fixation. Indeed Swanson himself is convinced that a lack of fixation is one of the causes of the success of his design (Swanson, 1972; Swanson et al, 1986). This may be in part due to the lower modulus of silicone rubber compared with bone. Silicone rubber has a modulus of elasticity of 0.01GPa, while bone has a modulus of 10 to 30GPa. In turn UHMWPE also has a modulus of elasticity lower than that of bone, at 0.5GPa (Dowson, 1989).

2.7.3 Durham Prosthesis Fixation

The diagrams below (Figures 2.2 to 2.11) show the various designs of mechanical fixation considered for the Durham MCP prosthesis, superimposed on scale drawings of metacarpal heads in the sagittal plane. All diagrams are based on a R7.5 metacarpal component.

Stokoe's (1990) design (Figure 2.2) was improved in three aspects (increased thickness, 200° cover and an anti-rotation lip) to give the design shown in Figure 2.3. Fixation was then considered. It was initially intended to fit circumferential fins to the stems of each prosthesis (Figure 2.4). These fins would provide location by obtaining purchase on the inner walls of the medullary canal. However, a series of tests were undertaken which showed that a hole size of (fin diameter minus 1mm) was necessary to allow the appropriately sized fins to fit without breaking. Therefore a drilled hole almost equal to the size of the medullary canal itself would be required (Figure 2.5). In such a case, the drilling process would remove most of the bone that was intended to be preserved, possibly removing the attachments of the ligaments too and necessitating major changes to the metacarpal prosthetic component itself (Figure 2.6). It was apparent then, that fixation based on the medullary canal could not be achieved within the constraints of the original MCP prosthesis design concept.

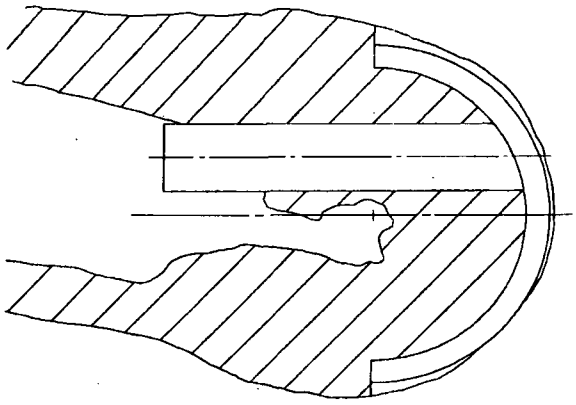

Figure 2.2 - Stokoe Design of MCP Prosthesis

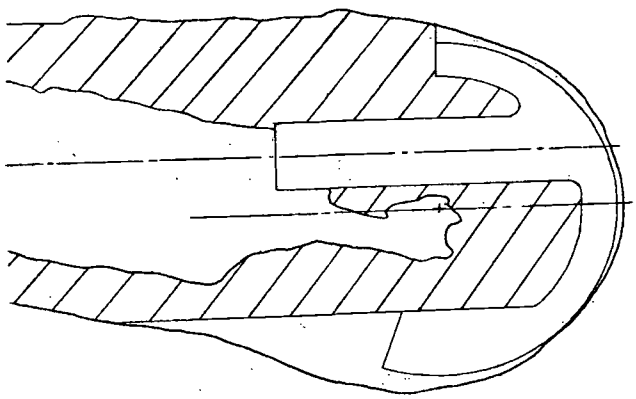

Figure 2.3 - Improved Design of MCP Prosthesis

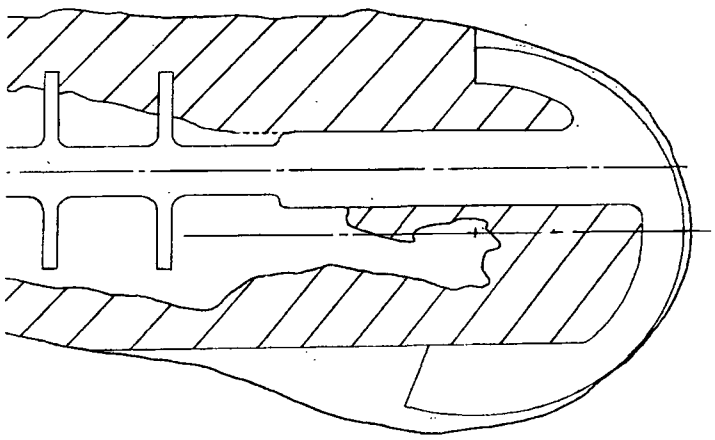

Figure 2.4 - Circumferential Fins Added to Prosthesis Stem

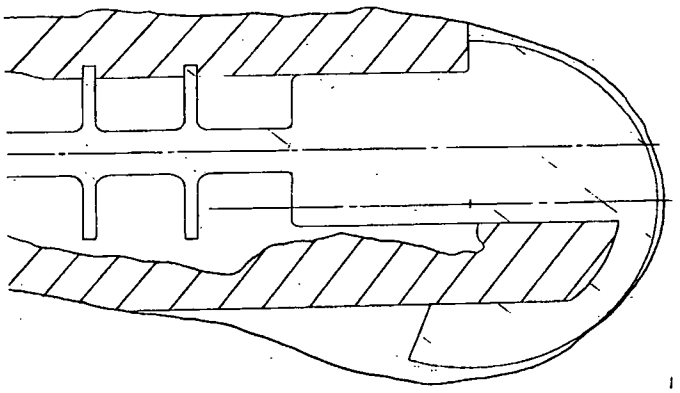

Figure 2.5 - Hole Size Required for Circumferential Fins

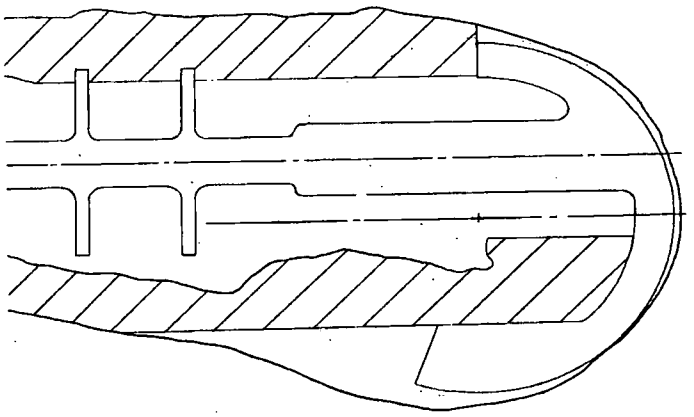

Figure 2.6 - Prosthesis Design Necessary to Accommodate Circumferential Fins

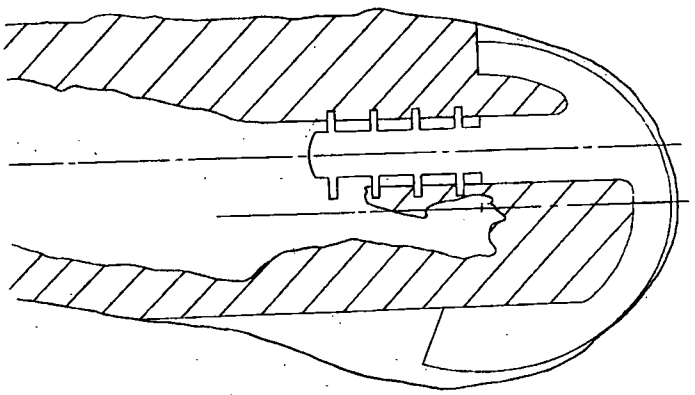

Figure 2.7 - Concept for Fixation Based Within Cancellous Bone

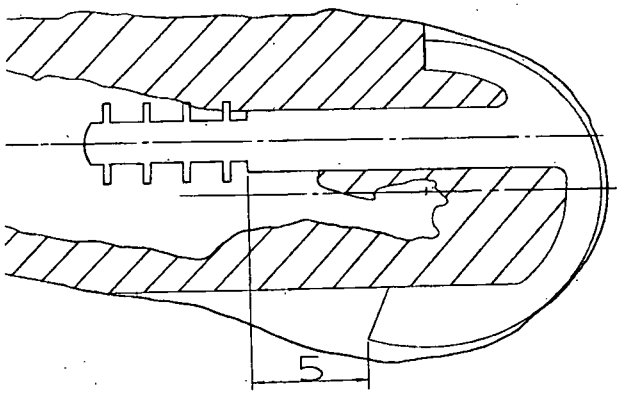

Figure 2.8 - Manufacturing Requirement for Cancellous Fins

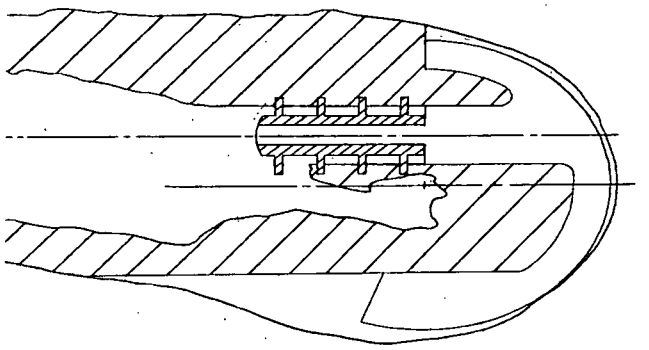

Figure 2.9 - Concept for Two-Piece Metacarpal Component to Give Fixation Within Cancellous Bone

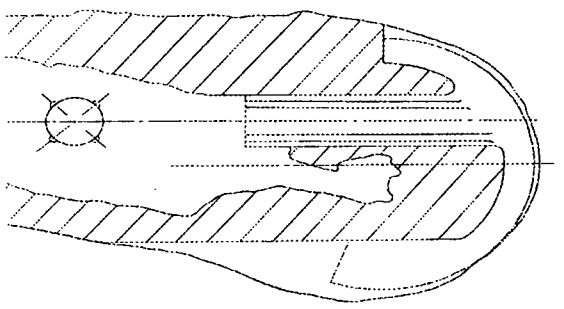

Figure 2.10 - Interference Fit With Ridges

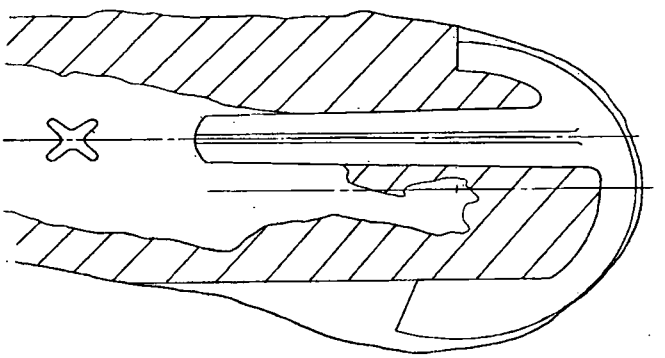

Figure 2.11 - Longitudinal Fins

Therefore fixation within the cortical bone of the metacarpal and phalanx was investigated (Figure 2.7). Again fins were considered of outer diameter = stem diameter + 1mm. Here differences between the two prosthetic components became apparent. Although such fins could be fitted to the phalangeal component, due to the injection moulding process they could not be applied to the metacarpal component. Specifically, at least 5mm was required between the end of the bottom lip of the metacarpal prosthetic component and the start of any fins. By such a point, the fins would be positioned within the medullary canal so fixation would not have been achieved (Figure 2.8). Further, although such manufacture was feasible it would be most complex, leading to increased production costs.

Therefore, to locate the fins within metacarpal head, the idea of a two piece metacarpal component was considered (Figure 2.9). The resulting prosthesis would obviously be more complicated and expensive. A means of joining the two parts also had to be considered. Such ideas included a rivet; an M2 thread; a taper of various sections, cylindrical, 3 or 4 fins; a rectangle and slip over design; splines; weld; and a circlip or spring washer. Each of these ideas had its own drawbacks but eventually all were rejected as separate fins would mean a central inner stem of some 1.5mm diameter, and therefore of dubious strength. Consequently, the original idea of a single piece stem was returned to. Again, various single piece stem designs were considered. Firstly, an interference fit (Figure 2.10), but rheumatoid bone may not be strong enough to act as a source of such location. Surgery is also made more difficult if it is necessary to wield a mallet within the confined space provided by a MCP joint during surgery. The use of longitudinal fins was also considered (Figure 2.11), but such a stem shape offered no advantages over a square section stem. Having considered the merits of all possible types of mechanical fixation, a plain stem was chosen for the Durham MCP prosthesis.

2.7.4 Summary of Fixation of Durham MCP Prosthesis

Cement has been shown to be inappropriate for use with MCP prostheses. The problem with fins based on medullary cavity fixation is that the necessary drilled hole size is so large it removes most of the bone that is intended to be preserved. However, a single piece prosthetic component with fins based on cortical bone

fixation cannot be manufactured by injection moulding. Further, a two piece component means additional cost and complexity, and there are problems with securely joining the two pieces due to the inherent weakness of such small parts. Therefore a plain stem was chosen, one which offered ease of fitting and was inexpensive to manufacture. It is intended to rely on fibrous encapsulation, the fact that the two components are always under compression, and the supportive nature of the prosthesis design, to ensure adequate fixation. Finally, it has to be remembered that the most successful MCP prosthesis, the Swanson, employs no fixation.

2.8 Variations to the Two Smallest Sizes of Metacarpal Component (R5.5 and R6.5)

Sketches showed that in the case of the R6.5 metacarpal prosthetic component, due to the 2.6mm offset of the stem, there was a very small gap between the stem and the top part of the inner sphere. So small a gap that the bone, even if it could be shaped during surgery, would probably necrose afterwards. Therefore the intersection between the top of the stem and the inner sphere became the rear face of the prosthesis. This decision resulted in slightly reduced coverage, but coverage still remained well within the functional range. Further, this solution had the advantage of not cutting any extra bone away instead only a reduced spherical cutter will be needed. Also, the complexity of the injection moulding tool is reduced, bringing costs down too. In the case of R5.5 there was no gap at all. However, the head blended in well to the stem and still gave the same 200° coverage as the larger prostheses.

2.9 Summary of Durham MCP Prosthesis Design and Dimensions

The Durham prosthesis is a two piece surface replacement design. It is made in five sizes, the range being R5.5 to R9.5mm in 1mm steps, where R is the radius of the outer articulating surface. Both components have conforming spherical articulating surfaces. The face of the metacarpal components is shaped as a trapezium, and the face of the phalangeal components is that of an ellipse (Stokoe, 1990). A metacarpal lip to counter coronal plane rotation has been added to the metacarpal component. Both prosthetic components have a wear face of

thickness 1.5mm, together with a stem of length 12mm and 3mm square section. Appendix 1 shows production drawings of the Durham MCP prosthesis.

Table 2.4 Metacarpal Component Dimensions

R	5.5	6.5	7.5	8.5	9.5
r	4.0	5.0	6.0	7.0	8.0
w	7.0	8.75	10.5	12.25	14.0
t	2.35	2.65	2.95	3.25	3.55

Key:

R = Articulating surface radius

r = Radius created on head of Metacarpal bone
= R - 1.5 (1.5mm = prosthesis thickness)

w = Width of metacarpal component. From Stokoe (1990) w = 1.75r

t = thickness of lower lip.

Table 2.5 Phalangeal Component Dimensions

R	5.5	6.5	7.5	8.5	9.5
s	7.0	8.0	9.0	10.0	11.0
a	8.50	9.66	10.82	11.98	13.14
b	6.34	7.53	8.72	9.91	11.10

Key:

R = Articulating surface radius

s = Distal prosthesis radius = R + 1.5mm. (1.5mm = prosthesis thickness)

b = minor axis length. Based on Stokoe (1990)
r = 0.84046b - 1.33145. Where r = metacarpal bone radius.

a = major axis length. Based on Stokoe (1990) a = 0.9772b + 2.2982.

CHAPTER THREE

Testing of the Durham Metacarpophalangeal Prosthesis

3.1 Description of Stokoe Finger Function Simulator

3.1.1 Apparatus

The Stokoe finger function simulator (Figure 3.1) has been shown to be a device which effectively simulates the loads and motions encountered by a finger prosthesis in vivo (Stokoe et al, 1990).

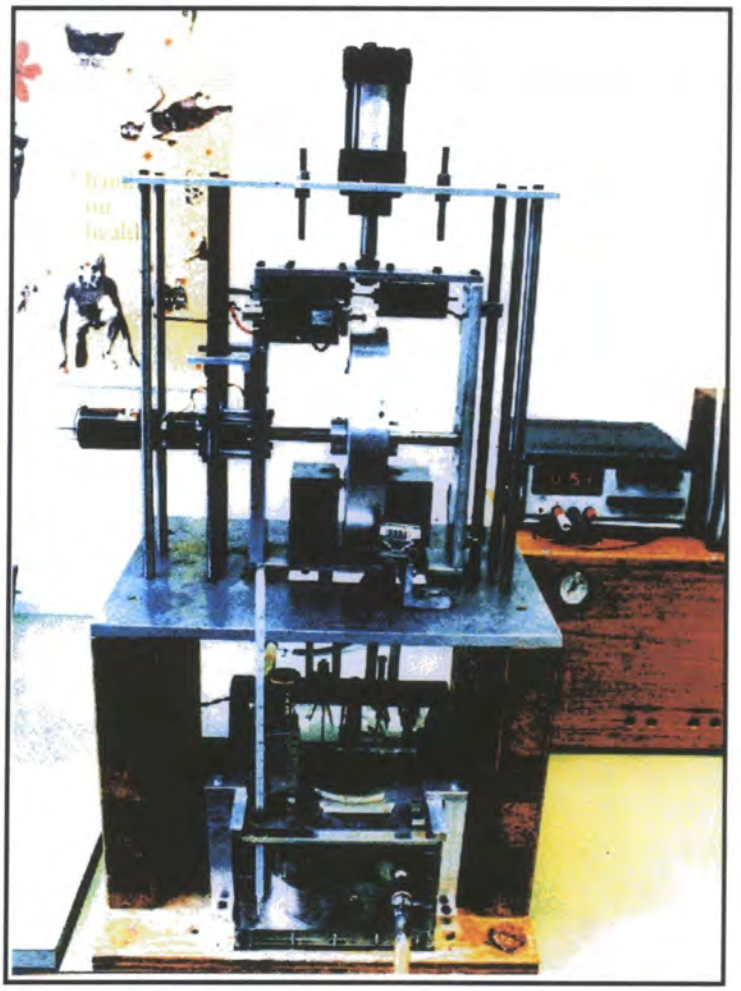

Figure 3.1 - The Stokoe Finger Function Simulator

The simulator flexed a test prosthesis cyclically over a 90° range of motion under light loading; then applied a heavy static load to imitate 'pinch' grip. Motion was uni-planar as flexion-extension is the predominant action of the finger. The light loading simulated those situations where loads were small (10-15N) but the finger was moving quickly (Tamai et al, 1988). In contrast, situations such as turning a key or holding a handle show minimal motion but large joint forces. These situations were therefore mimicked by the 'pinch' grip action of the simulator, which occurred once every 30 minutes, where a static load of 100N was applied. One hundred Newtons was calculated to be the maximum arthritic pinch grip force (Weightman and Amis, 1982; Jones et al, 1985).

The Stokoe finger function simulator can be described in three parts; the drive mechanism, the bath components and the control circuitry. The drive mechanism, which provided the flexion-extension motion of the test prosthesis and the static 'pinch' load, consisted of a 12V DC motor and gearbox unit turning a large aluminium flywheel (Figure 3.2). Into the flywheel a pair of eccentric grooves had been machined, into each of which fitted a follower. A single cord, which acted as an artificial tendon, was attached to each follower via a 'tendon' adjuster. Each adjuster contained a spring, the purpose of which was to smooth out motion during flexion-extension (Stokoe, 1990). Furthermore, the adjuster for the 'flexor tendon' contained a short spring within a collar, whereas the adjuster for the 'extensor tendon' contained a long spring. Therefore, during static loading, the short spring was soon compressed so that the collar was pressed against the base of its adjuster while the far longer spring on the 'extensor' side was hardly compressed at all. In this way the majority of the static force was carried through the flexor tendon, as is the case in vivo when 'pinch' loads are applied (Long et al, 1970). Above the drive mechanism was mounted a single 40mm bore pneumatic cylinder, which was used to provide the large load which mimicked 'pinch' grip. The motor and flywheel assembly was mounted in a cage which was free to move vertically on slides. During flexion-extension this cage rested on a lower shelf of the simulator, but during 'pinch' grip the cage was lifted vertically by the pneumatic cylinder.

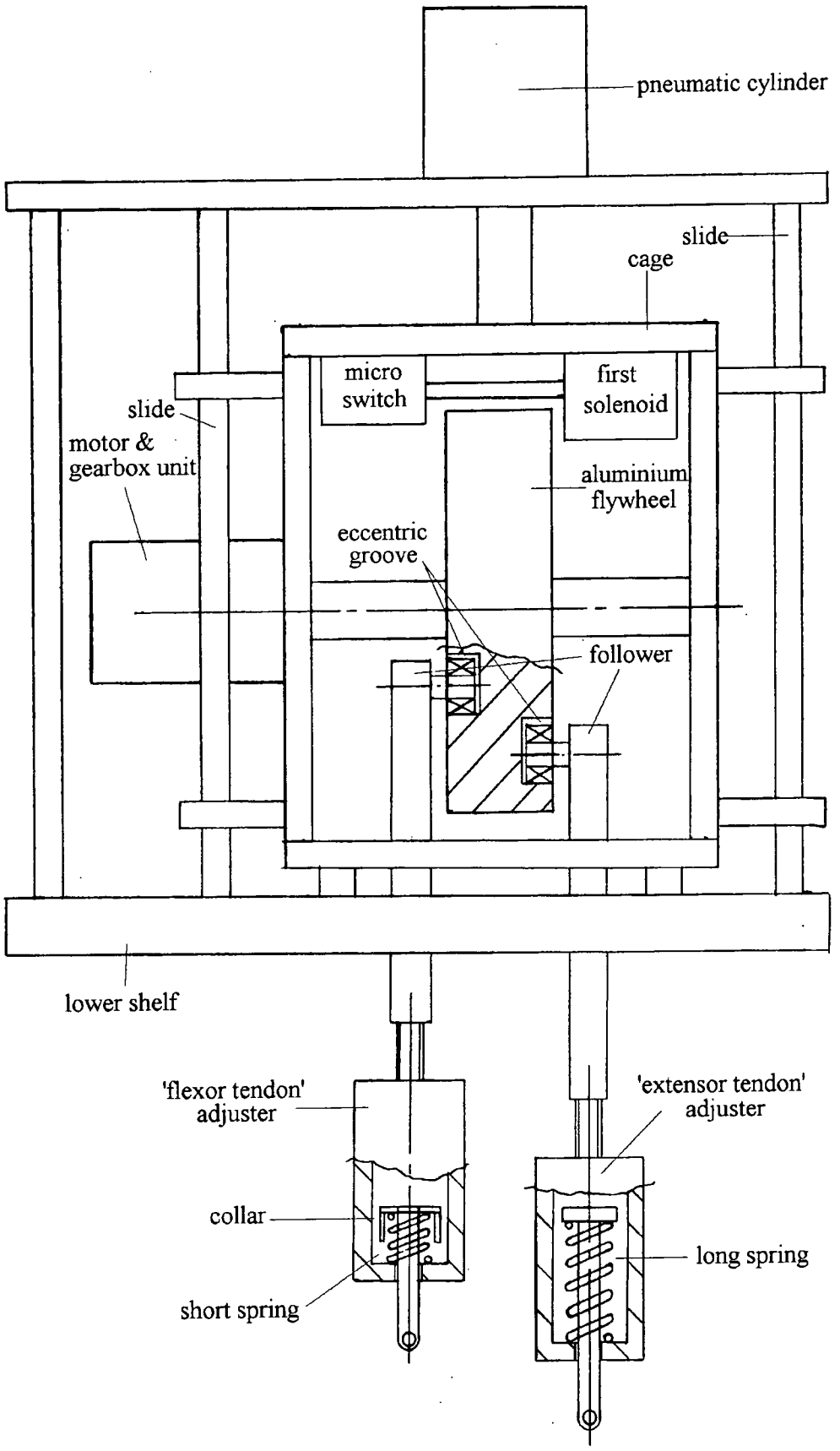

Figure 3.2 - Drive mechanism of finger function simulator

The artificial tendons, whose purpose was to represent the actions of the muscles associated with the MCP joint, were guided by pulleys into a perspex bath where the testing of the prosthesis took place (Figure 3.3). Each prosthetic component was mounted in an artificial bone. The metacarpal prosthetic component was held in an assembly which was connected to a square section cantilevered beam. On each face of this beam, but clear of the lubricant, were mounted two strain gauges. Together, these eight strain gauges comprised two full strain gauge bridges which measured the deflection of the beam in the axial and dorsal/palmar directions, and therefore the load across the prosthesis. The phalangeal prosthetic component was mounted in an assembly to which were attached the two artificial tendons, and this assembly was capable of being moved through an arc of 90°. Above this arc was mounted a stainless steel rod attached to a solenoid. This rod provided the 'thumb' resistance force during the 'pinch' grip part of the load cycle. Path restrictions normally imposed by tendon sheathes were provided by simple pulleys. The volar plate and metacarpoglenoidal ligament were simulated using a mobile pulley, whose point of attachment was offset from the centre of rotation of the artificial joint.

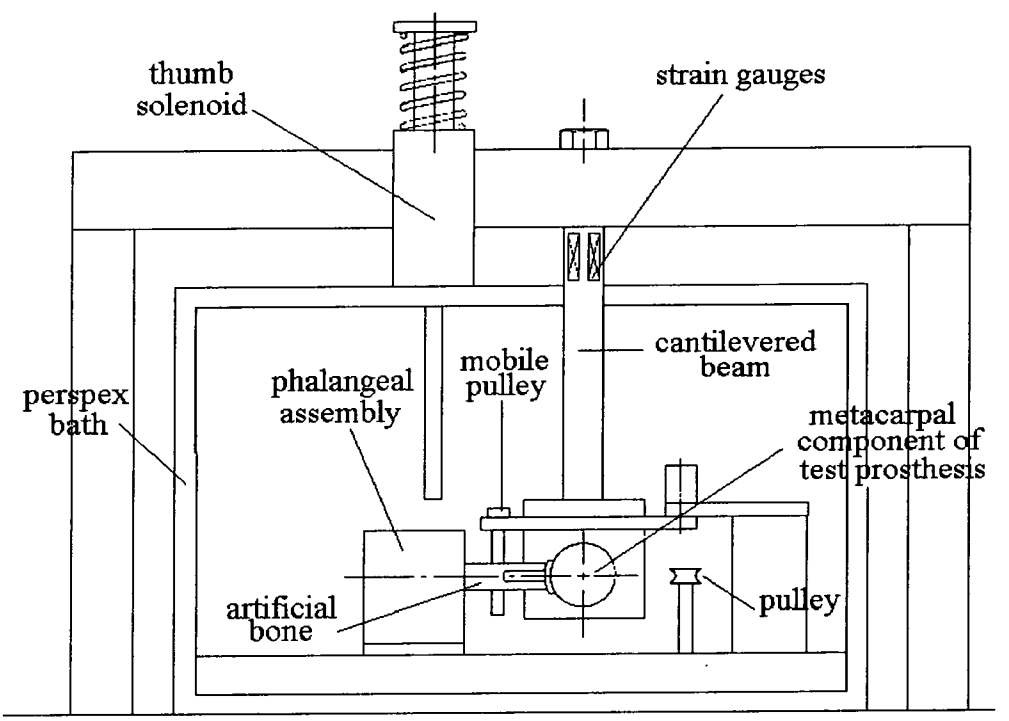

Figure 3.3 - Bath components of finger function simulator

An electrical timer was connected to a series of cams, and the motion of the cams provided the means of controlling the electrical and pneumatic components. The sequence of events was as follows. Once every thirty minutes the timer activated the first solenoid which pulled the micro-switch into the path of the aluminium flywheel. A lug on the circumference of the flywheel then hit the micro-switch which in turn deactivated the motor, and instead activated the 'thumb' solenoid. Following a brief pause the pneumatic cylinder was activated, lifting the cage and causing the phalangeal assembly to be pulled hard against the stainless steel pin of the 'thumb' solenoid. In this way, the 'pinch' load was achieved. After a pre set time the pneumatic cylinder was deactivated. Next the voltage to the first solenoid was cut, which restored the supply to the motor, released the 'thumb' solenoid and therefore flexion-extension re-commenced. Strain gauges provided the means of measuring the force across the test prosthesis. Load was measured in two directions, axial and dorsal/palmar, as the direction of the force across the test prosthesis was constantly changing during flexion-extension. The strain gauges were connected to a pair of strain gauge amplifiers and an analogue-digital (A-D) converter. The output was then displayed in millivolts on a pair of voltmeters. This voltage output was therefore directly proportional to the load across the prosthesis.

3.1.2 Upgrades and Modifications

3.1.2.1 Introduction

Problems with the finger function simulator were mainly associated with the drive mechanism and the constant need for re-adjustment of the tension in the artificial tendons, hence the move to pneumatic actuation in the new design of simulator (chapter 5).

3.1.2.2 Motor and Gearbox Unit

During the use of the finger function simulator by other researchers, the motor and gearbox unit had often failed due to the gears stripping. As a consequence, this old unit had required frequent overhaul and repair, with the result that it was due for replacement. An investigation of the design of the finger function simulator revealed two reasons for these gearbox failures. Firstly, if a solenoid elsewhere on the simulator stuck in position, then the flywheel would be locked in place while the motor was trying to turn it. To solve this problem, a fuse was

fitted in the electrical supply to the motor. Therefore, if the flywheel was held while the motor was trying to turn it, then the motor drew increased current until the fuse blew. Secondly, the old motor was found to be supporting, as well as driving, the flywheel and its associated driven components, so greatly increasing the load on the motor. To solve this problem, the rig framework was re-designed such that the weight of the flywheel and driven components was taken by a pair of bearings within the frame, rather than a single bearing and the motor, as had been the case. In tandem with these changes, a more powerful motor and gearbox unit was purchased and fitted to the simulator. The new motor and gearbox unit was a 40W motor with a planetary gearbox, code RE035.071.30 EAC200A, supplied by Trident Engineering Limited, Trident House, King Street Lane, Winnersh, Wokingham, Berks., RG11 5AS, tel. 01734 786444.

3.1.2.3 Bath/Pump Unit

A new bath with an integral heater and pump was obtained to warm and circulate the lubricant used to simulate in vivo conditions in the finger function simulator. Unlike earlier baths, the bath chosen had a lid to reduce the loss of lubricant through evaporation, a heater cut out protection to prevent the bath from burning out in the event of lubricant leakage, and sufficient capacity to supply two finger function simulators. The new bath was a Grant Y14-VFP, supplied by SH Scientific, Coniston Road, Blyth, NE24 4RG, tel. 01670 361661.

3.1.2.4 Other Modifications

Connections to a compressed air supply were arranged and new springs for the 'tendon' adjusters were purchased. These new springs were manufactured from 22 gauge stainless steel to resist the corrosive aspects of the Ringers solution which was initially used as a lubricant (spring supplier Red Rose, Patterson Street, Blaydon, NE21, tel. 0191 414 5012). Due to this corrosion, mechanical components were also replaced where appropriate. The electrical wiring of the simulator was overhauled which, as well as improving safety, led to a reduction in the simulator's overall size. Also in the interests of safety, a guard was manufactured and fitted around the flywheel.

Throttles were purchased and fitted to the pneumatic cylinder to minimise the shock which occurred when the 'pinch' load was applied. In this way, 'tendon' breakage was significantly reduced. As the 'tendon' substitute, 130lb (59kg) braking strain braided dacron fishing line was used. An air pressure of 40psi

($0.276MN/m^2$) supplied to the pneumatic cylinder was found to give the desired 'pinch' load of 100N across the test prosthesis. A flexible coupling was fitted between the first solenoid and the micro-switch, to accommodate their lack of alignment. This modification ensured the correct functioning of the solenoid and therefore of the 'pinch' load section of the load cycle. Finally, a means of securing the lid of the perspex bath was designed, manufactured and fitted. This modification, in preventing the 'thumb' solenoid from moving away from its correct position, ensured that the 'pinch' load operation was undertaken correctly.

3.2 Calibration and Operating Procedure

3.2.1 Calibration

Calibration of the strain gauges was performed so that the voltage output from the strain gauge amplifiers could be directly interpreted as a load reading. By applying set loads to the cantilevered beam, and noting the voltage produced, a graph of load against voltage for each of the axial and dorsal/palmar strain gauge bridges was obtained. From this graph (Figure 3.4) the reciprocal of the gradients gave calibration constants of 0.30N/mV in the axial direction and 0.45N/mV in the dorsal/palmar direction.

Figure 3.4 - Calibration Curves for Strain Gauges

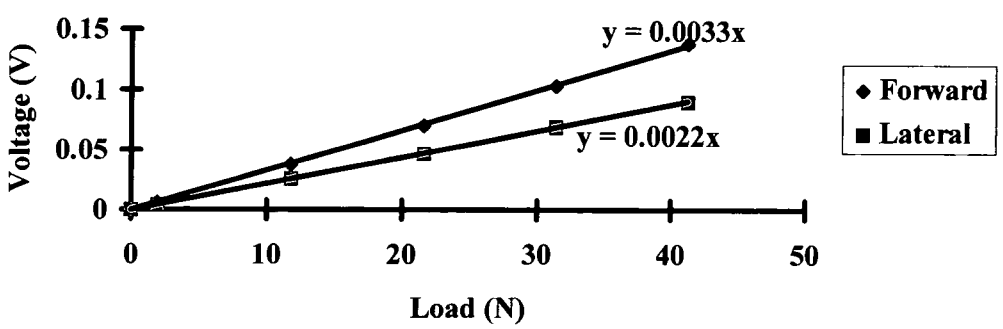

3.2.2 Operating Procedure

Set up of the simulator was initially both difficult and time consuming. Due to the independent positioning of the perspex bath, and each of the prosthetic component holders, with respect to each other and the rest of the simulator

components, a long learning curve had to be traversed, before the correct position of each of the components was found. Once these correct positions were discovered, the necessary arc of motion and loads could be achieved for legitimate operation of the simulator. The correct position of the perspex bath was then marked on the base of the simulator. Once these foundations were in place, set up was as follows. The flywheel was rotated by hand, while the arc of motion was noted. The 'tendon' adjusters were utilised so that a smooth 90° arc of motion together with the appropriate loads of 10-15N were applied across the prosthesis. This load was checked by noting the voltage output on the voltmeters. During the 'pinch' grip part of the simulator's operation, when the pneumatic cylinder was activated, the load was increased to 100N. This value of load was again checked using the voltmeters.

Prior to the commencement of a test, the prosthetic components were cleaned in acetone and weighed. An additional pair of prosthetic components was placed within a small cage in the perspex bath to act as control specimens. These control specimens were unloaded. The bath/pump unit was switched on and the lubricant allowed to reach a steady state temperature of 37°C. Testing then commenced. The number of cycles of the flywheel was recorded by a mechanical counter, 77 rotations of the flywheel being equal to one unit on the mechanical counter.

Frequent checking of loads and cycle speed were made. At regular intervals, the test was stopped, the prosthetic components were removed, cleaned in acetone and weighted. Test and control samples were weighed to the nearest 0.1mg using a Mettler AE200 balance. Wear of a test component was defined as the weight loss with respect to the initial weight, to which was added any weight gain of the control component. Therefore the weight gain of the control and test component was assumed to be identical. The control and test samples were very close in weight to each other. The biggest difference in weight was 2.3% in one case only (the phalangeal components of test 3) the majority were within 1% and many were identical in weight (to within the accuracy of the balance). Therefore these errors due to difference between control and test samples were small compared with weighing errors. The wear factor k (units $10^{-6}mm^3/Nm$) was determined from equation 1.1.

One complete operation of the simulator consisted of a 30 minute period. During the lightly loaded part of the operation, which lasted for almost 29 minutes, the simulator ran at 112 cycles per minute (cpm) with an average load of 12.5N during flexion-extension. One cycle being the movement of the phalangeal test component from 0 degrees to 90 degrees and back to 0 degrees. Towards the end of the operation, motion of the prosthesis ceased and, after a brief pause, a static load of 100N was applied for 45 seconds through the flexor 'tendon'. The static load, which mimicked 'pinch' grip, was then removed, there was another brief pause and, after this, a new operation started. Therefore at a speed of 112cpm, one operation consisted of 3,248 cycles and a single 'pinch' load. Test parameters for all six tests are summarised in table 3.1.

Table 3.1 General test parameters

Parameter	**Tests 1 to 3**	**Tests 4 to 6**
Lubricant Temperature	37°C	37°C
Mean Static Load	100N	100N
Prosthesis Outer Radius (R)	9.4mm	8.5mm
Wear Face Thickness	2mm	1.5mm
Arc Length (Rθ)	14.7mm	13.35mm
Cycles per Minute (cpm)	112	112
Average Velocity	54.9mm/s	49.8mm/s
Stroke	29.4mm	26.7mm
Nominal Stress at 100N Static Load	0.68MPa	0.82MPa
Nominal Stress at 12.5N Dynamic Load	0.08MPa	0.10MPa

3.3 Development of Tests

The first test was undertaken with irradiated, low gel content MCP prosthetic components to investigate whether a relationship between gel content (the percentage of cross-linking) and wear existed. The metacarpal component had a 36% mean gel content, while the phalangeal component had a 66% mean gel content. Cross-linking produces a lattice like structure between the polyethylene molecules, resulting in improved material properties. It was therefore expected that the low gel content metacarpal component would wear at a greater rate than the phalangeal component, which had a 30% higher gel content. De Puy International, who manufactured the prostheses, consider a gel content of greater than 70% to be acceptable for XLPE for use in a load bearing situation in vivo. These can be termed high percentage cross-linked components. The second and third tests employed MCP prostheses in which both the metacarpal and phalangeal components had a mean gel content of 87% after irradiation.

The first and second tests employed Ringers solution as the lubricant, while the third used distilled water. Therefore these tests permitted a comparison of lubricants. Earlier researchers at Durham (Stokoe 1990, Sibly and Unsworth 1991) had all used Ringers solution. The Ringers solution was made up as follows (for one litre):

Sodium chloride	7.5gm
Potassium chloride	0.075gm
Calcium chloride	0.1gm
Sodium hydrogen carbonate	0.1gm
Distilled water	to 1 litre

Each test was run for a minimum of 6 million cycles, although tests generally ran for a much greater duration. One million cycles includes just over 300 'pinch' operations. The third test had a duration of 633km which, at a rate of one million cycles per annum, was equivalent to 21.5 years in vivo.

The last three tests all employed irradiated 8.5mm radius production samples, of thickness 1.5mm, and all testing was done in distilled water. These production samples also had square section stems rather than the circular sections seen on

the prototype samples. Figure 3.5 shows a pair of production components, typical of those used in tests 4 to 6, together with a pair of prototype components, typical of those used in the first three tests.

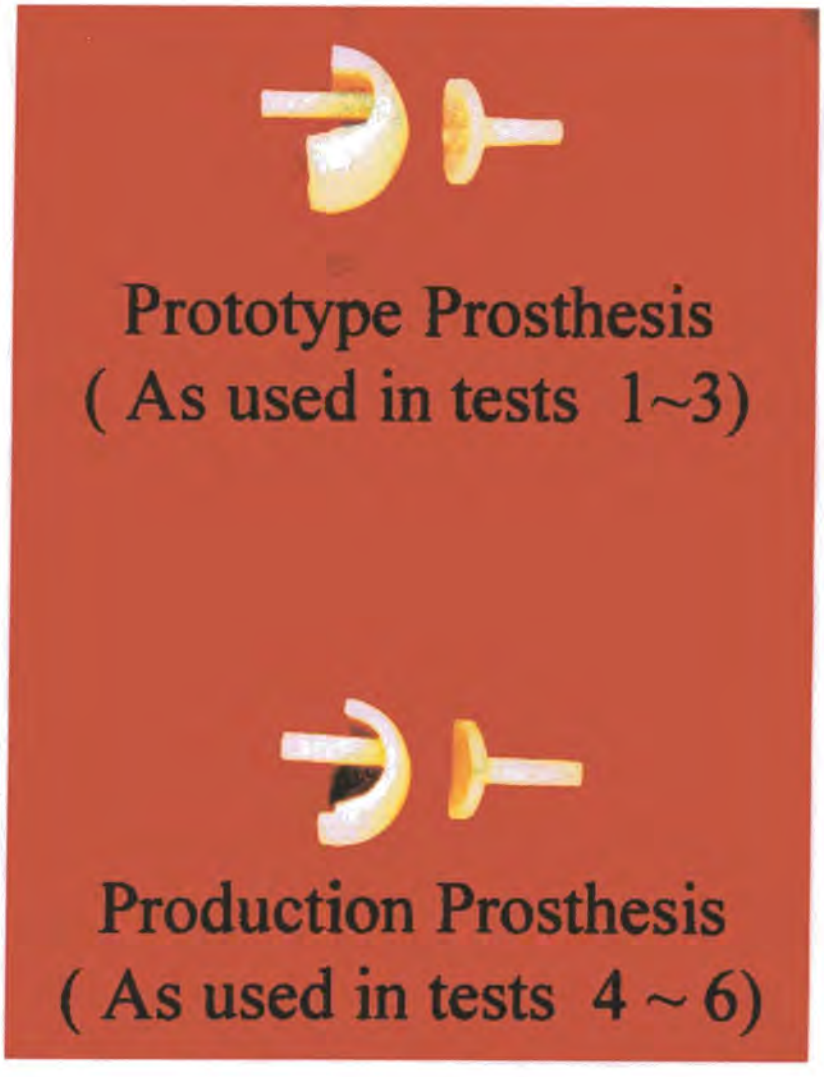

Figure 3.5 - Prototype and Production Prostheses

In tests 4 and 5 the phalangeal components had a mean gel content before irradiation of 80%, while the metacarpal components had a mean gel content before irradiation of 71%. In test 6, these figures were both 75%. In all six tests the density of XLPE was taken to be 949kg/m^3. Similarly all test components were irradiated, as would be the case for sterilising such products prior to implantation.

3.4 Finger Function Simulator Wear Test Results

Table 3.2 Summary of wear factors

Test	Aim of Test	Dist. (km)	R (mm)	k metacarpal x $10^{-6}mm^3/Nm$	k phalangeal x $10^{-6}mm^3/Nm$
1	low gel content	190	9.4	6.0 ± 0.1	2.1 ± 0.1
2	normal gel	224	9.4	0.72 ± 0.08	0.34 ± 0.08
3	+ distilled water	633	9.4	0.24 ± 0.03	0.12 ± 0.03
4	prodn thickness	252	8.5	0.40 ± 0.07	0.23 ± 0.07
5	prodn thickness	272	8.5	0.03 ± 0.06	0.12 ± 0.06
6	prodn thickness	247	8.5	0.13 ± 0.07	0.10 ± 0.04

The results in table 3.2 are shown graphically in Figures 3.6 to 3.21. The actual weight changes of test and control components are tabulated in appendix 3. The error was based on the accuracy of the Mettler balance. Allowing for an error of ± 1 x 10^{-4}g in weight measurement for each of the control and test samples gave a total error of ± 2 x 10^{-4}g for each prosthetic component.

3.5 Discussion of Results

Figure 3.6 - Effect of Percentage Cross-Linking on Wear of Prosthetic Components

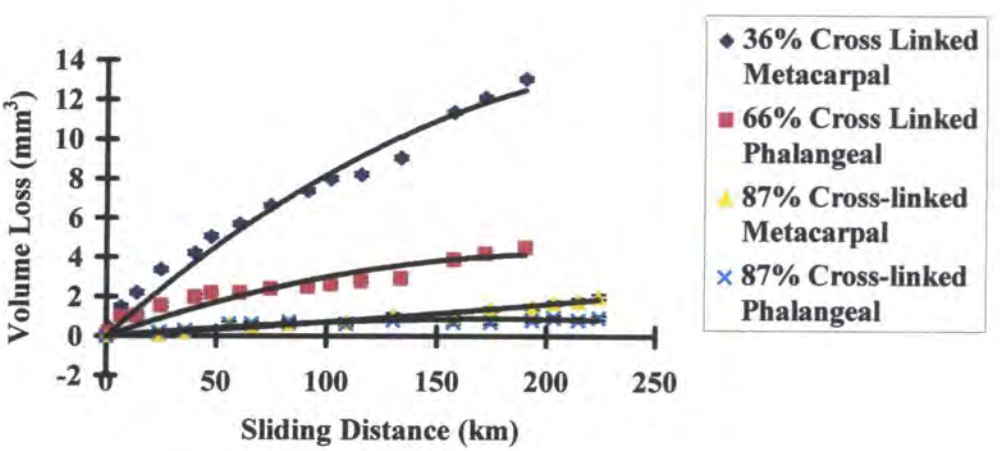

Figure 3.6 shows the results of tests 1 and 2 plotted on the same axes, and indicates an order of magnitude difference in wear factors between tests 1 and 2. In test 1, the metacarpal component had a gel content of 36%, while the

phalangeal component had a gel content of 66%. In test 2, both the metacarpal component and the phalangeal component had a gel content of 87%. Figure 3.6 clearly indicates the decrease in wear found with an increase in the percentage of cross-linking. Such a result is not unexpected, as it would be hoped that the cross-linking process would help to produce a stronger material, which was less likely to succumb to wear.

Figure 3.7 - Wear of High Percentage Cross-Linked Prostheses in Test 2

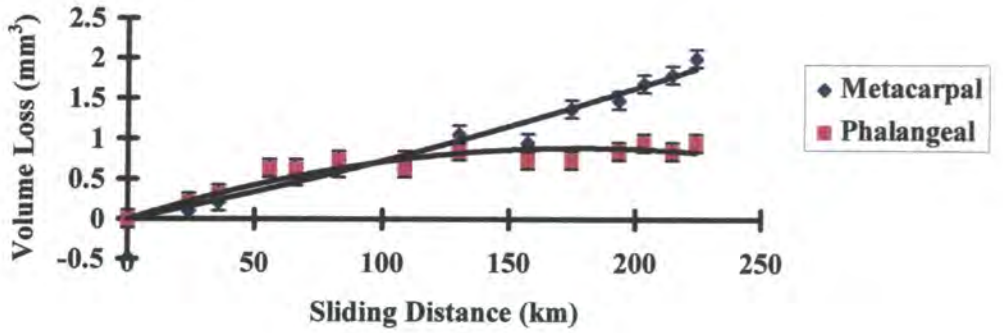

Figure 3.8 - Weight Change of Metacarpal Components in Test 2

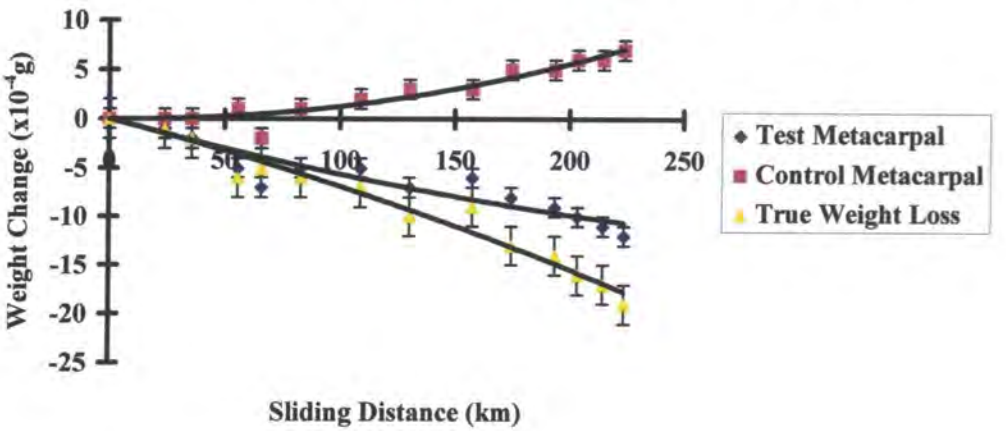

Figure 3.9 - Weight Change of Phalangeal Components in Test 2

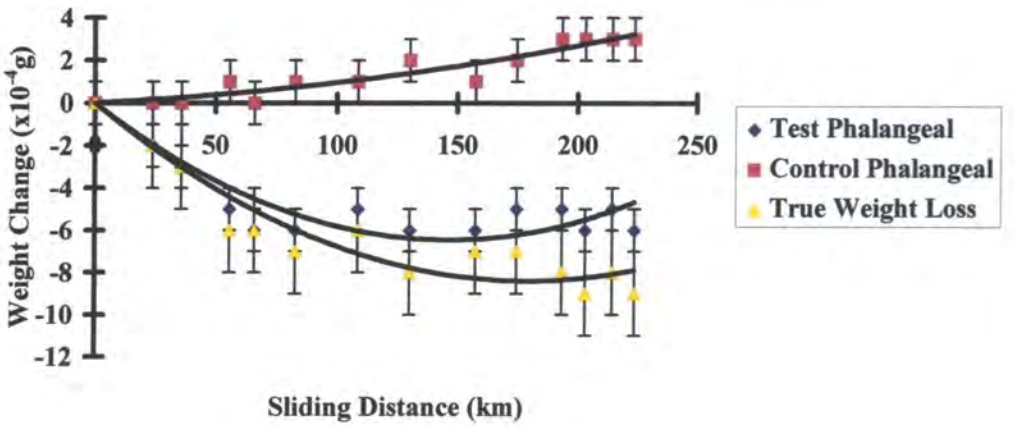

Figure 3.10 - Wear of High Percentage Cross-Linked Prostheses in Test 3

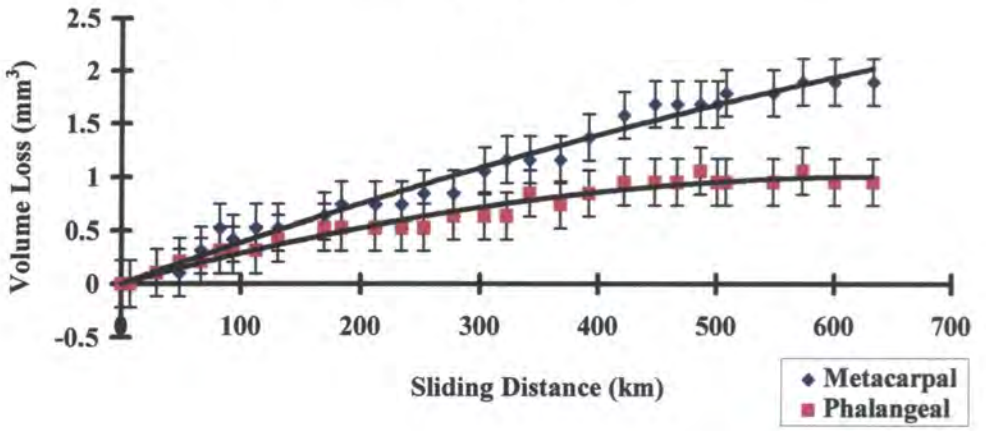

Figure 3.11 - Weight Loss of Metacarpal Prosthesis in Test 3

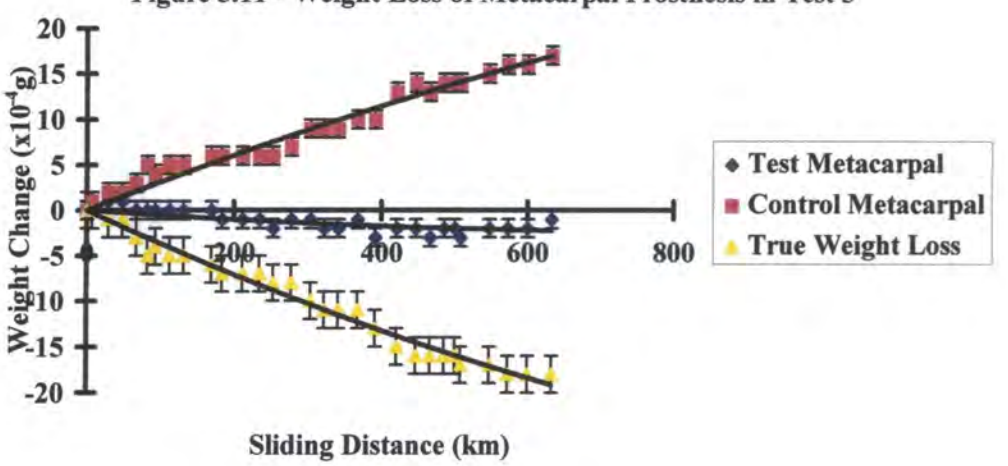

Figure 3.12 - Weight Change of Phalangeal Components in Test 3

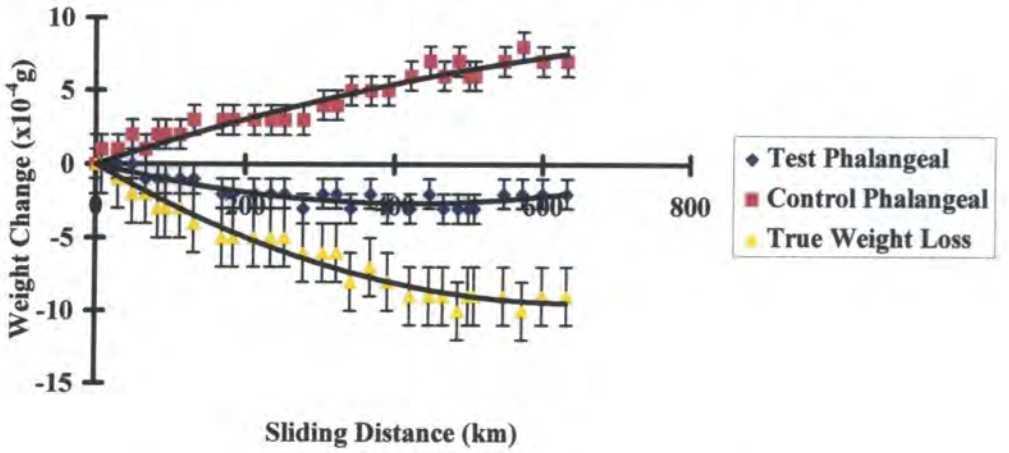

Figure 3.13 - Wear of High Percentage Cross-linked Prostheses in Test 4

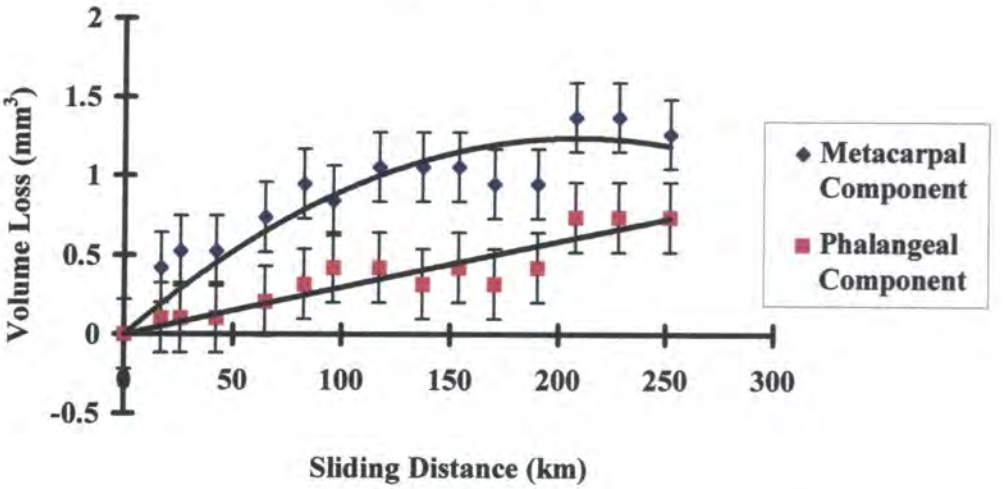

Figure 3.14 - Weight Change of Metacarpal Components in Test 4

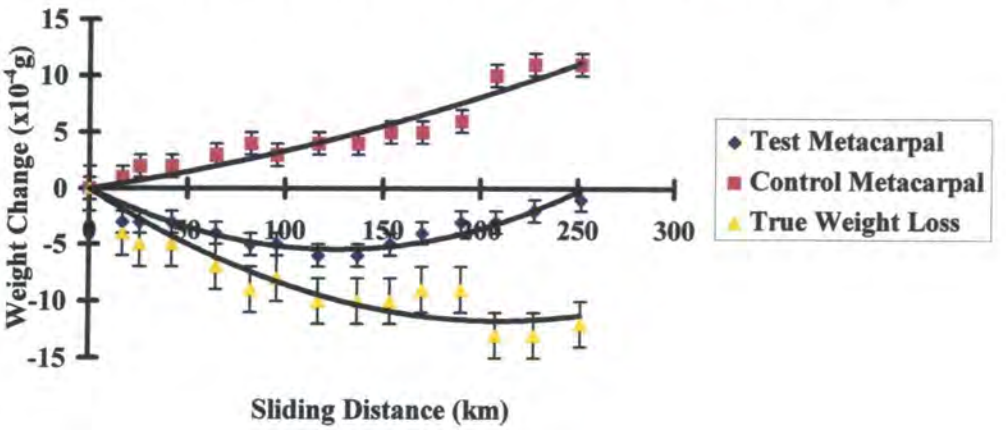

Figure 3.15 - Weight Change of Phalangeal Components in Test 4

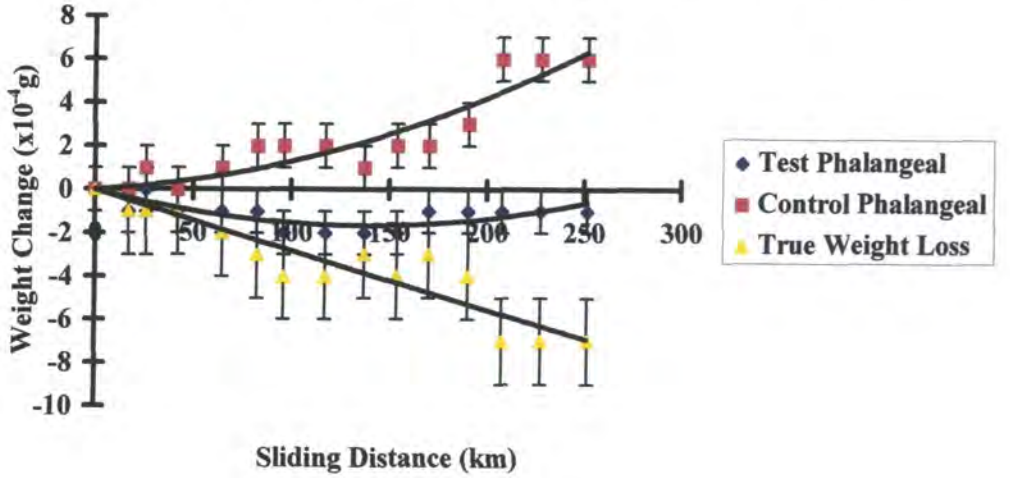

Figure 3.16 - Wear of High Percentage Cross-Linked Prostheses in Test 5

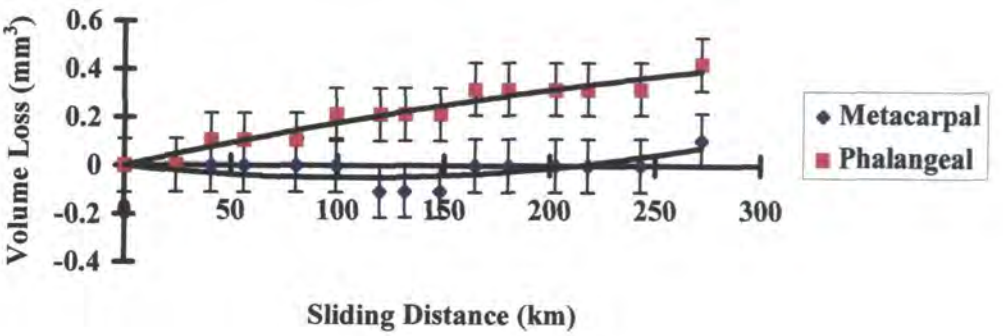

Figure 3.17 - Weight Change of Metacarpal Components in Test 5

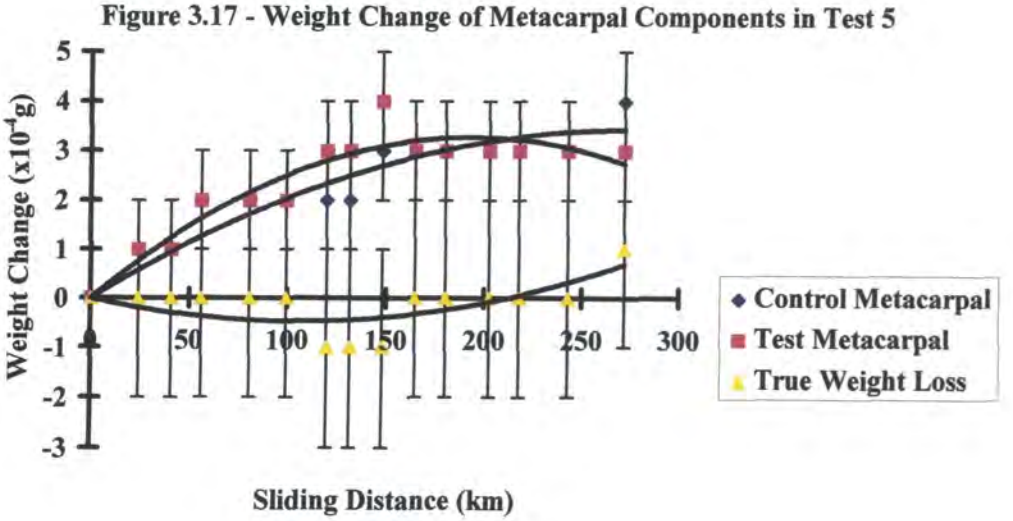

Figure 3.18 - Weight Change of Phalangeal Components in Test 5

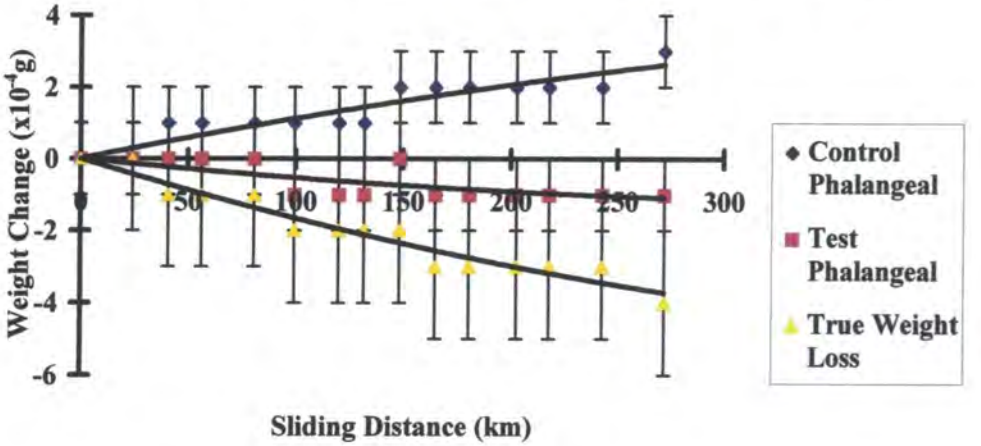

Figure 3.19 - Wear of High Percentage Cross-Linked Prostheses in Test 6

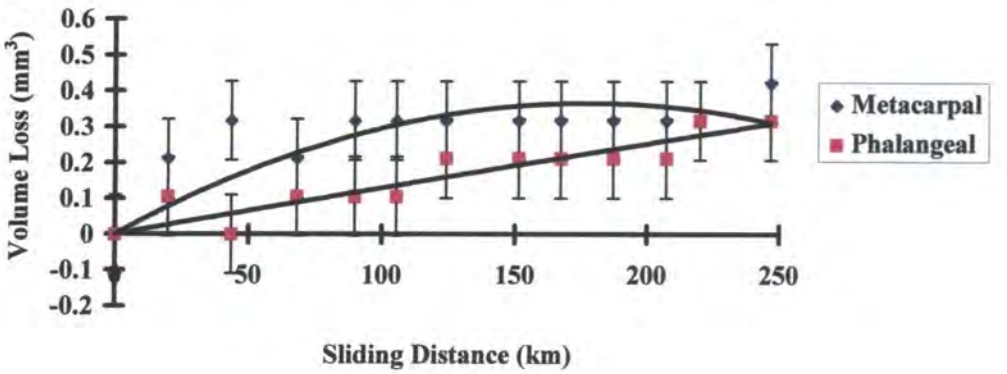

Figure 3.20 - Weight Change of Metacarpal Components in Test 6

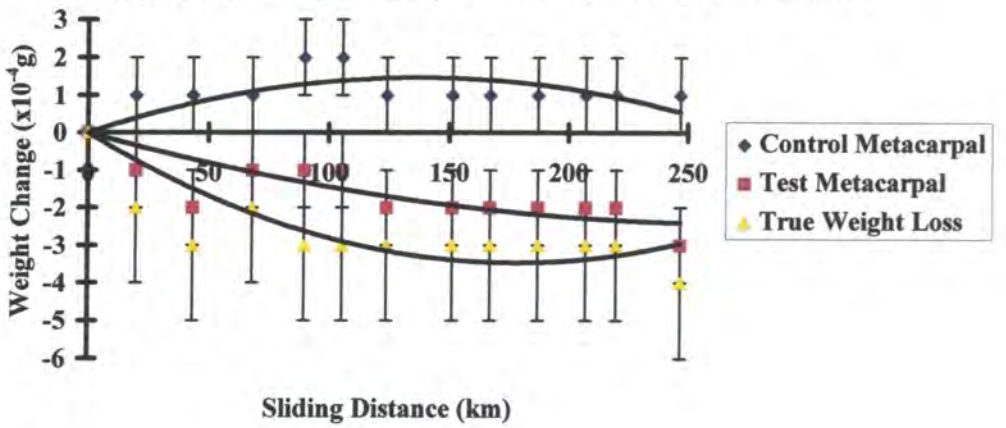

Figure 3.21 - Weight Change of Phalangeal Components in Test 6

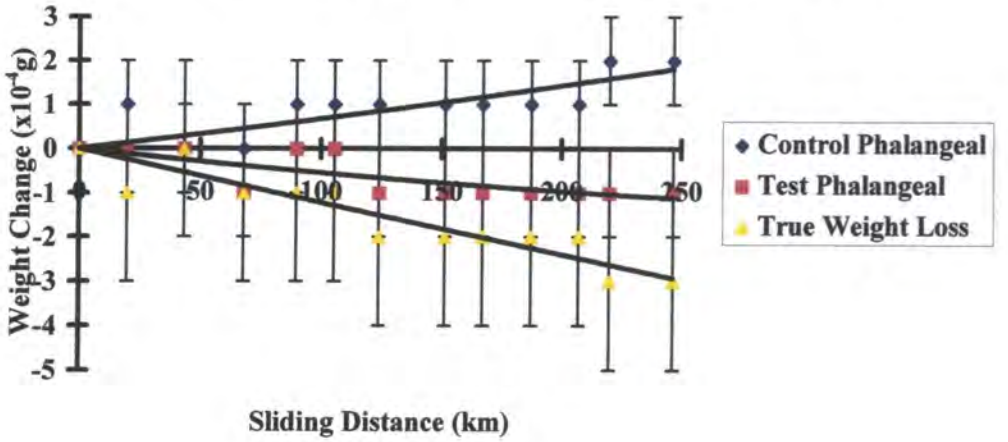

The test results of all the normal gel content prostheses were consistent (tests 2 to 6). Wear factors for the metacarpal components ranged from 0.03 x $10^{-6}$$mm^3$/Nm to 0.40 x $10^{-6}$$mm^3$/Nm, and from 0.10 x $10^{-6}$$mm^3$/Nm to 0.23 x $10^{-6}$$mm^3$/Nm for the phalangeal components of tests undertaken in distilled water (table 3.2). Tests 4 to 6 all involved production samples, and again consistent wear factors were measured. Test 5 was slightly unusual for the low wear of the metacarpal component that was measured. This result was due to an apparent weight gain by the test component together with a lower than average increase in weight by the control component.

If a normal MCP joint is considered to perform 1 million cycles per year, then the 633km (or 21.5 million cycles) achieved from the longest test (test 3) in the finger function simulator (Figures 3.10 to 3.12) is equivalent to 21.5 years. At this point, the XLPE test prostheses showed no cuts, no fractures and low wear. Further, the wear factors were calculated to be 0.24 x 10^{-6} mm^3/Nm for the metacarpal and 0.12 x 10^{-6} mm^3/Nm for the phalangeal component. These values correspond to wear volumes of 1.90mm^3 and 0.95mm^3 respectively. In turn, this total wear volume of 2.85mm^3 can be interpreted as a wear rate of 0.13mm^3 per million cycles, or per annum. Dowson (1994) states that, for an artificial hip joint, a wear rate of 38mm^3 per annum is considered acceptable. However, a hip joint of radius 20mm will have a capsule volume 23 times greater than that of a finger joint of radius 7mm. Therefore, for a finger joint, a wear rate of 1.65mm^3 per annum should be acceptable. Consequently, the 0.13mm^3 wear rate per million cycles determined from test 3 suggests that an all XLPE finger prosthesis will be acceptable from a wear point of view. Even if the results of test

2 are taken, which gave the highest wear rate of the high percentage cross-linked prostheses tested, of 0.39mm^3 per million cycles, then an all XLPE finger prosthesis remains feasible from a wear point of view.

Additionally, all of the XLPE prostheses tested had a wear curve which has a relatively constant gradient, or whose gradient decreased with time, indicating that a period of fatigue wear seems not to have occurred (Figures 3.6, 3.7, 3.10, 3.13, 3.16 and 3.19). This conclusion was supported by visual inspection which revealed neither pitting nor delamination. That the metacarpal components showed higher wear factors than those of their respective phalangeal components can explained by their geometrical differences, as it is known that convex surfaces tend to wear more than concave surfaces (Sibly and Unsworth, 1991).

Lubricant absorption was significant in comparison to apparent weight loss in those tests (tests 2 to 6) which employed high percentage cross-linked prostheses (Figures 3.7 to 3.21). Indeed, in tests 3 to 6 it accounted for the bulk of the 'wear' (i.e. the water uptake of the control component was greater than the apparent weight loss of the test component). Lubricant absorption was much less significant in the low gel contest test (test 1) where the weight loss of the test components was approximately an order of magnitude greater than the increase in weight of the control components due to water uptake.

A wide range of water uptake results can be seen in table 3.3, where the error of ±0.0001g was based on the accuracy of the Mettler balance. The control components in test 4 showed the greatest percentage weight increase per 100km and this fact accounts for test 4 giving the highest wear factors of all the distilled water tests. Apart from test 1, the phalangeal components showed greater percentage water uptake than the metacarpal components. To consider the 'worst case' influence of water absorption on wear factors, the maximum wear and maximum fluid uptake could be taken for those tests (3-6) in which water uptake accounted for the bulk of the 'wear'. The maximum wear due to weight loss occurred in test 6, and the maximum lubricant absorption per 100km took place in test 4. Neglecting the 2% difference in test duration between tests 4 and 6, and combining the weight change values will give a maximum weight loss for a metacarpal component of 0.0014g, and 0.0007g for a phalangeal component. These values correspond to a total volume loss of 1.48mm^3 and 0.74mm^3 respectively over the 9.3 million cycle test. In turn these volumetric values can be

used to calculate wear factors of 0.47 x $10^{-6}mm^3/Nm$ for the metacarpal component and 0.24 x $10^{-6}mm^3/Nm$ for the phalangeal component. Furthermore, if these wear factors are converted to volume loss per million cycles, as was discussed earlier for the results of test 3, then a total maximum wear of $0.24mm^3$ per million cycles can be calculated. This figure is still below the $1.65mm^3$ per million cycles specified as the maximum permissible wear. Therefore, even taking the 'worst case', the volume of wear should still be acceptable.

Tests 1 and 2 employed Ringers solution as a lubricant, while the remaining tests employed distilled water. However, the water absorption results indicated no difference in uptake between distilled water and Ringers solution. Similarly, there appeared to be no correlation between gel content and water uptake. Graphically, the water uptake results appear inconclusive. Some results (i.e. test 5, Figure 3.17) show a decline in the water uptake with time while others (i.e. test 4, Figure 3.15) show an increase with time. However, the longest test (to 633km, test 3) which therefore ought to be the most accurate, shows a linear relationship between test duration and water uptake (Figures 3.11 and 3.12).

Table 3.3 Summary of water absorption

Test Number	Dist. (km)	Component Initial Wt.	Weight Increase	% Weight Increase (WI)	% WI per 100km
1 m/c	190	0.7342g	+0.0011g	0.150 ± 0.014	0.079 ± 0.007
1 p		0.2299g	+0.0003g	0.130 ± 0.043	0.068 ± 0.023
2 m/c	224	0.7466g	+0.0007g	0.094 ± 0.013	0.042 ± 0.006
2 p		0.2295g	+0.0003g	0.131 ± 0.044	0.058 ± 0.019
3 m/c	633	0.7453g	+0.0017g	0.228 ± 0.013	0.036 ± 0.002
3 p		0.2327g	+0.0007g	0.301 ± 0.043	0.048 ± 0.007
4 m/c	252	0.4729g	+0.0011g	0.233 ± 0.021	0.092 ± 0.008
4 p		0.2341g	+0.0006g	0.256 ± 0.043	0.102 ± 0.017
5 m/c	272	0.4706g	+0.0004g	0.085 ± 0.021	0.031 ± 0.008
5 p		0.2335g	+0.0003g	0.128 ± 0.043	0.047 ± 0.016
6 m/c	247	0.4721g	+0.0001g	0.021 ± 0.021	0.009 ± 0.009
6 p		0.2313g	+0.0002g	0.086 ± 0.043	0.035 ± 0.018

p = phalangeal control component m/c = metacarpal control component

From table 3.3 it can be seen that the percentage weight increase per 100km varied from 0.009% ± 0.009% weight increase per 100km for the metacarpal component of test 6 to 0.102% ± 0.017% weight increase per 100km for the phalangeal component of test 4. The mean from all twelve control components can be calculated to be 0.054% weight increase per 100km. Using this value to give an average fluid uptake, the wear factors from each of the tests can be 'compensated' and re-calculated to be as shown in table 3.4

Table 3.4 Change in wear factors due to mean control component fluid uptake

	k Before Compensation ($\times 10^{-6}$ mm^3/Nm)		k After Compensation ($\times 10^{-6}$ mm^3/Nm)	
Test No.	Metacarpal	Phalangeal	Metacarpal	Phalangeal
1	6.0	2.1	5.9	2.1
2	0.72	0.34	0.80	0.34
3	0.24	0.12	0.36	0.13
4	0.40	0.23	0.23	0.13
5	0.03	0.12	0.12	0.12
6	0.13	0.10	0.29	0.13

As would be expected, the values given in table 3.4 indicate that when the test results are compensated for the average water uptake, the range of wear factors narrows. This is especially so for the four tests undertaken in distilled water with high percentage cross-linked prostheses (test 3 to 6).

When all of the wear factors were calculated, the sliding distance (D) was based upon the arc length $R\theta$ given in table 3.1. This same method was used by Stokoe (1990) and therefore permits a comparison of results (see section 3.6). However, for a spherical component in contact with another, the sliding distance varies across the face of the contact, and decreases with an increase in the distance away from the centre of contact (calculation A5.1). Therefore at the furthest point the sliding distance was determined to be 1.42 times less than at the centre, so the wear factor would be correspondingly higher. Based on the earlier 'worst case' of maximum wear plus maximum fluid uptake, then the calculated maximum wear will increase from 0.24mm^3/million cycles to 0.34mm^3/million cycles, still well below the 1.65mm^3/million cycles maximum allowed wear.

A comparison of the results of tests 2 and 3 indicate that the use of distilled water gave lower wear factors than Ringers solution. After each of the tests, the

prostheses showed no cuts and no fractures. Scratches in the direction of sliding could be seen on the rubbing surfaces of both components, indicating that abrasive wear was a dominant feature, although these scratches were not too prominent. Figure 3.22 shows the wear faces of the test components from test 1, in which the highest wear was measured. Scratches in the direction of sliding can only just be made out. In contrast Figure 3.23 shows the test components from test 6. On the wear faces of these components no surface defects can be seen.

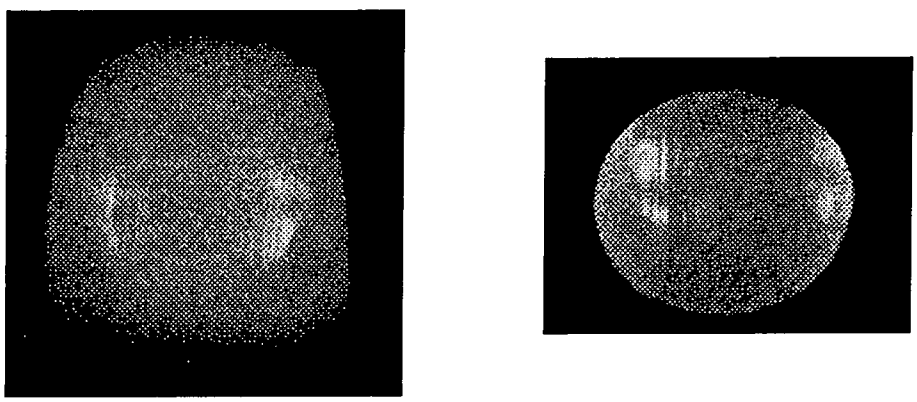

Figure 3.22 - Wear faces of test components from test 1

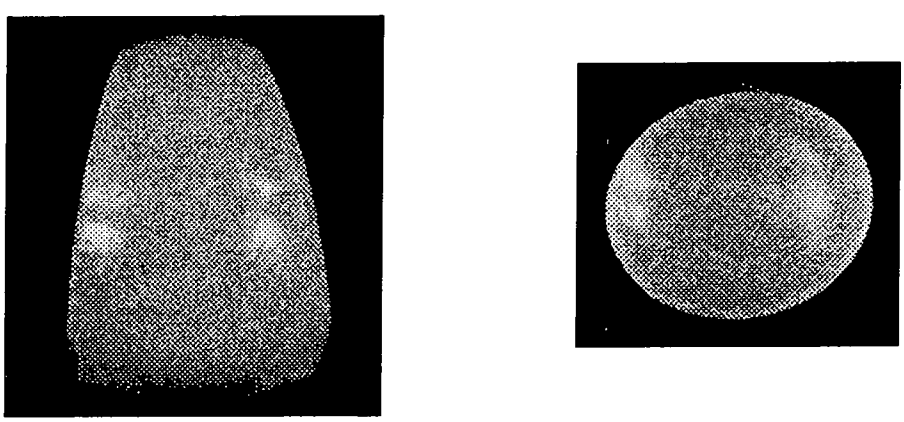

Figure 3.23 - Wear faces of test components from test 6

3.6 Comparison of Wear Results with Other Researchers

Cross-linked polyethylene MCP prostheses have only been tested at the University of Durham, and only one set of results had previously been published in a peer

reviewed journal (Sibly and Unsworth, 1991). The results of Stokoe are reproduced from her thesis (Stokoe, 1990).

Table 3.5 XLPE MCP prosthesis wear test results

Researcher	Dist. (km)	k metacarpal x $10^{-6}mm^3/Nm$	k phalangeal x $10^{-6}mm^3/Nm$
Stokoe 1	129	11.8	12.8
Stokoe 2	130	11.1	12.0
Stokoe 3	126	11.8	12.8
Stokoe 4	256	11.8	13.2
Stokoe 5	303	11.2	12.8
Sibly & Unsworth	267	2.4	1.3
Joyce 1	190	6.0	2.1
Joyce 2	224	0.72	0.34
Joyce 3	633	0.24	0.12
Joyce 4	252	0.40	0.23
Joyce 5	272	0.03	0.12
Joyce 6	247	0.13	0.10

All of the tests noted in table 3.5 shared the common features of employing the same test rig, a similar dynamic load of 12.5N, and a comparable cycle speed of approximately 110cpm. The differences were that Stokoe (1990) employed a static load of 181N, Sibly and Unsworth (1991) a static load of 150N and all of these researchers used Ringers solution as a lubricant. Stokoe (1990) employed test prostheses having and articulating radius of 8mm, but no such radius was stated by Sibly and Unsworth (1991).

The key reason for the differences in wear factors measured by the various researchers is shown by a comparison of the results of tests Joyce 1 and Joyce 2. Test 1 was undertaken with a low gel content prosthesis, while test 2 used a high gel content prosthesis. Gel content is obviously crucial to wear. Unfortunately, neither Stokoe (1990) nor Sibly and Unsworth (1991) stated the gel content of the prostheses they tested, nor whether their test components had been irradiated. This may have been because the state of development of the XLPE MCP prosthesis at the time was such that gel content was not considered to be important. Where low gel content prostheses were tested (test Joyce 1) the wear factors measured lie in the range between the results of Stokoe (1990) and those

of Sibly and Unsworth (1991). High gel content prostheses were used for the other five tests of Joyce. The order of magnitude difference in wear factors measured in these five tests compared with those found by the other researchers is remarkable.

A contrast in wear factors was noted between those tests employing Ringers solution (test Joyce 2), and those using distilled water as a lubricant (tests Joyce 3 to Joyce 6), all other researchers having used Ringers solution. This partially explains the differences in wear factors measured between the various researchers, but gel content is considered to be far more important.

Differences in the wear factors reported by the various researchers cannot be explained by the dissimilar static loads employed. Static load only accounts for some 2.2% of the time taken for one complete operation of the simulator. Next, the static loads used in the various tests (100N to 181N) correspond with contact stresses in the range 0.82MPa to 1.48MPa, values which are well below the strength of XLPE, which has a yield stress of 29.7MPa (Atkinson and Cicek, 1983). Finally, the wear factor is calculated from load during motion, not the static load.

Stokoe's (1990) values of wear factor are the highest of any reported, such that she was able to measure the wear depth on the phalangeal and metacarpal test components. She found the wear depth of the phalangeal component to be three to four times that of the metacarpal, yet she also found the wear factors to be almost identical. These two conclusions are contradictory. In contrast, it is interesting to note that the relationship between wear factor and wear depth shown by Sibly and Unsworth's (1991) result is as expected. Sibly and Unsworth (1991) measured the wear depth on the metacarpal component to be twice that of the phalangeal component.

3.7 Future Work

Consistent and low wear factors were found from all tests. Further, no cuts or fractures of the prosthetic components were seen. However there is a strong argument that in an application as critical as the human body itself, there can never be enough testing of a prosthetic device. Therefore, in the case of the

Durham prosthesis, testing could be undertaken using bovine serum as a lubricant. Before such testing could commence though, significant modifications to the Stokoe simulator would be required to permit heating of the bovine serum. Also, tests of the smallest size of Durham prosthesis currently available (R6.5mm) could be carried out, to ensure that it too will show no crucial surface damage.

CHAPTER FOUR

Material Wear Tests (pin on plate)

4.1 Summary

Fourteen wear tests were undertaken using pin on plate rigs. These machines are widely used as screening devices for biomaterials, and the results from them allow a comparison with those of other workers.

Five tests rubbing XLPE against XLPE, for a total sliding distance of 6,207km, were undertaken. Tests were carried out with 10N and 40N loads. All revealed pin wear factors of the order of 0.02 x $10^{-6}mm^3/Nm$ and plate wear factors of the order of 0.5 x $10^{-6}mm^3/Nm$. Except for later tests where the plate wear factors increased to 2.5 x $10^{-6}mm^3/Nm$, perhaps indicating an ageing effect to the XLPE material while it was in storage. All of these XLPE wear factors were lower than those found by earlier researchers.

Next, three tests rubbing UHMWPE against UHMWPE were undertaken for comparison with the earlier XLPE against XLPE tests. Due to the high UHMWPE pin and plate wear factors measured, approximately 80 x $10^{-6}mm^3/Nm$, these tests could only total a test pin sliding distance of 1580km. Further, the majority of the tests were undertaken at 10N load, as under 40N load the test lasted only 20km before what remained of the test pins sheared.

Based on the difference in wear rates measured, both XLPE and UHMWPE were tested against hard counterfaces. Therefore test plates manufactured from 316 stainless steel and zirconia were obtained and tests undertaken. Finally, stainless steel pins were manufactured and tested against plates made from each type of polyethylene. In all of these hard counterface tests, XLPE failed to show a superiority to UHMWPE in resisting wear.

4.2 Description of Pin on Plate Test Rigs

The pin on plate rigs employed a reciprocating motion which is consistent with the natural flexion-extension of the finger. Load, speed and stroke could all be varied as appropriate. Pin on plate machines are widely used as screening devices in wear studies and therefore permit comparison of results with other researchers (Dowson 1994).

The test rigs (Figures 4.1 and 4.2) consisted of an aluminium sledge reciprocating along two fixed parallel bars. On this sledge was positioned a heated bed and a stainless steel bath. The sledge was driven by a 125W DC shunt motor, with integral gearbox, to give a maximum speed of 100rpm. Motor speed was controlled by using a variable voltage supply and the stroke was altered by adjusting the crank radius of the drive shaft. Heating of the distilled water, which acted as a lubricant, was provided by 12V resistors positioned within the heated bed. These resistors, together with a thermocouple, were connected to a controller which maintained the lubricant at a constant, pre-set temperature.

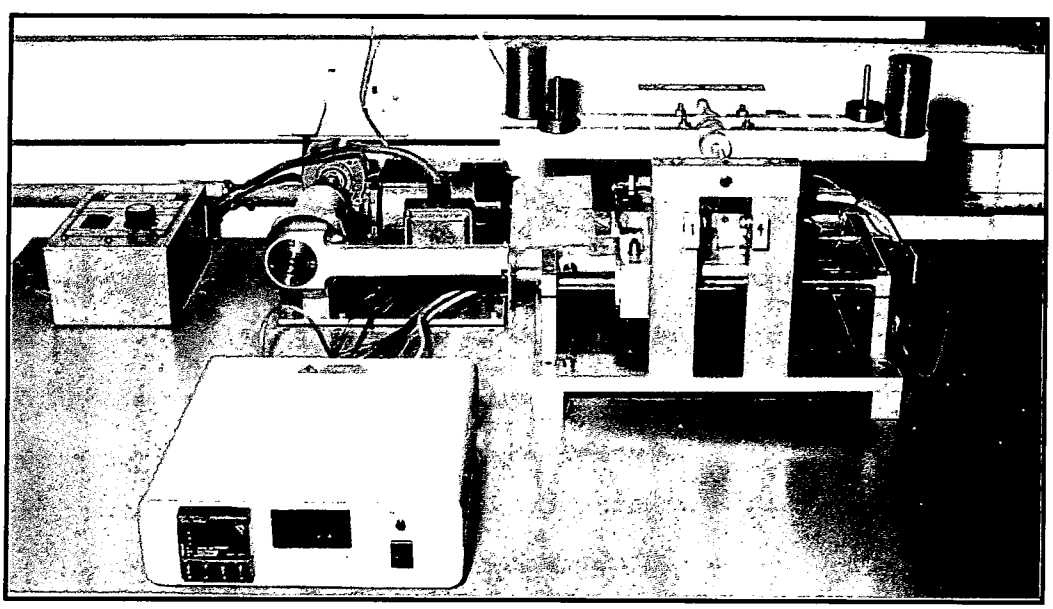

Figure 4.1 Pin on Plate Test Rig

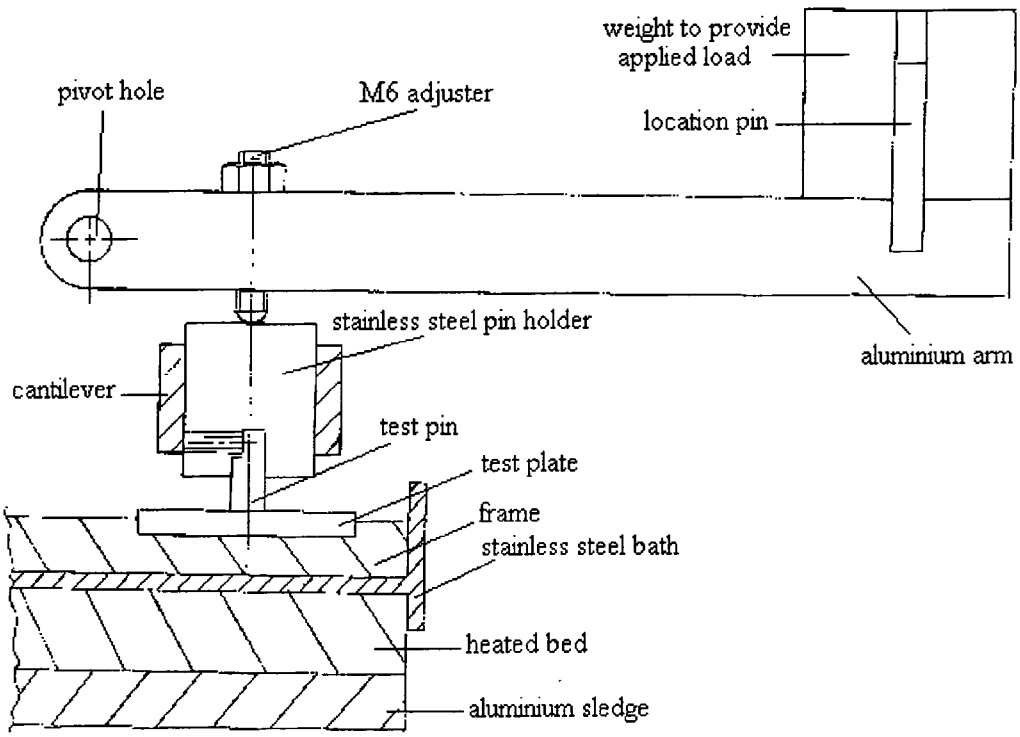

Figure 4.2 - Components within pin on plate test rig

Four test plates were located in the stainless steel bath using a frame into which suitable location slots had been milled. The design of this frame ensured that test plates were replaced in the exact position from which they were removed, without the need to remove the cantilevers which held the test pin holders. This scheme therefore permitted the rapid weighing of the test plates. Each test pin was held within an stainless steel holder and each holder fitted within a reamed hole in the end of a cantilever. Each pin was notched at the upper end to provide a good location in the pin holder, and also to prevent rotation. It also ensured that the pin was replaced in its original position after removal for weighing. On the top of each holder rested a pivoted aluminium arm to which weights were added to provide an applied load. An automatic lubricant level sensing gauge was fitted such that the lubricant within the bath was maintained between pre-set maximum and minimum levels and therefore to prevent the rig from operating without lubricant. A perspex cover minimised contamination from atmosphere.

4.3 Calibration and Operating Procedure.

4.3.1 Calibration of Pin on Plate Test Rig

This work was done by H. Ash, using a piezo-electric transducer positioned beneath a test pin, such that a set weight at a set distance gave the necessary 10N or 40N load desired. For a 10N load, a weight of 75g at a distance of 132mm was needed, and for a 40N load, a weight of 575g at a distance of 165mm was required.

4.3.2 Operating Procedure (polyethylene against polyethylene tests)

Prior to the commencement of a test, the polyethylene test plates and pins were carefully weighed, the appearance of each wearing surface noted and the roughness of the plates measured using a Taylor Hobson Talysurf 4. For each plate, the mean of eight roughness measurements was taken. The test plates were fitted into the insert, which was in turn fitted into the stainless steel bath. Distilled water filled the bath and was allowed to reach a steady state temperature of 37°C, with the thermocouple mounted close to a test plate. A control pin was included to take account of any lubricant absorption. This pin was unloaded and kept with its un-notched end in the same distilled water as the test pins at 37°C. Each test pin was carefully positioned in its holder and then fitted to the rig. The aluminium arms were lowered and weights added to give the desired load. Testing then commenced.

At regular intervals, the test was stopped, pins and plates were removed, cleaned in acetone, weighted to the nearest 0.1mg using a Mettler AE200 balance, and visually inspected. As considered appropriate, the roughness of the wear track on each of the plates was measured. Afterwards, pins and plates were replaced in their original positions, the loads were re-applied, the distilled water was allowed to reach its pre-set temperature and then testing recommenced.

Wear of a test pin was defined as the weight loss with respect to the initial weight, to which was added any weight gain of the control pin. Therefore the weight gain of the control and test pins was assumed to be equal. Test pins and control pins

were within 5% of the weight of each other. Except in those tests (tests 3, 4 and 5) where test pin diameter was reduced to 4mm. In such cases the control pins, which were 5mm diameter, were approximately 50% heavier, and therefore all the more likely to show water uptake when compared with the 4mm diameter test pins. However, as even these relatively heavier control pins in tests 3, 4 and 5 showed no water uptake outside of the error of the Mettler balance, then the potential error due to any discrepancy between control and test pin was negated. The wear factors (k, units mm^3/Nm) were calculated from equation 1.1.

4.3.3 General Test Parameters (polyethylene against polyethylene tests)

Distilled water was used as a medium to warm the pins and plates to 37°C. Loads of 10N and 40N were employed. The 10N load was regarded as a 'normal' load for the MCP joint during motion (Tamai et al, 1988), while the 40N load gave a factor of safety and provided the opportunity of discovering if wear factors increased with load. Further, these two values of load had been employed by earlier researchers at Durham who had investigated the wear of polyethylene sliding against itself (Stokoe 1990, Walker 1990, Sibly and Unsworth 1991, and Short 1993) and all of these researchers had used the original pin on plate rig. Similarly, these researchers had employed cylindrical pins of diameter 5mm, together with a stroke of approximately 20mm. Therefore these parameters were also reproduced in the polyethylene rubbing against polyethylene tests reported in this thesis. A test speed of 1Hz was chosen, where the rig was capable of it. The density of XLPE was taken to be $949kg/m^3$ (Sibly and Unsworth, 1991) and that of UHMWPE to be $953kg/m^3$ (Stokoe, 1990).

4.4 Development of Polyethylene Against Polyethylene Tests

Test 1 was undertaken to compare results of the XLPE sliding against itself with those of earlier workers at Durham (Short 1993, Sibly and Unsworth 1991, and Walker 1990) using similar test conditions. The lack of XLPE pin wear compared with plate wear encountered in test 1 led to test 2 investigating the effect of initial surface finish/work hardening on wear. At the same time, this test still served as a basis for comparison with the earlier work carried out at Durham. Test 2 considered whether the higher surface roughness of the pins due to their

manufacturing process could permit the pins to 'wear' the plates, which had a smoother, un-machined wear surface. Therefore, in test 2, two plates were milled to give a higher value of surface roughness (mean 2.25μm Ra), and two test pins were sliced using a microtome to give a lower value of surface roughness (mean 0.55μm Ra) compared with an average machined pin roughness of 1.70μm Ra. The other aspect considered in test 2 was the possible effect of the machining process on work hardening the pins and plates. Therefore, slicing the pins should have removed this 'work hardened' area and milling the plates should have produced a 'work hardened' surface. Test 2 was undertaken on the original pin on plate machine, before upgrading.

Tests 3, 4 and 5 investigated whether the moulding orientation of the supplied mouldings (see Figure 4.3) could explain the reason for negligible pin wear. The test pins used in these tests were taken from the 'flat' part of the moulding, rather than from the sprue. It was speculated that the pins manufactured from sprue, as in tests 1 and 2, as well as those from the 'flat' in test 3, would have a molecular structure which would be advantageous to resist wear. Implicit in this theory was that flow orientation due to the injection moulding process was crucial, and could have a vital effect on the performance of an injection moulded XLPE finger prosthesis. Tests 4 and 5 had pins again made from the 'flat' part of the moulding, but taken at 90° to those of test 3. A side effect of this investigation was that the pins of tests 3, 4 and 5 had their diameters reduced from 5mm to 4mm. Therefore a second aspect of these tests was to see if the higher contact stresses, due to the reduction in test pin diameter, would produce a greater amount of wear. According to the wear equation (equation 1.1) it should not. All of the XLPE tests employed distilled water as a lubricant and used XLPE from the same batch, with a gel content after irradiation of 86%.

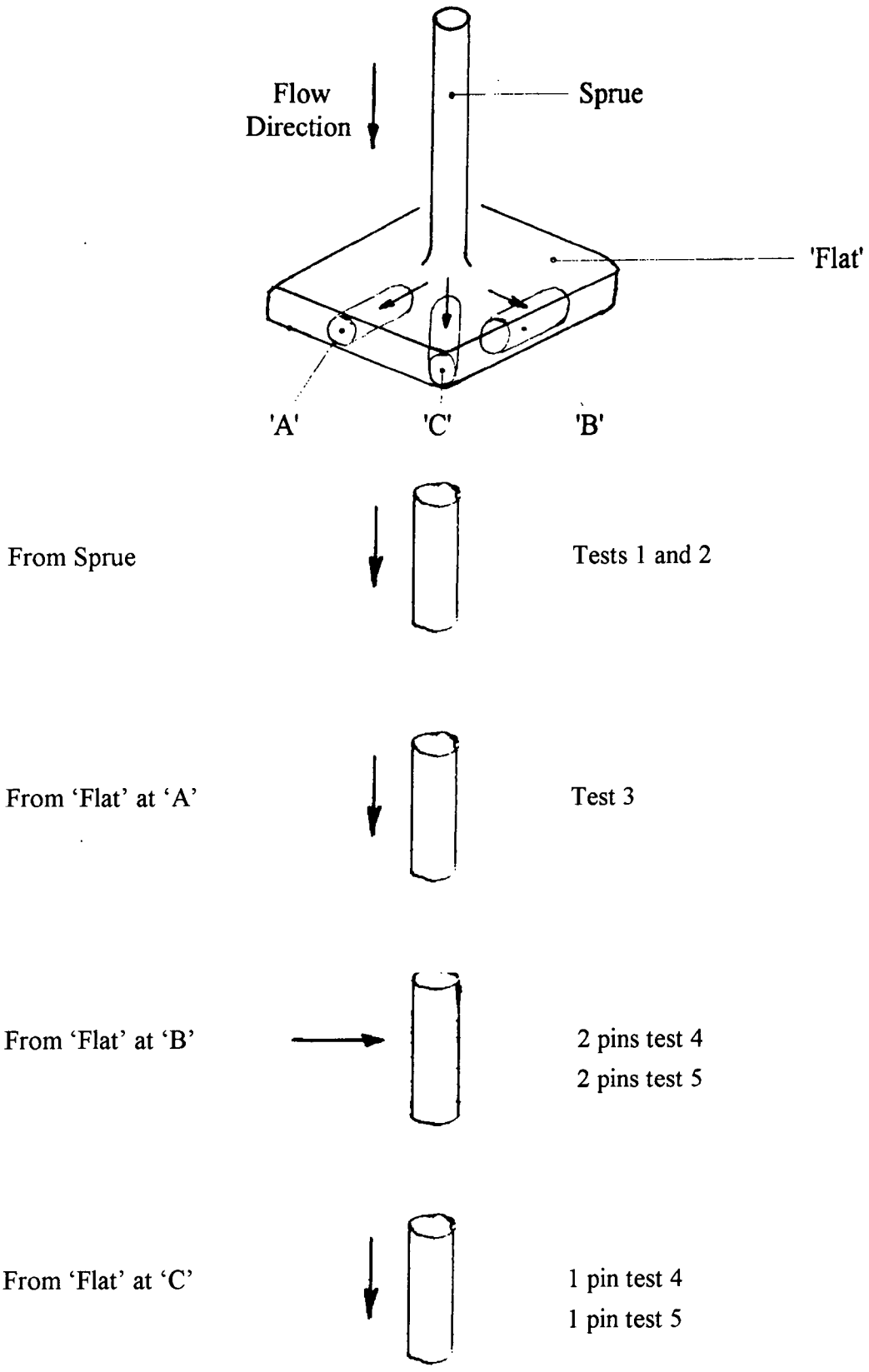

Figure 4.3 - Moulding Orientation of XLPE Pins

Tests 6, 7 and 8 all involved UHMWPE rubbing against itself under the same test conditions as the XLPE rubbing against XLPE tests. Test 6 used non-irradiated UHMWPE which was originally supplied by De Puy International Limited but was several months old. Test 7 used brand new, irradiated UHMWPE supplied by De Puy International Limited. Test 8 employed UHMWPE from the same batch as test 7, but the material was not irradiated. The aim of tests 6 and 7 was to compare irradiated and non-irradiated UHMWPE. The aim of tests 6 and 8 was to compare batch differences between non-irradiated UHMWPE.

4.5 XLPE Against XLPE Pin on Plate Tests

Table 4.1 Summary of XLPE Against XLPE Test Conditions and Wear Factors

Test No	1		2	3		4	5
Load (N)	10	40	40	10	40	40	40
No. of pins	2	2	2	2	2	3	3
mean k pin $x10^{-6}mm^3/Nm$	0.030 ±0.060	0.012 ±0.015	0.065 ±0.011	0 ±0.035	0.013 ±0.009	0.016 ±0.050	0.012 ±0.077
mean k plate $x10^{-6}mm^3/Nm$	0.50	0.42	0.52	0.49	0.33	1.14	2.45
Dist (km)	349	349	465	608	608	105	68
pin dia (mm)	5	5	5	4	4	4	4
No cyc. (,000)	8,725	8,725	6,835	15,197	15,197	2,751	1,800
Stroke (mm)	20	20	34	20	20	19	19
Speed (rpm)	53	53	41.7	56	56	61	59.3
Av. Vel (mm/s)	35.3	35.3	47.6	37.3	37.3	40.6	39.3

4.5.1 Discussion of XLPE Against XLPE Wear Results

Figures 4.4, 4.5, 4.6 and 4.7 show pin and plate wear for tests 1, 2, 3, and 4 and 5 respectively. The actual weight losses are tabulated in appendix 3. All results revealed similar characteristics of negligible pin wear of approximately 0.02 x $10^{-6}mm^3/Nm$ and plate wear of approximately 0.5 x $10^{-6}mm^3/Nm$ (for tests 1, 2 and 3).

Figure 4.4 - Mean Wear of XLPE Pins and Plates Under 10N and 40N Loads. Test 1.

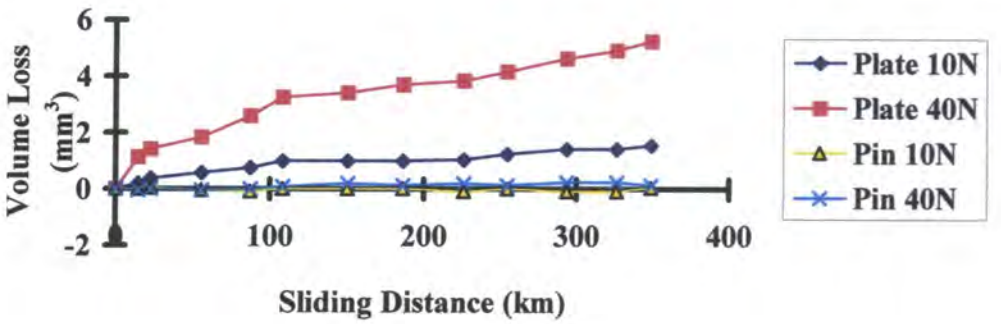

Figure 4.5 - Mean Wear of XLPE Pins and Plates Under 40N Loads. Test 2.

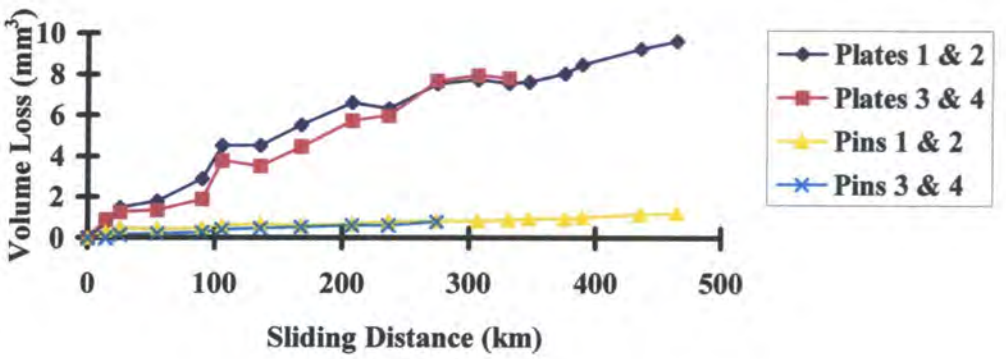

Figure 4.6 - Mean Wear of XLPE Pins and Plates Under 10N and 40N Loads. Test 3.

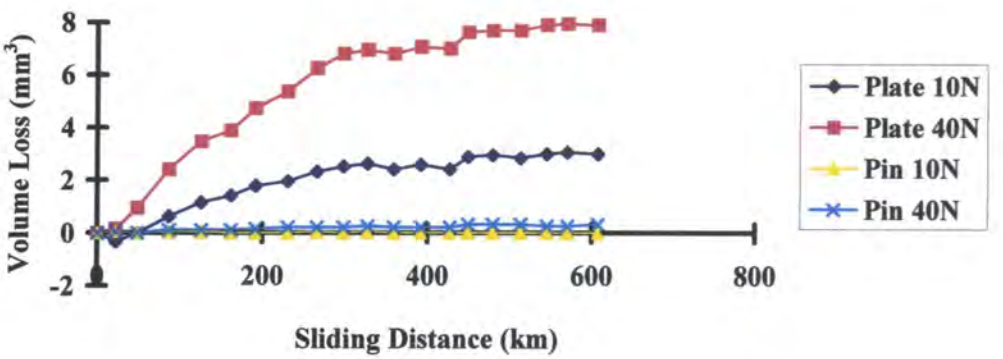

Figure 4.7 - Mean Wear of XLPE Pins and Plates Under 40N Loads. Tests 4 and 5.

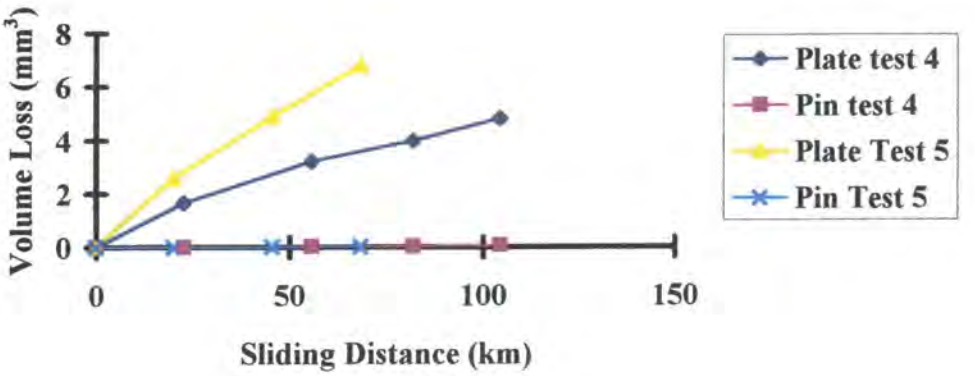

Figure 4.8 shows that XLPE plate wear factors have increased with each test, indicating an ageing affect on the wear of XLPE. Test results have been reported in chronological order, test 1 being the first test. XLPE mouldings were kept in sealed clear plastic bags exposed to sunlight, therefore it is speculated that the ageing was caused by sunlight. Further work may be of benefit here, for example if XLPE material were to be stored in darkness for a long duration, and then wear tested to investigate the apparent ageing affect due to sunlight.

Figure 4.8 - Mean Wear of XLPE Plates Loaded at 40N. Chronological Order of Tests Undertaken on the Same Rig.

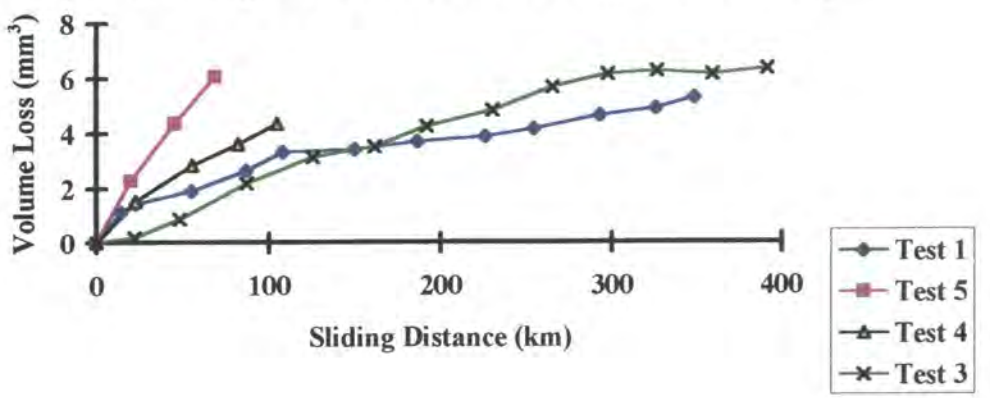

However, this same 'ageing' phenomenon was not seen with the XLPE pin wear factors. XLPE pin wear was negligible, one test pin in test 1 even gained in weight by 0.1×10^{-3}g. However, the accuracy of the Mettler AE200 balance was also $\pm 0.1 \times 10^{-3}$g, and the weight of the control pin in this test fluctuated by the same amount. Further, the original concentric machining marks were still visible

on the wear face of the XLPE test pins at the end of each of the tests (Figure 4.9). This fact proved that the pins were not wearing and also indicated that material transfer from plate to pin was not occurring. The XLPE pin wear factors found approach those of UHMWPE rubbing against ceramic (Saikko, 1993).

Lack of pin wear in all of the XLPE tests cannot be explained by the particular injection moulding orientation of the mouldings that were used for the test pins (Figure 4.3). No difference between pins made from 'flat' (tests 3, 4 and 5) and those made from sprue (tests 1 and 2) was noted. Similarly, the XLPE material used in each test was identical, having come from the same moulding. Instead, as the pins were constantly loaded whereas the individual parts of the wear track on the plates underwent a cyclic load, there may have been a fatigue mechanism producing the higher XLPE plate wear in contrast to the lower XLPE pin wear. This fatigue does not however refer to the severe wear known as delamination which is sometimes seen in retrieved tibial component of knee prostheses.

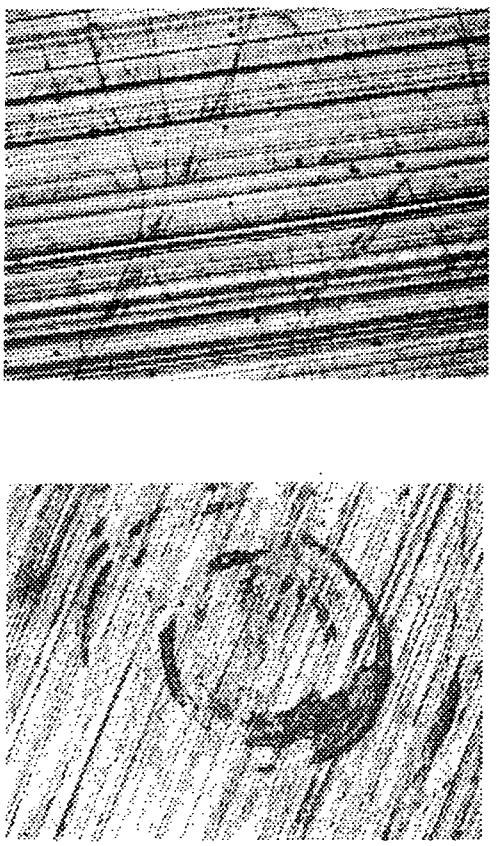

Figure 4.9 - XLPE Plate and Pin Visual Appearance

Test 2 was the only test to show any noticeable XLPE pin wear, if a mean wear factor of 0.065 x $10^{-6}mm^3/Nm$ can be described as noticeable. However, of the five XLPE tests, only this test showed any uptake of distilled water by the XLPE control pin outside of balance error. This weight increase may have been due to oil contamination of the control pin, as testing of two of the test pins later ceased at 332km due to such contamination. This contamination aspect will be discussed in appendix 7. However, if zero fluid uptake of the control pin (as occurred in all of the other XLPE against XLPE tests) is assumed then the mean wear factor can be re-calculated to be 0.030 x $10^{-6}mm^3/Nm$.

Pin weight was of the order of 0.36g for the 5mm diameter test and control pins. Due to this relatively low weight, and the lack of test pin wear, then errors were significant for the pins, as can be seen in table 4.1. The XLPE plate wear volumes were seen to be related to load. More wear debris was produced under 40N load than under 10N load, as would be expected. There was an initial bedding in period after which the slope of the wear curve became relatively constant with increased sliding distance. In all tests, the initial plate weight was of the order of 5g.

The results of test 2, which investigated the relationship between wear and initial surface finish, indicate that initial surface roughness had no effect on the wear mechanisms occurring when XLPE rubbed against itself. Further, that any work hardening of the XLPE test pins imparted due to their manufacture did not cause the high plate wear/low pin wear phenomenon seen in each of the five tests.

Cross contamination (third body wear by, in this instance, XLPE wear particles) was shown by test 2 not to be a problem, because when the testing of two of the four pins ceased, there was no decline in the amount of plate wear of the remaining two plates.

Comparison of the results of test 3 with test 1 indicates that nominal contact stress alone, based on pin diameter, seems to have little effect on wear, so confirming the use of the wear equation (equation 1.1). Stress values are indicated in table 4.2. For comparison, Tamai et al (1988) indicate MCP contact stress values of 0.35MPa and 0.53MPa at finger flexion positions of 0° and 45°. Interestingly, the 0.35MPa value quoted by Tamai et al (1988) corresponds to a value of 0.08MPa in the Durham prosthesis design, so indicating the degree to which totally conforming surfaces can reduce contact stresses.

Table 4.2 Relationship between pin diameter and nominal contact stress

Pin Dia	Area (mm^2)	Load (N)	Stress (MPa)
5mm	19.6	10	0.51
	19.6	40	2.04
4mm	12.6	10	0.80
	12.6	40	3.18

4.5.2 Comparison of XLPE Against XLPE Wear Results with Those of Other Workers

Table 4.3 XLPE against XLPE wear factors of other workers

Researcher	Walker (1990)		Sibly and Unsworth(1991)		Short (1993)	
Lubricant	Distilled Water		Distilled Water		Distilled Water	
Ave Vel (mm/s)	22.5		20		20	
Stroke (mm)	22.5		19.2		19	
Pin Diameter (mm)	4.7		4.7		4	
Distance (km)	27	30	100	100	46	53
k (10N load) ($x10^{-6}mm^3/Nm$)	2.1	0.9	1.3	0.9	1.7	2.4
k (40N load) ($x10^{-6}mm^3/Nm$)	0.8	5.5	2.8	2.3	0.8	2.5

In the tests summarised in table 4.3; lubricant, stroke, pin diameter and load were all similar parameters to those reported in this thesis. All earlier researchers measured XLPE pin wear, while XLPE plate wear was neglected. However, Sibly and Unsworth 1991 clearly show a wear track of a depth worth noting in their paper. That all earlier researchers obtained pin wear factors much greater than reported here, two orders of magnitude, could be explained by the fact that their material may have been of low gel content, that it was aged in sunlight, or some other as yet unknown factor. However, a similar difference in wear factors was seen with the comparison of the finger function simulator results obtained by Joyce and those obtained by Stokoe (1990). Further, the combined test distance of 256km reported by the earlier researchers is small in comparison with the 1,600km reported in this thesis.

4.5.3 XLPE Mean Plate Roughness Values

The measured Ra values of the wear track are tabulated in appendix 4. In general, all five tests revealed a similar phenomenon. In the longitudinal direction, or along the wear track, mean plate roughness values fell rapidly from the 'as-moulded' value of approximately 1μm Ra to a very low mean figure of approximately 0.05μm Ra. Transverse values, those across the wear track, showed a greater variation, falling to approximately 0.5μm Ra. The mean roughness values of the wear tracks of the plates of tests 1, 2, 3, and 4 and 5 are shown in Figures 4.10, 4.11, 4.12 and 4.13 respectively.

Figure 4.10 - Mean XLPE Plate Roughness Values in the Longitudinal (L) and Transverse (T) Directions Under 10N and 40N Loads. Test 1.

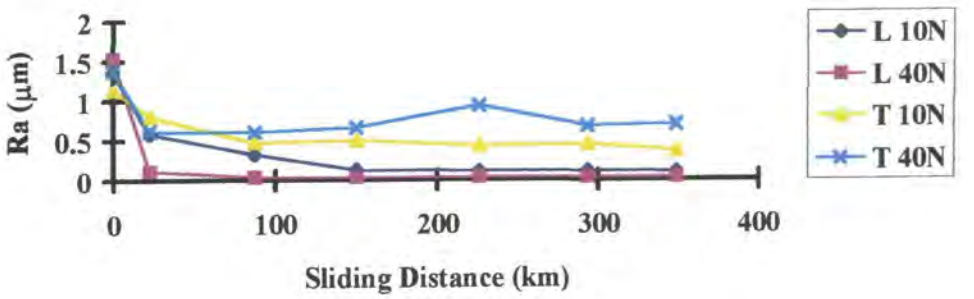

Figure 4.11 - Mean XLPE Plate Roughness Values in the Longitudinal (L) and Transverse (T) Directions Under 40N Loads. Test 2.

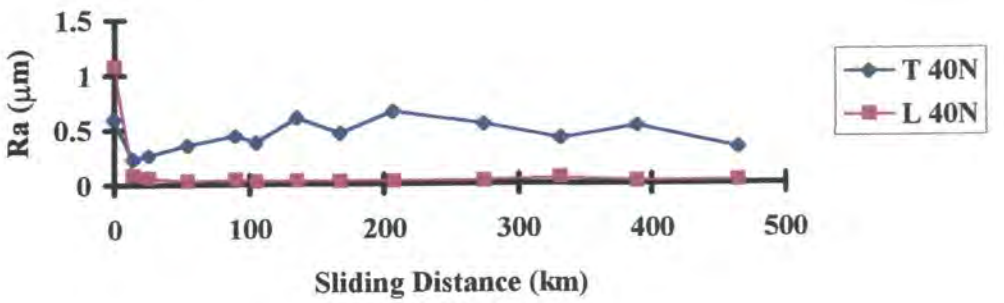

Figure 4.12 - Mean XLPE Plate Roughness Values in the Longitudinal (L) and Transverse (T) Directions Under 10N and 40N Loads. Test 3.

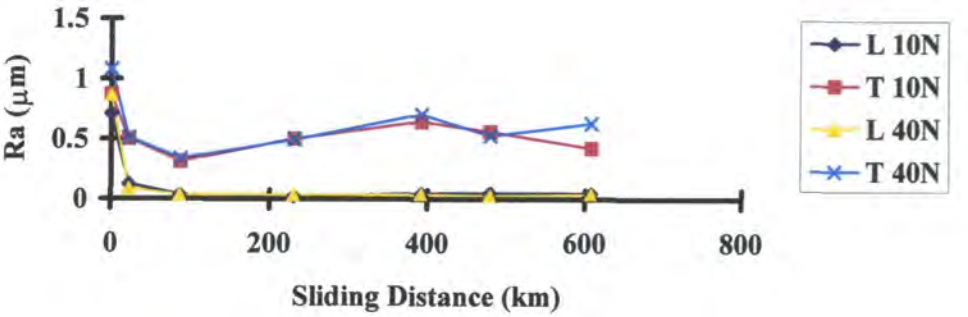

Figure 4.13 - Mean XLPE Plate Roughness Values in the Longitudinal (L) and Transverse (T) Directions Under 40N Loads. Tests 4 and 5.

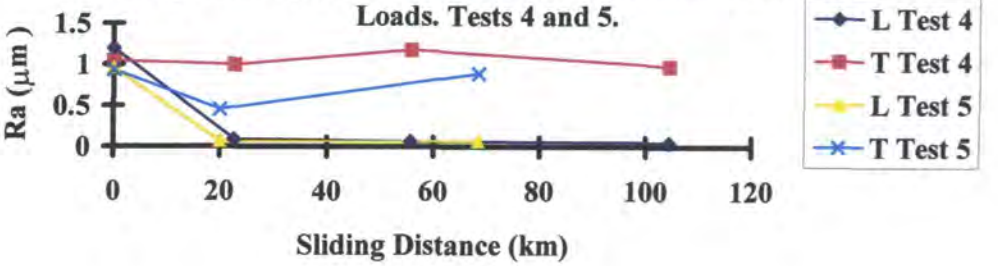

Concerning test 1, plate 1 ended with the highest mean longitudinal value of 0.16µm Ra, and its wear was the greatest of the four plates. Transverse roughness values also fell in test 1, from an initial mean of 1.26µm Ra for the four plates to a mean of 0.53µm Ra. Transverse values fell rapidly but tended to stabilise, especially in the case of the 10N load.

The aim of test 2 was to make the plates rougher than the pins, which was the opposite to the initial situation of test 1. Then, if high roughness was causing the wear of the smoother XLPE component, test 2 should see test plates wearing test pins. However, test 2 revealed no correlation between initial plate roughness and wear. Although the smooth plates had the greatest wear volumes, this higher wear only became evident at 90km. If the plate roughness was a crucial factor, then it should have been seen immediately.

With both XLPE test pins and XLPE test plates, the dominant feature of the wearing surfaces was parallel grooves in the direction of sliding (Figure 4.9) giving the appearance of abrasive wear. Once this surface finish was achieved, there was very little change. The relatively constant values of roughness which

were measured imply no evidence of a transfer film. It has been suggested that serum would be a more appropriate medium in which to run pin on plate tests involving potential biomaterials (Cooper et al, 1993, a). The reason being that, unlike distilled water, serum prevents the formation of a transfer film between UHMWPE and stainless steel and a transfer film is not found in vivo. Cooper et al (1993, a) indicated the presence of a transfer film by increased plate roughness at the cessation of a test. However, the XLPE plate roughness results reported here show no increase in the surface roughness of the plates and therefore indicate no evidence of a transfer film. Further, tests employing distilled water permit a fuller comparison with other researchers (Saikko, 1993; Dowson, 1994). Visual inspection of XLPE pins and plates revealed little evidence of adhesive or fatigue wear. In the case of the XLPE pin shown in Figure 4.9, the original concentric machining marks are still visible, indicating that the pins had experienced little wear, even after 349km. There appears to be little correlation between plate roughness and wear, except perhaps in the initial stages, when some 'bedding in' would be expected.

Pin roughness values could only be measured on the Alphastep, rather than the Talysurf, therefore parameters such as cut off (which is specified by BS 7252) could not be set. However, judging by their visual appearance, and knowledge of wear processes in general, pin roughness should match that of the plate. This assumption is supported by Figure 4.9, which shows scratches in the direction of sliding as the dominant feature on both test pin and test plate. Roughness values were not measured by Walker (1990) Sibly and Unsworth (1991) or Short (1993) although all stated that abrasive wear was the dominant wear mechanism.

Figure 4.14 shows the edge of a wear track from an XLPE test plate. The 'as moulded' surface is below and the wear track is shown above.

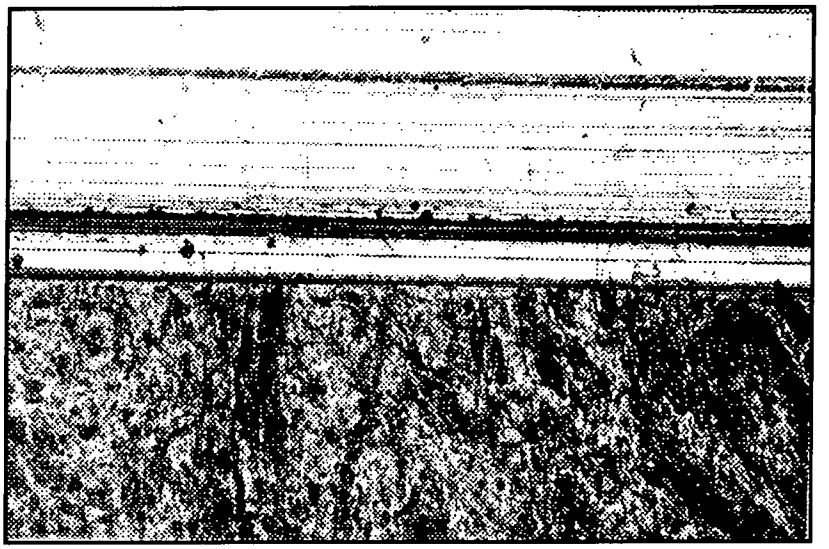

Figure 4.14 - Edge of wear track on XLPE test plate

4.5.4 Conclusions Regarding XLPE Against XLPE Pin on Plate Wear Results

Wear factors for XLPE rubbing against itself were considered to be low enough that, from a wear point of view, an all XLPE prosthesis, operating under dynamic loads of the order of tens of Newtons, should be viable. The lack of pin wear compared with plate wear was very interesting, especially as plate wear had been ignored in the past. Another important conclusion reached as a result of these wear tests was that ageing due to sunlight appeared to have an important effect on wear. Finally, there did not appear to be a transfer film produced when XLPE rubbed against itself.

4.5.5 Comparison of XLPE Against XLPE Pin on Plate Wear Test Results with those Involving Standard Biomaterials

If a comparison of wear factors is made between XLPE sliding against itself, and UHMWPE against a metallic counterface, where testing was undertaken using a reciprocating pin on plate rig, then similarity is seen. Cooper et al (1993) also employing reciprocating rigs, de-ionised water and a test distance of 350km (as was the case in test 1) obtained wear factors from 0.18 to 1.3 x $10^{-6}mm^3/Nm$ for UHMWPE pins rubbing against a metallic counterface. The laboratory values compare with $0 \pm 0.035 \times 10^{-6}mm^3/Nm$ to $0.065 \pm 0.011 \times 10^{-6}mm^3/Nm$ for the

XLPE test pins, and 0.33 x $10^{-6}mm^3/Nm$ to 0.52 x $10^{-6}mm^3/Nm$ for the XLPE plates, in the three long distance tests (greater than 300km) reported here.

However, Saikko (1993) obtained a wear factor of 0.1 x $10^{-6}mm^3/Nm$ for UHMWPE rubbing against cobalt chromium molybdenum alloy plates. In fact, wear factors as low as 0.019 x $10^{-6}mm^3/Nm$ have been reported by Dowson et al (1987) for UHMWPE rubbing against metal plates. If ceramics are considered, then wear factors are lower still, Saikko, (1993) reporting a value of 0.003 x$10^{-6}mm^3/Nm$ for UHMWPE rubbing against zirconia plates. However, such wear values are not found in vivo, where an average clinical wear factor of 2.1 x $10^{-6}mm^3/Nm$ for hip prostheses was measured (Hall et al, 1996). Therefore pin on plate machines are useful only as screening devices for potential biomaterial combinations. The XLPE against XLPE results were low enough so that, in the case of a finger joint where loads are relatively low, an all XLPE finger prosthesis should be viable from a wear point of view.

Further, if coefficients of friction are considered, then similar results are again seen. Tests using reciprocating pin on plate rigs gave a coefficient of friction of 0.14 for XLPE against itself (Sibly and Unsworth, 1991). This value compares with 0.1 reported for UHMWPE against cobalt chromium alloy (Saikko, 1993).

4.6 UHMWPE Against UHMWPE Pin on Plate Tests

4.6.1 Wear of UHMWPE Pins and UHMWPE Plates

Table 4.4 Summary of UHMWPE against UHMWPE test conditions and wear factors

Test Number	6		7	8
Load (N)	10	40	10	10
Number of pins/plates	2	2	4	4
Mean k pin ($x10^{-6}mm^3/Nm$)	81.3	85	31.1	101.4
Mean k plate ($x10^{-6}mm^3/Nm$)	84.0	158	59.8	50.7
Sliding Distance (km)	154	19.1	153	155.6
Pin diameter (mm)	5	5	5	5
Number of cycles (,000)	3,837	478	3,821	3,891
Stroke (mm)	20	20	20	20
Speed (rpm)	57	57	57	57

All the above tests employed distilled water as a lubricant. Test 6 used non-irradiated UHMWPE, which was several months old. Test 7 employed brand new irradiated UHMWPE, and test 8 was conducted with brand new, non-irradiated UHMWPE. Further, the material used in tests 7 and 8 came from the same batch. The actual weight losses that were measured during testing are tabulated in appendix 3.

4.6.2 Discussion of UHMWPE Against UHMWPE Wear Results

Figure 4.15 shows the mean UHMWPE pin and plate wear for test 6, under 10N and 40N loads. It can be seen that the wear volumes under 40N load are more than four times greater than under 10N loads. Figure 4.16 shows mean pin and plate wear, under 10N loads, for tests 6, 7 and 8. These results show a gentle increase in wear rate over the test distance. It was found that irradiated UHMWPE (test 7) wore less than non-irradiated UHMWPE (tests 6 and 8). Irradiation of UHMWPE increases the hardness of the material and cross-links some of the molecules. Therefore it can be speculated that irradiated UHMWPE should wear less than non-irradiated UHMWPE because as a general rule wear is

proportional to hardness. Also, at the molecular level, the cross-links should help to strengthen the material.

Figure 4.15 - Mean Wear of Non-Irradiated UHMWPE Pins and Plates Under 10N and 40N Loads. Test 6.

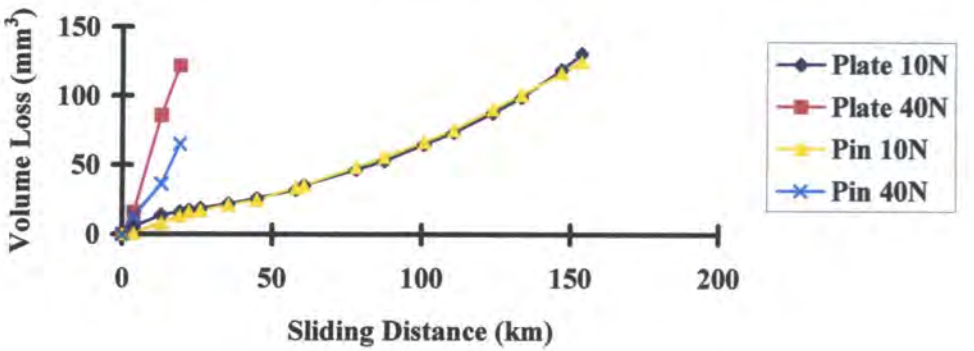

Figure 4.16 - Mean Wear of UHMWPE Pins and Plates Under 10N Loads. Tests 6, 7 and 8.

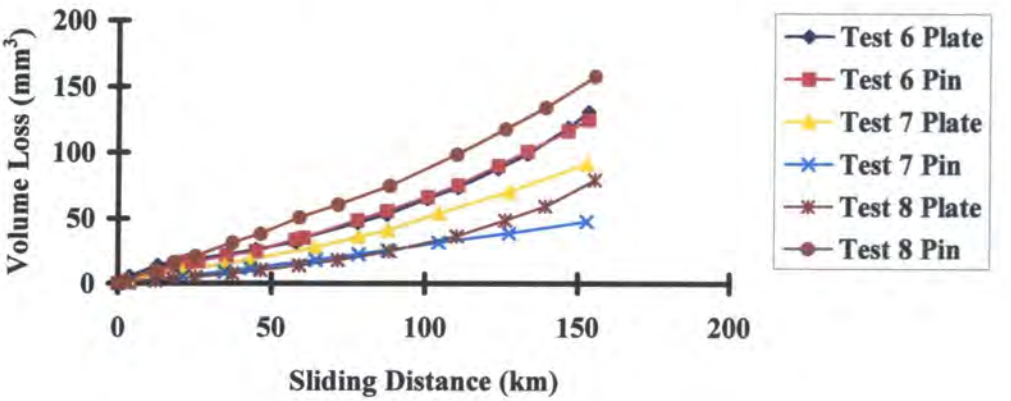

Dependent on which test is studied, pin wear can be seen to be greater than (test 8), equal to (test 6) or less than (test 7) plate wear under 10N loads! Interestingly though, if the system as a whole is taken for a comparison between non-irradiated tests (tests 6 and 8) then total wear volumes are similar. Further, the irradiated (test 7) result of lower pin wear matches that of the XLPE against XLPE tests, although the difference in wear rates is not as marked. It is known that an effect of irradiation is to cross-link some of the polyethylene molecules. However, the process of deliberate cross-linking, such as that produced by the silane method,

creates a more cross-linked material than would be created through the bi-product of irradiation.

The other question that can be asked is what wear mechanism, or combination of wear mechanisms, was occurring during the UHMWPE against UHMWPE tests? The scratches seen at a macroscopic level indicate that abrasive wear was occurring. The high values of wear factor measured implied that fatigue wear could also be taking place, and this was supported by tiny ripples perpendicular to the direction of sliding which are likely to be fatigue cracks. The pitting seen on the wear tracks of the test plates could also indicate either fatigue or adhesive wear. A final point worth noting is that the wear regimes may have acted in synergy to produce the high wear factors that were measured.

All of the test UHMWPE pins and plates had wear surfaces which had been machined, therefore all components would have been work hardened to the same degree. The results of test 6 indicate that cross contamination was not a problem, as wear volumes of the components under 10N load did not suddenly decrease after the 40N test samples were removed. Pins 2 and 4 had sheared by 22.3km, therefore tests under 40N loads ceased at this point. Testing under 10N loads continued to 153.5km.

In all UHMWPE against UHMWPE tests, the increase in weight due to water absorption of the control components was found to be trivial in comparison with weight loss of the test components. However, it was noted that water absorption by UHMWPE was greater than that by XLPE. In each of the UHMWPE tests reported, both a control pin and a control plate were included. Weighing errors, those due to the Mettler balance, were also small in comparison with the weight losses of the test pins and test plates.

4.6.3 Comparison of UHMWPE Against UHMWPE Wear Test Results With Those of Other Workers.

Table 4.5 UHMWPE against UHMWPE pin wear factors.

Researcher	Load (N)	Dist (km)	Stress (MPa)	Av. vel (mm/s)	k x 10^{-6} mm^3/Nm
Atkinson (mean of 2) 1976	12.7	38.3	0.10	18	9.4
Stokoe (mean of 3) 1990	8.5	67.5	0.43	38	12.4
Short (mean of 2) 1993	10	49.4	0.52	20	87.5
Joyce (mean of 2) non-irrad	10	153.5	0.51	38	81.3
Joyce (mean of 4) Irrad	10	152.8	0.51	38	31.1
Joyce (mean of 4) non-irrad	10	155.6	0.51	38	101.4

Note: wear factors refer to pins only.

The pin wear factors determined from the results of tests 6 and 8 (for non-irradiated material) are comparable with those of Short (1993). However, all of these results give wear factors several times greater than those measured by both Stokoe (1990) and Atkinson (1976).

Atkinson (1976) used larger diameter test pins which gave lower nominal contact stresses than those employed in the Durham tests, therefore the high (fatigue) wear component he identified was only seen in his highest stress test. This test was undertaken at 32N load which gave a nominal contact stress of 0.25MPa. Below this value of stress, Atkinson found no fatigue wear. Additionally, bovine synovial fluid was used as the lubricant, the test was undertaken at ambient temperature, and the material properties of UHMWPE could have changed in the last 20 years, so Atkinson's results are perhaps not suitable for a direct comparison.

Stokoe (1990) employed a speed identical to that used in tests 6, 7 and 8. Therefore speed cannot account for the differences in wear factor. This conclusion agrees with the results of tests 1 and 2, which were run at different speeds, and revealed no major difference in wear factors for XLPE. Further, Fisher et al (1994) indicated no difference in wear factor for UHMWPE sliding against stainless steel for velocities of between 24 and 240mm/s. The actual material may be of the greatest importance, as was found with the differences in

XLPE plate wear factors, possibly due to ageing, between tests 1 and 5. The results of tests 6, 7 and 8 indicate that differences in wear factors could, in part, be explained by whether irradiated or non-irradiated UHMWPE was used as the test material. Irradiated test pins were found to have wear factors less than half those of non irradiated test pins. Indeed, neither Atkinson (1976) Stokoe (1990) nor Short (1993) specified whether they tested irradiated or non-irradiated UHMWPE.

Atkinson (1976) and Stokoe (1990) found that pin wear factors were proportional to load, and therefore that more wear occurred at higher stresses. This conclusion is confirmed by the wear factors determined in test 6, which show a greater wear factor for the 40N load tests than for the 10N load tests. That wear factors in UHMWPE against UHMWPE tests increase with stress may in part explain the difference between the results of Short (1993) and those reported here; and those of Atkinson (1976) and Stokoe (1990). The former tests employed a higher stress than the latter tests.

4.6.4 UHMWPE Test Samples - Changes in Visual Appearance of Wear Faces

Changes in the topography of test pins and plates were far more dramatic than those of the equivalent XLPE against XLPE tests. In all of the UHMWPE against UHMWPE tests, the original machining marks on the test pins were removed by the first weighing point. After this, the pins assumed a matching wear profile to that of the plates, that of scratches in the direction of sliding. The pins of test 6 loaded under 40N snapped due to the wear tracks in the plates being so deep that the test pins impinged on each end of the wear track. These test pins were therefore subjected to a heavy shearing load at each end of the wear track. This impingement resulted in the test pin shearing in line with the base of the holder in which it was located.

For the plates of test 6 under 40N loads, after 3.9km heavy pitting was seen on the wear tracks. After 12.9km, this surface finish had been replaced by a deep, approximately 'V' shaped groove, overlaid with the long parallel scratches seen on all other pin on plate tests. The wear tracks on the 10N plates were different though. While plate 1 developed a highly polished surface finish, plate 3 showed

the rough, pitted topography seen on the 40N plates after 3.9km. However, after 26km both plates had developed a polished surface finish, the dominant feature being long scratches in the direction of sliding along the wear track. Towards the end of the test, also notable was the matching concave profile of the plates with the convex profile of the pins. Such plate topography was repeated in tests 7 and 8, again the amount of pitting on the wear tracks gradually declined throughout the duration of the test. Figure 4.17 shows a typical pit on the wear track of a test plate from test 7. This pitting may have indicated either fatigue or adhesive wear. When viewed under a microscope, fatigue cracks could be seen on the wear faces of the pins and plates from each test.

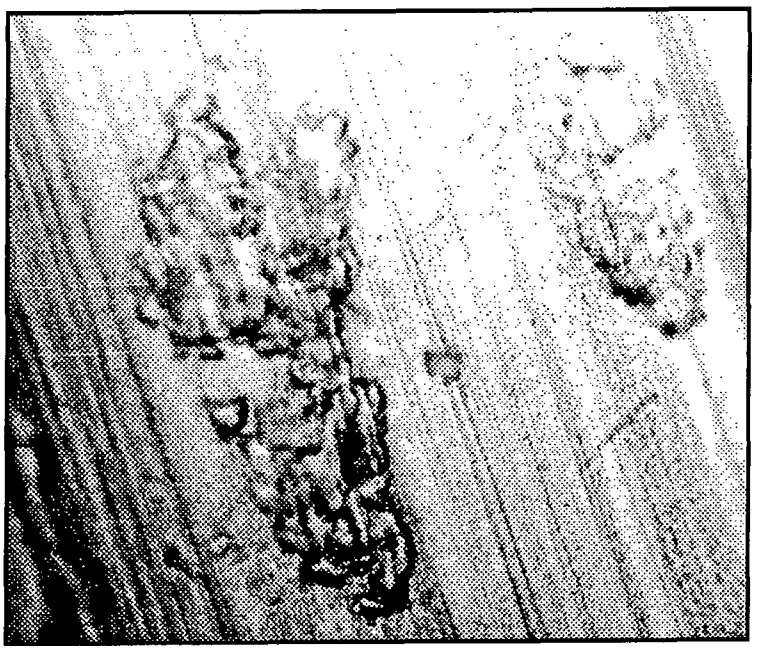

Figure 4.17 - Pit on wear track of UHMWPE test plate (magnification x200)

4.6.5 Comparison of XLPE Against XLPE with UHMWPE Against UHMWPE Results

Table 4.6 Comparison of XLPE against XLPE with UHMWPE against UHMWPE wear factors

Material	UHMWPE	XLPE
Load (N)	**10**	**10**
Distance (km)	153	150
k pin $x10^{-6}mm^3/Nm$	31.1	0.070
k plate $x10^{-6}mm^3/Nm$	59.8	0.78
Load (N)	**40**	**40**
Distance (km)	19	150
k pin $x10^{-6}mm^3/Nm$	85	0.035
k plate $x10^{-6}mm^3/Nm$	158	0.67

The large difference in wear factors between UHMWPE and XLPE is shown by table 4.6. The XLPE against XLPE test (test 3) continued to 608km. The UHMWPE against UHMWPE results under 10N loads are from test 7, as this test employed irradiated material. As no irradiated UHMWPE material was tested under 40N load, instead the results from test 6 are reported, therefore there can only be an indirect comparison between the wear of XLPE and UHMWPE under 40N loads.

From table 4.6, overall wear factors for irradiated XLPE and irradiated UHMWPE under 10N load can be taken as $0.85 \times 10^{-6}mm^3/Nm$ and $90.9 \times 10^{-6}mm^3/Nm$ respectively. If a finger joint is assumed to perform 1 million cycles per annum, in this case equivalent to 40km, then these wear factors can be interpreted as wear rates of $0.32mm^3$ per annum for irradiated XLPE and $36.4mm^3$ per annum for irradiated UHMWPE. Using the argument described previously in section 3.6, a polyethylene wear rate of $1.65mm^3$ per annum should be acceptable for an artificial finger joint. Consequently, based on the pin on plate results reported here, an all XLPE finger prosthesis would be acceptable from a wear point of view, while an all UHMWPE finger prosthesis would not.

Figure 4.18 - Mean Wear of Irradiated UHMWPE Pins and Plates Compared with Irradiated XLPE Pins and Plates Under 10N Loads. Tests 7 and 1.

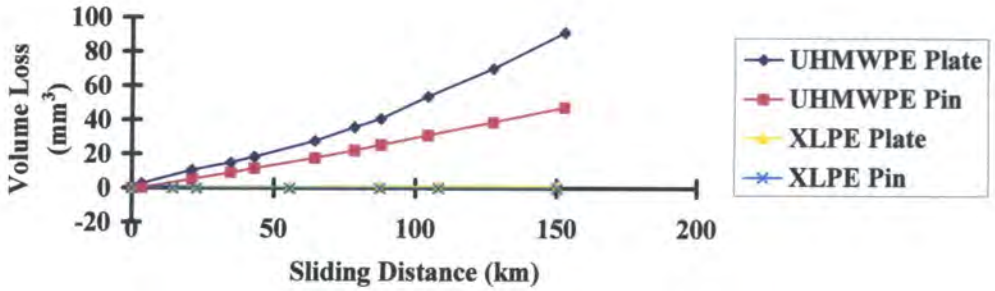

Figure 4.18 shows the wear of irradiated XLPE pins and plates compared with the wear of irradiated UHMWPE pins and plates, all under 10N loads. As well as showing the huge difference in wear rates, the UHMWPE gradients have a gentle increase in wear rate over the test distance. This result is in marked contrast to the gradient of the graphs of the XLPE against XLPE tests, Figures 4.4, 4.5 and 4.6, which show a decrease in wear rate. Wear factors for UHMWPE under 40N loads were found to be higher than for 10N loads, again distinct from XLPE. No XLPE pins loaded at 40N snapped, unlike the UHMWPE pins which did. Any material which shows increasing wear factors with increasing load should be avoided in a load bearing situation wherever possible. That the UHMWPE pin wear factors approached those of the UHMWPE plates is in contrast with the results from the XLPE rubbing against XLPE test results. Unsurprisingly, the UHMWPE rubbing against UHMWPE tests resulted in a large amount of debris, in marked contrast with the XLPE rubbing against XLPE tests. Figure 4.19 shows UHMWPE and XLPE test pins for comparison.

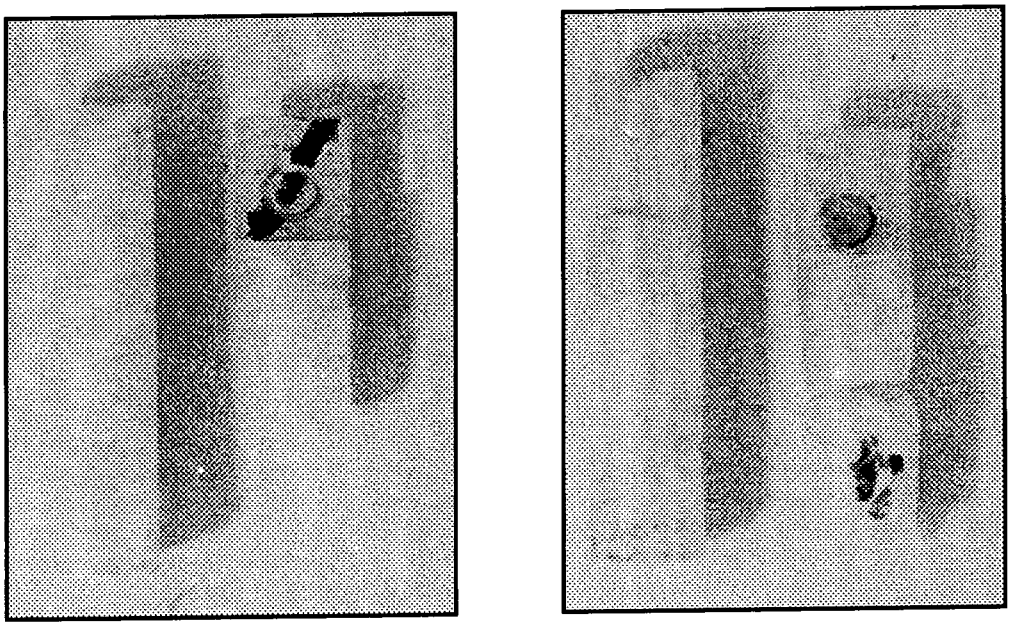

(Left) XLPE Pin after 349.0km under 10N load
(Right) UHMWPE Pin after 153.5km under 10N load

(Left) XLPE Pin after 349.0km under 40N load
(Right) UHMWPE Pin after 22.3km under 40N load

Figure 4.19 - Comparison of XLPE and UHMWPE test pins

It should be asked why did UHMWPE wear at such a higher rate than XLPE? The UHMWPE test components showed scratches in the direction of sliding, indicating abrasive wear; fatigue cracks, implying fatigue wear; and pitting (Figure 4.17), indicating adhesive wear. In contrast the XLPE test components only showed scratches in the direction of sliding (Figure 4.9). Figure 4.20 shows the wear tracks from an XLPE test plate (above) and an UHMWPE test plate (below). Scratches in the direction of sliding are prominent on both, but fatigue cracks can be made out on the UHMWPE test plate, but not on the XLPE test plate. Perhaps then the cross-links between the polyethylene molecules may have provided a mechanism which was sufficient to prevent adhesive and fatigue wear from occurring? Wear regimes are often synergistic, therefore it may be this synergy which led to the high wear of the UHMWPE test components.

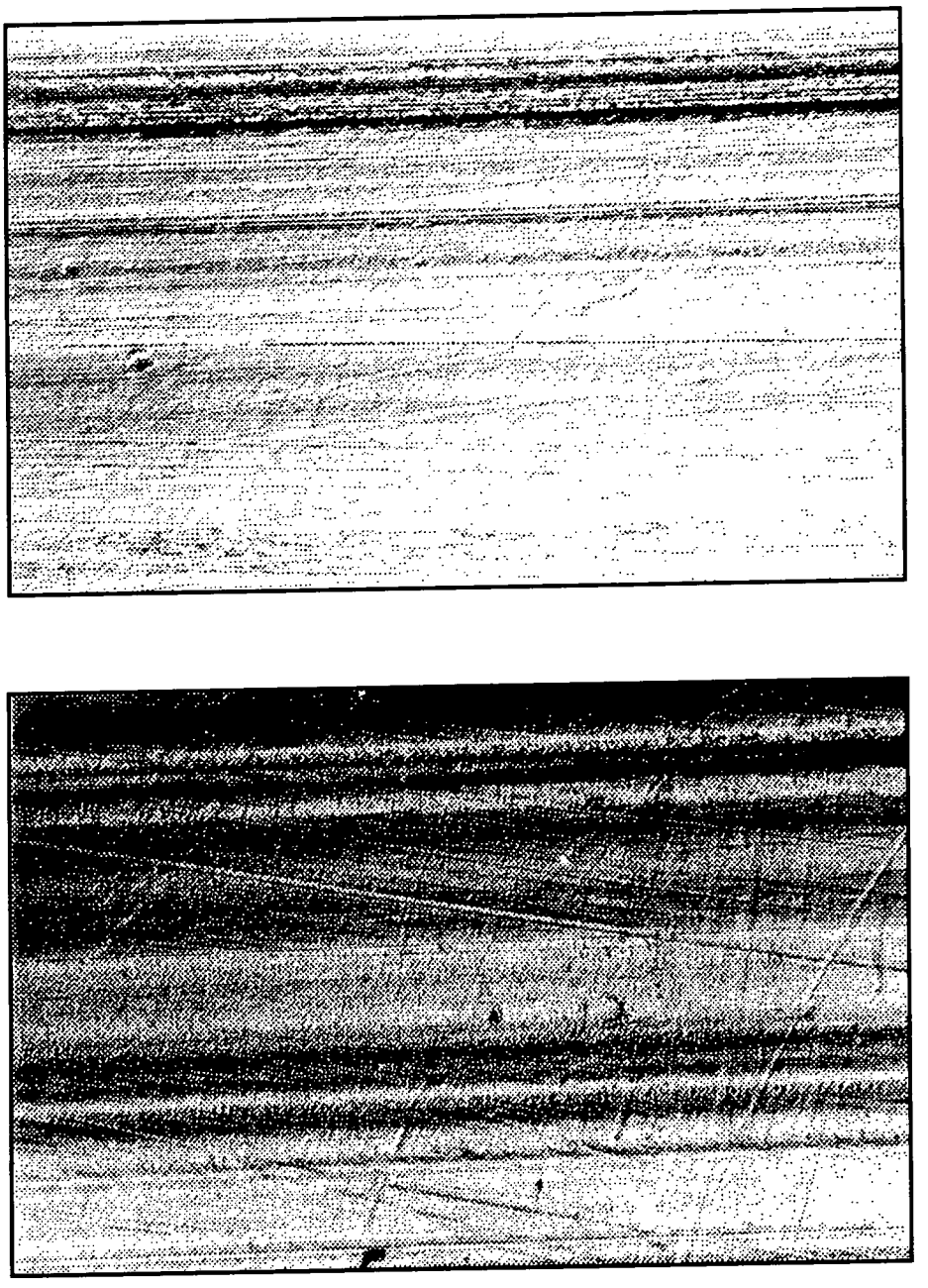

Figure 4.20 - Comparison of XLPE (above) and UHMWPE (below) wear tracks from test plates (magnification x 200)

4.7 XLPE and UHMWPE Pin on Plate Tests against hard counterfaces.

There are some 50,000 total hip replacement (THR) operations carried out in the UK each year, and a further 10,000 total knee replacement (TKR) operations. In both cases, the prosthesis usually consists of a hard metal component, commonly stainless steel or cobalt chromium molybdenum alloy, articulating against a softer UHMWPE component. While generally very successful, these artificial joints do not last forever, and some 13% of THR procedures are revisions. The reason for re-operation is frequently due to loosening of one or both components which in turn is thought to be due to the body's reaction to the polyethylene wear debris, with the inflammation caused leading to osteolysis (bone destruction). To reduce the production of such wear debris, a number of means have been tried, usually involving hardening of the hard component. Therefore coatings such as titanium nitride may be applied, or a ceramic used in place of a metal. Indeed in some recent designs, the concern over polyethylene wear has been such that the polyethylene component has been replaced altogether by a metal or a ceramic component (Müller, 1995).

The XLPE rubbing against XLPE wear test results were so remarkable, especially in comparison with the results of the tests in which UHMWPE rubbed against itself, that a direct comparison between UHMWPE and XLPE rubbing against harder materials was also made. This included an investigation of the basic wear mechanisms taking place. Further, there have been no such reported laboratory wear studies of XLPE in the literature, except for one single hip simulator study of an XLPE acetabular cup matched against an alumina ceramic femoral head (Wroblewski et al, 1996). Unfortunately, the gel content of the XLPE component was not stated.

Therefore, both polyethylenes were tested against 316 stainless steel, the material which is commonly used for the femoral components in THR and TKR. Ceramics, such as alumina, are increasingly used as materials for the spherical heads of femoral components in THR as they offer greater scratch resistance than an equivalent stainless steel component. Lately, it has been suggested that zirconia may be even more superior, as it has greater ductility than alumina. Therefore tests were also undertaken with XLPE and UHMWPE pins rubbing against zirconia plates.

Each test employed two UHMWPE test pins and two XLPE test pins. A secondary aspect of these wear tests was that they would permit a direct comparison with the polyethylene rubbing against polyethylene test results, as identical rigs and similar test conditions were being employed.

Finally, the fatigue effect discussed following the XLPE against XLPE results, which in part may explain the increased plate wear compared with pin wear, was investigated in a test which employed stainless steel pins loaded against XLPE and UHMWPE plates.

The pin on plate rigs used in these tests were identical to those described in section 4.2. Similarly, the calibration and operating procedures described in section 4.3 were identical.

4.8 XLPE and UHMWPE Against Stainless Steel Plates Pin on Plate Tests

4.8.1 Pin Wear Factors and Test Conditions

Table 4.7 Summary of XLPE and UHMWPE against stainless steel test conditions and wear factors.

Test Number	9	10
Plate Material	Stainless Steel	Stainless Steel
Distance (km)	471.5	448.5
No. cycles ($x10^6$)	7.858	7.478
Stroke (mm)	30	30
Load (N)	40	40
Pin Diameter (mm)	5	5
No. of XLPE Test Pins	2	2
No. of UHMWPE Test Pins	2	2
Lubricant	Distilled Water	Distilled Water
Speed (cycles per minute)	41.7	41.7
Av. Plate Ra (μm) - UHMWPE	0.025	0.031
Av. Plate Ra (μm) - XLPE	0.038	0.024
k UHMWPE ($x10^{-6}mm^3/Nm$)	0.011 and 0.022	0.26 and 0.45
k XLPE ($x10^{-6}mm^3/Nm$)	0.52 and 2.10	0.58 and 0.61

The UHMWPE material used for the pins in these tests was irradiated by exposure to gamma radiation, a dose not less than 25kGy. The minimum dose was 25.7kGy and the maximum dose was 33.2kGy. All of the UHMWPE material came from the same batch. The XLPE material used in these tests was irradiated and had a gel content after irradiation of 86%. All of the XLPE material came from the same batch.

The first stainless steel test, test 9, employed one UHMWPE control pin and one XLPE control pin. During this test, the wear of the UHMWPE test pins was so low that water absorption by the control pin had a significant affect on the calculated wear factors. To minimise the potential error from compensating for water absorption, the second stainless steel test employed two UHMWPE control pins and two XLPE control pins.

All plates were polished to have a surface finish of less that 0.05μm Ra, measured at a cut off of 0.8mm, as specified by British Standard BS 7252. The results of the first stainless steel test, test 9, indicated that XLPE wore at a significantly greater rate than UHMWPE, when rubbing against stainless steel. However, the XLPE pins rubbed against plates with higher Ra values than did the UHMWPE pins. To investigate further the effects of initial plate surface finish on pin wear, a second stainless steel test, test 10, was undertaken which put the UHMWPE pins against the slightly rougher plates.

Figures 4.21 and 4.22 show the wear results of each of the stainless steel tests. Appendix 3 gives the actual pin weight changes measured during the tests. Unlike the polyethylene against polyethylene tests, the test results against hard counterfaces did not produce consistent results. Therefore the individual hard counterface tests are considered and discussed separately.

Figure 4.21 - Wear of XLPE and UHMWPE Pins Against a Stainless Steel Counterface Under 40N Loads (Test 9).

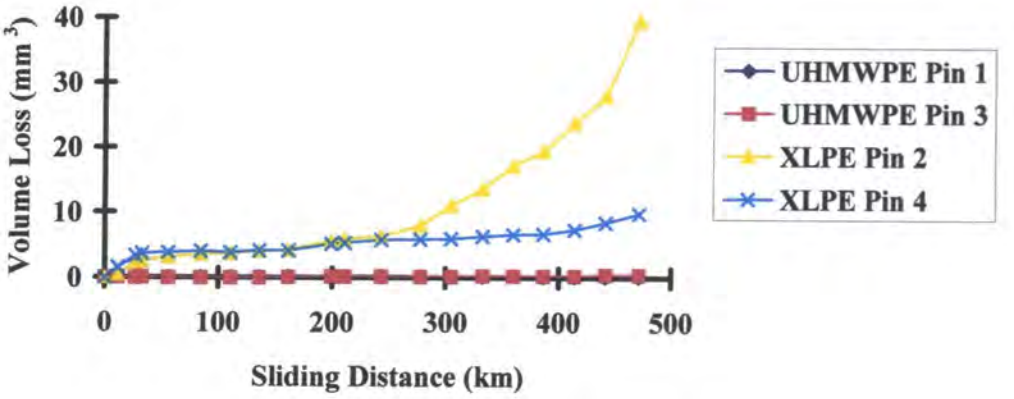

Figure 4.22 - Wear of XLPE and UHMWPE Pins Against a Stainless Steel Counterface Under 40N Loads (Test 10).

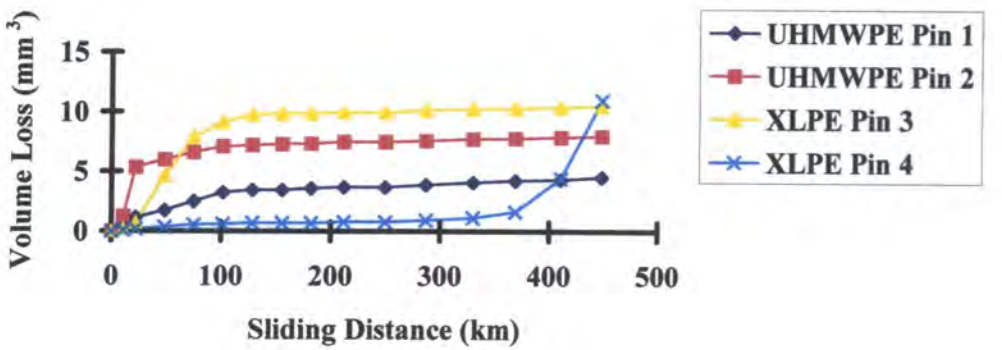

4.8.2 Changes in Test Pin Topography

4.8.2.1 First Stainless Steel Test (test 9)

4.8.2.1.1 Visual Changes

Overall, the significant feature on the wear face of each test pin was scratches in the direction of sliding. The original machining marks on the XLPE pins had been removed by 11.3km whereas, even after 471.5km, remnants of them were still visible on the UHMWPE pins. Polyethylene debris could be seen on the circumferences of the XLPE test pins throughout the test, although the amount

varied. This debris consisted of fine particles and was greatest during the early and final stages of the test (0 to 55km and after 199km). At the end of the test, fatigue cracks could be seen on the wear face of pin 2, although none could be seen on the other XLPE pin, pin 4. Figure 4.23 shows the wear face of this test pin at x200 magnification.

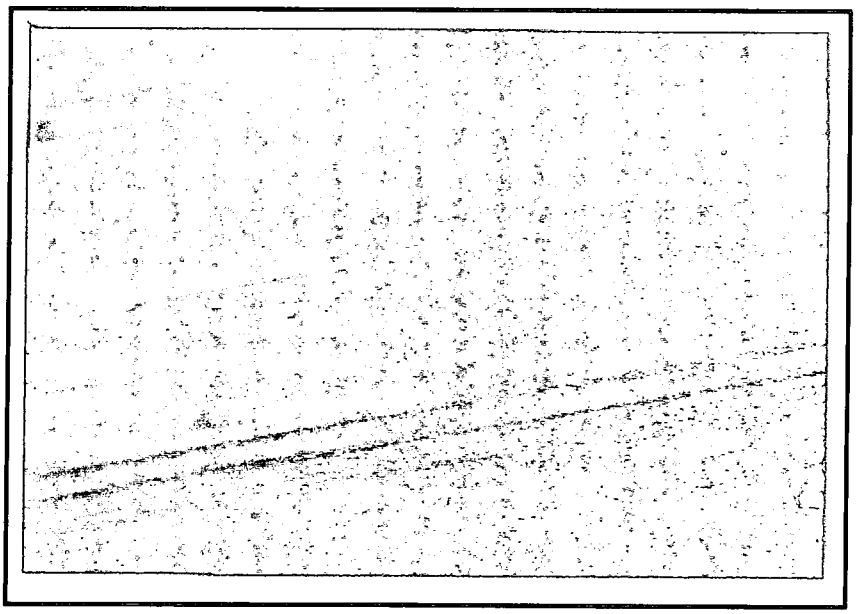

Figure 4.23 - Wear face of XLPE pin 4 test 9

4.8.2.2 Second Stainless Steel Test (test 10)

4.8.2.2.1 Visual Changes

Polyethylene debris could be seen on the circumferences of test pins 1 (UHMWPE), 2 (UHMWPE) and 3 (XLPE) during the early stages of the test. In the case of pin 2 (UHMWPE) debris was generated to 101.7km, and in the case of pins 1 (UHMWPE) and 3 (XLPE) debris was generated to 128.6km. Debris appeared on the circumference of test pin 4 (XLPE) at the last two weighing points only, i.e. beyond 400km. As in the previous stainless steel test, debris was of a fine particulate nature. Overall, the significant feature on the wear faces of all the pins was scratches in the direction of sliding. Inspection under a light microscope at a magnification of x200 revealed fatigue cracks on pin 3 (XLPE) at 155.7km, indicating that it had fatigued early in the test, and on pin 4 (XLPE) at 410.6km (Figure 4.24). This type of rippled surface was not seen on the UHMWPE test pins.

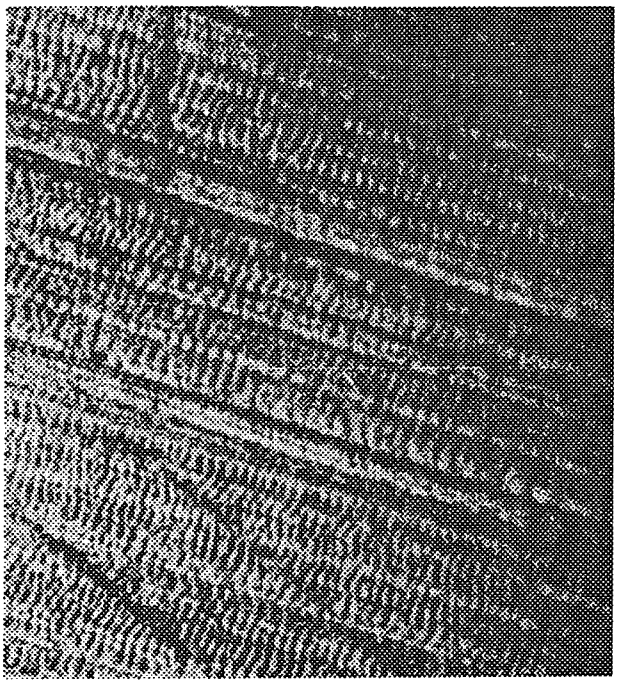

Figure 4.24 - Wear face of XLPE pin 4 test 10 showing fatigue cracks

4.8.3 Changes in Plate Topography

4.8.3.1 First Stainless Steel Test (test 9)

4.8.3.1.1 Mean Roughness Values of Wear Track on Plate (μm Ra)

These values were measured using a Taylor Hobson Talysurf 4, the mean of eight readings being tabulated. In table 4.8, L refers to a longitudinal measurement, while T indicates to a transverse measurement. Plates 1 and 3 rubbed against UHMWPE pins, while plates 2 and 4 rubbed against XLPE pins.

Table 4.8 Mean plate roughness values (test 9)

km	1L	2L	3L	4L	1T	2T	3T	4T
0	0.030	0.029	0.019	0.041	0.025	0.038	0.026	0.042
471.5	0.031	0.258	0.096	0.176	0.069	0.294	0.157	0.187

4.8.3.1.2 Visual Changes

A 'wear' track the width of the test pin could be clearly seen on each of the stainless steel plates at the end of the test. Each 'wear' track had the appearance of parallel lines in the direction of sliding, with each end being semi-circular to match the shape of the test pin.

4.8.3.1.3 Stainless Steel Plate Weight Changes

Table 4.9 Stainless steel plate weight changes (test 9)

Plate No.	Pin Material	Initial Plate Weight (g)	Final Plate Weight (g)	Difference ($x10^{-4}g$)
1	UHMWPE	18.6521	18.6525	+2
2	XLPE	18.7835	18.7839	+4
3	UHMWPE	18.6992	18.6996	+4
4	XLPE	18.7717	18.7721	+4

At the end of the test, each plate had increased in weight. The error in weight measurement was taken to be $\pm$ 1 x 10^{-4} grammes. It was assumed that a material as hard and as dense as stainless steel would not absorb any of the distilled water lubricant.

4.8.3.2 Second Stainless Steel Test (test 10)

4.8.3.2.1 Mean Roughness Values of Wear Track on Plate (μm Ra)

These values were measured using a Taylor Hobson Talysurf 4, the mean of eight readings being tabulated. In table 4.10, L refers to a longitudinal measurement, while T indicates to a transverse measurement. Plates 1 and 2 rubbed against UHMWPE pins, plates 3 and 4 rubbed against XLPE pins.

Table 4.10 Mean plate roughness values (test 10)

km	**1L**	**2L**	**3L**	**4L**	**1T**	**2T**	**3T**	**4T**
0	0.033	0.029	0.018	0.029	0.036	0.025	0.023	0.025
448.5	0.201	0.042	0.038	0.112	0.269	0.064	0.043	0.133

4.8.3.2.2 Visual changes

A 'wear' track equal to the width of the test pins was again seen on each of the test plates at the cessation of the test. Alphastep traces of plates 1 and 4 revealed a transfer film of depth 0.4μm to 0.6μm (XLPE) for plate 4 (Figure 4.25) and 0.8μm to 1.0μm (UHMWPE) for plate 1 (Figure 4.26).

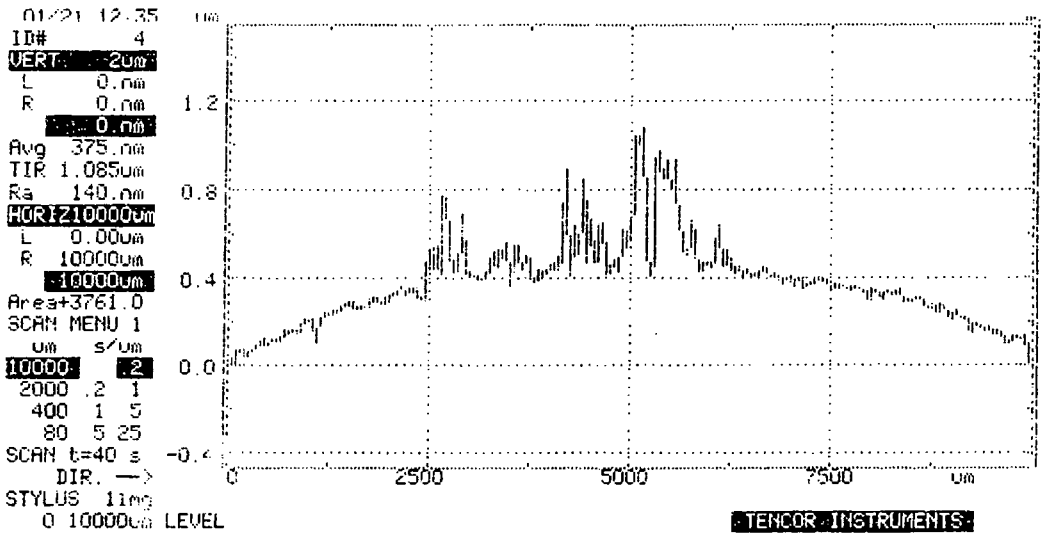

Figure 4.25 - Alphastep trace of Stainless Steel plate 4 showing XLPE transfer film (test 10).

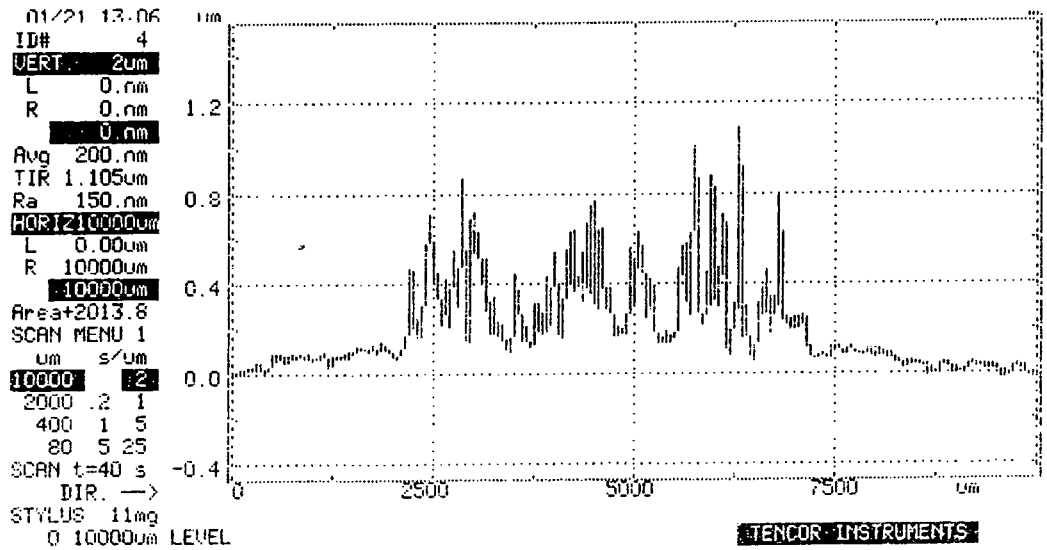

Figure 4.26 - Alphastep trace of Stainless Steel plate 1 showing UHMWPE transfer film (test 10).

4.8.3.2.3 Stainless Steel Plate Weight Changes

Table 4.11 Stainless steel plate weight changes (test 10)

Plate No.	Pin Material	Initial Plate Weight (g)	Final Plate Weight (g)	Difference ($x10^{-4}g$)
1	UHMWPE	18.6502	18.6509	+7
2	UHMWPE	18.7813	18.7818	+5
3	XLPE	18.6980	18.6983	+3
4	XLPE	18.7706	18.7710	+4

The weight differences indicate that a slightly heavier transfer film occurred with UHMWPE than with XLPE. The measurement error was taken to be $\pm$ 1 x 10^{-4} grammes. It can be seen that the greatest increase in plate weight corresponds with the greatest increase in Ra values (plate 1). Further, the least increase in plate weight corresponds with the least increase in Ra values (plate 3).

4.8.4 Discussion of Stainless Steel Results

4.8.4.1 First Stainless Steel Test (test 9)

At the end of the test, after 471.5km, wear factors were measured to be 0.011 x $10^{-6}mm^3/Nm$ and 0.022 x $10^{-6}mm^3/Nm$ for the UHMWPE test pins; and 0.52 x $10^{-6}mm^3/Nm$ and 2.10 x $10^{-6}mm^3/Nm$ for the XLPE test pins. In each case, the error in the wear factor was taken to be $\pm$ 0.011 x $10^{-6}mm^3/Nm$, based on a weighing error of $\pm$ 0.0001g, which was the accuracy of the Mettler balance.

Part of the reason for the greater wear of the XLPE pins compared with the UHMWPE pins may have been due to the initial surface finish of the stainless steel plates. The XLPE pins (numbers 2 and 4) were rubbing against the plates with the higher initial Ra values. Further, these two plates, plates 2 and 4, also had the highest Ra values at the end of the test. It is possible that this difference in Ra values between the plates rubbing against XLPE pins, and those rubbing against UHMWPE pins, accounts for the high initial wear (to 32.9km) of the XLPE pins (figure 4.21). During this initial period, XLPE material may have been transferred from pin to plate, to fill in some of the troughs on the plate. It is well known that surface finish affects the wear of UHMWPE (Cooper et al, 1993, a).

Further, Fisher (1995) states that a 5 fold increase in roughness leads to a 50 fold increase in wear. Additionally, the transverse roughness is considered to be of greater significance than longitudinal roughness (Dowson et al, 1987; Fisher et al, 1995). The transverse roughness (Ra) values of the plates at the end of the test are then in the same order as the wear factors, as shown in table 4.12. A high Ra value corresponds to a high wear factor. Although plates 3 and 4 had similar transverse Ra values at the end of the test, it is worth noting that plate 4 had a final longitudinal roughness value twice that of plate 3. Longitudinal roughness also affects wear, though to a lesser extent than transverse roughness (Dowson et al, 1987; Fisher et al, 1995). This fact may account for the differences in wear factors between pins 3 and 4.

The increase in roughness of the plates at the end of the test is likely to be due to the build up of a transfer film; a phenomenon which is commonly found when a test is undertaken with distilled water as a lubricant (Cooper et al, 1993, a). Other indicators of a transfer film, apart from an increase in the Ra values, were an increase in the weight of each plate, and the appearance of a 'wear' track on each of the plates.

Table 4.12 Comparison of Ra values and wear factors (test 9)

Plate	Pin Material	Ra (transverse) start of test	Ra (transverse) end of test	k x $10^{-6}mm^3/Nm$
1	UHMWPE	0.025μm	0.069μm	0.011
3	UHMWPE	0.026μm	0.157μm	0.022
4	XLPE	0.042μm	0.187μm	0.52
2	XLPE	0.038μm	0.294μm	2.10

However, roughness effects alone could not be the whole story. Figure 4.21 shows that, above 277.8km, the wear of one of the XLPE pins (pin 2) increased markedly, in turn implying fatigue wear. When the wear face of this pin was viewed beneath a microscope, tiny ripples perpendicular to the direction of motion were seen, and these were thought to be fatigue cracks.

4.8.4.2 Second Stainless Steel Test (test 10)

At the end of the test, after 448.5km, wear factors were measured to be 0.26 x $10^{-6}mm^3/Nm$ and 0.45 x $10^{-6}mm^3/Nm$ for the UHMWPE test pins; and 0.58 x

$10^{-6}mm^3/Nm$ and 0.61 x $10^{-6}mm^3/Nm$ for the XLPE test pins. In each case, the error in the wear factor was taken to be ± 0.012 x $10^{-6}mm^3/Nm$, based on a weighing error of ± 0.0001g, which was the accuracy of the Mettler balance.

This test showed that initial surface roughness could not alone explain the greater wear of XLPE compared with UHMWPE. The figures in table 4.13 show that transverse Ra values at the end of the test and wear factors did not correspond. In fact the highest transverse Ra value at the end of the test (that of plate 1) gave the lowest wear factor!

Table 4.13 Comparison of Ra values and wear factors (test 10)

Plate	Pin Material	Ra (transverse) start of test	Ra (transverse) end of test	k x $10^{-6}mm^3/Nm$
1	UHMWPE	0.036μm	0.269μm	0.26
2	UHMWPE	0.025μm	0.064μm	0.45
3	XLPE	0.023μm	0.043μm	0.58
4	XLPE	0.025μm	0.133μm	0.61

Alphastep traces of the 'wear' tracks on plates 1 and 4 (figures 4.25 and 4.26) show that a transfer film had occurred on both a plate rubbing against a XLPE pin (plate 4) and on a plate rubbing against an UHMWPE pin (plate 1). These traces also indicate that the transfer film was deeper and wider on plate 1 than plate 4. This fact is supported by the changes in weight of the test plates, plate 1 increasing in weight by a greater amount than plate 4. In turn, these weight increases imply that the transfer film was greater in the case of UHMWPE than in the case of XLPE. Based on these two pieces of evidence it can be speculated that XLPE is superior to UHMWPE in resisting the adhesive attraction which creates a transfer film; the molecular bonds are stronger, which would be expected due to the cross-linking process.

However, for most of the duration of the test it was likely that abrasive wear was the dominant mechanism, as shown by the scratches on both the test pins and the test plates. It may be that, as the stainless steel plates were significantly harder than either the XLPE or UHMWPE pins, then the steel gouged its way through both polymers to the same degree. Nevertheless, lacking the same number of cross-links between molecules, the UHMWPE may have produced a transfer film quicker that the XLPE, filling in any prominent (primarily transverse) scratches on its stainless steel test plates. Indeed, over the initial 22.3km the wear of the

UHMWPE pins was greater than that of the XLPE pins. This deposition of a transfer film would perhaps have continued, gradually declining to around 100km, after which point wear of the test pins was low and steady state. In fact both polyethylenes showed a substantial period of low, steady state wear. For each of the test pins, Figure 4.22 shows there to be a significant period (over some 300km) during which wear was low (i.e. of the order of 0.064 x $10^{-6}mm^3/Nm$ for pin 2 (UHMWPE) between 101.7km and 448.5km).

As with the previous stainless steel test, this second test also showed fatigue of a XLPE pin. This phenomenon is indicated for XLPE pin 4 in Figure 4.22, and was confirmed by viewing the wear face of the XLPE pin under a microscope which revealed fatigue cracks (Figure 4.24). Why should any of the XLPE pins have fatigued, while the UHMWPE pins did not? If both polyethylenes are considered to be rubbing against a roughish steel surface, it can be speculated that both polymers will have wear faces deformed by the metal, and that the degree of deformation will depend on the Ra value of the metal surface. Therefore the higher the Ra value, the greater the deformation. Although XLPE has a higher yield strength than UHMWPE, as well as a greater resistance to creep (Atkinson and Cicek, 1983), this strength may also make XLPE more brittle than UHMWPE and eventually XLPE fatigues (in this test, test 10, after 350km or 6 million cycles). In contrast, UHMWPE has a greater ductility than XLPE, as its percentage elongation is greater (Atkinson and Cicek, 1983), and this ductility may have prevented the occurrence of fatigue wear before the test ended at 7.5 million cycles.

4.8.5 Comparison of Stainless Steel Results With Those of Other Workers

This section involves a comparison with tests which have used metal counterfaces having Ra values of less than 0.05μm, reciprocating rigs, UHMWPE test pins and distilled water as a lubricant. Only UHMWPE results have been discussed as the wear of silane cross-linked polyethylene against hard counterfaces has not been described elsewhere. A comparison of the wear of XLPE with that of UHMWPE, both rubbing against hard counterfaces, will be discussed in section 4.9.8.

Table 4.14 UHMWPE against stainless steel wear factors

Researcher	No. of pins	Load N	Dist km	Stress MPa	k x 10^{-6} mm^3/Nm
Saikko (1993)	3	225	250	4.8	0.11 (mean)
Cooper et al (1993) 2	6	80	350	12	0.18-1.3
Derbyshire et al (1994)	3	80	419	11.3	0.035 (mean)
Dowson et al (1987)	2	100	440	14.1	0.019 & 6.0
Kumar et al (1991)	3	219	65	3.45	0.112 (mean)
Joyce - test 9	2	40	472	2.04	0.011 & 0.022
Joyce - test 10	2	40	449	2.04	0.26 & 0.45

A large number of such reciprocating tests have been undertaken by various researchers in the past and a huge range of wear factors for UHMWPE rubbing against metal counterfaces have been reported. For example, Dowson et al, 1987, report wear factors of 0.019 x $10^{-6}mm^3/Nm$ and 6.0 x $10^{-6}mm^3/Nm$, for plate Ra values of 0.012 and 0.013μm respectively. The results reported in this thesis for UHMWPE cover a similar range, from 0.011 x $10^{-6}mm^3/Nm$ to 0.45 x $10^{-6}mm^3/Nm$. An explanation for such a range of wear factors has been said to lie in the counterface roughness (Fisher, 1995) and the transfer film found with tests which have employed distilled water as a lubricant (Cooper et al, 1993, a). Secondly, a wide scatter of results is frequently found in wear tests (Wallbridge and Dowson, 1987).

4.9 XLPE and UHMWPE Against Zirconia Plates Pin on Plate Tests

4.9.1 Development of Tests

The aim of the first zirconia test, test 11, was to determine the wear factors of irradiated XLPE and irradiated UHMWPE pins rubbing against zirconia ceramic plates. The test would therefore give a direct comparison between the two types of polyethylene. Test 12 repeated the loading conditions of test 11, to see if the same results would be obtained. Additionally during test 12, the roughness of the 'wear' track on the zirconia plates was regularly monitored. Test 13 was conducted with zirconia plates which had two different magnitudes of surface finish, to investigate whether initial surface finish of the hard counterface could have a significant effect on the wear of the polyethylene test pins.

All zirconia plates were polished to have a surface finish of less than or equal to 0.005μm Ra, except for the final zirconia test, test 13, which included two plates with higher Ra values. All roughness values were measured at a cut off of 0.8mm, as specified by British Standard BS 7252.

4.9.2 Pin Wear Factors and Test Conditions

Table 4.15 Zirconia test conditions and wear factors

Test Number	11	12	13
Plate Material	Zirconia	Zirconia	Zirconia
Distance (km)	391.9	298.8	130.7
No. cycles (x10^6)	10.314	7.115	2.841
Stroke (mm)	19	21	23
Load (N)	40	40	40
Pin Diameter (mm)	5	5	5
No. of UHMWPE Pins	2	2	2
No. of XLPE Pins	2	2	2
Lubricant	Distilled Water	Distilled Water	Distilled Water
Speed (cpm)	60	59	60
Av. Plate Ra (μm) UH	0.005	0.005	N/A
Av. Plate Ra (μm) XL	0.005	0.005	N/A
k UH (x$10^{-6}$$mm^3$/Nm)	4.14 and 2.35	0.005 and 0.015	30.6 and 10.2
k XL (x$10^{-6}$$mm^3$/Nm)	0.38 and 0.10	0.013 and 0.013	2.56 and 1.89

Details of the polyethylene material used for the pins were as follows. The UHMWPE material was irradiated by exposure to gamma radiation, at a dose of not less than 25kGy. The maximum dose was 33.2kGy. All of the UHMWPE material came from the same batch. The XLPE material had a gel content after irradiation of 86%, and all of the XLPE material came from the same batch. Four polyethylene control pins were included in each test, as it was expected that pin wear would be small, and therefore that lubricant absorption would be significant.

Figures 4.27, 4.28 and 4.29 show the results of the three zirconia tests (tests 11, 12 and 13). To permit a comparison between the tests, the overall wear factor from each test is quoted in table 4.16. However, during tests 11 and 13, regions

of high and low wear were seen. The actual weight changes of the test pins are given in appendix 3.

Figure 4.27 - Wear of XLPE and UHMWPE Pins Against a Zirconia Counterface Under 40N Loads (Test 11).

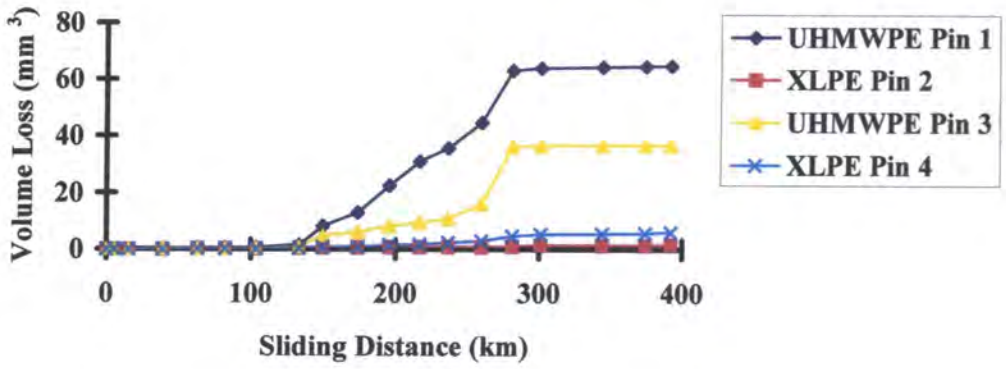

Figure 4.28 - Wear of XLPE and UHMWPE Pins Against a Zirconia Counterface Under 40N Loads (test 12)

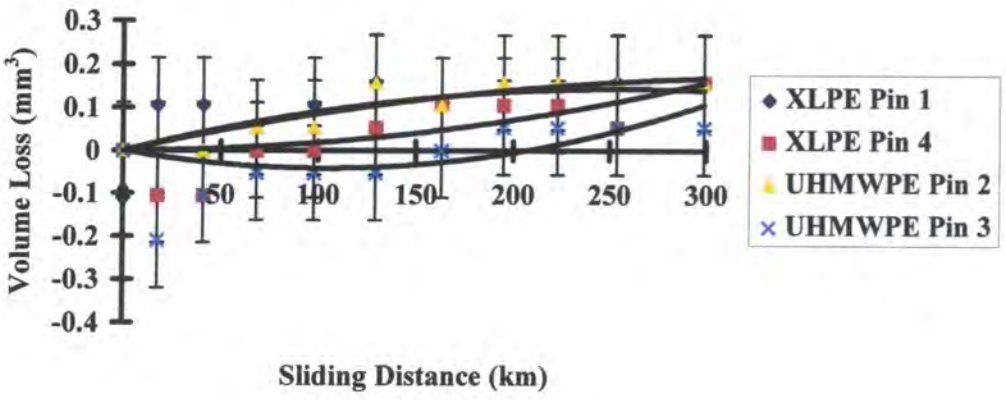

Figure 4.29 - Wear of XLPE and UHMWPE Pins Against a Zirconia Counterface Under 40N Loads (test 13)

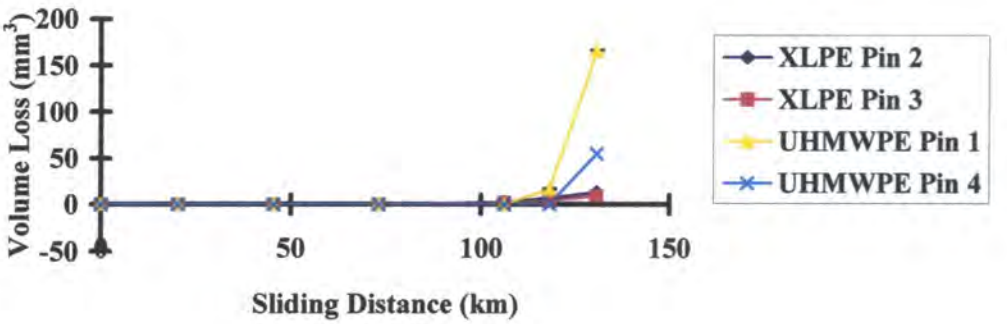

4.9.3 Changes in Test Pin Topography

4.9.3.1 Visual Changes (test 11)

On the wear face of each test pin, scratches in the direction of sliding had replaced concentric machining marks as the dominant feature by the 133.4km weighing point. Inspection of the wear faces of the UHMWPE test pins during the 133.4km to 281.4km period, using a 500 times magnification microscope, revealed the presence of small wavy cracks perpendicular to the sliding direction which were thought to be fatigue cracks. Wear of the UHMWPE test pins was such that, by the end of the test, they were noticeably shorter (17mm and 18mm) than the 20mm long XLPE test pins. Between 133.4km and 281.4km, UHMWPE debris took the form of fine wear particles bunched together around the circumference of the test pin, as sketched in Figure 4.30. The XLPE test pins occasionally showed similar particulate debris, but the amount was always much less than with the UHMWPE test pins.

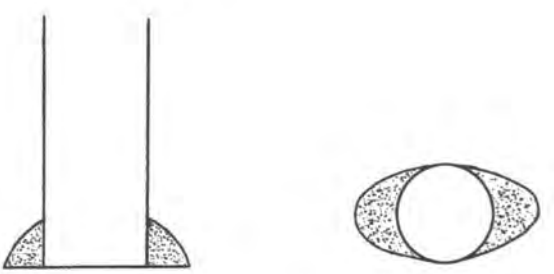

Figure 4.30 - Build up of wear debris on UHMWPE pins during Zirconia test 11, over the period 133.4km to 281.4km

4.9.3.2 Visual Changes (test 12)

The wear face of each test pin had acquired a polished finish, overlaid with fine scratches in the direction of sliding, by the end of this test. No wear debris was seen around the circumference of any of the test pins, and no fatigue cracks could be seen.

4.9.3.3 Visual Changes (test 13)

Visual changes in this test were similar to those noted in test 11, including the build up of wear debris around the periphery of the test pins. All of the machining marks on the wear face of each of the test pins had disappeared by the 106.1km weighing point. Due to the high wear of the UHMWPE test pins, they were noticeably shorter at the end of the test than at the beginning, being 12mm and 17mm long rather than the initial 20mm in length. Fatigue cracks were visible on the wear face of pin 4 (UHMWPE) at the end of the test but not on XLPE pin 2 (Figure 4.31).

Figure 4.31 - Comparison of XLPE (left) and UHMWPE (right) test pins (x200 magnification)

4.9.4 Changes in Plate Topography

In the following three tables (tables 4.16 to 4.18) L refers to longitudinal values and T to transverse values. The units are μm Ra, measured using Taylor Hobson Talysurf 4, with a cut off set at 0.8mm, as specified by BS7252: Part 4: 1990. The mean of 8 readings is given.

4.9.4.1 Mean Plate Roughness Values (test 11)

Table 4.16 Mean plate roughness values (test 11)

km	1L	2L	3L	4L	1T	2T	3T	4T
0	0.005	0.004	0.005	0.005	0.004	0.005	0.004	0.005
149.6	--	--	0.017	0.020	--	--	0.018	0.022
391.9	0.032	0.013	0.011	0.009	0.037	0.013	0.012	0.008

Plates 1 and 3 rubbed against UHMWPE pins, plates 2 and 4 rubbed against XLPE pins. All plates showed a small increase in roughness from those measured at the beginning of the test. Interestingly, little difference was seen between the transverse and longitudinal values of each plate at the end of the test. The few readings that were taken during the test indicated that the Ra values appeared to increase during the test but had decreased by the end. However, there were perhaps an insufficient number of results upon which a definite conclusion could be made.

4.9.4.2 Mean Plate Roughness Values (test 12)

Table 4.17 Mean plate roughness values (test 12)

km	1L	2L	3L	4L	1T	2T	3T	4T
0	0.005	0.005	0.005	0.005	0.005	0.005	0.005	0.005
17.6	0.007	0.007	0.005	0.005	0.006	0.006	0.006	0.005
68.4	0.005	0.008	0.007	0.007	0.006	0.007	0.008	0.008
129.2	0.008	0.007	0.008	0.009	0.008	0.008	0.008	0.009
195.1	0.005	0.005	0.005	0.005	0.006	0.005	0.005	0.006
253.7	0.008	0.007	0.007	0.007	0.008	0.007	0.008	0.009
298.8	0.009	0.005	0.005	0.007	0.009	0.005	0.005	0.008

Plates 2 and 3 rubbed against UHMWPE pins. Plates 1 and 4 rubbed against XLPE pins. The results in table 4.17 indicated that there was no major change in

plate roughness values during the test, either along or across the 'wear' track. As in the previous test, test 11, longitudinal and transverse values of roughness corresponded closely.

4.9.4.3 Mean Plate Roughness Values (test 13)

Table 4.18 Mean plate roughness values (test 13)

km	1L	2L	3L	4L	1T	2T	3T	4T
0	0.005	0.091	0.005	0.096	0.005	0.025	0.005	0.077
130.7	0.066	0.096	0.005	0.112	0.055	0.017	0.006	0.046

Plates 1 and 4 rubbed against UHMWPE pins, plates 2 and 3 rubbed against XLPE pins. The initially 'rough' plates, plates 2 and 4, showed a slight increase in longitudinal Ra values and a decrease in transverse Ra values. This result can perhaps be explained by the transfer film filling in the 'troughs' of these 'rough' plates. Plate 1, an initially 'smooth' plate, showed the greatest increase in Ra values, and this plate corresponded with the pin which showed the greatest wear. However, the longitudinal Ra values of plate 1 at the end of the test were still less than those of either of the 'rough' plates, plates 2 and 4, although the transverse Ra value of plate 1 was greater. In contrast, the Ra values of the other smooth plate, plate 3 remained virtually unchanged from those at the beginning of the test. For all the plates, longitudinal Ra values were approximately equal to transverse Ra values, this being the same result as found in the other two zirconia tests (tests 11 and 12).

4.9.4.4 Visual Appearance of Zirconia Plates (test 11)

All of the plates were discoloured by an initially yellow 'wear' track which darkened to a brown colour. However, the least discolouration occurred with the two plates which rubbed against the XLPE test pins. The least discoloured plate of all was plate 4, although this did not correspond with the XLPE pin which showed the least wear (which was pin 2). Instead the lack of discolouration corresponded with the smallest increase in plate Ra values (table 4.16). Each 'wear' track was composed of parallel lines in the direction of sliding, with each end of the 'wear' track being semi-circular to match the shape of the test pin.

4.9.4.5 Visual Appearance of Zirconia Plates (test 12)

After 68km (1.6 million cycles) a transfer film at the ends of the 'wear' track was just visible. Although all of the transfer films were inconspicuous, the most noticeable by 98km (2.3 million cycles) were those on plates 2 and 3, the plates which rubbed against the UHMWPE test pins. By the termination of the test, all of the transfer films were only faintly visible to the eye.

4.9.4.6 Visual Appearance of Zirconia Plates (test 13)

A transfer film was visible on all plates by the 106km (2.3 million cycles) mark. As in the earlier zirconia tests this transfer film was yellow in colour. The transfer film on plate 2 was the darkest. Plate 2 was the 'rough' plate which rubbed against one of the two XLPE test pins. However, in contradiction, the least prominent transfer film was that on plate 3, the 'smooth' plate which rubbed against the other XLPE test pin.

4.9.5 Zirconia Plate Weight Changes

Table 4.19 Zirconia Plate Weight Changes (test 11).

Plate No.	Pin Material	Initial Plate Weight (g)	Final Plate Weight (g)	Difference ($x10^{-4}g$)
1	UHMWPE	36.2038	36.2038	0
2	XLPE	36.2247	36.2248	+1
3	UHMWPE	36.2145	36.2146	+1
4	XLPE	36.2180	36.2181	+1

These measurements show that the plates had not lost any weight. Any increase in weight may be explained by polyethylene transferring from pin to plate due to adhesive wear, i.e. a transfer film. The above measurements were made after 392km (10.3 million cycles). Fluid uptake of the zirconia plates was assumed to be zero. The measurement error due to the Mettler balance was taken to be ± 1 $x10^{-4}g$. Therefore by the end of the test the weights of the test plates were almost within the error of the Mettler balance.

Table 4.20 Zirconia Plate Weight Changes (test 12).

Plate No.	Pin Material	Initial Plate Weight (g)	Final Plate Weight (g)	Difference ($x10^{-4}g$)
1	XLPE	39.5324	39.5326	+2
2	UHMWPE	39.4126	39.4127	+1
3	UHMWPE	39.4713	39.4715	+2
4	XLPE	39.5874	39.5876	+2

The weight increase of the plates approximately corresponds to the weight loss of the test pins, which in all cases was no greater than 2 $x10^{-4}g$. Once more, the error in the Mettler balance was taken to be $\pm$ 1 $x10^{-4}g$.

Table 4.21 Zirconia Plate Weight Changes (test 13).

Plate No.	Pin Material	Initial Plate Weight (g)	Final Plate Weight (g)	Difference ($x10^{-4}g$)
1	UHMWPE	39.4361	39.4365	+4
2	XLPE	36.2145	36.2147	+2
3	XLPE	39.3803	39.3804	+1
4	UHMWPE	36.1885	36.1885	0

Although this test was the shortest of the three zirconia tests, there was again a general trend towards an increase in plate weight, which may be explained by the deposition of a transfer film. Interestingly, the plate which showed the greatest increase in weight, plate 1, also showed the most significant increase in Ra values of the 'wear' track. Plates 2 and 4 were the 'rough' plates, therefore it may have been expected that a heavier transfer film would have been deposited to 'fill-in' the valleys of these plates. As can be seen from table 4.21 however, this was not the case.

4.9.6 Discussion of Zirconia Results

4.9.6.1 First Zirconia Test - Test 11

Figure 4.27 graphically indicates the wear of the polyethylene pins against the zirconia plates. These results imply that, up to approximately 133km, wear was increasing in the reported way of reciprocating tests which employed distilled water as a lubricant (Cooper et al, 1993, a). That is, a transfer film was building

up, leading to an increase in surface roughness which in turn caused a gradual increase in wear. However, between 133.4km and 281.4km, the wear of the UHMWPE pins increased markedly, indicating fatigue wear. Further, examination using a microscope at x500 magnification revealed the presence of tiny, wavy cracks perpendicular to the direction of sliding. Such cracks are a classic sign of fatigue wear (Brown et al, 1976).

As can be seen from Figure 4.27 the 'steps' in the UHMWPE results are remarkable. The mean wear factors for the UHMWPE pins between the periods of 0 to 133.4km, 133.4km to 281.4km and beyond 281.4 km were calculated to be 0.21 x $10^{-6}mm^3/Nm$, 8.24 x $10^{-6}mm^3/Nm$ and 0.21 x $10^{-6}mm^3/Nm$ respectively. However, such incremental wear is not unknown (Cooper et al, 1993, b). On the 'incline' of the 'step', fatigue cracks were seen at x500 magnification at 216.8km on the wear face of UHMWPE pin 1, whereas at this sliding distance XLPE pin 4 showed none. Further, after 259.9km, at x500 magnification, the UHMWPE pin 3 also showed the same tiny fatigue cracks perpendicular to the direction of motion on its wear face. The levelling out of the 'step' above 281.4km could be due to the fatigued surface layer being completely removed from the wear face of the test pin (Cooper et al, 1993, b). Indeed, at 344.1km the fatigue cracks seen earlier on the UHMWPE pins 1 and 3 had been removed. This new visual appearance coincided with a reduction in wear due to weight loss which implied that, for the UHMWPE pins, fatigue wear ceased around 300km.

Table 4.22 Comparison of Ra values and wear factors (test 11)

Plate	Pin Material	Ra (transverse) start of test	Ra (transverse) end of test	wear factor, k x $10^{-6}mm^3/Nm$
2	XLPE	0.005	0.013	0.10
4	XLPE	0.005	0.008	0.38
3	UHMWPE	0.004	0.012	2.35
1	UHMWPE	0.004	0.037	4.14

The average wear factors of the test pins compared with the transverse roughness values of the 'wear' tracks of the plates, are given in table 4.22. The error in wear factors due to the Mettler balance was calculated to be ± 0.013 x $10^{-6}mm^3/Nm$, which was small in comparison with the wear factors determined. Pin 1 (UHMWPE) showed the greatest amount of wear, and rubbed against the plate which had the highest Ra values by the end of the test. However, the pin which

showed the least wear (pin 2, XLPE) did not rub against the plate which had the lowest Ra values at the end of the test. The plate with the lowest Ra of its 'wear' track was plate 4. As an aside, even after 10.3 million cycles, all of the Ra values measured would have been within the tolerance specified by BS7252, if they were measured from the head of a femoral component of a THR. Alphastep traces of the 'wear' tracks on plates 1 and 4 indicated the presence of a transfer film (Figures 4.32 and 4.33). Together with visual appearance and Talysurf Ra values, these Alphastep traces re-confirm that the transfer film was more significant in the case of UHMWPE than in XLPE. This result matches that found in the second stainless steel test (test 10). The implication then is that XLPE resists adhesive wear to a greater degree than UHMWPE, and it could be argued that such a result should be expected due to the stronger molecular links within XLPE compared with UHMWPE.

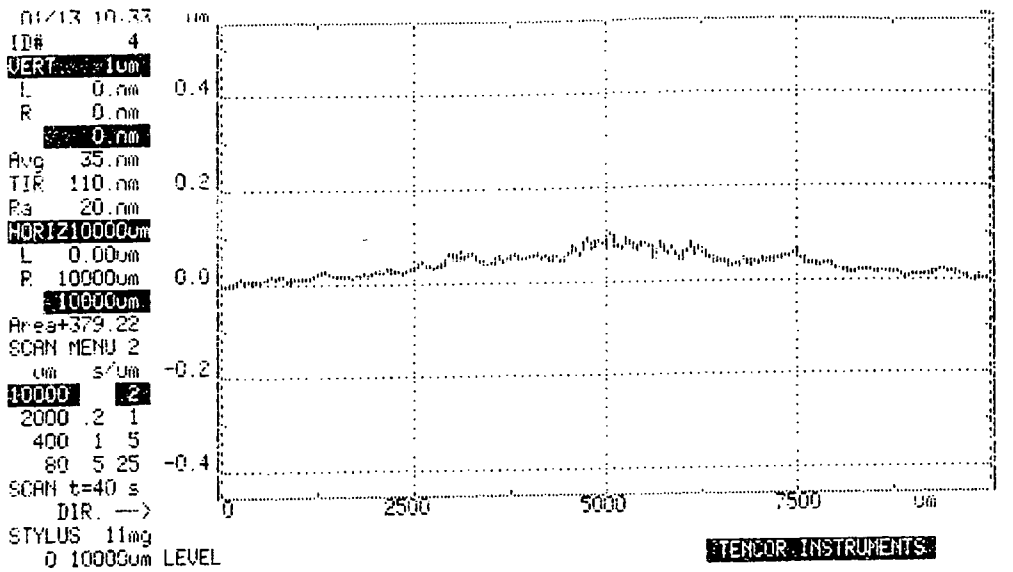

Figure 4.32 - Alphastep trace of Zirconia plate 4 showing XLPE transfer film (test 11).

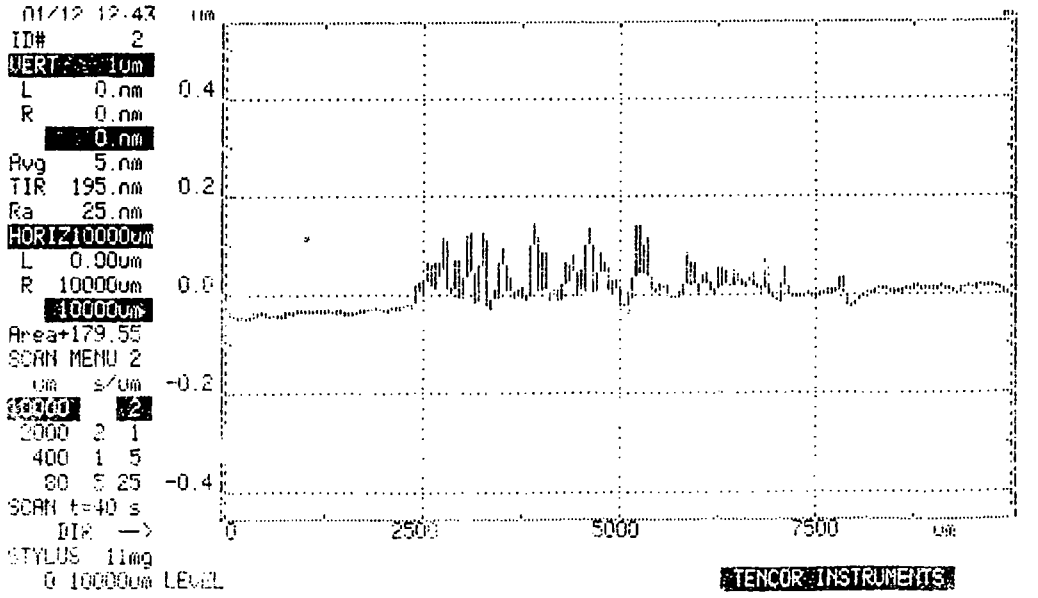

Figure 4.33 - Alphastep trace of Zirconia plate 1 showing UHMWPE transfer film (test 11).

4.9.6.2 Second Zirconia Test - Test 12

After 299km (7.1 million cycles) average wear factors for the UHMWPE pins of 0.009 x $10^{-6}mm^3/Nm$, and 0.013 x $10^{-6}mm^3/Nm$ for the XLPE pins, were measured. An error for the wear factors of ± 0.018 x $10^{-6}mm^3/Nm$ due to the Mettler balance was also calculated, which can be seen to be significant. Therefore it can be seen that the amount of wear measured was very low. In turn, lubricant absorption by the control pins was of the order of the weight loss of the test pins. The fatigue of the UHMWPE test pins seen in tests 11 and 13 was not repeated in this particular test. On each of the plates, a transfer film could be seen, but it was far less prominent than those seen in the other two zirconia tests. Also, Ra values remained almost unchanged throughout the duration of the test. Therefore the question must be asked whether regular cleaning of the plates during the test (a necessary pre-requisite to their Ra measurement) may have reduced the transfer film. A reduced transfer film in turn could explain the low Ra values, and therefore the low wear. Plate weight had shown a slight increase by the end of the test, probably caused by the transfer film. Figure 4.28 shows a graph of pin wear against test duration.

4.9.6.3 Third Zirconia Test - Test 13

The results of this test implied that initial surface roughness of the test plates had little affect on the test pins, because up to 73km, wear of all the test pins was within the error of the Mettler balance (±0.0001g). Instead fatigue of the UHMWPE test pins was significant (Figure 4.29). Between 2.3 and 2.6 million cycles (106km and 118km) the UHMWPE test pins fatigued, then between 2.6 and 2.8 million cycles (118km and 131km) at which point the test ceased, a massive increase in wear of the UHMWPE test pins took place. After 131km (2.8 million cycles) average wear factors for the UHMWPE pins of 20.4 x $10^{-6}mm^3/Nm$, and 2.23 x $10^{-6}mm^3/Nm$ for the XLPE pins, were measured. Obviously such a large amount of wear in turn generated a large amount of wear debris, which may have led to third body wear. Weight losses from the test pins in this test were greater than in the other two zirconia tests and was such that errors due to the Mettler balance were negligible in comparison.

4.9.7 Comparison of Zirconia results with those of other workers

Table 4.23 Comparison of zirconia results

Researcher	Load N	Dist km	No. cycles ($x10^6$)	k x 10^{-6} mm^3/Nm
Saikko 1993 (mean of 3)	225	350	7	0.0026
Derbyshire et al 1994 (2 off)	80	173	2.06	0.01 & 0.1
Kumar et al 1991 (mean of 3)	219	65	1.3	0.038
Joyce (test 11)	40	392	10.3	4.14 & 2.35
Joyce (test 12)	40	299	7.1	0.013 & 0.005
Joyce (test 13)	40	131	2.8	30.6 & 10.2

To permit an approximate comparison, wear factors from tests 11, 12 and 13 are given for the total weight loss over the total distance. All of the results above are associated with zirconia plates having a Ra value of less than or equal to 0.005μm, except in test 13 where two plates deliberately had a higher Ra value. All tests were undertaken using reciprocating rigs, UHMWPE test pins and de-ionised water as a lubricant.

No wear tests of XLPE rubbing against zirconia ceramic have been reported in the literature. Therefore this section refers only to a comparison of the wear of

UHMWPE test pins against zirconia. The results reported by other researchers cover three orders of magnitude, but despite this fact, the results returned from tests 11 and 13 are still outside of this range. How can this discrepancy be explained?

In part, an explanation may lie in the fact that a transfer film was built up over the duration of the test. As this transfer film increased in magnitude, so the equivalent roughness of the plates increased and in turn so did the wear of the test pins. Indeed, where a low Ra value of the 'wear' track was maintained (test 12) negligible wear occurred. Both Saikko (1993) and Derbyshire et al (1994) found a transfer film for UHMWPE rubbing against zirconia in distilled water. Crucially, their results indicate the range of wear factors - three orders of magnitude - all attributable to either a beneficial or a destructive transfer film. Kumar et al (1991) did not find a transfer film, although this fact may be explained by the short duration of their tests which, at 1.3 million cycles, may have been insufficient to produce a transfer film. Indeed in all three zirconia tests reported in this thesis, at 1.3 million cycles and below, there was negligible pin wear, giving results which compare favourably with those of Kumar et al (1991).

The second element of an explanation regarding the wear of the UHMWPE pins, was that they showed fatigue wear which greatly increased the overall wear factors measured. It is interesting to note that fatigue of the UHMWPE pins was found to occur after 3.46 million cycles in test 11, and after 2.31 million cycles in test 13. Fatigue wear is, by definition, related to the number of cycles undertaken. Both Kumar et al (1991) and Derbyshire et al (1994) undertook tests which ceased before such a number of cycles had been completed. However, the tests carried out by Saikko (1993) reached 7 million cycles and found no fatigue wear, although test 12 also passed 7 million cycles without finding fatigue wear.

4.9.8 Comparison of Zirconia and Stainless Steel Results

Table 4.24 Comparison of zirconia and stainless steel results

Test Number	9	10	11	12	13
Plate Material	Stainless Steel	Stainless Steel	Zirconia	Zirconia	Zirconia
Distance (km)	471.5	448.5	391.9	298.8	130.7
No. cycles ($x10^6$)	7.858	7.478	10.314	7.115	2.841
Stroke (mm)	30	30	19	21	23
Load (N)	40	40	40	40	40
Pin Diameter (mm)	5	5	5	5	5
No. of UHMWPE Pins	2	2	2	2	2
No. of XLPE Pins	2	2	2	2	2
Lubricant	Distilled Water	Distilled Water	Distilled Water	Distilled Water	Distilled Water
Av. plate wt. change UHMWPE ($x10^{-4}g$)	+3	+6	+0.5	+1.5	+2
Av. plate wt. change XLPE ($x\ 10^{-4}g$)	+4	+3.5	+1	+2	+1.5
Av. initial plate Ra (μm)	0.031	0.027	0.005	0.005	N/A
Speed (cpm)	41.7	41.7	60.4	60.4	60.4
Mean k UHMWPE ($x10^{-6}mm^3/Nm$)	0.017	0.35	3.24	0.009	20.4
Mean k XLPE ($x10^{-6}mm^3/Nm$)	1.31	0.60	0.24	0.013	2.23

On first viewing there appears to be little that can definitely be said about the wear of the two types of polyethylene against the stainless steel and zirconia plates. For example, the greatest and the least wear both occurred with zirconia plates, and UHMWPE test pins showed the greatest and the least wear factors. Further the wear factors measured covered three orders of magnitude.

One reason for the range of reported wear factors is wear data variability (Wallbridge and Dowson, 1987). The second reason is the build up of a transfer film in tests which employed distilled water as a lubricant (Cooper et al, 1993, a). This transfer film can serve either to reduce the roughness of the counterface, and

therefore reduce the amount of wear; or to increase the roughness of the counterface, and therefore increase the amount of wear (Brown et al, 1976).

All five tests reported in this thesis also showed that each of the test pins had a period of low wear, which is indicated graphically by a flat gradient, as shown in Figures 4.21, 4.22, 4.27, 4.28 and 4.29.

A final common point is that each test found fatigue wear of one material. This fatigue wear was indicated by the visual appearance of the wear faces of the test pins, and graphically by the steep gradient of the wear curve. However, for the stainless steel tests the fatigued material was the XLPE, but for the zirconia tests it was the UHMWPE test material that tended to fatigue.

Regarding the fatigue of the UHMWPE pins, such a phenomenon has been reported elsewhere in the literature (Cooper et al, 1993, a and b). This fatigue has been explained by the build up of plastic shear strains under the peaks of the polymer, which are developed during long periods of sliding against a hard, smooth counterface (Ra consistently less than 0.02μm). Therefore the theory indicates that fatigue is dependent on the Ra value, and will occur if the Ra value of the hard counterface is maintained below 0.02μm. The theory continues that, for higher Ra values, the roughness of the hard counterface then becomes the dominant factor, with the dominant wear regime changing to abrasive.

On the basis of the wear factors reported from the two stainless steel tests undertaken, XLPE shows higher wear against stainless steel than does UHMWPE. More importantly, the high XLPE wear factors reported were thought to have been due to fatigue wear. This conclusion is based upon visual appearance of the wear faces of the XLPE test pins and the shape of the XLPE wear graphs (Figures 4.21 and 4.22). It has been proposed that the cross-linking process may have reduced the material's ductility. Ductility which was required to cope with repeated deformation by the hard stainless steel counterface which occurred during the reciprocating tests.

A transfer film was found on all test plates at the cessation of each of the five tests. However, the transfer film was less significant in the case of the zirconia tests than in the stainless steel tests. Why should this be? In part the greater roughness of the stainless steel plates may be the reason. Also, ceramics are said to possess a higher degree of wettability than metals, that is they attract liquids

more, so that the solid to solid interaction necessary for adhesive wear is less likely to occur.

Further, with both the stainless steel and the zirconia test plates, Alphastep traces of the 'wear' tracks revealed the transfer film to be deeper and wider in the case of the UHMWPE pins than in the case of the XLPE pins (Figures 4.25, 4.26, 4.32 and 4.33). As UHMWPE produces a heavier transfer film than XLPE, therefore it can be argued that XLPE resists adhesive wear to a greater degree than UHMWPE. This would be expected as the cross-links between the molecules, much fewer in UHMWPE, resist material being removed from the bulk material.

From the zirconia tests (tests 11, 12 and 13) it was noted that longitudinal Ra values of the wear track were measured to be approximately equal to those transversely (both during and at the end of the test). This fact is in opposition to the XLPE against XLPE results (in which the transverse Ra values were very much greater than the longitudinal Ra values) and to the polyethylene against stainless steel results (in which the transverse Ra values were greater than the longitudinal Ra values). This result may be a further indication that the transfer film on to zirconia plates was less significant than that occurring on the stainless steel plates.

In the third zirconia test, test 13, the high initial surface roughness of two of the test plates appeared to have little effect on the wear of the test pins rubbing against them. Up to 73km, all test pins showed negligible wear.

On the basis of the five tests reported in this thesis, XLPE shows higher wear against hard counterfaces than UHMWPE. However, some recent work has called into question the validity of reciprocating tests with respect to the wear of UHMWPE. Wang et al (1996) investigated the discrepancy between wear factors achieved from reciprocating rigs with those obtained from joint simulators. Often the case was that two orders of magnitude difference existed between wear factors, with reciprocating rigs showing the lower wear. Wang et al (1996) proposed that the reason for this difference was that the UHMWPE test specimens in reciprocating tests showed a molecular re-alignment which was condusive to low wear. However, in a joint simulator with three degrees of motion, this molecular re-alignment could not occur and therefore wear factors approached those found in vivo. In addition, visual appearance of test specimens from a simulator matched that of the multi-directional scratches seen on explanted

femoral heads (Hall et al, 1996) whereas wear faces from reciprocating tests did not show such scratches.

Wang et al (1996) further proposed that the wear of UHMWPE components could be reduced if links between the polyethylene molecules could be strengthened. One method suggested was cross-linking. These researchers therefore undertook tests in which they achieved cross-linking by irradiating their UHMWPE test specimens. They then compared the wear of the irradiated and non-irradiated UHMWPE. In the reciprocating tests the irradiated UHMWPE showed the greater wear, but on the simulator test, the irradiated UHMWPE showed less wear. Wang et al (1996) quoted a cross-linking of 45% to 60% in their irradiated samples. It is unlikely that the irradiation process could hope to achieve the degree of cross-linking seen with the silane method. Further, the results of the finger simulator tests reported in this thesis indicate that the greater the degree of cross-linking, the lower the wear of the test component. Therefore potential for the use of silane cross-linked polyethylene as a replacement for UHMWPE as a load bearing biomaterial does exist.

The importance of multi-directional motion, as opposed to the bi-directional motion found in reciprocating tests, has also been pointed out lately by Bragdon et al (1996). For the tests reported in their paper, with unidirectional motion no measurable wear of the (UHMW) polyethylene components was found. When multi-directional motion was introduced, wear volumes comparable with those found in vivo were measured. Further, the surface topography of the wear surface of components tested using multi-directional motion was also found to be similar to that found from explanted polyethylene components.

4.9.9 Future tests

Part of the reason for the wear of the test pins has been speculated as being due to the presence of a transfer film which has served to increase the counterface roughness and in turn, the wear of the test pins. By changing to bovine serum as a lubricant, the formation of a transfer film should be prevented. Therefore it is suggested that the tests be repeated with this lubricant.

The recent work by Bragdon et al (1996) and Wang et al (1996) proposes that a test which moves away from reciprocating motion, and includes a third direction of motion, would provide in vitro wear factors closer to those found in vivo. Therefore it is suggested that a rotational element be added to the test pins in the reciprocating rigs, and that the tests be repeated. Perhaps, in such an instance, the wear of XLPE against hard counterfaces would be found to be less than that of UHMWPE.

4.10 Test of Polyethylene Plates Rubbing Against Stainless Steel Pins

4.10.1 Aim

The aim of this test was to compare the wear of irradiated UHMWPE with that of irradiated XLPE, both being rubbed against stainless steel pins. By reversing the 'soft pin, hard counterface' situation of the previous stainless steel and zirconia tests, it was intended to investigate whether cyclic loading of a polyethylene plate, rather than the constant loading of a polyethylene pin, as seen in all earlier hard counterface tests, could cause greater plate wear through a fatigue process.

4.10.2 Pin Wear Factors and Test Conditions

Table 4.25 Summary of test conditions and polyethylene plate wear factors

Test Number	14
Plate Material	UHMWPE and XLPE
No. cyc ($x10^6$)	1.894
Stroke (mm)	28
Load (N)	40
Pin Diameter (mm)	5
Pin Material	Stainless Steel
No. of XLPE Test Plates	2
No. of UHMWPE Test Plates	2
Lubricant	Distilled Water
Speed (cycles per minute)	60
k UHMWPE ($x10^{-6}mm^3/Nm$)	45.9 and 74.7
k XLPE ($x10^{-6}mm^3/Nm$)	45.7 and 38.9

The stainless steel pins were manufactured with a 5mm diameter wear face to give the same nominal contact stress as that in the earlier pin on plate tests, but had the addition of a large radius around the periphery of the test pin in an aim to minimise any cutting of the polyethylene by any sharp edges on the rim of the metal test pin. All pins were manufactured from 316 stainless steel, and a test pin is shown in Figure 4.34. The wear faces of the pins were finished by the same method as applied to the stainless steel plates. Therefore it was assumed that a similar roughness value, of less than 0.05μm Ra, would be achieved. Two control plates, one UHMWPE and one XLPE, were also included to give an indication of the amount of water absorption by the test plates.

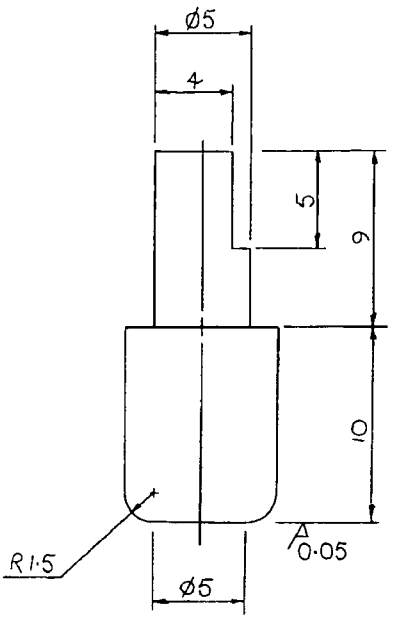

Figure 4.34 - Drawing of a stainless steel test pin

4.10.3 Visual Changes

Scratches in the direction of sliding were seen on the wear face of each of the pins at the cessation of the test. A fully formed wear track had appeared on each of the XLPE plates by 23.4km. For the UHMWPE plates, this situation was reached at 36.9km. Long ribbons of polyethylene debris were produced from all test plates. This fact is in contrast to all earlier tests where debris was of a more particulate form, and may indicate that tearing of the polyethylene plates was occurring at the periphery of the pins. A side effect of the high wear measured was that a great deal of wear debris was generated. As with the pins, the

dominant feature of the wear track of the plates was scratches in the direction of sliding. Due to the high yet different amounts of wear measured, testing of plate 2 (UHMWPE) ceased at 54.7km, plates 1 and 3 (both XLPE) at 63.9km and plate 4 (UHMWPE) at 106.1km.

4.10.4 Pin Weight Changes

Table 4.26 Stainless steel pin weight changes

Pin No.	Initial Pin Weight (g)	Final Pin Weight (g)	Difference ($x10^{-4}g$)
1	4.9170	4.9169	-1
2	4.9965	4.9964	-1
3	4.8661	4.8860	-1
4	4.9727	4.7223	-4

For three of the test pins, the difference in weight between the beginning and the end of the test was within measurement error of the Mettler balance, which was taken to be $\pm$ 1 $x10^{-4}g$. Pin 4, which was involved in the longest test, showed the greatest weight loss. However, pin weight change was negligible compared with plate weight change. It was assumed that there would be no increase in weight due to water absorption by the stainless steel pins.

4.10.5 Discussion of Results

The plate weight change results indicated that wear was relatively low up to approximately 9.4km. After this point however, the XLPE wear increased markedly but remained linear. In contrast, the UHMWPE maintained a lower overall wear until the wear suddenly increased; above 36.9km for one UHMWPE plate (plate 2) and above 64.3km for the other UHMWPE plate (plate 4). The plate wear results are shown graphically in figure 4.35.

Figure 4.35 - Wear of XLPE and UHMWPE Plates Under 40N Loads Against Stainless Steel Pins

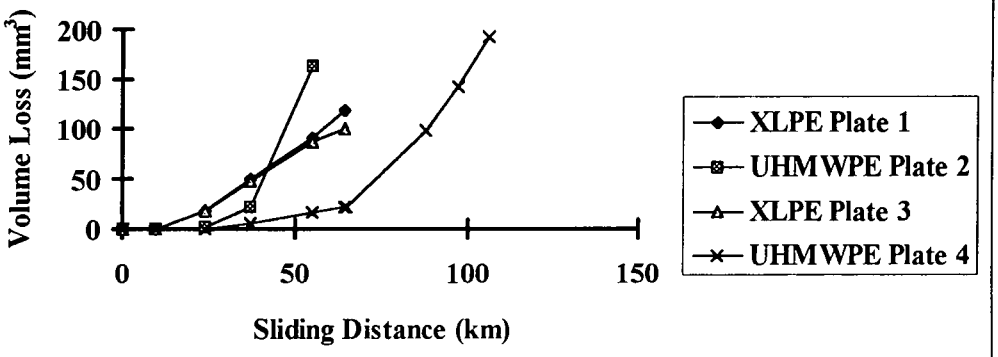

The wear factors at the cessation of the test for each plate were as follows. For the XLPE plates, wear factors of 45.7 x $10^{-6}mm^3/Nm$ for plate 1 and 38.9 x $10^{-6}mm^3/Nm$ for plate 3 after 63.9km were calculated. For the UHMWPE plates, the wear factors were measured to be 74.7 x $10^{-6}mm^3/Nm$ after 54.7km for plate 2 and 45.9 x $10^{-6}mm^3/N$ after 106.1km for plate 4.

The amount of water absorption by the control plates was small in comparison with the loss of weight of the test plates due to wear. The actual values of weight change due to water absorption are given in table A6.6 of appendix 6, and are discussed there.

For both test pins and test plates the dominant visual appearance of the wear face was scratches in the direction of sliding, indicating abrasive wear. Although test pin weight loss was negligible in comparison with that of the test plates, it was interesting to note that in the two tests involving stainless steel plates (tests 9 and 10) an increase in the weight of the stainless steel component, however slight, was always found.

The wear factors measured in this test were greater than in any of the other polyethylene against hard counterface tests. This fact indicates that cyclic loading was important in the wear of the polyethylene material.

4.10.6 Comparison With Other Researchers

Only rarely have other researchers employed metal pins against a polyethylene counterface. Wright et al (1982) undertook a test using a pin and disc machine. They used a test pin of 8mm diameter, with the rubbing end having a spherical radius of 200mm together with a surface finish of better than 0.05μm Ra. They found all wear against time graphs of the UHMWPE discs to be linear, and a wear factor of 0.26 x $10^{-6}mm^3/Nm$ was calculated. Unfortunately, Wright et al (1982) did not repeat their tests with pin and plate material reversed.

Barbour et al (1996) conducted a reciprocating pin on plate test with a cobalt chrome pin articulating against an UHMWPE plate. The pin had a spherical wear face. Wear factors were found to be approximately ten times greater than those where a UHMWPE pin rubbed against a cobalt chrome plate. Specifically, wear factors of 0.13 x $10^{-6}mm^3/Nm$ for the metal pin test and 0.01 x $10^{-6}mm^3/Nm$ for the polymeric pin test were measured.

The plate wear factors reported in this thesis are higher than those reported by Barbour et al (1996) and by Wright et al (1982). It may be that the edge of the metal test pins tore the polyethylene plates, therefore it is suggested that the tests be repeated with pins having spherical wear faces.

However, as with the work of other researchers it was again seen that, by having a 'hard' pin articulating against a 'soft' counterface, higher wear factors than the reverse situation were found.

4.11 Comparison of Finger Function Simulator (XLPE Prostheses) and Pin on Plate (XLPE against XLPE) Results

All test specimens, both those from the pin on plate machine and those from the finger function simulator, showed wear surfaces with scratches in the direction of sliding. This fact indicated that the same macroscopic wear mechanism of abrasive wear appeared to be dominant in each of the tests. For the same (distilled water) lubricant, corresponding gel content and equal sliding distance, each of the prosthetic components had wear factors approximately half those of

the plates from the pin on plate machines (figure 4.36). However, when the total wear was considered, then a much closer similarity was seen (figure 4.37). That the prosthetic components had slightly lower wear factors may be explained by the lower stress values across the test components in the simulator, or perhaps by higher speeds of the test components in the simulator leading to increased hydrodynamic lubrication.

Figure 4.36 - Comparison of Finger Function Simulator and Pin On Plate Wear Results - Individual Components

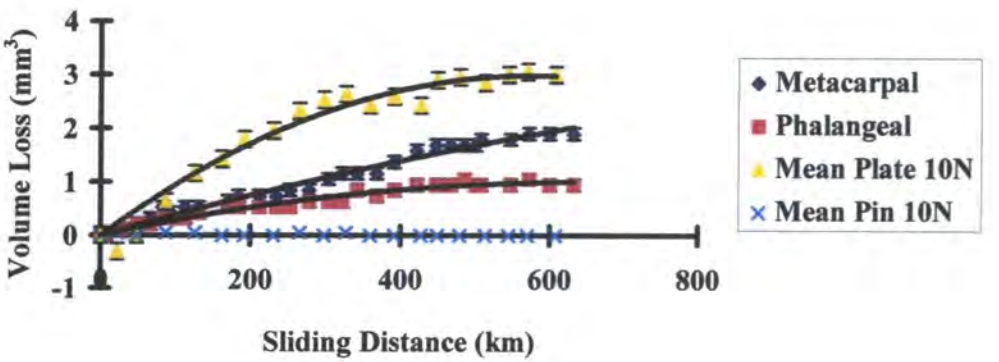

Also, the wear factors for the prosthetic components were calculated from a sliding distance based on the maximum radius of the spherical contact. For such a spherical contact, the sliding distance varies with the further away from the centre of the contact (Calculation A5.1). Therefore it could be argued that the actual wear factors of the prosthetic components should be higher and therefore approach those of the total pin on plate wear factors.

Figure 4.37 - Comparison of Finger Function Simulator and Pin on Plate Results

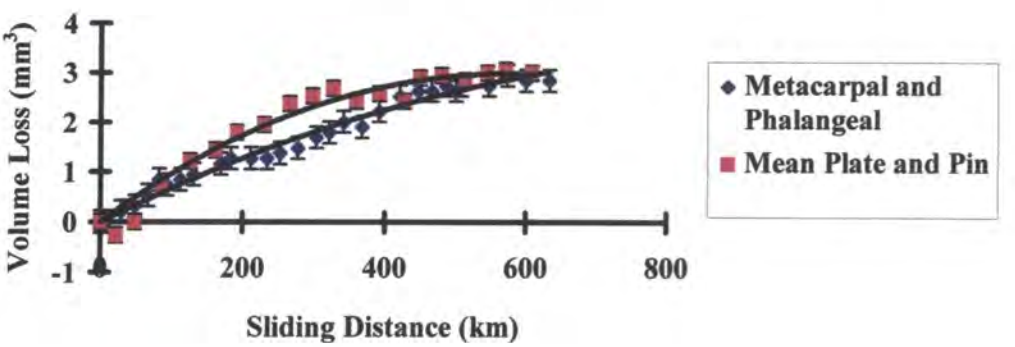

Table 4.27 Comparison of simulator and pin on plate results

Rig	Finger Simulator	Pin On Plate
Sliding Distance (km)	600	608
Load (N)	12.5	10
Test Number	3	3
Stress (MPa)	0.08	0.80
Gel Content	87%	86%
Av. speed (mm/s)	55	37
k ($x10^{-6}mm^3/Nm$)	Metacarpal 0.25 ±0.03 Phalangeal 0.13 ±0.03	Pin 0 ±0.04 Plate 0.49
k 'total' ($x10^{-6}mm^3/Nm$)	0.38 ±0.06	0.49 ±0.04

The fairly close match in wear factors from simulator and reciprocating machine shown in table 4.27 is not always reported in the literature. For example Wang et al (1996) report wear factors for UHMWPE rubbing against cobalt chromium alloy in a reciprocating machine of $4.75 \times 10^{-9}mm^3/Nm$, while the same material combinations in a hip simulator gave wear factors of $5.3 \times 10^{-7}mm^3/Nm$. A difference of two orders of magnitude. Derbyshire et al (1993), while trying to explain the lower wear factors obtained from their pin on plate machines in comparison with their joint simulators, postulated that wear may be accelerated by cyclic loading rather than constant load. Indeed the differences between XLPE plate wear and XLPE pin wear reported in this thesis imply such a 'fatigue' theory to be feasible. Also the importance of the correct type of motion during laboratory testing has been seen to increase wear factors to values comparable with those found in vivo (Bragdon et al, 1996).

Water absorption of XLPE control components was found to be significant in the simulator tests but the situation was different for the control components in the pin on plate tests.

The XLPE control pins in the pin on plate tests showed no lubricant absorption outside of the accuracy of the weight measuring equipment. Although typically some 50% heavier than a phalangeal control component (which did show significant water uptake) this lack of lubricant absorption for the control pins may be explained by a number of points. Firstly the control pins were not fully submerged whereas the prosthetic controls were. Furthermore the prosthetic controls had a large surface area for their low weight, compared with the relatively compact control pins which had a higher surface area to weight ratio.

Regarding XLPE control plates, appendix 6 indicates that beyond approximately 100 days, all control plates had a weight below that originally measured. Such a result was both unexpected and remarkable. It may be that in the environment of 37°C water the XLPE control plates continued slowly to cross-link, and as these new molecular bonds were formed the distilled water that had originally been soaked up, was pushed out. The effect of the compensation for fluid uptake on an XLPE test plate (mean of test 3 plates under 10N load) can be seen in Figure 4.38. Although the initial 'weight loss' is increased, over time the overall effect is to reduce the 'wear', and to a level closer to that indicated by the wear factors for the prosthetic components.

Figure 4.38 - Weight change of test plate compensated for fluid uptake of control plate

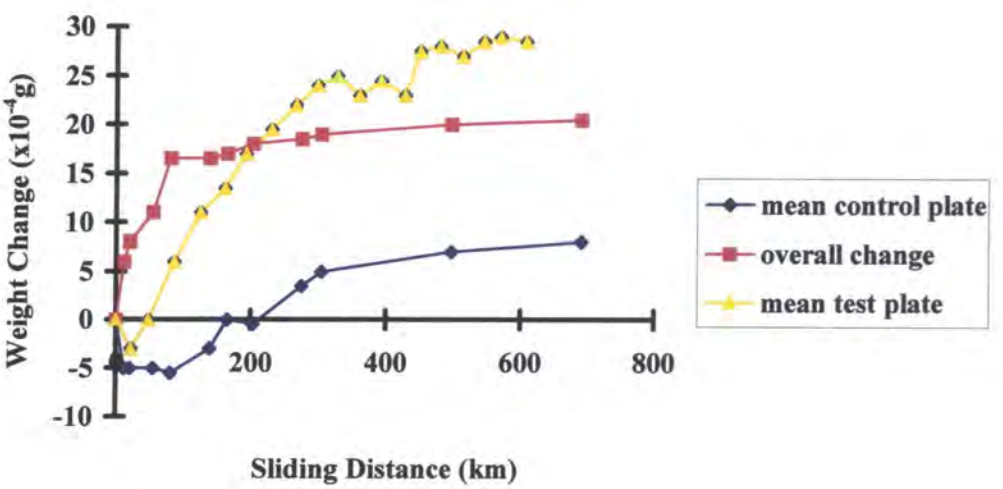

CHAPTER FIVE

New Finger Function Simulator Design

5.1 Introduction

While wear testing the Durham metacarpophalangeal (MCP) prosthesis, several problems with the Stokoe finger function simulator were revealed. These were therefore eliminated. In addition, a second finger function simulator was designed which maintained the positive aspects of the Stokoe simulator while overcoming its faults.

5.2 Assessment of Stokoe Finger Function Simulator

5.2.1 Positive Aspects

The synergistic action of pinch load applied regularly in between flexion-extension had been shown to reproduce failures of the Swanson prosthesis in a time and a manner comparable with surgical experience (Stokoe et al, 1990). In tandem with realistic loads, the re-creation of natural MCP joint motion using artificial 'tendons' was considered to be important. The cantilever and strain gauges combination offered a simple yet effective load measuring mechanism. All of these aspects were therefore carried forward to the new simulator design.

5.2.2 Faults

Experience of operation had shown that the 'tendons' stretched, leading to a gradual reduction in the load across the test prosthesis and necessitating regular manual re-tensioning to restore the desired load. Therefore a new method of drive and load actuation which would overcome these problems was sought. The positions of the metacarpal prosthetic component, phalangeal prosthetic

component and the centre of joint rotation were all independent of each other. Additionally, the bath in which testing took place was not fixed relative to the rest of the mechanical components. Therefore a long learning curve had to be traversed before suitable positions for each of these components could be found which achieved the desired 90° arc of motion together with the loads required across the test prosthesis. In the thesis (Stokoe, 1990), no reference was given as to how the positions of the pulleys which represented the tendon sheathes and ligaments were chosen, therefore concern existed that joint motion may not have been exactly reproduced. Smaller problems included rotation of the cantilever, which meant that the metacarpal component moved from its original position, and many of the mechanical components were overly complex. Finally, problems with the electronic components and computer software meant that load measurement from the BBC computer was unavailable. Instead two voltmeters were used to measure the load across the test prosthesis in the axial and dorsal/palmar directions.

5.3 Summary of Improvements in the New Finger Function Simulator

5.3.1 Load Actuation

The challenge was to apply two different magnitudes of load successfully and reliably. Loads from 10-15N were required for flexion-extension, while a load of up to 322N was necessary to simulate pinch grip. Pneumatics were chosen for load actuation as they offered an inexpensive, reliable, clean, and effective means of driving the new finger function simulator, which is intended to be run continuously for several weeks. One size of pneumatic cylinder could not alone provide both the flexion-extension and 'pinch' grip loads, therefore separate sizes of cylinder were chosen. Crucially, the use of pneumatics would automatically counter any stretching of the 'tendons' by taking up this stretching, as air pressure and therefore load remained constant. Further, the potential of closed loop control of the pneumatic circuit was available.

Other options of load actuation were also considered, but eventually rejected. Use of a rotary actuator would have necessitated a spring mechanism to ensure that most of load was applied through the flexor 'tendon', leading to the same

problems of load reduction when the 'tendons' stretched as in the Stokoe design. Similarly, a rack and pinion drive mechanism would not have offered the opportunity for closed loop control. Hydraulics are significantly more expensive than comparable pneumatic components, and low cost was an important consideration in the design of the new simulator.

5.3.2 Location of Components

The positional inaccuracies associated with the Stokoe simulator were eliminated in the new design. The bath in which testing took place was bolted to the main frame so that the exact location of components within the bath became fixed. Similarly, the position of the metacarpal prosthetic holder was also fixed. Set up therefore became much simplified and repeatable.

Stokoe (1990) did not specify how the tendon pulley positions were chosen, therefore MCP joint geometry was re-examined and, with exact dimensions from references, the precise positions of the necessary 'pulleys' with respect to the centre of rotation of the metacarpal head was recreated (Appendix 8).

5.3.3 Electronic Components

A 386 computer facilitated both force measurement and simulator control. A direct value of load across the prosthesis was output to screen. Being computer controlled, software could be easily altered to vary the make up of a load cycle. Further, the option remained of upgrading to closed loop control of the pneumatic components should it ever be required. The other part of the control circuit was an input/output (I/O) card together with a bespoke electronic control circuit mounted on its own board. In total, these components provided control signals for the pneumatic circuit, rather than the mechanical mechanism used on the Stokoe simulator. The use of the combined 'PC-Alpha-G' strain gauge amplifier/A-D card significantly reduced the overall size of the simulator.

5.3.4 Design of Individual Mechanical Components

The cantilever was designed with a square section upper stem, to fit within a milled slot in the bridge. In this way, cantilever rotation was prevented and removal and refitting of the cantilever became much simplified. Both of these problems afflicted the Stokoe simulator. The design of components to fit in the test bath was also simplified, which permitted their rapid manufacture with subsequent cost savings and led to the new simulator being smaller than the Stokoe design.

5.4 Description of New Finger Function Simulator

5.4.1 Introduction

The new simulator can be described in three parts. These are the bath components, the drive and pinch mechanism, and the control and measurement circuitry. In the following sections; 5.4.2, 5.4.3 and 5.4.5; the values in curved brackets correspond with those shown on the general arrangement drawings in appendix 9.

5.4.2 Bath

At the heart of the new simulator is the bath (1) where testing took place. Each prosthetic component was mounted in its own holder (3, 15) and each holder represented the appropriate finger bone. Both holders had shoulders to fix their location so that the prosthetic components could be placed in exactly the same position from test to test. The nylon phalangeal clamp (2) contained two magnets (29), each of which acted as a signalling device to control the flexion-extension motion. The phalangeal clamp was positioned between the phalangeal arc (4) and the base plate (28). Therefore motion of the joint was limited to the plane of flexion-extension. By making this plane horizontal, any gravitational effects on the motion of the joint were removed. The clamp also showed low friction against the stainless steel base (28) and the UHMWPE arc (4).

The metacarpal component was held stationary, and the phalangeal component oscillated against it under the action of the 'tendons' (20). Load was measured via 8 strain gauges, mounted on a square section cantilever (30). These were protected from the ingress of any lubricant by a layer of silicone sealant. Two artificial 'tendons' (20) were used to represent the action of all the tendons and muscles associated with the MCP joint. The 'tendons' were 130lb breaking strain braided nylon fishing line. These 'tendons' were retained at the back of the phalangeal clamp by stainless steel split pins.

The use of magnets (17), positioned in slots cut in to the ends of the phalangeal clamp arc (4), allowed adjustment of the movement of the phalangeal clamp, so that a 90° arc of motion could be achieved. The heights of the prosthetic components and the 'tendon' guide pulleys (27) were equalised so that the faces of the prosthetic components sat together correctly.

A free moving pulley (16) attached to the base plate, represented the volar plate and metacarpoglenoidal ligaments. The base plate (28) was attached to the bridge (14) by a brace of stainless steel support columns (32). Therefore the bath components were fixed in position relative to each other.

On the lid of the bath was mounted a 24V 'thumb' solenoid with a stainless steel rod inserted (31). The stainless steel rod acted as a 'thumb' against which the 'pinch' load was applied. When activated this rod passed through the phalangeal arc (4) at a position equivalent to 30° of MCP joint flexion, and into a hole drilled in the base plate (28). 30° flexion is a typical 'pinch' grip position for the MCP joint.

The base plate (28) was attached to the phalangeal arc (4) by three stainless steel columns (18). The base plate (28) sat in a perspex bath (1), so that the operation of the joint could be visually monitored. The same Grant circulating bath that supplied the Stokoe finger function simulator also supplied the new simulator with lubricant at 37°C. Again there was a gravity return for the overflow.

Figure 5.1 shows a test Durham prosthesis in place. The metacarpal component can be clearly seen, although the phalangeal component is hidden by its holder (3) which in turn is mounted in the phalangeal clamp (2). Figure 5.2 shows the test bath in place, and also the phalangeal arc (4) has been added. Mounted within the phalangeal arc, the two arc magnets (17) can be clearly seen. Lastly, Figure

5.3 gives a general view of the simulator, with the flexor (8) and extensor (12) pneumatic cylinders pictured on the aluminium slider (6). Behind these cylinders, their regulators controlling the air supply to them can be seen. The lid of the test bath is in place, with the 'thumb' solenoid (31) mounted on it, and the lubricant supply pipe threaded through it.

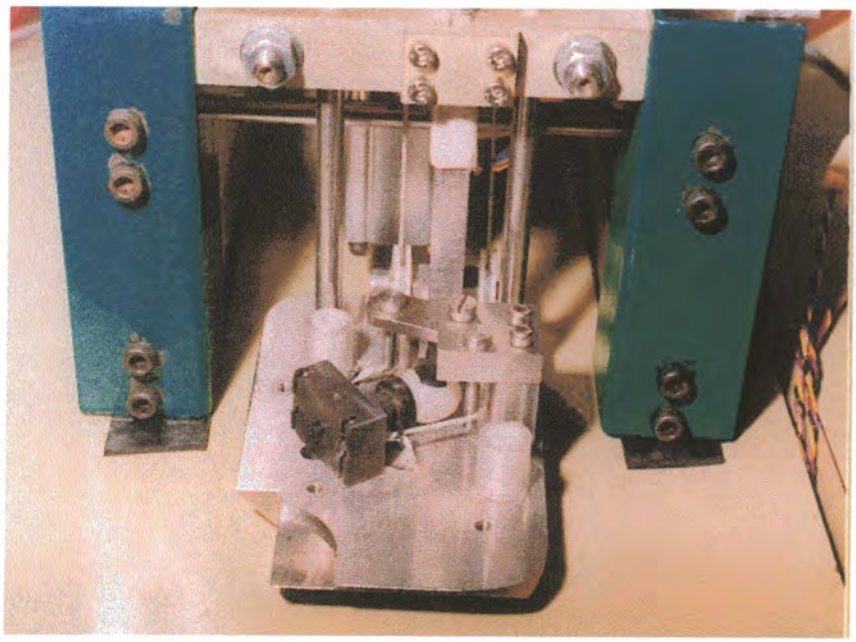

Figure 5.1 - New finger function simulator - test components in place

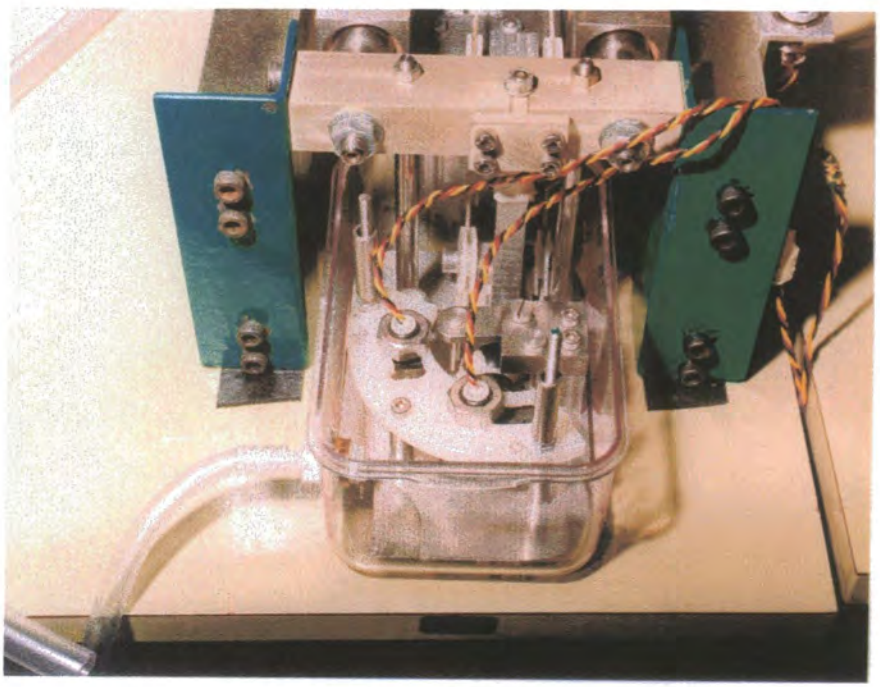

Figure 5.2 - New finger function simulator - test bath in place

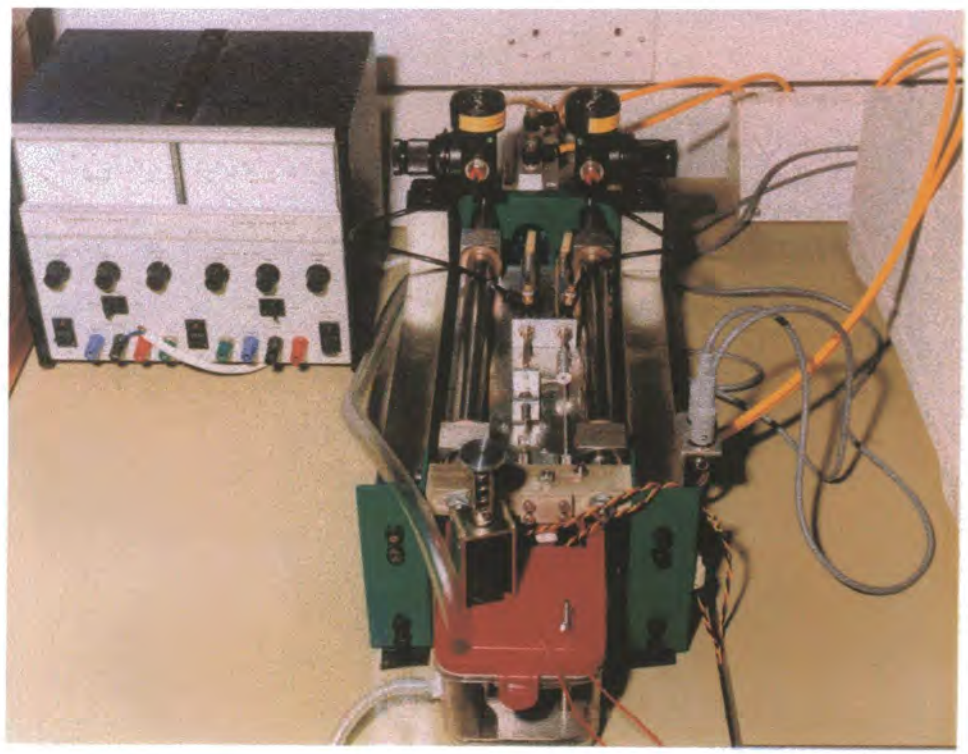

Figure 5.3 - New finger function simulator - general view

5.4.3 Drive and Pinch Mechanisms

Behind and above the bath were the pneumatic cylinders which provided the drive and pinch mechanisms. By mounting the cylinders in a horizontal position, rather than vertically as in the Stokoe design, the need to lift components against gravity was removed. Pulleys (19) guided the 'tendons' (20) to the two 10mm bore cylinders which provided flexion and extension (8, 12). These were mounted on an aluminium slider (6) which in turn was connected by a universal coupling (11) to the larger 32mm bore cylinder (24) which provided the 'pinch' load. Two 20mm diameter stub steel rods (7) each mounted within a pair of oil-lite bushes (9) allowed movement of the light aluminium slider when the 32mm bore cylinder was activated.

The framework consisted of 30mm x 30mm mild steel bar (5) with a mild steel plate (10) at the rear, on which the 32mm bore pneumatic cylinder was mounted. The framework had been nickel coated to protect it from corrosion. All the pneumatic cylinders were fitted with throttles to smooth the application of load

and permit the speed of cylinder operation to be controlled. The rod of each 10mm bore cylinder was fitted with an adjuster (13, 21) to permit the optimisation of 'tendon' length. The flexor adjuster also doubled as one of the components which facilitated 'pinch' load to be applied to the test prosthesis.

The throttle (22) and restrictor (23) mounted on each of the flexion and extension cylinders ensured that there was a residual air pressure in each cylinder during flexion and extension. Together with compressed air always being supplied to one cylinder, this set up assured that the phalangeal component was always held against the metacarpal component and that load always passed across the artificial joint. This situation therefore mimicked the support of the collateral ligaments. An inherent cushioning during flexion-extension was provided by the 10mm bore cylinders always being operated near mid-stroke and by throttles which ensured a base pressure was maintained in each. A range of speeds of flexion-extension were available. Speed was controlled by air pressure and by the throttles mounted on the 10mm bore cylinders. However, most important of all, the 10mm bore cylinders would each pull to a position given by the magnets. Therefore any slack and stretching of the 'tendons' was automatically taken up. This arrangement served as intrinsic compensation for any stretching of the 'tendons'.

A separate pressure regulator for each of the 10mm bore pneumatic cylinders provided the opportunity of increasing load with angle of flexion, as occurs in the natural MCP joint (Stokoe et al, 1990). Calculations A5.4 to A5.7 in appendix 5 show how the bore and stroke of all the pneumatic cylinders were determined.

During 'pinch' grip, most of the load is carried through the flexor apparatus, with the extensors relaxed (Smith et al, 1964, Weightman and Amis, 1982, Long et al, 1970). To simulate this relaxation of the extensor apparatus, the appropriate directional control valve was activated such that no air was supplied to the extensor cylinder.

However, some means had to be determined so that the load was carried through the flexor apparatus. Here, a load of up to 322N was required to be applied to the artificial finger joint. The value of 322N was calculated to be the maximum load developed across the MCP joint during pinch grip by 'normals' (appendix 5, calculation A5.7). As such, this load was far beyond the capacity of the 10mm bore cylinder. Indeed, such a load would damage a 10mm bore cylinder,

therefore a larger 32mm bore cylinder had to be used to apply the required load through the flexor apparatus, while ensuring that the 10mm bore cylinders were not damaged. To facilitate pinch load, air was first exhausted from the extensor cylinder, and then the fork cylinder (26) was activated so that load was taken through the aluminium slider (6) via the flexor stop fork (25) when the 32mm bore cylinder was activated. The fork cylinder (26) was chosen on the basis of cost. While its stroke was important, its bore size was less so. An inexpensive 25mm bore x 15mm stroke cylinder was therefore chosen.

To minimise the stroke required during 'pinch' grip (appendix 5, calculation A5.5), a pinch guide bar (33) was located on the main frame. This bar had the additional advantage of preventing the 'tendons' from fouling on the rear of the bath during 'pinch' grip. A pair of M6 bolts (34) served to control the maximum pull of the heavy load cylinder, by acting as physical stops on the aluminium slider. A 24V, 2.4A power supply (appendix 5, calculation A5.9) was used to activate the solenoid and all the pneumatic directional control valves. A silencer reduced noise from the 10mm bore cylinders when exhausting.

5.4.4 Control and Measurement

Eight strain gauges made up two full bridges (one for the forward direction and the other for the lateral direction) and connections from these went to a 386 computer, into which a combined A-D converter and strain gauge amplifier card was fitted. This 'PC-Alpha G' was a 4 channel, 16 bit strain gauge board. It had programmable circuitry for each bridge allowing adjustment of bridge balance, energising voltage and gauge factor. Supplied with the board was a small example program which activated the board to provide a numerical output from the attached strain gauges. This example program formed the nucleus of a larger program, written in Quick C by the author of this thesis, which converted the numerical output to a value of load and displayed it on the screen of the computer. The same Quick C program also controlled the new simulator by activating the various directional control valves in a pre-determined order to produce a load cycle of 3,000 counts of flexion-extension followed by one minute of 'pinch' grip. The complete Quick C program is given in appendix 11. Therefore the computer served both to control the simulator and to measure the load across the test prosthesis. By making the simulator computer controlled, it

could be left running unattended for long periods, constantly repeating load cycles.

The combined strain gauge amplifier/AD converter, 'PC Alpha G' card, was manufactured and supplied by Computer Instrumentation Limited, 4 Wayside, Commerce Way, Lancing, West Sussex, BN15 8SW. Tel. 01903 765225.

5.4.5 Control Sequence and Description of a Load Cycle

Magnets (17) were mounted on the phalangeal arc (4) at positions which ensured that the phalangeal clamp (2) moved from 0° to 90°. These each sent a signal via a control board to a pneumatic control valve which switched alternately each of the 10mm bore cylinders.

After 3,000 counts, pre-set into the computer program, flexion-extension stopped and the phalangeal clamp (2) was pulled to the 0° position. (Therefore the flexor cylinder (8) was mostly out and the extensor cylinder (12) was mostly in. Their exact positions could not be fixed due to stretching of the 'tendons').

A valve exhausted air from the extensor cylinder (12). (This was done to prevent damage to the extensor cylinder (12) during the 'pinch' grip part of the load cycle. There was already no compressed air supply to the flexor cylinder).

The 'thumb' solenoid (31) operated, sending a rod through a hole in the phalangeal arc (4) and into the base plate (28). The fork cylinder (26) operated, and the 'flexor stop' fork came through the aluminium slider (6) in front of the flexor adjuster (21).

The 32mm bore heavy load cylinder (24) operated. The flexor adjuster (21) was pulled against the 'flexor stop' fork (25). Load was then transmitted to the flexor 'tendon' which pulled the phalangeal clamp (2) against the thumb rod. The heavy load cylinder continued pulling until it hit a mechanical stop. (All this time the rod of the extensor cylinder was being extended, but remained undamaged as its stroke was greater than the 'heavy load' distance pulled). The load was held for 1 minute to simulate 'pinch' load.

The heavy load cylinder (24) was de-activated. The fork cylinder (26) was de-activated. The 'thumb' solenoid (31) was de-activated. Flexion-extension began again.

5.5 Calibration

Eight strain gauges were bonded to the cantilever, to form two full strain gauge bridges. One for dorsal/palmar load, and the other at 90° to it for the axial load. Connections from these gauges went to the 'PC-AlphaG' card located within the simulator's computer. The strain gauges were calibrated in the following way. The test bath and base plate were removed from the simulator, leaving only the cantilever protruding from the bridge. The cantilever was then removed, rotated through 180° then re-fitted. This was done so that the tensile load during calibration would be equal to the compressive load during operation. 'Forward' calibration could then be undertaken. The computer was switched on and the program 'A_3_G_2' was selected to be used for calibration. A spare artificial 'tendon' was used, the 'eye' of which was slipped around an M3 screw tightened through the tapped hole in the cantilever. Such a procedure ensured that the calibration load would have the same line of action as that applied during normal running of the simulator. The other end of the artificial 'tendon' passed over a pulley and was attached to a tray to which weights could be added. At each different weight, the numerical mV output to the screen was noted. The entire procedure was then repeated for the dorsal/palmar direction. The values measured were plotted against the loads applied (Figure 5.4). From this graph, the reciprocal of the gradient gave the calibration factors. These factors, 0.1063N/mV for the dorsal/palmar load and 0.1067N/mV for the axial load, were incorporated into the control program 'meas.c' such that direct values of load were output to the screen when the simulator was in operation.

Figure 5.4 - New Finger Function Simulator - Strain Gauge Calibration Curves

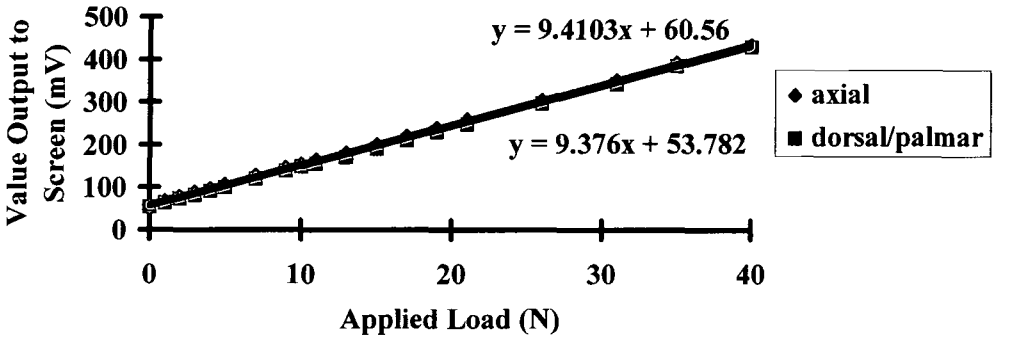

5.6 Operation

Each prosthesis holder was designed so that it could only be fitted in one position, having a shoulder to locate against the face of its clamp, and a flat on its stems for the locking grub screw. Once the holders were in place, the test prosthetic components could be fitted. The two artificial 'tendons' were threaded from their respective adjusters, around the pulleys, and through the phalangeal clamp. At the rear face of the phalangeal clamp, the 'tendons' were held by stainless steel split pins. The phalangeal arc was re-fitted, followed by the lid of the test bath, and tightened down. Then the test bath was fitted from beneath and clamped onto the lid itself. The lubricant supply pipe was pushed through the appropriate hole in the lid and fed down into the bath. Next, the lubricant supply was switched on, at the Grant bath, and the lubricant allowed to reach a steady temperature of 37°C. As an air lock could occur, the return pipe from the test bath was checked to ensure that the lubricant was flowing back to the Grant bath.

Next, the compressed air supply was turned on, and the reading on the pressure regulator was set to 3 bar, as this value gave the 10-15N load desired across the test prosthesis. The power was switched on to a transformer which gave a 24V output which in turn supplied the pneumatic valves and the 'thumb' solenoid. The computer was switched on, and the program 'meas.c' selected to commence operation of the simulator.

5.7 New Finger Function Simulator Validation Test

5.7.1 Aim

The aim of the validation test was to test 2.0mm thick prototype prostheses, under similar test conditions to those used with the Stokoe simulator, and to compare the results with those given by the Stokoe simulator.

Table 5.1 General Test Parameters

Parameter	Test 1
Lubricant Temperature	37°C
Lubricant	Distilled Water
Average Dynamic Load	12.5N
Mean Static Load	100N
Metacarpal Outer Radius (R)	9.4mm
Wear Face Thickness	2mm
Arc Length (Rθ)	14.7mm
Cycles per Minute	80
Average Velocity	39.2mm/s
Stroke	29.4mm
Nominal Stress at 100N Static Load	0.68MPa
Nominal Stress at 12.5N Dynamic Load	0.08MPa

The XLPE material had a mean gel content before irradiation of 87% for both the phalangeal and metacarpal components. Prostheses came from the same batch as those tested in tests 2 and 3, and reported earlier in this thesis. Therefore the material was again XLPE irradiated by exposure to a dose of not less than 25kGy of gamma radiation. The minimum dose was 25.7kGy, and the maximum dose was 32.9kGy. Again, the density of the XLPE was taken to be 949kg/m^3. The only difference in test parameters between the new simulator and the Stokoe simulator was the cycle speed. A cycle speed of 112 cycles per minute could not be achieved with the new simulator. Instead a consistent cycle speed of 80 cycles per minute was achieved, and this speed was considered to be adequate.

5.7.2 Test Procedure

The test procedure was similar to that used for the testing of a prosthesis on the Stokoe finger function simulator. Prior to the commencement of a test, the prosthetic components were cleaned in acetone and weighed. An additional pair of prosthetic components was placed within a small container in the Grant bath (which supplied and circulated the lubricant used in the test) to act as control specimens. These control specimens were unloaded. The Grant bath was switched on and the lubricant allowed to reach a steady state temperature of 37°C. Testing then commenced. The number of flexion - extension cycles was recorded by a dedicated pneumatic counter.

Frequent checking of loads and cycle speed were made. Any necessary adjustments to the speed of the simulator were achieved using the throttles fitted to the flexion and extension pneumatic cylinders. At regular intervals, the test was stopped, the prosthetic components were removed, cleaned in acetone and weighted. Test and control samples were weighed to the nearest 0.1mg using a Mettler AE200 balance. Wear of a test component was defined as the weight loss with respect to the initial weight, to which was added any weight gain of the control component. Therefore the weight gain of the control and test component was assumed to be identical. The control and test samples were very close in weight to each other. The metacarpal components were within 2.3% of each other, and the phalangeal components within 0.96% of each other. Therefore these errors due to weight differences were small compared with errors due to the accuracy of the Mettler balance. The wear factor k (units $10^{-6}mm^3/Nm$) was determined, as before, from equation 1.1.

5.7.3 Discussion of Results

Weight changes of the prosthetic components are tabulated in appendix 2 (table A2.7). These results are shown graphically in figures 5.5, 5.6 and 5.7. At the end of the test, after 140km, wear factors of $0.24 \pm 0.12 \times 10^{-6}mm^3/Nm$ and $0.36 \pm 0.12 \times 10^{-6}mm^3/Nm$ were measured for the phalangeal and metacarpal components respectively.

Figure 5.5 - Wear of High Percentage Cross-Linked Prostheses in New Finger Simulator Test

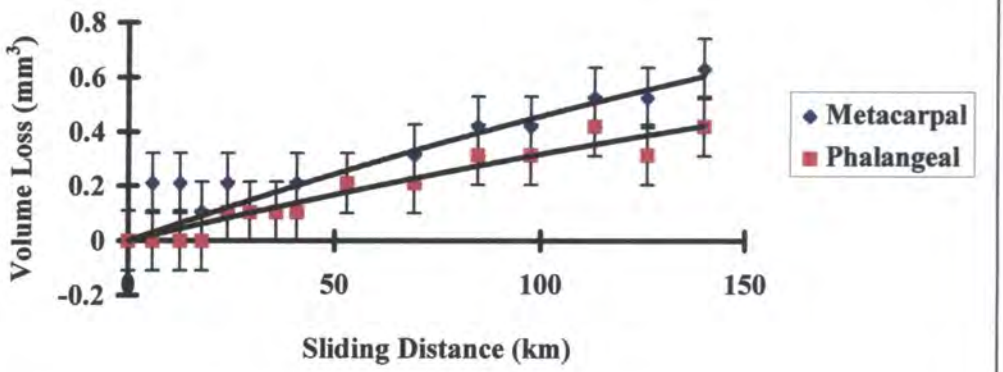

Figure 5.6 - Weight Change of Metacarpal Components in New Finger Simulator Test

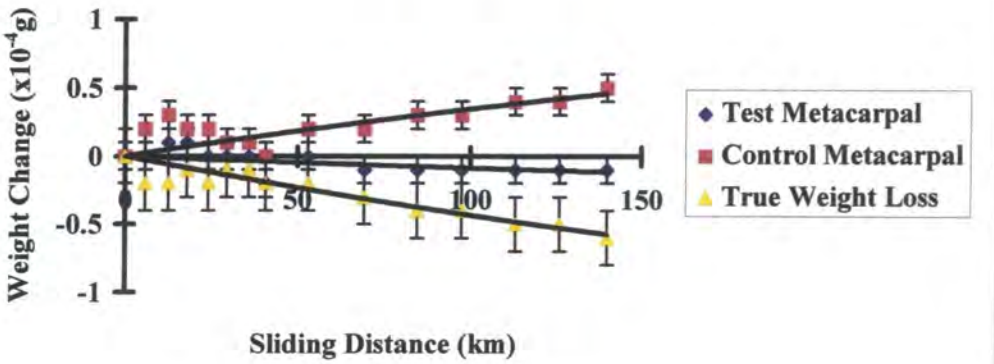

Figure 5.7 - Weight Change of Phalangeal Components in the New Finger Simulator

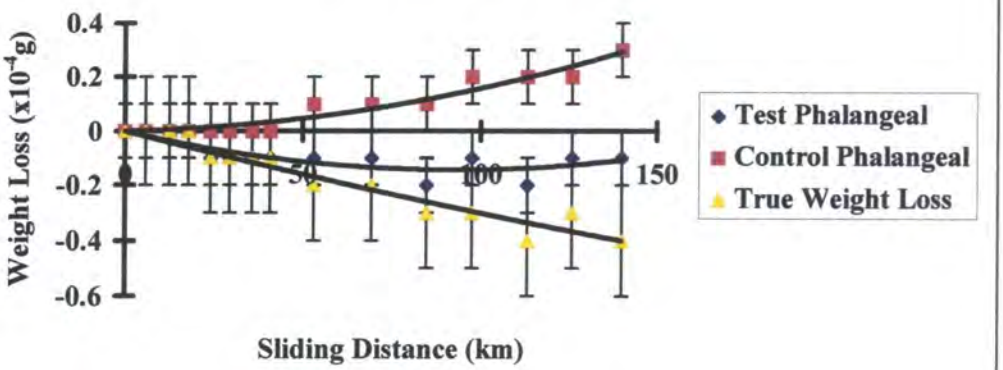

These wear factors correspond well with results from test 3 undertaken on the Stokoe simulator, where prostheses from the same batch were used, and also distilled water was the lubricant. After 131.3km, test 3 had wear factors of 0.26 $\pm$ 0.12 x $10^{-6}mm^3/Nm$ and 0.32 $\pm$ 0.12 x $10^{-6}mm^3/Nm$ for the phalangeal and metacarpal components respectively. Therefore it can be seen that the wear factors from the new simulator are slightly higher than from the old simulator. This may be because the load across the test prosthesis was maintained at the desired 10 to 15N, whereas frequent re-tensioning was required on the Stokoe simulator to maintain such a load.

Scratches in the direction of sliding were seen on the wear face of each of the test prosthetic components, although these were not too prominent (Figure 5.8). The metacarpal component showed greater wear than the phalangeal component. The bulk of the 'wear' was due to water absorption by the control components, rather than weight loss of the test components. Each of these observations agree with the findings of the six tests carried out using the Stokoe simulator.

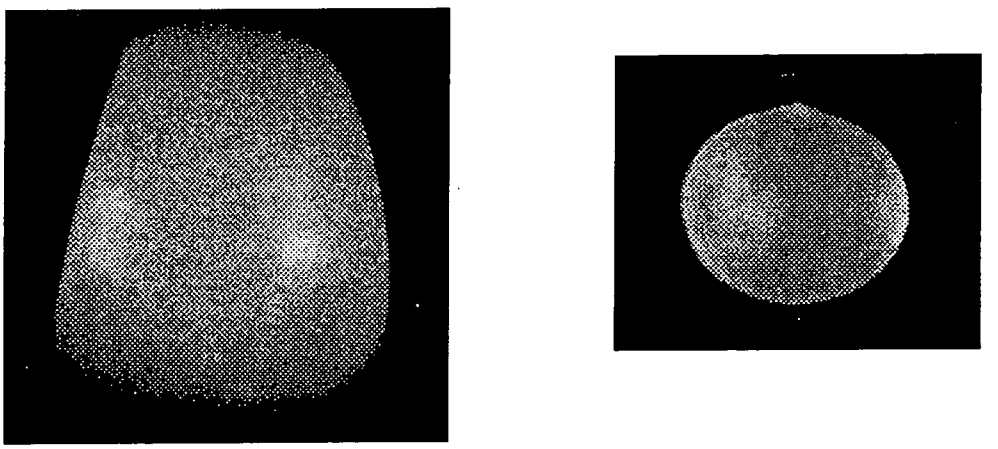

Figure 5.8 - Wear faces of prosthetic components at end of test

5.8 Modifications Made and Future Work

5.8.1 Mechanical Modifications

Needle roller bearings were mounted in the upper pulleys, as these bearings served to minimise frictional losses. Nylon sleeves were fitted over the stainless steel guide pins in the test bath, again to minimise frictional losses along the 'tendon' routes, but also to protect the artificial 'tendons' from abrasion.

Physical stops were added at positions which prevented the phalangeal component from moving beyond 0° or 90° to the metacarpal component. The 0° stop ensured that the phalangeal component was not pulled off the metacarpal component immediately prior to 'pinch' grip. The 90° stop acted to prevent the phalangeal and metacarpal components rotating beyond 90° and this prevented the phalangeal clamp from becoming wedged behind the cantilever.

5.8.2 Modifications to the Pneumatic System

The speed of flexion-extension was found gradually to slow down towards the 'pinch' grip part of a load cycle. After 'pinch' grip, the higher original speed was resumed, before the speed once again progressively decreased. The problem was found to be residual air pressure in the flexion-extension circuit. The solution consisted of fitting a check valve in each the flexion and extension air lines, with the result that this residual air pressure was prevented from building up. Silencers were fitted on the pneumatic solenoid valves to minimise noise due to venting.

5.8.3 Possible Future Improvements

The phalangeal clamp could be redesigned so that the magnets within it are moved outwards relative to the position of the phalangeal holder. In this way it is hoped that the 0° and 90° signals will be sent to the pneumatic valve sooner during flexion-extension, and therefore that the cycle speed of the simulator during flexion-extension can be increased. Smaller pneumatic solenoid valves are now available. Being smaller, their internal components will have lower inertia than those in the valves currently fitted. Also, such new valves are small enough

to be mounted on the rig itself, rather than, at present, hidden below the test bench on which the simulator sits. The closer the valve to its slave pneumatic cylinder, the shorter the air line required and the quicker the circuit response time. Therefore the combination of low inertia valves plus shorter air lines would also be hoped to permit an increase in the speed of the simulator during flexion - extension.

5.8.4 Future Tests

Tests of greater duration ought to be undertaken on the new simulator to compare results with those from the Stokoe simulator. Also, it would be a useful exercise to test a Swanson prosthesis on the new simulator, to see if failure in a time and a manner comparable with surgical experience can be obtained.

CHAPTER SIX

Towards Implantation

6.1 Summary

The design of the new prosthesis having been completed, and substantial testing of both the wear of the material and the actual components carried out, the next stage was implantation in patients. However, more work was required before this implantation could be achieved. Approval from the relevant statutory bodies had to be obtained, the surgical tools required for implantation of the prosthesis had to be manufactured and objective measures of the outcome of surgery had to be developed.

6.2 Protocol for Ethical Approval

New designs of prosthesis cannot be implanted into human subjects without statutory ethical approval first being given. Currently, the process of obtaining such approval falls into two stages. A protocol describing the proposed study has to be approved by the local research ethics committee and then this same document has to be approved by the Medical Devices Agency, which is the designated authority under EU regulations.

The necessary protocol was therefore produced in liaison with De Puy International Limited, entitled 'Protocol for a Pilot Study of a Clinical Trial of the Durham Surface Replacement Metacarpophalangeal Prosthesis'. The objective of the protocol was to evaluate the safety of the surgical procedure and to evaluate the efficacy of the procedure. The protocol's secondary objectives were stated as being to measure the grip and pinch strength of the patient; measurement of the patient's metacarpophalangeal joint stiffness and range of motion; and to obtain the patient's assessment, through the use of a questionnaire. The study was an open, single-centre, prospective investigation. Forty joints in 10 hands were required, and inclusion and exclusion criteria for patients were specified. The study would run for twelve months from the date of the final implantation. A risk

benefit analysis was described in the protocol. This last section included a description of the design of the Durham prosthesis, and details of the XLPE material from which it was manufactured.

Patient management was also described, as well as surgical technique. A patient explanation leaflet was written and included in the protocol, and the means by which informed patient consent would be obtained was described. Primary assessments would consist of radiological evaluation, a clinical questionnaire, and adverse event reporting. The secondary assessments would be those of hand strength, finger strength, metacarpophalangeal joint range of motion and stiffness, and completion of a patient satisfaction questionnaire. The questionnaire and the section on stiffness assessment were written by Ms H Ash. All assessments would be undertaken immediately prior to the joint replacement operation, then at 3, 6, 9, and 12 months post operatively. The primary assessments would be undertaken by Mr C Viva, the hand surgeon who performed the operation, with independent clinical evaluation being by Prof. John Stothard, a consultant orthopaedic surgeon. Appendices to the protocol included the World Medical Association Declaration of Helsinki, and the appropriate section of British Standard EN 540 - Clinical Investigation of Medical Devices for Human Subjects. Complication and case report forms were also produced for the clinical trial and included as appendices in the protocol. The protocol is given in appendix 12, and approval for the clinical trial described in it was given by the local research ethics committee and then by the Medical Devices Agency.

6.3 Surgical Instruments

A complete set of the surgical instrumentation necessary for the implantation of the Durham prosthesis was manufactured by De Puy International Limited, based on prototype designs from Durham. All instruments were manufactured from stainless steel, which could be repeatedly sterilised. The set came in three sizes, to suit the R6.5, R7.5 and R8.5 size prostheses which had been manufactured. Figure 6.1 shows the set for the R8.5 size. After the metacarpophalangeal joint had been exposed, and a complete synovectomy performed, the metacarpal head was measured using the template. Then the appropriate size of cutter was used to produce a part-sphere on the metacarpal head. Using the guide tool, a palmar flat was made on the metacarpal head with a power saw, and an offset hole was drilled in the head using the second guide tool. This second tool had a lip which

fitted underneath, and against, the flat just produced on the metacarpal head. In this way the offset hole was precisely and correctly located. Finally the hole was reamed out to a square section, before the metacarpal component of the appropriate size was inserted. The cartilage on the proximal phalanx was cleaned away, then a hole reamed into the medullary canal of the proximal phalanx and the phalangeal component of the prosthesis was push fitted. The capsule was repaired, the collateral ligaments released or re-tensioned as appropriate, and the extensor tendons reefed back to the radial side of the joint to complete the operation.

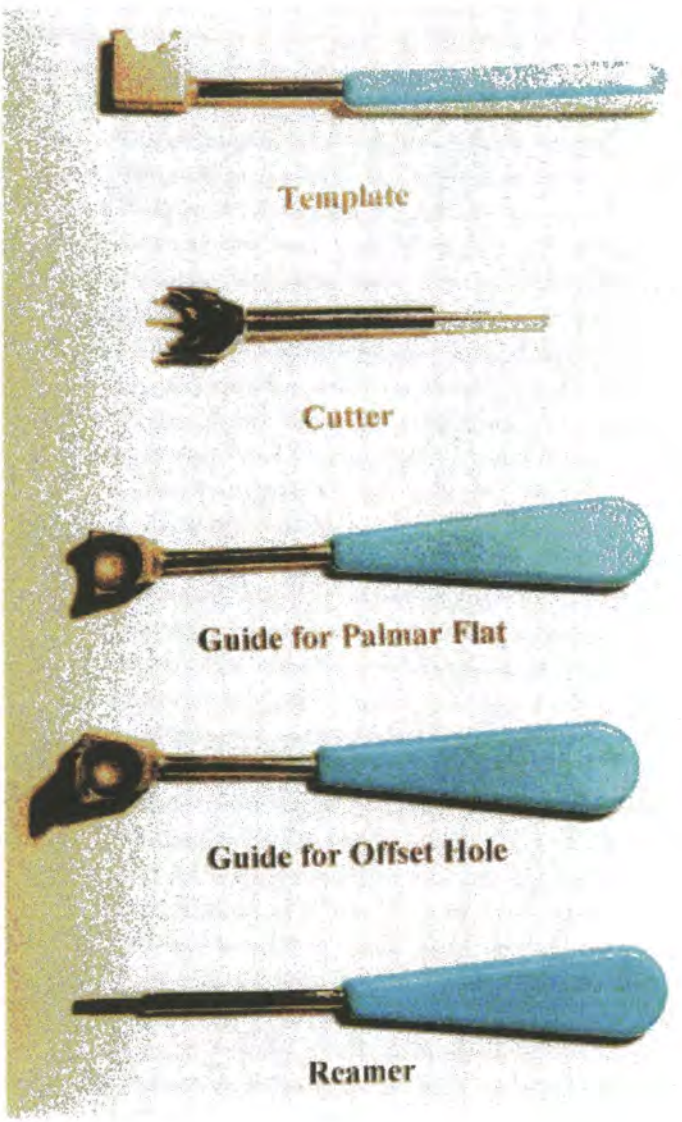

Figure 6.1 - Surgical Instruments

6.4 Assessment of Hand Strength

6.4.1 Overview

It has been shown that one of the significant effects of rheumatoid arthritis on the hands of a sufferer is a reduction in strength. Both individual finger strength, and total hand grip strength are affected (Jones et al, 1985; Walker et al, 1978). This loss of strength is likely to be due to several causes. The disease weakens the muscles, and produces swelling of the tendon sheathes which makes tendon movement difficult. Further, painful joints cease to be used so that further muscle wastage occurs and, once muscle balance is lost, the hand ceases to be fully effective (Lister, 1993).

Once MCP joint arthroplasty has been performed, pain should be much reduced, and the joint re-balanced as far as possible. Therefore, with a pain free, more functional joint, an opportunity should exist for an increase in grip strength. With the Swanson prosthesis, it has been shown that arthroplasty provides no increase in grip strength (Helliwell et al, 1988; Blair et al, 1984 a). This result may be attributable to the prosthesis design. As a single piece, flexible prosthesis, the patient's strength may be required simply to bend the prosthesis, therefore any increase in strength due to surgery may be wasted in inducing the Swanson to bend. However, such a situation should not occur with the Durham prosthesis. This design is two piece, with each piece showing a low coefficient of friction against the other. Therefore, the two pieces should slide over each other freely, thus allowing the patient's strength to be used to grip or to pinch, rather than simply dissipated in the fabric of the prosthesis.

The clinical measurement of hand strength allows the response to treatments to be assessed, and the effectiveness of different surgical procedures to be compared (Mathiowetz et al, 1985). In comparison, such an assessment is difficult when a parameter as subjective as hand 'pain' is used. Due to factors such as circadian variation, and patient to patient differences, grip strength measurement must be reliable and valid, necessitating the use of standardised equipment, procedures and positioning of the hand.

A popular method of measuring grip strength is to squeeze an inflated bag connected to a manometer and to note the increase in pressure. However, different techniques of squeezing will give different results, as indeed will different original bag volumes or pressures (Unsworth et al, 1990). Additionally,

the contribution of individual fingers cannot be determined (Jones et al, 1985). Instead strain-gauged devices offer the ability to measure the force of a grip, rather than the pressure indicated by an inflated bag. Further, with certain strain-gauged devices, the magnitude and contribution of the individual fingers, and finger segments, to the overall grip strength can also be determined.

6.4.2 Grip Strength Measurement Device

A strain gauged, grip strength measurement device, or 'gripper', was available (Porter, 1993), but two deficiencies were discovered with it. Most importantly, the 'gripper' was inaccurate. This was caused by poor bearing design within the unit (Figure 6.2). The plain bushes used as bearings were short in relation to the length of the stems. This situation permitted the point of application of the load on the cantilever to vary which, in conjunction with the sensitivity of the strain gauges, led to a wide spread of measured forces. Additionally, the stems would sometimes stick in their bushes. This meant that a load would be indicated when none was applied. The second problem was that the size of the 'gripper' could not be adjusted to cope with the different sizes of hand that are normally found in a population.

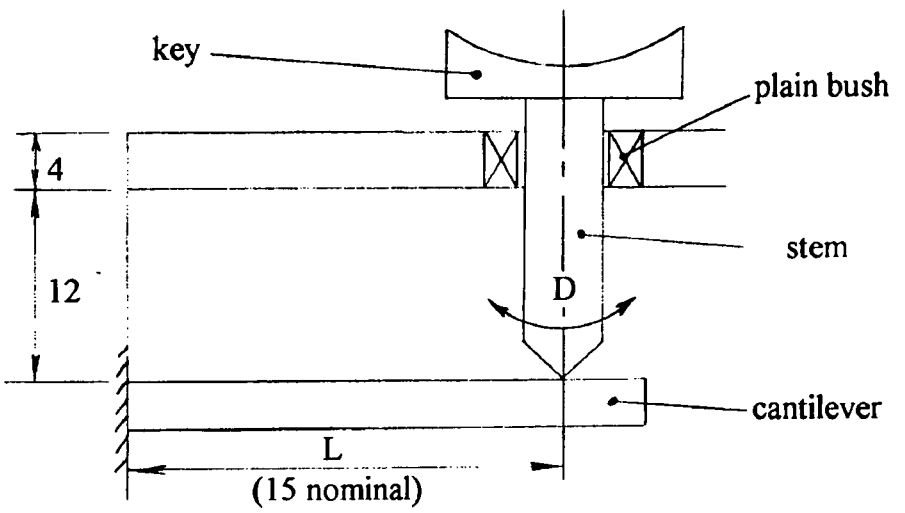

Figure 6.2 - Bush Design in the Original 'Gripper'

Measured play D = 1.4mm, therefore L = 15mm ± 0.7mm = 14.3mm to 15.7mm. For a cantilever, deflection of cantilever $\delta \propto$ length L^3 Therefore $\delta \propto$ 2924 to 3870 (a 32% difference) Also, bush height to stem length ratio is 4 : (4+12) or 1:4

Therefore a new 'gripper' was designed to overcome these problems. A general arrangement drawing of it is shown in Figure 6.3. Linear bearings (Figure 6.4) were fitted instead of plain bushes, which resulted in consistent results being measured, along with no sticking of the stems in the bearings. Secondly, the unit was free to move on two locating spindles, which permitted four different 'hand' sizes to be accommodated.

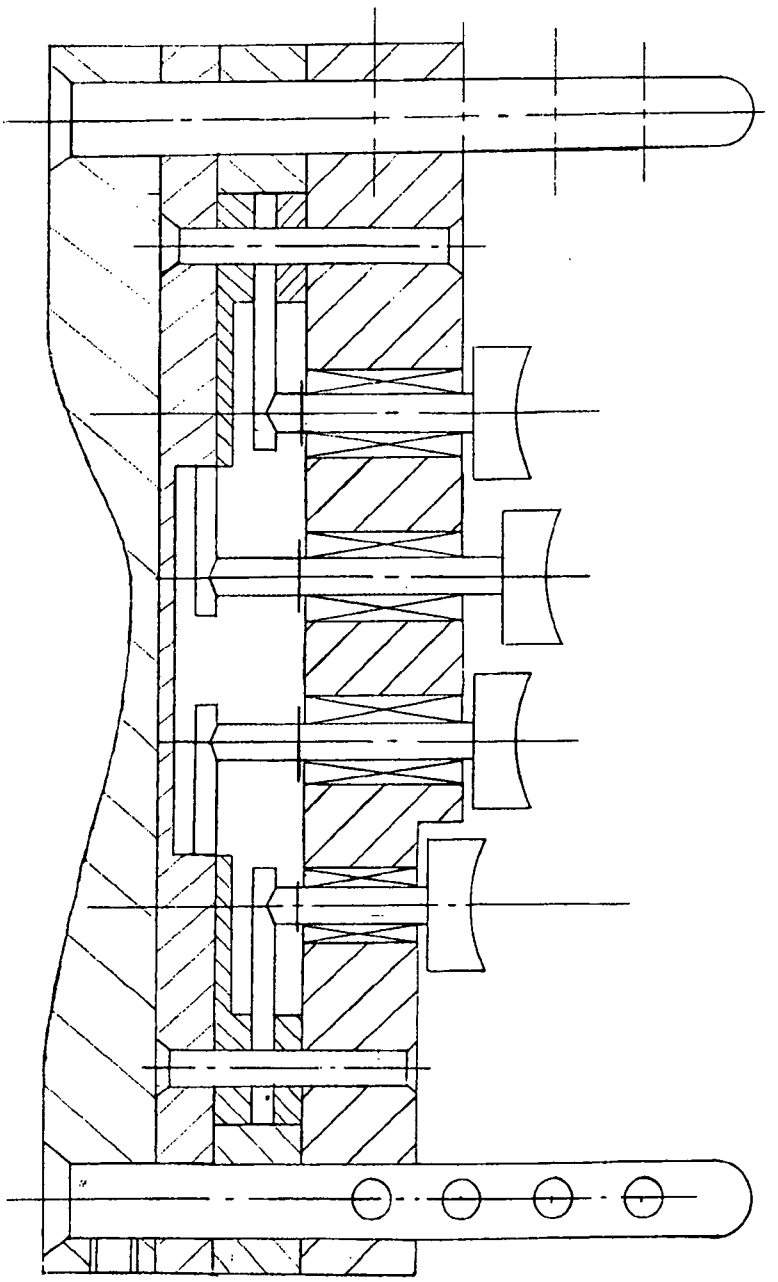

Figure 6.3 - General Arrangement Drawing of the New 'Gripper'

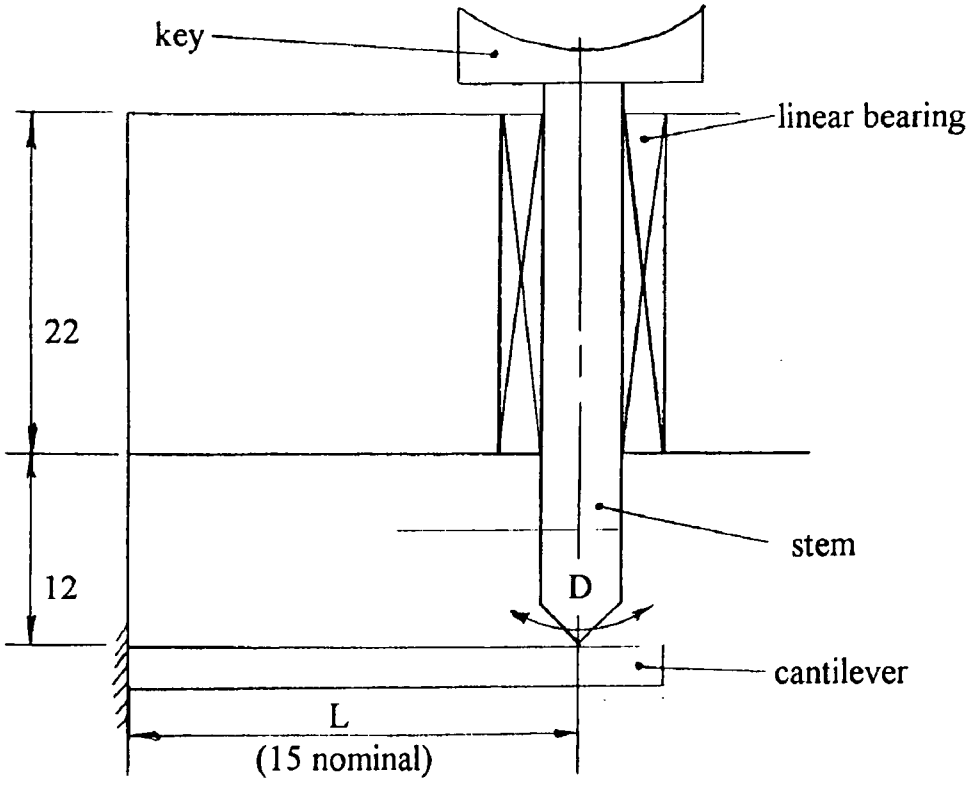

Figure 6.4 - Bearing Arrangement in the New 'Gripper'

Measured play D = 0.2mm, therefore L = 15mm ± 0.1mm = 14.9mm to 15.1mm
For a cantilever, deflection of cantilever $\delta \propto$ length L^3 $\delta \propto$ 3308 to 3443 (a 4% difference)
Also, bearing height to stem length ratio is 22 : (22+12) or 1:1.5

The 'gripper' consisted of an aluminium body which fitted into the palm of the hand (Figure 6.5). The rear of the housing was designed to follow the contours of the palm and to fit against the abductor pollicis muscle of the thumb. Each of the four keys had a front face which was contoured to sit comfortably beneath the finger pad of the middle phalanx. The force from each finger was transmitted via the key, through a stem, to a cantilever housed within the body of the 'gripper'. Each cantilever had four strain gauges attached to it, and these 4 strain gauges together made up a full strain gauge bridge. Having four independent cantilevers permitted the contribution of the individual fingers to the overall grip strength to be measured.

Figure 6.5 - The 'Gripper' in Use

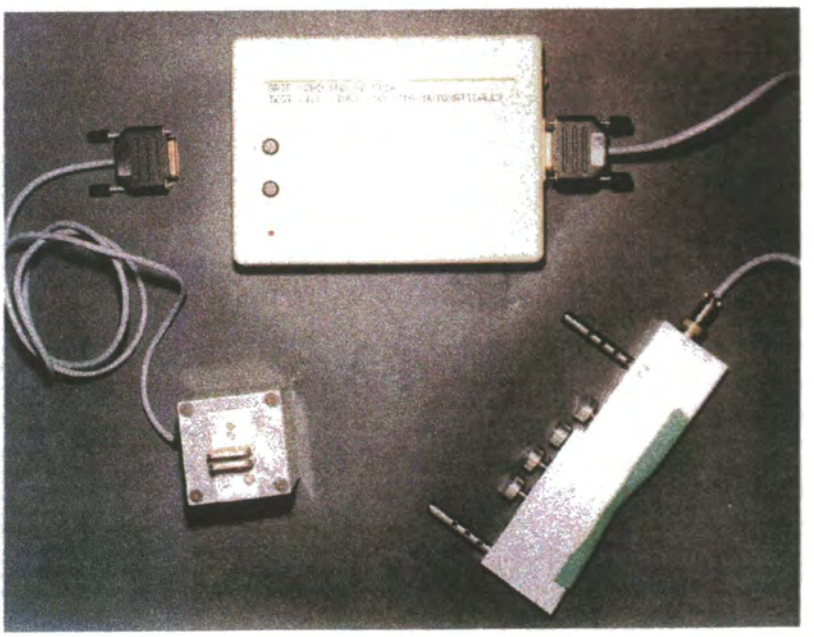

Figure 6.6 - The Hand Strength Measurement Equipment
'Pinch' Unit, Monitor and 'Gripper'

The 'gripper' plugged into a small hand assessment monitor, as did a 'pinch' unit which was also available (Porter, 1993). The 'pinch' unit was intended to be used to measure the pulp pinch and lateral pinch strength of a patient. The hand assessment monitor was an intelligent, four channel strain gauge amplifier. It had balanced voltage outputs and four independently zeroable, dual gain millivoltmeter inputs. At its core was a microprocessor (a K100 mini module manufactured by PSI Systems Limited, 17-18 Chelmsford Road Industrial Estate, Great Dunmow, Essex, CM6 1XG). The software permitted two ranges of amplification of the signal from the strain gauges. High amplification, intended for arthritic patients, and low amplification, intended for 'normals'. A 2 line by 40 character LCD provided the means of communication with the operator. The monitor was powered by—rechargeable batteries, and an LED indicator supplied a warning if their power became low. The batteries supplied power for approximately half an hour so, whenever possible, the unit was powered from a mains supply. The software for the monitor consisted of a menu with a number of options relevant to the 'gripper' and 'pinch' unit. The options could be scrolled through and selected using the two buttons located on the front of the monitor. The complete system of monitor, 'pinch' unit and 'gripper' is shown in Figure 6.6.

Despite being manufactured from aluminium, and designed to be of a minimum weight, arthritic patients still found the 'gripper' to be uncomfortably heavy, therefore a combined arm rest and gripper support device was designed and manufactured. This device had the additional advantage of guiding the patient's arm to the correct, repeatable position desired for grip strength measurement. Calibration of the gripper was achieved by attaching weights to individual finger pads and noting the output on the display of the hand assessment monitor. For each finger, and for high and low amplification, a graph was plotted and the calibration constants determined. (see Figures 6.7 to 6.10).

Figure 6.7 - Gripper Calibration Curve: Index Finger

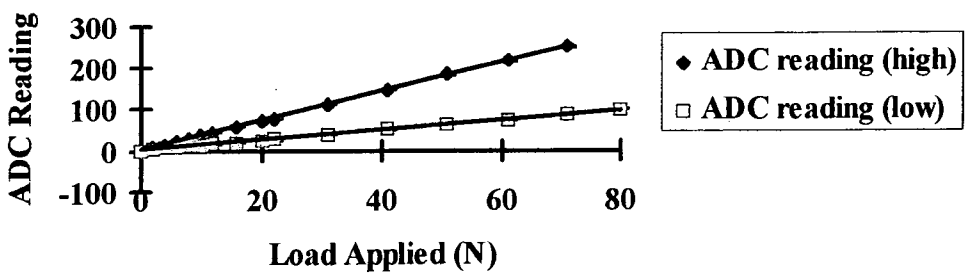

Figure 6.8 - Gripper Calibration Curve: Middle Finger

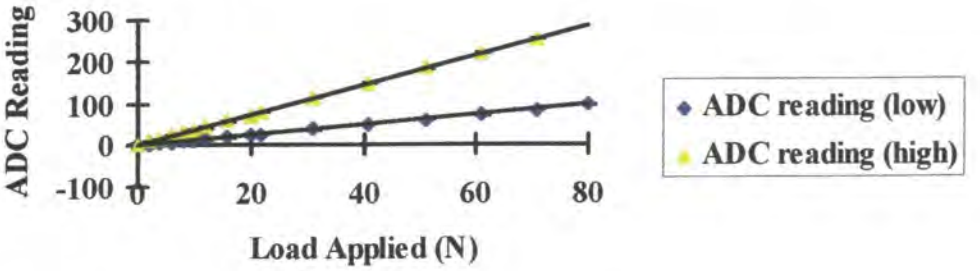

Figure 6.9 - Gripper Calibration Curve: Ring Finger

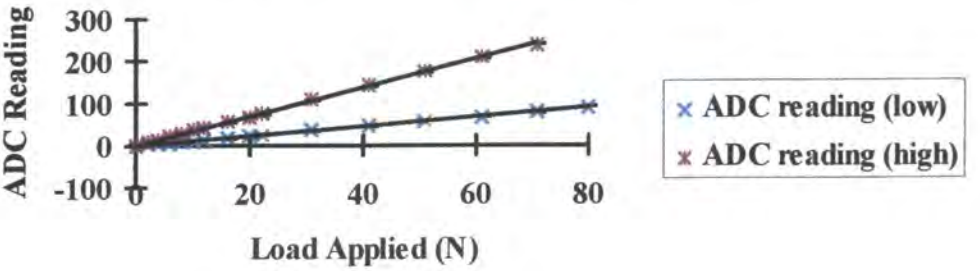

Figure 6.10 - Gripper Calibration Curve: Little Finger

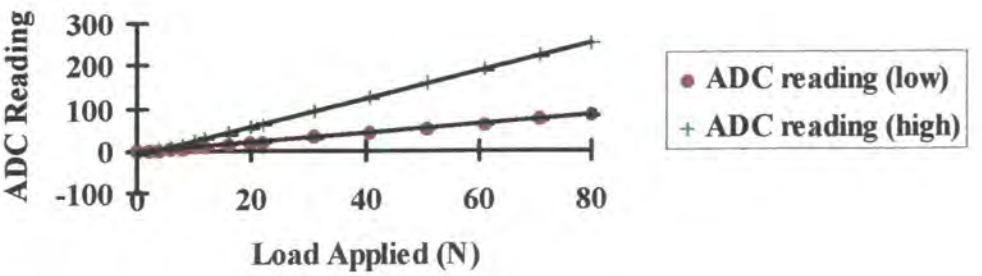

CHAPTER SEVEN

Summary and Further Work

7.1 Summary

Based on the dimensions of the natural MCP joint, the design of the Durham prosthesis has been completed. It is suggested that a range of five sizes (R5.5 to R9.5mm in 1mm steps, where R is the radius of the outer articulating surface) would cover the population. The Durham prosthesis is a surface replacement design, having a metacarpal and a prosthetic component. Both components have conforming spherical articulating surfaces. The face of the metacarpal components is shaped as a trapezium, and the face of the phalangeal components is that of an ellipse. The prosthesis is manufactured from XLPE and is intended to be uncemented in vivo. A lip to counter coronal plane rotation has been added to the metacarpal component, full details of both components are given in chapter 2. Production examples of the prosthesis have been manufactured in the middle three sizes, together with the appropriate surgical instrumentation.

Six examples of the Durham prosthesis were tested using a finger function simulator to over 70 million cycles, equivalent to over 70 years in vivo. Total wear factors of the order of 0.4 x $10^{-6}mm^3/Nm$ were measured and such values, lower than previously measured, should make the prosthesis acceptable from a wear point of view (chapter 3). Furthermore the test prostheses showed no cuts and no fractures and abrasive wear appeared to be the dominant wear mechanism. The link between the degree of cross-linking and the amount of wear of the prosthesis has been shown. While the simulator was modified to improve its reliability, a new simulator has been designed, manufactured and commissioned (chapter 5). Results from this commissioning test gave wear factors comparable with those from the older simulator. The new simulator should have the advantage over its older counterpart of maintaining the desired load across the test prosthesis through pneumatic actuation.

In tandem with these simulator tests, fundamental wear tests on XLPE rubbing against itself have been carried out on reciprocating pin on plate rigs and again show total wear factors of the order of 0.4 x $10^{-6}mm^3/Nm$ and the prominence of abrasive wear

(chapter 4). Testing has extended over 6000km or 130 million cycles, at loads of 10N and 40N, with distilled water at 37°C as a lubricant. Interestingly, it was found that pin wear was very much less than plate wear, indicating a fatigue effect on wear of the plates. Previously in such polyethylene against polyethylene tests, the wear of the plates has not been measured. Other conclusions reached as a result of these wear tests was that ageing due to sunlight appeared to have an important effect on wear and there did not appear to be a transfer film produced when XLPE rubbed against itself. The pin on plate tests were extended to include testing of UHMWPE against UHMWPE, as well as both polyethylenes against hard counterfaces. UHMWPE rubbing against itself showed wear factors of the order of 80 x $10^{-6}mm^3/Nm$, such high values possibly being due to a combination of abrasive, adhesive and fatigue wear. Tests of the two polyethylenes against hard counterfaces (stainless steel and zirconia) revealed the importance of the roughness of the counterfaces but further testing is suggested.

The XLPE against XLPE wear test results were encouraging enough to consider a trial of the Durham prosthesis in human subjects. However, before surgery could begin, ethical approval had to be obtained. Therefore, the necessary 'protocol' was written and submitted to the local Research Ethics Committee. Once their approval was received, then the protocol was submitted to the Medical Devices Agency who in turn gave their approval to a clinical trial. A grip strength device (Porter, 1993) has been further developed so that objective measurements of patients, at pre and post operation, can be made as part of a series of evaluations of the new prosthesis. All of this work towards implantation is described in chapter 6.

7.2 Further Work

The most important work to be carried forward is the implantation of the prosthesis. This is where much of the work described in this thesis will be judged. In tandem with the design of the prosthesis the skill of the surgeon in successfully achieving soft tissue rebalancing will be critical to the success of the Durham prosthesis.

Consistent and low wear factors were found from all simulator tests. However there is a strong argument that in an application as critical as the human body there can never be enough testing of a prosthetic device. Therefore, further testing of the Durham prosthesis could be undertaken using bovine serum as a lubricant. Before such testing

could commence though, significant modifications to the simulators would be required to permit heating of the bovine serum. Also, tests of the smallest size of Durham prosthesis currently available (R6.5mm) could be carried out, to ensure that it too will show no crucial surface damage.

Tests of greater duration ought to be undertaken on the new simulator to compare results with those from the Stokoe simulator. Also, it would be a useful exercise to test a Swanson prosthesis on the new simulator, to see if failure in a time and a manner comparable with surgical experience can be obtained.

Regarding the XLPE against XLPE pin on plate tests, it may be worth undertaking tests with material that has been aged in sunlight as well as material that has aged in darkness. The results of such tests should indicate whether ageing alone or ageing in sunlight can increase the wear of XLPE. More work on the water uptake of XLPE control plates also ought to be carried out.

Part of the reason for the wear of the test pins in the hard counterface tests has been speculated as being due to the presence of a transfer film, which has served to increase the counterface roughness and in turn the wear of the test pins. By changing to bovine serum as a lubricant the formation of a transfer film should be prevented. Therefore it is suggested that the tests be repeated with this lubricant. The recent work by Bragdon et al (1996) and Wang et al (1996) proposes that a test which moves away from reciprocating motion, and includes another direction of motion, would provide in vitro wear factors closer to those found in vivo. Therefore it is suggested that a rotational element be added to the test pins, and that the 'hard counterface' tests be repeated. Perhaps, in such an instance, the wear of XLPE against hard counterfaces would be found to be less than that of UHMWPE. If XLPE can be shown to be superior to UHMWPE in resisting wear then this result could have a significant impact on the longevity of artificial joints. Test 14, which had stainless steel pins loaded against polyethylene plates could be repeated with pins having spherical wear faces.

REFERENCES

Adams B D, Blair W F and Shurr D G. (1990) Schultz metacarpophalangeal arthroplasty: a long term follow up study. Journal of Hand Surgery. **15A**, 4, 641-645.

Alexander W J. (1972) The design of a bearing for a human finger joint. M.Sc Report. University of Leeds.

Amis A A. (1987) Variation of finger forces in maximal isometric grasp tests on a range of cylinder diameters. J Biomedical Engineering. **9**, 313-320.

An K N, Chao E Y, Cooney W P and Linscheid R L. (1985) Forces in the normal and abnormal hand. Journal of Orthopaedic Research. **3**, 2, 202-211.

An K N, Cooney W P, Chao E Y and Linscheid R L. (1978) Functional strength measurement of normal fingers. ASME Advances in Bio-engineering. 89-90.

Arthritis and Rheumatism Council. (1992). Annual Summary. St. Mary's Gate, Chesterfield, S41 7BR.

Atkinson J R and Cicek R Z. (1983) Silane cross-linked polyethylene for prosthetic applications. Part 1. Certain physical and mechanical properties related to the nature of the material. Biomaterials. **4**, 267-275.

Atkinson J R. (1976) An investigation into the wear of UHMWPE when a polyethylene pin is loaded against a reciprocating polyethylene counterface lubricated by bovine synovial fluid at ambient temperature. Report, Department of Metallurgy, Leeds University, 1-12.

Backhouse K M. (1968) The mechanics of normal digital control in the hand and an analysis of the ulnar drift of rheumatoid arthritis. Annals of the Royal College of Surgeons of England. **43**, 154-173.

Barbour P S M, Barton D C and Fisher J. (1996) The influence of temporal and spatial variations in stress on the wear of UHMWPE for total joint prostheses. Fifth World Biomaterials Congress, Toronto, Canada, 579.

Beckenbaugh R D and Linscheid R L. (1989) Arthroplasty in the hand and wrist p141-184 from Operative Hand Surgery (Ed D P Green) 2nd edition, Churchill-Livingstone, New York.

Beckenbaugh R D, Dobyns J H, Linscheid R L & Bryan R S. (1976) Review and analysis of silicone-rubber metacarpophalangeal implants. J Bone Joint Surgery. **58A**, 4, 483-487

Beckenbaugh R D. (1983) Preliminary experience with a non-cemented non-constrained total joint arthroplasty for the metacarpophalangeal joints. Orthopaedics. **6**, 8, 962-965.

Beevers D J and Seedhom B B. (1993) Metacarpophalangeal joint prostheses: a review of past and current designs. Proc Instn Mech Engrs. **207**, 195 - 206.

Berme N, Paul J P and Purves W K. (1977) A biomechanical analysis of the metacarpophalangeal joint. Journal of Biomechanics. **10**, 409-412.

Black J. (1988) Orthopaedic Biomaterials in Research and Practice. Churchill Livingstone.

Blair W F, Shurr D G and Buckwalter J A. (1984) Metacarpophalangeal joint arthroplasty with a silastic spacer. J Bone Joint Surgery. **66A**, 365-370. a

Blair W F, Shurr D G and Buckwalter J A. (1984) Metacarpal joint arthroplasty with a metallic hinged prosthesis. Clinical Orthopaedics and Related Research. **184**, 156-163. b

Bosch Pneumatics Catalogue. (1993) Robert Bosch GmbH, Stuttgart, Germany.

Bragdon C R, O'Connor D O, Jasty M and Syniuta W D. (1996) The importance of multidirectional motion on the wear of polyethylene. Proc Instn Mech Engrs. **210**, 157-165.

Brannon E W and Klein G. (1959) Experiences with a finger-joint prosthesis. J Bone Joint Surgery. **41A**, 87-102.

Brown K J, Atkinson J R, Dowson D and Wright V. (1976) The wear of ultrahigh molecular weight polyethylene and a preliminary study of its relation to the in vivo behaviour of replacement hip joints. Wear. **40**, 255-264.

Brummitt K and Hardaker C S. (1996) Estimation of wear in total hip replacement using a ten station hip simulator. Proc Instn Mech Engrs. **210**, 187-190.

Brummitt K, Hardaker C S, McCullagh P J J, Drabu K J and Smith R A. (1996) Effect of counterface material on the characteristics of retrieved uncemented cobalt-chromium and titanium alloy total hip replacements. Proc Instn Mech Engrs. **210**, 191-195.

BS7252: Part 4: 1990. Specification for bearing surfaces of hip joint prostheses. BSI publications, Milton Keynes.

Caravia L, Dowson D, Fisher J and Jobbins B. (1990) The influence of bone and bone cement debris on counterface roughness in sliding wear tests of ultra-high molecular weight polyethylene on stainless steel. Proc Instn Mech Engrs. **204**, 65-70.

Chao E Y and An K Y. (1978) Determination of internal forces in the human hand. J Engin Mechanics Div. ASCE. **104**, 255-272.

Chao E Y, Opgrande J D and Axmear F E. (1976) 3D force analysis of finger joints in selected isometric hand functions. Journal of Biomechanics. **9**, 387-96.

Condamine J L, Benoit J Y, Comtet J J and Aubroit J H. (1988) Proposed digital arthroplasty, critical study of the preliminary results. Ann Chir Main. 7, 4, 282-297.

Cook S D, Beckenbaugh R D, Weinstein A M and Klawitter J J. (1983) Pyrolite carbon implants in the metacarpophalangeal joint of baboons. Orthopaedics. **6**, 8, 952-961.

Cooper J R, Dowson D and Fisher J. (1993) The effect of transfer films and surface roughness on the wear of lubricated ultra-high molecular weight polyethylene. Clinical Materials. **14**, 295-302. a

Cooper J R, Dowson D and Fisher J. (1993) Macroscopic and microscopic wear mechanisms in ultra-high molecular weight polyethylene. Wear. **162-164**, 378-384. b

Cutts A and Bollen S R. (1993) Grip strength and endurance in rock climbers. Proc Instn Mech Engrs. **207**, 87-92.

Davidson J A and Lynch G E. (1988) The effect of human synovial lubricant and temperature of in vitro friction and torque of the prosthetic hip. Proc 12th annual meeting, American society Biomechanics, Univ III, Urbana, Sept 28-30, 4-5.

Derbyshire B, Fisher J, Dowson D, Hardaker C and Brummitt K. (1994) Comparative study of the wear of UHMWPE with zirconia ceramic and stainless steel femoral heads in artificial hip joints. Med Eng Phys. **16**, 229-236.

Derkash R S, Niebauer J J and Lane C S. (1986) Long-term follow up of metacarpal phalangeal arthroplasty with silicon dacron prostheses. Journal of Hand Surgery. **11A**, 4, 553-558.

Devas M and Shah V. (1985) Link arthroplasty of the metacarpophalangeal joints. J Bone Joint Surgery. **57B**, 1, 72-77.

Dickob M and Martini T. (1996) The cementless PM hip arthroplasty. J Bone Joint Surgery. **78B**, 2, 195-199.

Dieppe P. (1994) Towards preventing osteoarthritis. Arthritis Today. **90**, 3-5.

Doi K, Kuwata N and Kawai S. (1984) Alumina ceramic finger implants: a preliminary biomaterial and clinical evaluation. Journal of Hand Surgery. **9A**, 5, 740-749.

Dowson D & Wright V (eds). (1981) An introduction to the biomechanics of joints and joint replacements. Mechanical Engineering Publications Limited.

Dowson D, Taheri S and Wallbridge N C. (1987) The role of counterface imperfections in the wear of ultra-high molecular weight polyethylene. Wear. **119**, 277-293.

Dowson D. (1989) 'Are our joint replacement materials adequate?', in I. Mech. E conference on 'The changing role of engineering in orthopaedics'. Paper C384, 1-6.

Dowson D. (1994) A comparative study of the performance of metallic and ceramic femoral head components in total replacement hip joints. Proceedings of Austrib '94, 59-73.

Drabu K J, Michaud R J, McCullagh P J J, Brummitt K and Smith R A. (1994) Assessment of titanium alloy on polyethylene bearing surfaces in retrieved uncemented total hip prostheses. Proc Instn Mech Engrs. **208**, 91-96.

El-Gammal T A and Blair W F. (1993) Motion after metacarpophalangeal joint reconstruction in rheumatoid disease. Journal of Hand Surgery. **18A**, 504-511.

Fisher J, Firkins P, Reeves E A, Hailey J L and Issac G H. (1995) The influence of scratches to metallic counterfaces on the wear of ultra-high molecular weight polyethylene. Proc Instn Mech Engrs. **209**, 263-264.

Fisher J. (1995) Wear of ultra-high molecular weight polyethylene in total artificial joints. Current Orthopaedics, 164-169.

Flatt A E and Fischer G W. (1969) Biomechanical factors in the replacement of rheumatoid finger joints. Ann Rheum Dis. **28** (Suppl) 36-41.

Flatt A E. (1983) 'Care of the Arthritic Hand'. 4th edition, St Louis, C V Mosby Co., London.

Fleming S G and Hay E C. (1984) Metacarpophalangeal arthroplasty - eleven year follow up study. Journal of Hand Surgery. **9B**, 300-302.

Geborek P and Wollheim F A. (1993) Synovial fluid in Wright V and Radin E L, (eds) Mechanics of human joints: physiology, pathophysiology and treatment. Marcel Dekker, New York.

Geesink R G T and Hoefnagels N H M. (1995) Six year results of hydroxyapatite-coated total hip replacement. J Bone Joint Surgery. **77B**, 4, 534-547.

Gillespie T E, Flatt A E, Youm Y and Sprague B L. (1979) Biomechanical evaluation of metacarpophalangeal joint prosthesis designs. Journal of Hand Surgery. **4**, 508-521.

Gordon M and Bullough P G. (1982) Synovial and osseous inflammation in failed silicon-rubber prostheses. J Bone Joint Surgery. **64A**, 4, 574-580.

Hagert C G, Branemark P I, Albrektsson T, Strid K G and Irstram L. (1986) Metacarpophalangeal joint replacement with osseointegrated endoprostheses. Scand J Plast Reconstr Surg. **20**, 207-218.

Hagert C G. (1975) Metacarpophalangeal joint implants: III. Roentgenographic study of the in vivo function. Scand J Plast Reconstr Surg. **9**, 147-157.

Hakstain R W and Tubiana R. (1967) Ulnar deviation of the fingers. The role of joint structure and function. J Bone Joint Surgery. **49A**, 299-316.

Hall R M, Unsworth A, Siney P and Wroblewski B M. (1996) Wear in retrieved Charnley acetabular sockets. Proc Instn Mech Engrs. **210**, 197-208.

Harrison S H. (1978) The rheumatoid hand. Clinics in Rheumatic Diseases. **4**, 2, 403-13.

Helliwell P S, Howe A and Wright V. (1988) An evaluation of the dynamic qualities of isometric grip strength. Ann Rheum Dis. **47**, 934-939

Howie D W, Roberts B V, Oakeshott R and Manthey B A. (1988) A rat model of bone resorption at the cement bone interface in the presence of polyethylene wear particles. J Bone Joint Surgery. **70A**, 256-263.

Jones A R, Unsworth A and Haslock I. (1985) A microcomputer controlled hand assessment system used for clinical measurement. Engineering in Medicine. **14**, 4, 191-198.

Kay A G L, Jeffs J V and Scott J T. (1978) Experience with silastic prostheses in the rheumatoid hand. Ann Rheum Dis. **37**, 3, 255-258.

Kessler I. (1974) A new silicon implant for replacement of destroyed metacarpal heads. The Hand. **6**, 308-310.

Khoo C T K. (1993) Silicone synovitis. Journal of Hand Surgery. **18B**, 6, 679-686.

Kjeldsen-Kragh J, Haugen M, Borchgrevink C F, Laerum E, Eek M, Mowinkel P, Hovi K and Forre O. (1991) Controlled trial of fasting and one-year vegetarian diet in rheumatoid arthritis. The Lancet. **338**, 899-902.

Kumar P, Oka M, Ikeuchi K, Shimizu K, Yamamuro T, Okumura H and Koloura Y. (1991) Low wear rates of UHMWPE against zirconia ceramic in comparison to alumina ceramic and SUS 316L alloy. J Biomed Mat Res. **25**, 813-828.

Lazar G and Schulter-Ellis F P. (1980) Intramedullary structure of human metacarpals. Journal of Hand Surgery. **5A**, 477-481.

Leijnse J N A L, Snijders C J, Bonte J E, Landsmeer J M F, Kalker J J, van der Meulen J C, Sonneveld G J and Hovius S E R. (1993) The hand of the musician; the kinematics of the bidigital finger system with anatomical restrictions. Journal of Biomechanics. **26**, 10, 1169-1179.

Levack B, Stewart H D, Hanska Flierenga and Helal B. (1987) Metacarpophalangeal joint replacement with a new prosthesis: description and preliminary results of treatment with the Helal flap joint. Journal of Hand Surgery. **12B**, 3, 377-381.

Linscheid R L and Dobyns J H. (1979) Total Joint Arthroplasty. The Hand. Mayo Clinic Proc. **54**, 516-526.

Lister, G. (1993) The Hand. Diagnosis and Indications. Third edition. Churchill Livingstone. 0443 045 453

Long C, Conrad P W, Hall E A and Furler S L. (1970) Intrinsic-extrinsic muscle control of the hand in power grip and precision handling. J Bone Joint Surgery. **52A**, 5, 853-867.

Lundborg G, Branemark P I, and Carlsson I. (1993) Metacarpophalangeal joint arthroplasty based on the osseointegration concept. Journal of Hand Surgery. **18B**, 693-703.

Malcolm A J. (1988) Pathology of longstanding cemented total hip replacements in Charnley's cases. J. Bone Joint Surgery. **70B**, 153.

Mathiowetz V, Weber K, Volland G and Kashman N. (1984) Reliability and validity of grip and pinch strength evaluations. Journal of Hand Surgery. **9A**, 222-226.

Mathiowetz V, Kashman N, Volland G, Weber K, Dowe M and Rogers D. (1985) Grip and pinch strength: normative data for adults. Arch Phys Med Rehab. **66**, 69-74.

McKellop H. (1981) Wear of artificial joint materials II. 12 channel wear screening device: correlation of experimental and clinical results. Engineering in Medicine. **10**, 3, 123-136.

McMaster M. (1972) The natural history of the rheumatoid metacarpophalangeal joint. J Bone Joint Surgery. **54B**, 4, 687-697.

Minami A, An A K, Cooney W P, Linscheid R L and Chao E Y S. (1984) Ligamentous structures of the metacarpophalangeal joint: a quantitative anatomic study. Journal of Orthopaedic Research. **1**, 4, 361-368.

Minami A, An K N, Cooney W P, Linscheid R L and Chao E Y S. (1985) Ligament stability of the metacarpophalangeal joint: a biomechanical study. Journal of Hand Surgery. **10A**, 2, 255-260.

Minami M, Yamazaki J, Kato S and Ishii S. (1988) Alumina ceramic prosthesis arthroplasty of the metacarpophalangeal joint in the rheumatoid hand. Journal of Arthroplasty. **3**, 2, 157-166.

Mirra J H, Marder R A and Amstutz H C. (1982) The pathology of failed total joint arthroplasty. Clinical Orthopaedics and Related Research. **170**, 175-183.

Müller M E. (1995) The benefits of metal-on-metal total hip replacements. Clinical Orthopaedics and Related Research. **311**, 54-59.

Nalebuff E A. (1984) The rheumatoid hand. Clinical Orthopaedics and Related Research. **182**, 150-159.

Nicolle F V and Calnan J S. (1972) A new design of the finger joint prosthesis for the rheumatoid hand. The Hand. **4**, 135-146.

Niebauer J J, Shaw J L and Doren W W. (1969) Silicone-dacron hinge prosthesis. Design, evaluation and application. Ann Rheum Dis. **28** (Suppl) 56-58.

Ohtsuki T. (1981) Inhibition of individual fingers during grip strength exertion. Ergonomics. **24**, 21-36.

Pagowski S and Piekarski K. (1977) Biomechanics of the metacarpophalangeal joint. J Biomechanics. **10**, 205-209.

Pearson R, MacKinnon M J and Meek A P. (1982) Diurnal and sequential grip function in normal subjects and effects of temperature change and exercise of the forearm on grip functions in patients with rheumatoid arthritis and in normal controls. Scand J Rheumatology. **11**, 113-118.

Phillips T W and Messieh S S. (1988) Cementless hip replacement for arthritis. J Bone Joint Surgery. **70B**, 5, 750-755.

Porter A E D J. (1993) A portable hand assessment system. Final year project. University of Durham.

Profio A E. (1993) 'Biomedical Engineering'. 1st edition, John Wiley & Sons Inc., New York. ISBN 0-471-57768-5.

Rae T, Rushton N, Thomson L, Lardner A and Martin S. (1988) Biocompatibility studies of cross-linked polyethylene. J Bone Joint Surgery. **70B**, 5, 852.

Reis N D and Calnan J S. (1969) Integral hinge joint. Ann Rheum Dis. **28** (Suppl) 59-62.

Rose R M, Schneider H, Reis M, Paul I, Crugnola A, Simon S R and Radin E L. (1978) A method for the quantitative recovery of polyethylene wear debris from the simulated service of total joint prostheses. Wear. **51**, 77-84.

Saikko V. (1993) Wear and friction properties of prosthetic joint materials evaluated on a reciprocating pin on flat apparatus. Wear. **166**, 169-178

Schetrumpf J. (1975) A new metacarpophalangeal joint prosthesis. The Hand. 7, 1, 75-77.

Schultz R J, Johnston A D and Krishnamurthy S. (1987) Thermal effects of polymerisation of methyl-methacrylate on small tubular bones. International Orthopaedics. **11**, 277-282.

Short C. (1993) Wear testing of polyethylene for finger joint replacement. Final year project, University of Durham.

Sibly T F and Unsworth A. (1991) Fixation of a surface replacement endoprosthesis of the metacarpophalangeal joint. Proc Instn Mech Engrs. **205**, 227-232.

Sibly T F and Unsworth A. (1991) Wear of cross linked polyethylene against itself: a material suitable for surface replacement of the finger joint. Journal of Biomedical Engineering. **13**, 217-220.

Smith E M, Juvinall R C, Bender L F and Pearson T R. (1964) Role of the finger flexors in rheumatoid deformities of the metacarpophalangeal joints. Arthritis Rheum. 7, 467-480.

Smith R J and Kaplan E B. (1967) Rheumatoid deformities at the metacarpophalangeal joints of the fingers. J Bone Joint Surgery. **49A**, 31-47.

Stokoe S M, Unsworth A, Viva C and Haslock I. (1990) A finger function simulator and the laboratory testing of joint replacements. Proc Instn Mech Engrs. **204**, 233-240.

Stokoe S M. (1990) A finger function simulator and surface replacement prosthesis for the metacarpophalangeal joint. PhD thesis, University of Durham.

Sturrock R. (1992) Rheumatoid arthritis. The Practitioner. **236**, 1077-1082.

Swanson A B & de Groot Swanson G. (1984) Flexible implant arthroplasty in the rheumatoid metacarpophalangeal joint. Clinics in Rheumatoid Disease. **10**, 3, 609-629

Swanson A B, Poitevin L A, DeGroot-Swanson G and Kearney J. (1986) Bone remodelling phenomena in flexible implant arthroplasty in the metacarpophalangeal joints. Long term study. Clinical Orthopaedics and Related Research. **205**, 254-262.

Swanson A B. (1972) Flexible implant arthroplasty for arthritic finger joints. J Bone Joint Surgery. **54A**, 435-456.

Szivek J A, Weatherly G C, Pilliar R M and Cameron H U. (1981) A study of bone remodelling using metal-polymer laminates. J Biomedical Materials Research. **15**, 853-865.

Tamai K, Ryu J, An K N, Linscheid R L, Cooney W P and Chao E Y S. (1988) Three dimensional geometric analysis of the metacarpophalangeal joint. Journal of Hand Surgery. **13A**, 4, 521-529.

Unsworth A and Alexander W J. (1979) Dimensions of the metacarpo-phalangeal joint with particular reference to joint prostheses. Engineering in Medicine. **8**, 2, 75-80.

Unsworth A, Dowson D and Wright V. (1971) Cracking joints - a bioengineering study of cavitation in the metacarpophalangeal joint. Ann Rheum Dis. **30**, 348-357.

Unsworth A, Haslock, I, Vasandakumar V and Stamp J. (1990) A laboratory and clinical study of pneumatic 'grip strength' devices. Br J Rheumatology. **29**, 440-444.

Unsworth A, White E F T and White G. (1987) Soft layer lubrication of artificial hip joints. Proc I Mech E. Int. Vol. Trib. London. 715-724.

Unsworth A. (1993) Lubrication of Human Joints in Wright V and Radin E L, (eds) Mechanics of human joints: physiology, pathophysiology and treatment, Marcel Dekker, New York.

Varma S K and Milward T M. (1991) The Nicolle finger joint prosthesis: a reappraisal. Journal of Hand Surgery. **16B**, 2, 187-190.

Walker D A. (1990) An investigation into the wear of a cross-linked polyethylene finger prosthesis. Final year project, University of Durham.

Walker P S and Erkman M J. (1975) Laboratory evaluation of a metal plastic type of metacarpophalangeal joint prosthesis. Clinical Orthopaedics and Related Research. **112**, 349-356.

Walker P S and Straub L R. (1977) Development and evaluation of a mechanical finger prosthesis. C168/77, IMechE. 127-132.

Walker P S, Davidson W and Erkman M J. (1978) An apparatus to assess function of the hand. Journal of Hand Surgery. **3**, 2, 189-193.

Walker P S, Nunamaker D, Huiskes R, Parchinski T and Greene D. (1983) A new approach to the fixation of a metacarpophalangeal joint prosthesis. Engineering in Medicine. **12**, 3, 135-140.

Wallbridge N C and Dowson D. (1987) Distribution of wear rate data and a statistical approach to sliding wear theory. Wear. **119**, 295-312.

Wang A, Stark C and Dumbleton J H. (1996) Mechanistic and morphological origins of UHMWPE wear debris in total joint replacement prostheses. Proc Instn Mech Engrs. **210**, 141-155.

Weightman B and Amis A A. (1982) Finger joint force predictions related to design of joint replacements. J Biomedical Engineering. **4**, 197-205.

Weightman B, Evans D M and Light D. (1983) The laboratory development of a new metacarpophalangeal prosthesis. The Hand. **15**, 1, 57-69.

Welsh R P, Hastings D E and White R. (1982) Resurfacing arthroplasty for the metacarpophalangeal joint. Acta Orthopaedica Belgica. **48**, 924-927.

Williams D. (1990) Biomaterials for tomorrow. Professional Engineering. **3**, 12, 38-39.

Wilson Y G, Sykes P J and Niranjan N S. (1993) Long term follow up of Swanson's silastic arthroplasty of the metacarpophalangeal joints in rheumatoid arthritis. Journal of Hand Surgery. **18B**, 1, 81-91.

Wood V E, Ichtertz D R and Yahiku H. (1989) Soft tissue metacarpophalangeal reconstruction for treatment of rheumatoid hand deformity. Journal of Hand Surgery. **14A**, 2, 1, 163-174.

Wright K W J, Dobbs H S and Scales J T. (1982) Wear studies on prosthetic materials using the pin-on-disc machine. Biomaterials. **3**, 41-48.

Wroblewski B M, Siney P D, Dowson D and Collins S N. (1996) Prospective clinical and joint simulator studies of a new total hip arthroplasty using alumina ceramic heads and cross-linked polyethylene cups. J Bone Joint Surgery. **78B**, 2, 280-285.

Youm Y, Gillespie, T E, Flatt A E and Sprague B L. (1978) Kinematic investigation of normal MCP joint. J Biomechanics. **11**, 109-118.

Appendix 1

The Durham Metacarpophalangeal Prosthesis Production Drawings

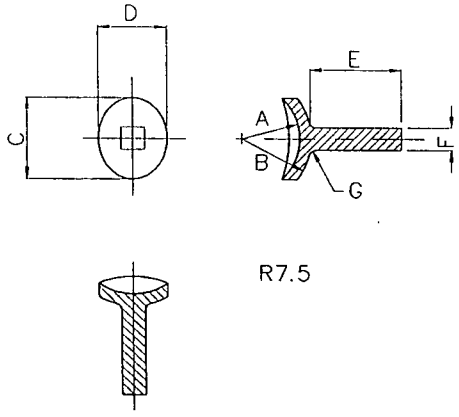

A	B	C	D	E	F	G
5.5	7.0	8.50	6.34	12.0	3.0 SQ	R1.0
6.5.	8.0	9.66	7.53	12.0	3.0 SQ	R1.0
7.5	9.0	10.82	8.72	12.0	3.0 SQ	R1.0
8.5	10.0	11.98	9.91	12.0	3.0 SQ	R1.0
9.5	11.0	13.14	11.10	12.0	3.0 SQ	R1.0

PHALANGEAL TABLE OF DIMENSIONS.

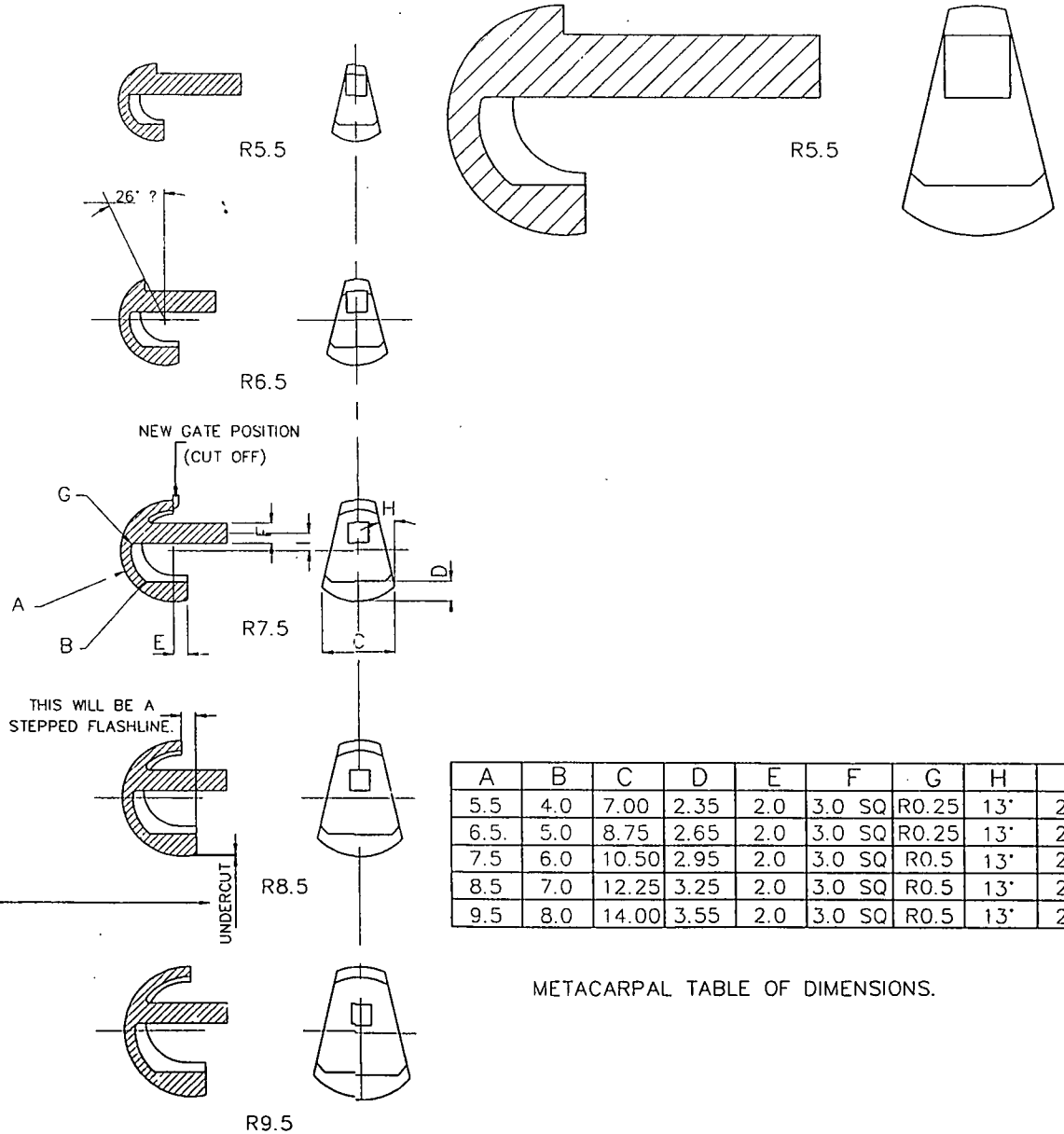

A	B	C	D	E	F	G	H	I
5.5	4.0	7.00	2.35	2.0	3.0 SQ	R0.25	13°	2.6
6.5.	5.0	8.75	2.65	2.0	3.0 SQ	R0.25	13°	2.6
7.5	6.0	10.50	2.95	2.0	3.0 SQ	R0.5	13°	2.6
8.5	7.0	12.25	3.25	2.0	3.0 SQ	R0.5	13°	2.6
9.5	8.0	14.00	3.55	2.0	3.0 SQ	R0.5	13°	2.6

METACARPAL TABLE OF DIMENSIONS.

All unspecified dimensions are mm

To Dept.	Date Issued
Prod. Eng.	
Prod. Cont.	
Qual. Cont.	

Catalogue Number

Computer Number

Alterations

Number	Issue	Signed	Date

Material X.L.P.E

Quantity Per Assy

Scale

Drawn G.M. Date

Checked Date

Project Leader P.KILBURN Date

General specifications

Surface Finish N8 N7 N6

Metric tolerances

0; ±0.5 0.0; ±0.25 0.00; ±0.10

Imperial tolerances

Fractional dims ±1/64" Decimal dims ±0.005"

Angular tolerance ±0.5°

Geometrical tolerances

As implied by linear tolerances except where specified See B.S.5100 & 308 Pt.2 for symbols

Product Title
PHALANGEAL AND METACARPAL COMPONENTS.

Drg. Title
COMPONENT DRAWING.

O DePuy
International Ltd.

Drg.No B000294A

Appendix 2

Finger Function Simulator
Test Results:
Tables of Weight Loss

Table A2.1 Test 1 Results

Test Duration		Metacarpal Wt. Change ($x10^{-4}g$)			Phalangeal Wt. Change ($x10^{-4}g$)			Volume Loss (mm^3)	
Dist. km	Fwheel cyc $x10^3$	Test	Con-trol	O/all	Test	Con-trol	O/all	Meta-carpal	Phalan-geal
0	0	---	0	0	---	0	0	0	0
1.2	42	-2	+2	-4	-3	-1	-2	0.4	0.2
6.7	235	-12	+2	-14	-11	1	-10	1.5	1.1
13.7	465	-16	+5	-21	-10	0	-10	2.2	1.1
24.7	841	-28	+4	-32	-15	0	-15	3.4	1.6
40.2	1368	-33	+7	-40	-18	1	-19	4.2	2.0
47.5	1615	-42	+6	-48	-20	1	-21	5.1	2.2
60.3	2052	-48	+6	-54	-20	1	-21	5.7	2.2
74.4	2496	-55	+8	-63	-22	1	-23	6.6	2.4
91.0	3094	-63	+7	-70	-23	1	-24	7.4	2.5
101.5	3451	-68	+8	-76	-24	1	-25	8.0	2.6
115.3	3923	-68	+10	-78	-24	3	-27	8.2	2.8
133.5	4540	-77	+9	-86	-26	2	-28	9.1	3.0
157.6	5358	-97	+11	-108	-34	3	-37	11.4	3.9
171.9	5847	-112	+13	-115	-35	5	-40	12.1	4.2
190.3	6471	-113	+11	-124	-40	3	-43	13.1	4.5

Table A2.2 Test 2 Results

Test Duration		Metacarpal Wt. Change ($x10^{-4}g$)			Phalangeal Wt. Change ($x10^{-4}g$)			Volume Loss (mm^3)	
Dist. km	Fwheel cyc $x10^3$	Test	Con-trol	O/all	Test	Con-trol	O/all	Meta-carpal	Phalan-geal
0	0	---	0	0	---	0	0	0	0
23.9	814	-1	0	-1	-2	0	-2	0.11	0.21
35.7	1215	-2	0	-2	-3	0	-3	0.21	0.32
55.7	1896	-5	+1	-6	-5	+1	-6	0.63	0.63
65.9	2242	-7	-2	-5	-6	0	-6	0.53	0.63
82.9	2819	-5	+1	-6	-6	+1	-7	0.63	0.74
108.8	3701	-5	+2	-7	-5	+1	-6	0.74	0.63
130.2	4429	-7	+3	-10	-6	+2	-8	1.05	0.84
157.4	5353	-6	+3	-9	-6	+1	-7	0.95	0.74
174.6	5941	-8	+5	-13	-5	+2	-7	1.37	0.74
193.5	6581	-9	+5	-14	-5	+3	-8	1.48	0.84
203.4	6919	-10	+6	-16	-6	+3	-9	1.69	0.95
214.6	7299	-11	+6	-17	-5	+3	-8	1.79	0.84
223.9	7615	-12	+7	-19	-6	+3	-9	1.99	0.95

Table A2.3 Test 3 Results

Test Duration		Metacarpal Wt. Change ($x10^{-4}g$)			Phalangeal Wt. Change ($x10^{-4}g$)			Volume Loss (mm^3)	
Dist. km	Fwheel cyc $x10^3$	Test	Con-trol	O/all	Test	Con-trol	O/all	Meta-carpal	Phalan-geal
0	0	---	0	0	---	0	0	0	0
7.2	244	+1	+1	0	+1	+1	0	0	0
29.5	1004	+1	+2	-1	0	+1	-1	0.11	0.11
48.7	1656	+1	+2	-1	0	+2	-2	0.11	0.21
66.7	2274	0	+3	-3	-1	+1	-2	0.32	0.21
82.6	2809	0	+5	-5	-1	+2	-3	0.53	0.32
93.4	3176	0	+4	-4	-1	+2	-3	0.42	0.32
112.6	3830	0	+5	-5	-1	+2	-3	0.53	0.32
131.3	4465	0	+5	-5	-1	+3	-4	0.53	0.42
169.6	5769	0	+6	-6	-2	+3	-5	0.63	0.53
183.7	6250	-1	+6	-7	-2	+3	-5	0.74	0.53
212.0	7212	-1	+6	-7	-2	+3	-5	0.74	0.53
234.6	7981	-1	+6	-7	-2	+3	-5	0.74	0.53
253.1	8607	-2	+6	-8	-2	+3	-5	0.84	0.53
277.8	9448	-1	+7	-8	-3	+3	-6	0.84	0.63
304.0	10338	-1	+9	-10	-2	+4	-6	1.05	0.63
322.4	10965	-2	+9	-11	-2	+4	-6	1.16	0.63
341.8	11627	-2	+9	-11	-3	+5	-8	1.16	0.84
367.8	12511	-1	+10	-11	-2	+5	-7	1.16	0.74
391.7	13323	-3	+10	-13	-3	+5	-8	1.37	0.84
421.4	14335	-2	+13	-15	-3	+6	-9	1.58	0.95
447.4	15217	-2	+14	-16	-2	+7	-9	1.69	0.95
466.7	15876	-3	+13	-16	-3	+6	-9	1.69	0.95
486.0	16532	-2	+14	-16	-3	+7	-10	1.69	1.05
500.4	17019	-2	+14	-16	-3	+6	-9	1.69	0.95
507.9	17276	-3	+14	-17	-3	+6	-9	1.79	0.95
547.6	18625	-2	+15	-17	-2	+7	-9	1.79	0.95
572.7	19480	-2	+16	-18	-2	+8	-10	1.90	1.05
600.1	20412	-2	+16	-18	-2	+7	-9	1.90	0.95
632.8	21525	-1	+17	-18	-2	+7	-9	1.90	0.95

Table A2.4 Test 4 Results

Test Duration		Metacarpal Wt. Change ($x10^{-4}g$)			Phalangeal Wt. Change ($x10^{-4}g$)			Volume Loss (mm^3)	
Dist. km	Fwheel cyc $x10^3$	Test	Con-trol	O/all	Test	Con-trol	O/all	Meta-carpal	Phalan-geal
0	0	---	0	0	---	0	0	0	0
17.0	638	-3	+1	-4	-1	0	-1	0.42	0.11
25.9	971	-3	+2	-5	0	+1	-1	0.53	0.11
42.2	1581	-3	+2	-5	-1	0	-1	0.53	0.11
64.8	2425	-4	+3	-7	-1	+1	-2	0.74	0.21
82.6	3095	-5	+4	-9	-1	+2	-3	0.95	0.32
96.1	3600	-5	+3	-8	-2	+2	-4	0.84	0.42
117.2	4390	-6	+4	-10	-2	+2	-4	1.05	0.42
137.3	5141	-6	+4	-10	-2	+1	-3	1.05	0.32
154.0	5769	-5	+5	-10	-2	+2	-4	1.05	0.42
170.3	6377	-4	+5	-9	-1	+2	-3	0.95	0.32
190.4	7130	-3	+6	-9	-1	+3	-4	0.95	0.42
207.9	7788	-3	+10	-13	-1	+6	-7	1.37	0.74
227.8	8530	-2	+11	-13	-1	+6	-7	1.37	0.74
251.8	9431	-1	+11	-12	-1	+6	-7	1.26	0.74

Table A2.5 Test 5 Results

Test Duration		Metacarpal Wt. Change ($x10^{-4}g$)			Phalangeal Wt. Change ($x10^{-4}g$)			Volume Loss (mm^3)	
Dist. km	Fwheel cyc $x10^3$	Test	Con-trol	O/all	Test	Con-trol	O/all	Meta-carpal	Phalan-geal
0	0	---	0	0	---	0	0	0	0
24.2	907	+1	+1	0	0	0	0	0	0
40.8	1528	+1	+1	0	0	+1	-1	0	0.11
56.2	2105	+2	+2	0	0	+1	-1	0	0.11
80.7	3021	+2	+2	0	0	+1	-1	0	0.11
99.4	3724	+2	+2	0	-1	+1	-2	0	0.21
119.8	4486	+3	+2	+1	-1	+1	-2	-0.11	0.21
131.8	4938	+3	+2	+1	-1	+1	-2	-0.11	0.21
148.2	5550	+4	+3	+1	0	+2	-2	-0.11	0.21
164.8	6173	+3	+3	0	-1	+2	-3	0	0.32
180.5	6760	+3	+3	0	-1	+2	-3	0	0.32
202.7	7593	+3	+3	0	-1	+2	-3	0	0.32
218.0	8164	+3	+3	0	-1	+2	-3	0	0.32
243.0	9102	+3	+3	0	-1	+2	-3	0	0.32
272.0	10187	+3	+4	-1	-1	+3	-4	0.11	0.42

Table A2.6 Test 6 Results

Test Duration		Metacarpal Wt. Change ($x10^{-4}g$)			Phalangeal Wt. Change ($x10^{-4}g$)			Volume Loss (mm^3)	
Dist. km	Fwheel cyc $x10^3$	Test	Con-trol	O/all	Test	Con-trol	O/all	Meta-carpal	Phalan-geal
0	0	---	0	0	---	0	0	0	0
19.9	747	-1	+1	-2	0	0.1	-1	0.21	0.11
43.6	1631	-2	+1	-3	0	0	0	0.32	0
68.2	2554	-1	+1	-2	-1	0	-1	0.21	0.11
89.8	3363	-1	+2	-3	0	+1	-1	0.32	0.11
105.5	3950	-1	+2	-3	0	+1	-1	0.32	0.11
124.0	4642	-2	+1	-3	-1	+1	-2	0.32	0.21
151.5	5675	-2	+1	-3	-1	+1	-2	0.32	0.21
167.2	6261	-2	+1	-3	-1	+1	-2	0.32	0.21
187.2	7012	-2	+1	-3	-1	+1	-2	0.32	0.21
207.2	7762	-3	+1	-4	-1	+1	-2	0.42	0.21
220.0	8315	-2	+1	-3	-1	+2	-3	0.32	0.32
246.8	9242	-3	+1	-4	-1	+2	-3	0.42	0.32

Table A2.7 New Finger Simulator Test - Table of Results

f-e = flexion - extension.

Test Duration		Metacarpal Wt. Change ($x10^{-6}kg$)			Phalangeal Wt. Change ($x10^{-6}kg$)			Volume Loss (mm^3)	
Dist. km	f-e cyc $x10^3$	Test	Con-trol	O/all	Test	Con-trol	O/all	Meta-carpal	Phalan-geal
0	0	---	0	0	---	0	0	0	0
5.9	202	0	+0.2	-0.2	0	0	0	0.21	0
12.6	430	+0.1	+0.3	-0.2	0	0	0	0.21	0
17.9	608	+0.1	+0.2	-0.1	0	0	0	0.11	0
24.1	820	0	+0.2	-0.2	-0.1	0	-0.1	0.21	0.11
29.5	1004	0	+0.1	-0.1	-0.1	0	-0.1	0.11	0.11
35.8	1216	0	+0.1	-0.1	-0.1	0	-0.1	0.11	0.11
40.8	1388	-0.2	0	-0.2	-0.1	0	-0.1	0.21	0.11
53.0	1803	0	+0.2	-0.2	-0.1	+0.1	-0.2	0.21	0.21
69.3	2356	-0.1	+0.2	-0.3	-0.1	+0.1	-0.2	0.32	0.21
84.7	2881	-0.1	+0.3	-0.4	-0.2	+0.1	-0.3	0.42	0.32
97.6	3320	-0.1	+0.3	-0.4	-0.1	+0.2	-0.3	0.42	0.32
113.2	3850	-0.1	+0.4	-0.5	-0.2	+0.2	-0.4	0.53	0.42
126.0	4286	-0.1	+0.4	-0.5	-0.1	+0.2	-0.3	0.53	0.32
140.0	4762	-0.1	+0.5	-0.6	-0.1	+0.3	-0.4	0.63	0.42

Appendix 3

Pin On Plate Test Results:
Tables of Weight Loss

Wear of XLPE Pins against XLPE Plates

Test 1 (XLPE v XLPE)

Note: 1 - 4 = pin/plate numbers Co = Control Pin

1 and 3 had 10N loads, 2 and 4 had 40N loads

Table A3.1 Wear of XLPE Plates

Test Duration		Plate weight change $x10^{-4}g$			
Cycles	**km**	**1**	**2**	**3**	**4**
0	0	0	0	0	0
360,600	14.4	-2	-17	-2	-7
570,000	22.8	-3	-20	-5	-10
1,386,802	55.5	-6	-25	-6	-14
2,182,531	87.3	-7	-33	-9	-22
2,705,137	108.2	-8	-39	-13	-30
3,754,710	150.2	-8	-42	-13	-30
4,639,510	186.6	-8	-45	-13	-33
5,654,160	226.2	-9	-46	-13	-35
6,368,020	254.7	-11	-49	-15	-39
7,337,912	293.5	-12	-52	-18	-46
8,158,710	326.3	-12	-54	-18	-50
8,724,960	349.0	-13	-56	-20	-55

Table A3.2 Wear of XLPE Pins

Test Duration		Pin weight change $x10^{-4}g$				
Cycles	**km**	**Co**	**1**	**2**	**3**	**4**
0	0	0	0	0	0	0
360,600	14.4	0	-1	+1	+1	0
570,000	22.8	0	-1	0	0	0
1,386,802	55.5	0	0	+1	+1	0
2,182,531	87.3	-1	-1	-1	+1	-1
2,705,137	108.2	0	-1	-1	+1	-1
3,754,710	150.2	+1	-1	-1	+1	-1
4,639,510	186.6	0	-1	-1	+1	-2
5,654,160	226.2	+1	-1	0	+1	-2
6,368,020	254.7	0	-1	-1	+1	-2
7,337,912	293.5	+1	-1	-1	+1	-2
8,158,710	326.3	+1	-1	-1	+1	-2
8,724,960	349.0	0	-2	-1	+1	-2

Test 2 (XLPE v XLPE)

Table A3.3 Wear of XLPE Plates *** Test Ceased

Test Duration		Plate weight change $x10^{-4}g$			
Cycles	**km**	**1**	**2**	**3**	**4**
0	0	0	0	0	0
206,558	14.1	-6	-8	-10	-7
375,282	25.5	-9	-19	-14	-10
803,204	54.6	-10	-24	-14	-12
1,205,800	90.0	-8	-47	-14	-22
1,553,079	105.6	-18	-68	-27	-45
1,993,000	135.5	-15	-71	-24	-43
2,462,440	167.4	-22	-83	-30	-55
3,046,700	207.2	-30	-96	-42	-67
3,475,300	236.3	-27	-93	-43	-71
4,034,120	274.3	-38	-105	-58	-88
4,512,742	306.9	-40	-107	-61	-90
4,876,812	331.6	-38	-106	-60	-88
5,109,081	347.4	-39	-106	***	***
5,524,683	375.7	-43	-110	***	***
5,723,351	389.2	-48	-113	***	***
6,415,196	436.2	-58	-118	***	***
6,834,697	464.8	-62	-121	***	***

Table A3.4 Wear of XLPE Pins

Test Duration		Pin weight change $x10^{-4}g$				
Cycles	**km**	**Co**	**1**	**2**	**3**	**4**
0	0	0	0	0	0	0
206,558	14.1	0	0	-6	+1	-1
375,282	25.5	+1	-1	-6	0	-1
803,204	54.6	+2	+2	-6	+1	-1
1,205,800	90.0	+2	+1	-6	0	-1
1,553,079	105.6	+2	0	-7	-2	-2
1,993,000	135.5	+4	0	-5	-1	0
2,462,440	167.4	+3	-1	-4	-2	-2
3,046,700	207.2	+3	-3	-4	-4	-2
3,475,300	236.3	+4	-3	-4	-2	-2
4,034,120	274.3	+4	-3	-5	-4	-3
4,512,742	306.9	+4	-3	-5	***	***
4,876,812	331.6	+5	-3	-4	***	***
5,109,081	347.4	+5	-3	-5	***	***
5,524,683	375.7	+5	-4	-4	***	***
5,723,351	389.2	+5	-5	-4	***	***
6,415,196	436.2	+5	-7	-5	***	***
6,834,697	464.8	+5	-8	-5	***	***

Test 3 (XLPE v XLPE)

Note: 1 and 3 had 10N loads, 2 and 4 had 40N loads.

Pins 3 and 4 manufactured from plate material.

Pins 1 and 2 manufactured from sprue material. See figure 4.3.

1 - 4 = plate/pin numbers. Co = control pin.

Table A3.5 Wear of XLPE Plates

Test Duration		Plate weight change $x10^{-4}g$			
Cycles	**km**	**1**	**2**	**3**	**4**
0	0	0	0	0	0
547,400	21.9	+3	-2	+3	-1
1,208,260	48.3	0	-12	0	-6
2,178,025	87.1	-8	-27	-4	-19
3,141,462	125.7	-15	-35	-7	-31
4,039,570	161.6	-18	-38	-9	-36
4,798,984	192.0	-21	-45	-13	-45
5,759,532	230.4	-24	-52	-13	-50
6,642,000	265.7	-28	-63	-16	-56
7,449,500	298.0	-30	-68	-18	-61
8,172,500	326.9	-31	-70	-19	-62
8,981,650	359.3	-30	-68	-16	-61
9,793,800	391.8	-31	-70	-18	-64
10,676,400	427.1	-30	-69	-16	-64
11,235,547	449.4	-34	-74	-21	-71
11,985,158	479.4	-35	-76	-21	-70
12,828,300	513.1	-34	-76	-20	-70
13,627,200	545.1	-36	-78	-21	-72
14,254,500	570.2	-37	-79	-21	-72
15,196,800	607.9	-36	-78	-21	-72

Table A3.6 Wear of XLPE Pins

Test Duration		Pin weight change x10^{-4}g				
Cycles	**km**	**Co**	**1**	**2**	**3**	**4**
0	0	0	0	0	0	0
547,400	21.9	0	0	0	-1	-1
1,208,260	48.3	0	0	0	0	0
2,178,025	87.1	0	0	-1	-1	-1
3,141,462	125.7	0	0	-1	-1	-1
4,039,570	161.6	0	0	-1	0	-1
4,798,984	192.0	0	0	-1	0	-2
5,759,532	230.4	0	0	-2	0	-2
6,642,000	265.7	-1	-1	-2	0	-2
7,449,500	298.0	-1	-1	-2	0	-2
8,172,500	326.9	-1	-1	-2	0	-3
8,981,650	359.3	0	0	-2	0	-2
9,793,800	391.8	0	0	-2	0	-2
10,676,400	427.1	0	0	-2	0	-2
11,235,547	449.4	0	0	-3	0	-3
11,985,158	479.4	-1	0	-3	0	-3
12,828,300	513.1	-1	0	-3	0	-3
13,627,200	545.1	-1	0	-2	0	-3
14,254,500	570.2	0	0	-2	0	-3
15,196,800	607.9	0	0	-3	0	-3

Test 4 (XLPE v XLPE)

All pins were manufactured from 'flat' material. See figure 4.3.

All loads were 40N. 3, 4 and 5 = pin/plate numbers.

Table A3.7 Wear of XLPE Plates

Test Duration		Plate weight change $x10^{-4}g$		
Cycles	km	3	4	5
0	0	0	0	0
594,000	22.6	-16	-16	-15
1,466,615	55.7	-32	-27	-32
2,158,135	82.0	-40	-31	-42
2,750,700	104.5	-50	-36	-51

Table A3.8 Wear of XLPE Pins

Test Duration		Pin weight change $x10^{-4}g$			
Cycles	km	Co	3	4	5
0	0	0	0	0	0
594,000	22.6	0	+1	0	0
1,466,615	55.7	+1	0	-1	0
2,158,135	82.0	0	0	-1	0
2,750,700	104.5	0	0	-2	0

Test 5 (XLPE v XLPE)

All pins were manufactured from 'flat' material. See figure 4.3.

All loads were 40N. 1, 2 and 6 = pin/plate numbers.

Table A3.9 Wear of XLPE Plates

Test Duration		Plate weight change $x10^{-4}g$		
Cycles	km	1	2	6
0	0	0	0	0
527,478	20.0	-22	-23	-28
1,198,338	45.5	-46	-42	-51
1,800,000	68.4	-62	-56	-75

Table A3.10 Wear of XLPE Pins

Test Duration		Pin weight change $x10^{-4}g$			
Cycles	km	Co	1	2	6
0	0	0	0	0	0
527,478	20.0	0	0	0	0
1,198,338	45.5	0	0	0	-1
1,800,000	68.4	0	0	0	-1

Wear of UHMWPE pins against UHMWPE plates.
Weight changes

Test 6 Non-irradiated UHMWPE, several months old.

Note: 1 - 4 pin or plate numbers. Co = control pin or plate.
1 and 3 had 10N loads, 2 and 4 had 40N loads.

Table A3.11 Wear of UHMWPE Plates

Test Duration		Plate Weight Change ($x10^{-4}g$)				
Cycles	km	1	2	3	4	Co
0	0	0	0	0	0	0
97,500	3.9	-56	-187	-43	-114	+3
323,000	12.9	-183	-734	-71	-892	+6
478,050	19.1	-207	-1054	-87	-1256	+7
557,560	22.3	-219	-1229	-96	---	+7
651,756	26.1	-232	---	-107	---	+8
884,700	35.4	-269	---	-131	---	+9
1,119,190	44.8	-319	---	-154	---	+10
1,446,337	57.9	-396	---	-192	---	+11
1,512,908	60.5	-415	---	-230	---	+11
1,946,400	77.9	-550	---	-319	---	+11
2,185,200	87.4	-610	---	-372	---	+12
2,521,000	100.8	-747	---	-467	---	+12
2,763,929	110.6	-840	---	-537	---	+14
3,094,104	123.8	-1006	---	-636	---	+15
3,335,750	133.4	-1136	---	-726	---	+14
3,669,500	146.8	-1339	---	-896	---	+17
3,387,000	153.5	-1447	---	-1011	---	+19

Test 6 (continued)

Table A3.12 Wear of UHMWPE Pins

Test Duration		Pin Weight Change ($x10^{-4}g$)				
Cycles	**km**	**Co**	**1**	**2**	**3**	**4**
0	0	0	0	0	0	0
97,500	3.9	0	-11	-141	-9	-121
323,000	12.9	0	-84	-464	-77	-232
478,050	19.1	0	-138	-705	-124	-536
557,560	22.3	0	-161	---	-151	---
651,756	26.1	+1	-172	---	-160	---
884,700	35.4	0	-217	---	-193	---
1,119,190	44.8	0	-258	---	-215	---
1,446,337	57.9	0	-342	---	-300	---
1,512,908	60.5	0	-353	---	-315	---
1,946,400	77.9	+1	-476	---	-444	---
2,185,200	87.4	0	-550	---	-509	---
2,521,000	100.8	0	-660	---	-607	---
2,763,929	110.6	0	-746	---	-691	---
3,094,104	123.8	0	-890	---	-828	---
3,335,750	133.4	0	-998	---	-927	---
3,669,500	146.8	0	-1153	---	-1073	---
3,387,000	153.5	0	-1239	---	-1143	---

Test 7 Irradiated UHMWPE, new.

Note: 1 - 4 pin or plate numbers. Co = control pin or plate.
All had 10N loads.

Table A3.13 Wear of UHMWPE Plates

Test Duration		Plate Weight Change ($x10^{-4}g$)				
Cycles	**km**	**1**	**2**	**3**	**4**	**Co**
0	0	0	0	0	0	0
87,500	3.5	-26	-30	-19	-24	+2
528,893	21.2	-111	-124	-65	-85	+4
868,531	34.7	-160	-171	-104	-113	+6
1,076,549	43.1	-190	-220	-124	-133	+9
1,610,934	64.4	-278	-344	-165	-217	+15
1,958,000	78.3	-350	-454	-205	-285	+18
2,193,151	87.7	-406	-523	-233	-339	+17
2,608,141	104.3	-524	-679	-306	-462	+20
3,185,700	127.4	-682	-864	-409	-645	+21
3,821,000	152.8	-873	-1093	-548	-881	+22

Table A3.14 Wear of UHMWPE Pins

Test Duration		Pin Weight Change ($x10^{-4}g$)				
Cycles	**km**	**Co**	**1**	**2**	**3**	**4**
0	0	0	0	0	0	0
87,500	3.5	0	-2	-2	-3	-2
528,893	21.2	0	-38	-48	-69	-42
868,531	34.7	0	-75	-90	-107	-74
1,076,549	43.1	+1	-98	-113	-132	-94
1,610,934	64.4	+1	-159	-176	-190	-151
1,958,000	78.3	+1	-198	-221	-235	-194
2,193,151	87.7	+1	-228	-252	-263	-224
2,608,141	104.3	+1	-281	-312	-313	-279
3,185,700	127.4	+1	-355	-388	-377	-354
3,821,000	152.8	+1	-437	-479	-450	-441

Test 8 Non-irradiated UHMWPE, new.

Note: 1 - 4 pin or plate numbers. Co = control pin or plate.
All had 10N loads.

Table A3.15 Wear of UHMWPE Plates

Test Duration		Plate Weight Change ($x10^{-4}g$)				
Cycles	**km**	**1**	**2**	**3**	**4**	**Co**
0	0	0	0	0	0	0
62,000	2.5	-8	-11	-14	+10	+0
307,506	12.3	-18	-21	-30	-21	+1
455,700	18.2	-26	-30	-42	-28	+2
627,000	25.1	-36	-42	-56	-41	+3
929,070	37.2	-54	-66	-84	-74	+2
1,158,341	46.3	-75	-95	-107	-105	+3
1,471,940	58.9	-100	-130	-130	-151	+4
1,791,200	71.6	-138	-171	-161	-200	+4
2,209,667	88.4	-199	-234	-204	-277	+5
2,759,500	110.4	-291	-351	-315	-408	+5
3,156,150	126.2	-367	-465	-438	-563	+4
3,485,000	139.4	-440	-565	-529	-698	+7
3,891,000	155.6	-571	-727	-727	-982	+6

Table A3.16 Wear of UHMWPE Pins

Test Duration		Pin Weight Change ($x10^{-4}g$)				
Cycles	**km**	**Co**	**1**	**2**	**3**	**4**
0	0	0	0	0	0	0
62,000	2.5	+0	-22	-18	-24	-22
307,506	12.3	+1	-96	-99	-78	-124
455,700	18.2	+1	-151	-151	-126	-186
627,000	25.1	+0	-199	-200	-170	-235
929,070	37.2	+0	-309	-305	-263	-321
1,158,341	46.3	+0	-375	-376	-323	-382
1,471,940	58.9	+1	-507	-497	-443	-487
1,791,200	71.6	+1	-603	-596	-539	-564
2,209,667	88.4	+1	-741	-740	-688	-674
2,759,500	110.4	+1	-987	-953	-937	-874
3,156,150	126.2	+0	-1185	-1133	-1115	-1056
3,485,000	139.4	+1	-1337	-1287	-1273	-1218
3,891,000	155.6	+1	-1539	-1488	-1507	-1480

Hard Counterface Tests **Weight Change of Test Pins** ($x10^{-4}$ g)

UC = UHMWPE Control Pin. XC = XLPE Control Pin. XL = XLPE. UH = UHMWPE.

Table A3.17 First Stainless Steel Test - Test 9

Cycles	km	1 UH	2 XL	3 UH	4 XL	UC	XC
0	0	0	0	0	0	0	0
188,294	11.3	0	-3	0	-14	+1	+1
448,927	26.9	0	-22	+1	-31	+1	+0
548,570	32.9	+1	-23	+1	-34	+2	+1
928,100	55.7	+1	-29	+2	-36	+2	+1
1,405,761	84.3	+1	-33	+2	-37	+2	+1
1,836,528	110.2	+1	-35	+2	-37	+2	+0
2,262,271	135.7	+1	-37	+2	-38	+2	+1
2,692,951	161.6	+1	-39	+2	-38	+3	+1
3,318,005	199.1	+1	-53	+1	-49	+3	+0
3,515,153	210.9	+1	-55	+1	-50	+3	+1
4,052,589	243.2	+0	-60	+1	-55	+3	+0
4,629,963	277.8	+1	-76	+1	-56	+3	+0
5,080,101	304.8	+1	-105	+1	-57	+3	+0
5,543,601	332.6	+2	-128	+1	-59	+4	+1
5,994,201	359.7	+1	-162	+1	-62	+4	+1
6,444,002	386.7	+2	-184	+1	-64	+4	0
6,904,000	414.2	+2	-225	+1	-69	+4	+1
7,360,448	441.6	+2	-264	0	-79	+4	+1
7,858,090	471.5	+2	-375	0	-92	+4	+1

Table A3.18 Second Stainless Steel Test - Test 10

Cycles	km	1 UH	2 UH	3 XL	4 XL	UC1	XC1	UC2	XC2
0	0	0	0	0	0	0	0	0	0
178,924	10.7	-5	-12	-2	-1	0	0	0	0
371,348	22.3	-10	-50	-7	-2	+1	0	+1	0
809,044	48.5	-16	-57	-45	-4	0	-1	+1	0
1,254,273	75.3	-24	-63	-76	-6	0	-1	0	-1
1,695,754	101.7	-30	-67	-87	-6	+1	-1	+1	0
2,142,986	128.6	-32	-68	-93	-7	+1	-1	+1	0
2,594,976	155.7	-32	-69	-94	-7	+1	-1	+1	0
3,036,205	182.2	-33	-69	-94	-7	+1	-1	+2	0
3,533,601	212.0	-34	-70	-95	-8	+1	-1	+2	0
4,161,481	249.7	-34	-70	-95	-8	+1	-1	+2	0
4,784,305	287.1	-36	-71	-97	-10	+1	-1	+2	-1
5,505,551	330.3	-37	-72	-98	-12	+2	-1	+2	-1
6,152,247	369.1	-38	-72	-98	-16	+2	-1	+3	0
6,843,111	410.6	-39	-73	-99	-43	+2	-1	+3	0
7,478,000	448.5	-41	-74	-100	-105	+2	-1	+3	0

Table A3.19 First Zirconia Test - Test 11

Cycles	km	1 UH	2XL	3UH	4XL	UC1	XC1	UC2	XC2
0	0	0	0	0	0	0	0	0	0
139,500	5.3	+1	+1	+1	+1	+1	+1	0	+1
410,819	15.6	+1	+1	+1	0	+1	+1	+1	+1
1,024,750	38.9	0	0	0	0	+1	+1	+1	0
1,669,224	63.4	-2	-1	-1	-1	+1	+1	+1	0
2,162,000	82.2	-2	-2	-1	-1	+1	+1	+1	0
2,731,165	103.8	-4	-2	-2	-1	+2	+1	+1	0
3,457,087	133.4	-11	-3	-6	-4	+2	+1	+2	0
3,935,661	149.6	-77	-5	-44	-7	+1	0	+1	0
4,573,781	173.8	-123	-6	-57	-8	+2	0	+1	0
5,154,212	195.9	-211	-7	-76	-13	+2	0	+2	0
5,706,293	216.8	-293	-8	-88	-17	+2	0	+1	-1
6,232,223	236.8	-337	-9	-99	-22	+2	0	+2	-1
6,839,220	259.9	-423	-9	-149	-29	+2	0	+2	-1
7,404,994	281.4	-599	-11	-344	-44	+2	0	+2	-1
7,924,141	301.1	-606	-14	-345	-49	+2	0	+2	+1
9,055,953	344.1	-611	-14	-347	-52	+2	0	+2	0
9,843,246	374.0	-613	-15	-347	-55	+2	0	+2	-1
10,314,125	391.9	-614	-15	-347	-57	+3	0	+2	0

Table A3.20 Second Zirconia Test - Test 12

Cycles	km	1XL	2UH	3UH	4XL	UC1	XC1	UC2	XC2
0	0	0	0	0	0	0	0	0	0
420,147	17.6	0	0	+2	+2	0	+1	0	+1
979,418	41.1	-1	0	+1	+1	0	0	0	0
1,627,622	68.4	0	0	+1	0	0	0	+1	0
2,330,470	97.9	-1	0	+1	0	0	0	+1	0
3,076,214	129.2	-1	0	+2	0	+1	0	+2	+1
3,882,781	163.1	-1	0	+1	-1	+1	0	+1	0
4,645,534	195.1	-1	0	+1	-1	+1	0	+2	0
5,309,596	223.0	-1	0	+1	-1	+1	0	+2	0
6,040,671	253.7	-2	0	+1	-1	+1	-1	+2	0
7,115,000	298.8	-2	0	+1	-2	+1	-1	+2	0

Table A3.21 Third Zirconia Test - test 13

Cycles	km	1UH	2XL	3XL	4UH	UC1	XC1	UC2	XC2
0	0	0	0	0	0	0	0	0	0
441,837	20.3	+1	0	0	0	0	0	+1	+1
986,300	45.4	+2	+1	+1	+1	+1	0	+2	+1
1,585,933	73.0	0	0	-1	+1	+1	0	+2	+1
2,305,465	106.1	-3	-24	-20	-3	+1	0	+2	+1
2,570,302	118.2	-155	-67	-44	-11	0	+1	+1	+2
2,840,943	130.7	-1522	-127	-94	-506	+1	0	+2	0

"rough" plates were plates 2 and 4

Test 14 - Weight Change of Test Plates ($x10^{-4}$ g)

UH = UHMWPE plate. XL = XLPE plate. XC = XLPE control plate. UC = UHMWPE control plate. XC and UC were within 3.3% of each other's initial weight. All test plates were within 1.1% of each other's initial weight.

Table A3.22 Test against stainless steel pins

Cycles	km	1 XL	2 UH	3 XL	4 UH	UC	XC
0	0	0	0	0	0	0	0
167,240	9.4	+3	+4	0	+4	+4	+6
417,890	23.4	-171	-16	-164	-1	+5	+6
659,201	36.9	-460	-203	-443	-41	+8	+8
976,262	54.7	-854	-1552	-821	-144	+9	+8
1,141,244	63.9	-1110	/	-945	**	**	**
1,147,806	64.3	/	/	/	-202	+10	+6
1,560,020	87.4	/	/	/	-929	+11	+6
1,730,021	96.9	/	/	/	-1345	+12	+6
1,894,000	106.1	/	/	/	-1818	+14	+7

** = no measurement taken. / = test ceased.

Appendix 4

XLPE Plate Ra Values
Across and Along Wear Tracks

In all of the following tables, L = Longitudinal direction, T = Transverse direction. Units μm Ra. Measured using Taylor Hobson Talysurf 4. Mean of 8 readings.

Table A4.1 Test 1 Mean XLPE Plate Roughness Values

1 - 4 = plate number.

Test Duration		Mean Ra Values							
Cycles	**km**	**1L**	**2L**	**3L**	**4L**	**1T**	**2T**	**3T**	**4T**
0	0	1.85	1.53	0.88	1.55	1.60	1.36	0.68	1.40
570,000	22.8	1.04	.069	0.11	0.15	0.85	0.76	0.74	0.48
2,182,531	87.3	0.49	.031	0.14	.057	0.54	0.61	0.40	0.59
3,754,710	150.2	0.21	.033	.043	.028	0.57	0.55	0.42	0.76
5,654,160	226.2	0.19	.035	.034	.051	0.43	0.91	0.42	0.96
7,337,912	293.5	0.20	.033	.039	.036	0.45	0.69	0.42	0.67
8,724,960	349.0	0.16	.033	.036	.033	0.43	0.31	0.28	1.08

Table A4.2 Test 2 Mean XLPE Plate Roughness Values

Plates 1 and 3 were milled with a large cutter, hence their relatively high longitudinal values and low transverse values. 1 - 4 = plate number.

Test Duration		Mean Ra Values							
Cycles	km	1L	2L	3L	4L	1T	2T	3T	4T
0	0	2.6	0.97	1.9	1.19	0.16	0.98	0.11	1.14
206,558	14.1	0.88	0.06	0.74	0.11	0.16	0.45	0.12	0.21
375,282	25.5	0.78	.029	*	.094	0.20	0.37	0.25	0.24
803,204	54.6	*	.025	*	.041	.55~	0.37	0.30	0.21
1,205,800	90.0	*	.027	*	.060	0.34	0.32	0.47	0.64
1,553,079	105.6	*	.023	*	.030	0.51	0.30	0.29	0.42
1,993,000	135.5	*	.034	*	.029	1.27	0.33	0.35	0.47
2,462,440	167.4	*	.025	*	.028	1.06	0.33	0.26	0.20
3,046,700	207.2	*	.025	*	.030	0.97	0.34	0.95	0.37
4,034,120	274.3	.032	.032	.030	.023	0.71	0.30	0.75	0.43
4,876,812	331.6	.033	.020	.023	.092	0.46	0.25	0.47	0.48
5,723,351	389.2	.062	.024	***	***	0.72	0.34	***	***
6,834,697	464.8	.031	.029	***	***	0.42	0.24	***	***

*** Test Ceased

~ Readings exaggerated by ridge and groove.

* Mean roughness no longer applicable. Roughness varied across the wear path by a factor greater than 10. Visual inspection of the plates during the test revealed offset wear patterns on plates 1 and 3. This wear was offset in two directions, being greatest at the ends of the wear track and towards one of the longitudinal edges. Therefore, inertial effects at each end of the stroke could be important, and also the load could be offset to one side.

Table A4.3 Test 3 Mean XLPE Plate Roughness Values

1 - 4 = plate number.

Test Duration		Mean Ra Values							
Cycles	km	1L	2L	3L	4L	1T	2T	3T	4T
0	0	0.44	1.21	0.99	0.52	0.41	1.27	1.33	0.89
547,400	21.9	0.17	0.12	0.09	.067	0.50	0.56	0.51	0.47
2,178,025	87.1	.026	.042	.052	.032	0.21	0.36	0.42	0.32
5,759,532	230.4	.022	.030	.028	.042	0.38	0.47	0.63	0.52
9,793,800	391.8	.043	.035	.054	.051	0.43	0.57	0.87	0.85
15,196,800	607.9	.056	.026	.044	.060	0.44	0.53	0.42	0.74

Table A4.4 Test 4 Mean XLPE Plate Roughness Values

3 - 5 = plate number.

Test Duration		Mean Ra Values					
Cycles	km	3L	4L	5L	3T	4T	5T
0	0	1.38	0.77	1.44	0.87	0.84	1.41
594,000	22.6	.072	.146	.056	0.98	1.0	1.01
1,466,615	55.7	.065	.060	.072	1.47	0.98	1.10
2,750,700	104.5	.056	.041	.050	1.06	0.78	1.10

Table A4.5 Test 5 Mean XLPE Plate Roughness Values

1, 2 and 6 = plate number.

Test Duration		Mean Ra Values					
Cycles	km	1L	2L	6L	1T	2T	6T
0	0	0.85	1.06	0.96	1.01	0.73	1.07
527,478	20.0	.070	.056	.070	0.46	0.34	0.58
1,800,000	68.4	.040	.053	.106	0.49	0.32	1.87

Appendix 5

Calculations

A5.1 To determine the difference between the maximum and the minimum sliding distance in the spherical contact of the prosthetic components

The least wear occurred with the high percentage cross-linked prostheses in the distilled water tests (tests 3 to 6) so in these tests the largest error due to differences in sliding distance could occur. For these prostheses, R = 8.5mm.

The shortest sliding distance occurred where the outer edge of the phalangeal component rubbed against the metacarpal component, at a radius H. The width of the R8.5 phalangeal component was 6mm. Therefore:

Figure A5.1 Difference in sliding distance in spherical contact

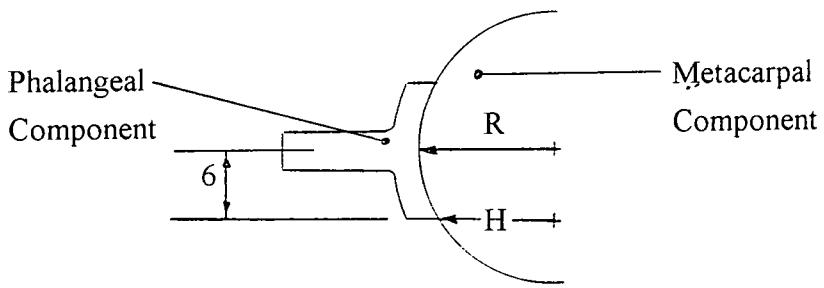

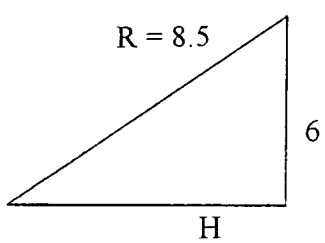

$H^2 = 8.5^2 - 6^2$ $H = 6.0mm$

In the worst case the wear factor would be increased in proportion to the difference in sliding distance:

$\frac{R}{H} = \frac{8.5}{6.0} = 1.42$ times

A5.2 To Determine Cross Section of Cantilever.

Let b = dimension of cross section. Cantilever needs to be of square section to suit the strain gauges.

$\sigma = \frac{My}{I}$ (Eqn. 1)

σ = yield stress
M = moment = force (F) x distance (L)
y = b/2
I = second moment of area = $b^4/12$

Equation 1, re-arranged to give

$\sigma = \frac{6FL}{b^3}$ or $b^3 = \frac{6FL}{\sigma}$

now, L = 83mm (from scale drawings, appendix 9)
F = 322N maximum, but allowing for a safety factor, take F = 500N
σ = 250×10^6 Pa

therefore $b^3 = \frac{6 \times 500 \times 83 \times 10^{-3}}{250 \times 10^6}$

$= 996 \times 10^{-9} m^3$ **b = 10mm**

A5.3 Distance moved by phalangeal clamp from 0 to 90°

Figure A5.2 - Distance moved by phalangeal clamp

0° Initial Position

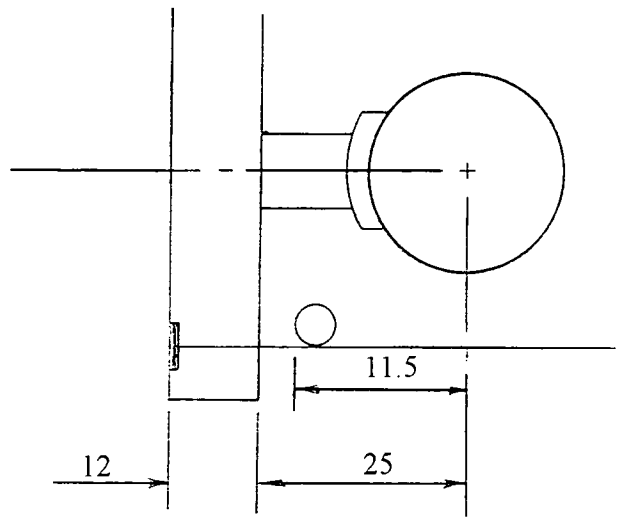

90° Final Position

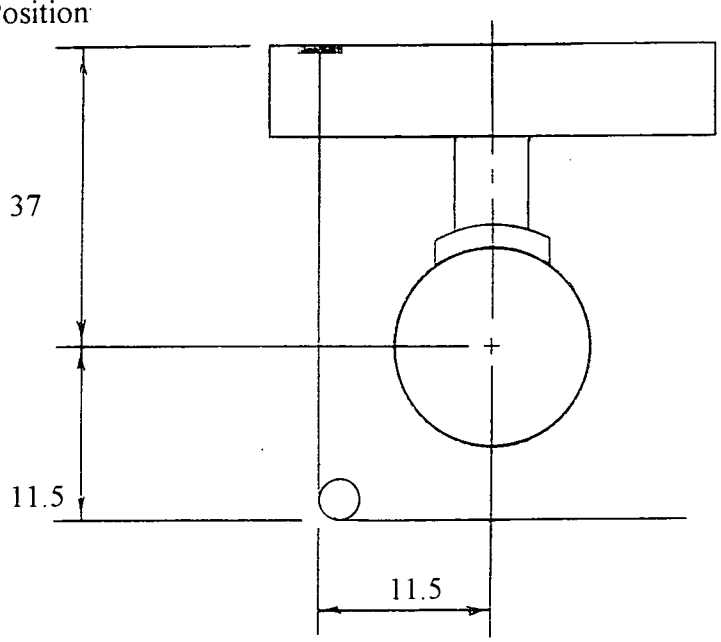

Base length = 37mm. At 90° require 11.5 + 11.5 + 37 = 60mm.
Difference = 60 - 37 = 23mm
Therefore distance moved from 0° to 30° (pinch grip position) is a third of this = 8mm. On some occasions it may be necessary to increase the arc of motion to a maximum of 120°. In such instances, a stroke of 23mm + 8mm = 31mm would be required.

A5.4 Stroke of Flexor and Extensor Cylinders

Based on calculation A5.3, a 120° arc would necessitate a stroke of 31mm. Allowing for a safety gap between the flexor adjuster and the flexor stop fork of 3mm, gave a maximum stroke of 34mm. However, experience with the Stokoe finger function simulator had shown that the 'tendons' stretched by a maximum of 6%. Especially the flexor 'tendon', as the 'pinch' load was applied through it.

On the new simulator, the 'tendon' length was 260mm, so a maximum stretching of 16mm had to be accommodated. Therefore, total stroke required = 34mm + 16mm = 50mm. Allowing a factor of safety, the next size of cylinder up had a 60mm stroke.

stroke chosen = 60mm

A5.5 Stroke of Heavy Load Cylinder

From calculation A5.3, the distance to travel from 0° (starting position) to 30° (pinch position) is 7mm. An allowance for a safety gap of 3mm between the flexor adjuster and the flexor stop fork was made. Plus a maximum 'tendon' stretching distance of 16mm for the flexor cylinder to extend before hitting the fork, gave a total of 26mm.

As the slider is pulled back, so the 'tendon' is pulled backwards, until it impinges on the pinch guide bar. The pinch guide bar was set slightly back from the 'tendons' during flexion-extension. In this way, there was no chance of the 'tendons' fraying against it. However, this arrangement meant that the stroke calculation was somewhat complicated, as follows:

Figure A5.3 To determine stroke of heavy load cylinder

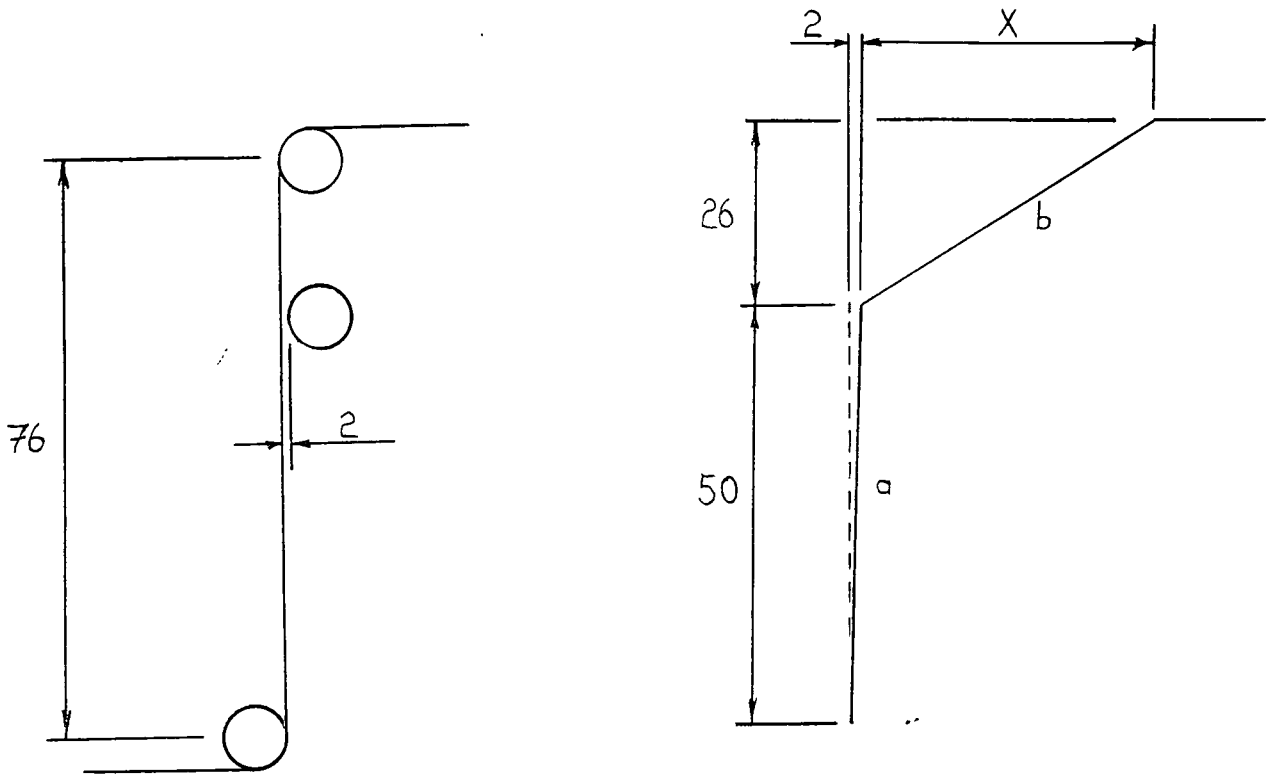

Let stroke required = S mm

Need to take up 26mm (from above)

(a + b) - original length > 26

Now, a = 50, original length = 76

therefore (50 + b) - 76 > 26

or b > 52.

If b = 52, then as $b^2 = 26^2 + X^2$.

Minimum stroke S = X + 2 = 47mm

therefore X = S - 2

$X^2 = 52^2 - 26^2 = 45^2$

Therefore, including a factor of safety, the next size of cylinder up had a 50mm stroke.

stroke chosen = 50mm

A5.6 Bore of Flexor and Extensor Cylinders

It should be noted that the minimum air pressure required to activate the pneumatic valves was 2 bar, while the maximum air pressure available in the lab was 5.5 bar.

A load of 15N across the test prosthesis during flexion-extension (Tamai et al, 1988) was desired. Due to the token 13g mass of the nylon phalangeal clamp, its friction and inertia were negligible in comparison. However, the Bosch pneumatics catalogue recommended the use of a safety factor of 1/0.5, in this high speed application (to account for wear or leakage due to ageing or pressure drops in the system). Therefore the load required was 15N x 1/0.5 = 30N. From the Bosch pneumatics catalogue it was seen that a pneumatic cylinder of bore size 10mm would provide, from an available air supply pressure range of 2 to 5.5 bar, a load between 14.3N and 78.5N.

bore size = 10mm

A5.7 Bore of Heavy Load Cylinder

It should be noted that the minimum air pressure required to activate the pneumatic valves was 2 bar, while the maximum air pressure available in the lab was 5.5 bar.

For 'normals', the maximum pinch grip (P) is 70N (Walker et al, 1978; An et al, 1978; Mathiowetz et al, 1985). In comparison, for rheumatoid patients, P is 20N (Linscheid and Dobyns, 1979). The force across the MCP joint during pinch grip has been given as 4.6P (Weightman and Amis, 1982).
Therefore maximum 'normal' force = 4.6 x 70 = 322N.
Therefore maximum 'rheumatoid' force = 4.6 x 20 = 92N.

Friction force to move aluminium slider = $\mu N = \mu mg = 0.2 \times 9.81 \times 1kg = 2N$
(The inertia of the aluminium slider is negligible as it moves at a low speed due to the use of throttles on the heavy load cylinder).

It was desired to be able to simulate both rheumatoid and 'normal' MCP joint loads. Therefore the required range of load to be provided by the heavy load cylinder was 94N to 324N. The Bosch pneumatics catalogue states that a

cylinder of bore size 32mm will provide, from an available air supply pressure range of 2 to 5.5 bar, a load between 121N and 330N. The 121N 'minimum' can in practice be reduced further by appropriate adjustment of the slider stop bolts to reduce the tension in the flexor 'tendon' during 'pinch' grip.

bore size = 32mm

A5.8 Speed of Flexor and Extensor Pneumatic Cylinders

At the maximum desired speed of the simulator of 120cpm, and a stroke of 31mm (see calculation A5.3)
velocity = distance/time = 31mm/0.25s = 124 mm/sec.
Bosch pneumatics catalogue gives operating speed range of these cylinders as 5 to 500 mm/sec, therefore the maximum desired speed of the simulator is achievable.

A5.9 Power Supply Required

A voltage of 24V was required for all of the solenoids.

Power requirements for the individual solenoids were as follows:

'thumb' solenoid	10W
flexion-extension pneumatic solenoid	10W
'dump' pneumatic solenoid	5W
'pinch' pneumatic solenoid	5W
'fork' pneumatic solenoid	5W
Therefore maximum power =	**35W**

Power (P) = Voltage (V) x Current (I)

or $I = \frac{P}{V} = \frac{35}{24} = \mathbf{1.46A}$

From the RS catalogue, the next size up of power supply is a 2.4A unit, RS number 593-899.

Appendix 6

Absorption of Distilled Water by XLPE and UHMWPE Control Components in Pin on Plate Tests

6.1 Control Pins

Polyethylene control pins were included so that any weight change due to lubricant absorption could be accounted for, and therefore the true wear of the test pins determined. Each control pin was positioned on the edge of the test bath so that it was partially immersed, like the test pin, in the same distilled water at 37°C. The water uptake results for the XLPE and UHMWPE control pins are shown in tables A6.1 and A6.2 respectively.

The fourteen XLPE control pins showed, apart from one debatable case, no fluid absorption outside of error due to the Mettler balance, which was taken to be ± 0.0001g. Only the control pin of test 2 showed any significant weight increase. However, this may have been due to oil contamination, which affected two of the test pins of test 2.

Regarding the twelve UHMWPE control pins, water absorption outside of error due to the Mettler balance did occur. From a comparison of the results it was clear that UHMWPE absorbed more distilled water than XLPE.

Table A6.1 Absorption of Distilled Water by XLPE Control Pins

Test Duration	Initial Weight (g)	Test No.	Weight Increase (g)	% Weight Increase (WI)	%WI per 100km
349km	0.3631	1	0	0	0
465km	0.3622	2	+0.0005	0.138	0.030
608km	0.3605	3	0	0	0
105km	0.3623	4	0	0	0
68km	0.3564	5	0	0	0
472km	0.3607	9	+0.0001	0.028	0.006
449km	0.3604	10	-0.0001	-0.028	-0.006
	0.3600	10	0	0	0
392km	0.3604	11	0	0	0
	0.3621	11	0	0	0
299km	0.3569	12	-0.0001	-0.028	-0.006
	0.3594	12	0	0	0
131km	0.3519	13	0	0	0
	0.3556	13	0	0	0

Table A6.2 Absorption of Distilled Water by UHMWPE Control Pins

Test Duration	Initial Weight (g)	Test No.	Weight Increase (g)	% Weight Increase (WI)	%WI per 100km
154km	0.3206	6	0	0	0
153km	0.3507	7	+0.0001	0.029	0.019
156km	0.3449	8	+0.0001	0.029	0.019
472km	0.3460	9	+0.0004	0.116	0.025
449km	0.3544	10	+0.0002	0.056	0.013
	0.3567	10	+0.0003	0.084	0.019
392km	0.3564	11	+0.0002	0.056	0.014
	0.3553	11	+0.0003	0.084	0.022
299km	0.3588	12	+0.0001	0.028	0.009
	0.3604	12	+0.0002	0.055	0.018
131km	0.3506	13	+0.0001	0.029	0.022
	0.3549	13	+0.0002	0.056	0.043

6.2 Control Plates

XLPE control plates were not employed during the first five tests, instead the emphasis during these tests was on maximising the number of test plates. However, the potential for errors due to water absorption was recognised. By switching from Ringers solution to distilled water in the finger function simulator tests, a distilled water environment at 37°C, in which to submerge polyethylene control plates, became available. This environment was provided by the Grant Y14-VFP bath. Control plates were then used for all of the following tests which employed polyethylene plates.

Chronologically, these tests commenced with the first UHMWPE against UHMWPE test, test 6. After the three UHMWPE against UHMWPE tests, in order to gain an indication of the fluid uptake of XLPE plates, a set of four XLPE control plates were manufactured and submerged in the Grant bath, with their weights being regularly checked. These four plates, which were submerged for a over a year, showed an initial increase in weight, followed by a decrease which continued below the initial weight of the plate! These results (table A6.3) are shown graphically in Figure A6.1. Although the longest pin on plate test (test 3) lasted 210 days, measurements of the weight of the XLPE control plates beyond this 210 day point indicated a continued decrease.

Figure A6.1 - Uptake of Distilled Water by XLPE Control Plates (first set of four plates)

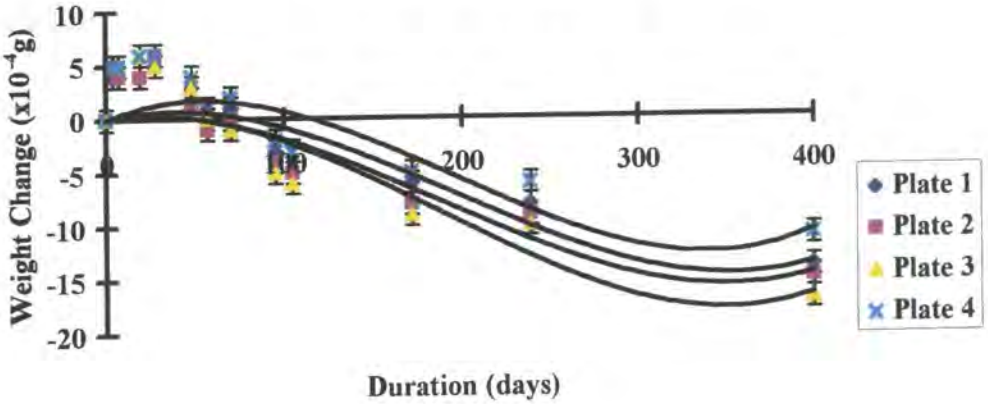

So surprising were these results that a second set of four XLPE control plates were manufactured and submerged in the distilled water environment at 37°C. Once again, plate weight increased then decreased. This second set of results (table A6.4) is shown graphically in Figure A6.2. As can be seen, twice the weight increase due to water absorption occurred in the second set as in the first, despite the mean initial difference in control plate weight being only some 3.6%.

Figure A6.2 - Uptake of Distilled Water by XLPE Control Plates (second set of four plates)

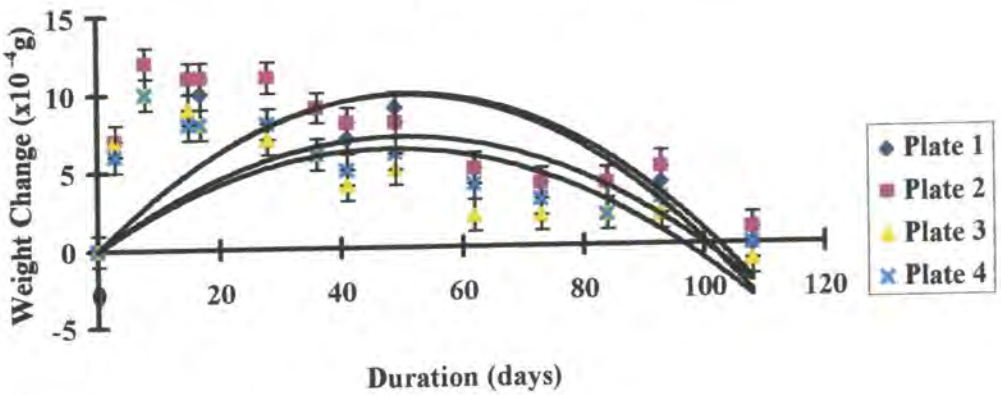

The absorption of distilled water by the XLPE control plates require further study as the result was both interesting and unexpected. The solution would be to repeat the test, but with a control plate positioned in the rig itself. Of relevance is the effect of the absorption of distilled water on the plate wear results of the XLPE against XLPE tests (tests 1 to 5). To take the worst case, consider the maximum water absorption by a control plate and the minimum weight loss of a test plate due to wear. Obviously the minimum weight loss due to wear occurred

under 10N load, therefore the 40N results will be less sensitive to errors due to fluid uptake.

From the second set of XLPE control plates, a maximum increase of 0.0012g due to water absorption was recorded at day 8. However, the shortest XLPE against XLPE tests (tests 4 and 5) lasted 34 and 23 days respectively, and both of these tests were only undertaken with 40N loads. In contrast the shortest duration 10N load test (test 1) lasted to 127 days. At such a point in time, the first four XLPE control plates had all fallen below their initial weight. As regards the second set of XLPE control plates, after 108 days the maximum weight increase was +0.0001g.

Taking both sets of four XLPE control plates into consideration, it appears that a weight increase due to water absorption occurred up to around day one hundred. Day one hundred, at 2.89km per day, corresponds to a test duration of 289km. As tests 1, 2 and 3 ceased at 349km, 465km and 608km respectively, so the final results should not be affected.

Table A6.3 - Absorption of Distilled Water by First Set of Four XLPE Control Plates

Duration	**Weight Increase (g)**			
Day	**Plate 1**	**Plate 2**	**Plate 3**	**Plate 4**
(Initial Weight)	(4.7719g)	(4.7624g)	(4.7646g)	(4.7402g)
0	0	0	0	0
4	+0.0004	+0.0005	+0.0005	+0.0005
7	+0.0005	+0.0004	+0.0005	+0.0005
19	+0.0004	+0.0004	+0.0006	+0.0006
28	+0.0005	+0.0006	+0.0005	+0.0006
48	+0.0003	+0.0001	+0.0003	+0.0004
57	0	-0.0001	0	+0.0001
70	+0.0001	0	-0.0001	+0.0002
95	-0.0003	-0.0004	-0.0005	-0.0002
105	-0.0005	-0.0005	-0.0006	-0.0003
172	-0.0006	-0.0008	-0.0009	-0.0005
239	-0.0008	-0.0009	-0.0010	-0.0006
400	-0.0014	-0.0015	-0.0017	-0.0011

All control plates were within 0.7% of the initial weight of each other.

Table A6.4 Absorption of Distilled Water by Second Set of Four XLPE Control Plates.

Duration	Weight Increase (g)			
Day	Plate 1	Plate 2	Plate 3	Plate 4
(Initial Weight)	(4.6317g)	(4.6060g)	(4.6300g)	(4.6366g)
0	0	0	0	0
3	+0.0007	+0.0007	+0.0007	+0.0006
8	+0.0012	+0.0012	+0.0010	+0.0010
15	+0.0011	+0.0011	+0.0009	+0.0008
17	+0.0010	+0.0011	+0.0008	+0.0008
28	+0.0011	+0.0011	+0.0007	+0.0008
36	+0.0009	+0.0009	+0.0006	+0.0006
41	+0.0007	+0.0008	+0.0004	+0.0005
49	+0.0009	+0.0008	+0.0005	+0.0006
62	+0.0005	+0.0005	+0.0002	+0.0004
73	+0.0004	+0.0004	+0.0002	+0.0003
84	+0.0004	+0.0004	+0.0002	+0.0002
93	+0.0004	+0.0005	+0.0002	+0.0003
108	0	+0.0001	-0.0001	0

All control plates were within 0.7% of the initial weight of each other.

As indicated in table A6.5, all of the UHMWPE control plates showed an increase in weight due to distilled water absorption. The 'percentage weight increase per 100km' (0.008% to 0.033%) was of a similar order to that of the UHMWPE control pins (0% to 0.043%). All of the UHMWPE control plate results are shown in Figure A6.3 which describes a gradual increase of weight with time, and no downward trend, unlike the XLPE control plates (Figures A6.1 and A6.2). The maximum difference between the initial weight of the UHMWPE control plates was some 17%, however this figure is small in comparison with the greater than 400% variation in 'percentage weight increase per 100km' measured at the end of the four tests.

Figure A6.3 - Uptake of Distilled Water by UHMWPE Control Plates

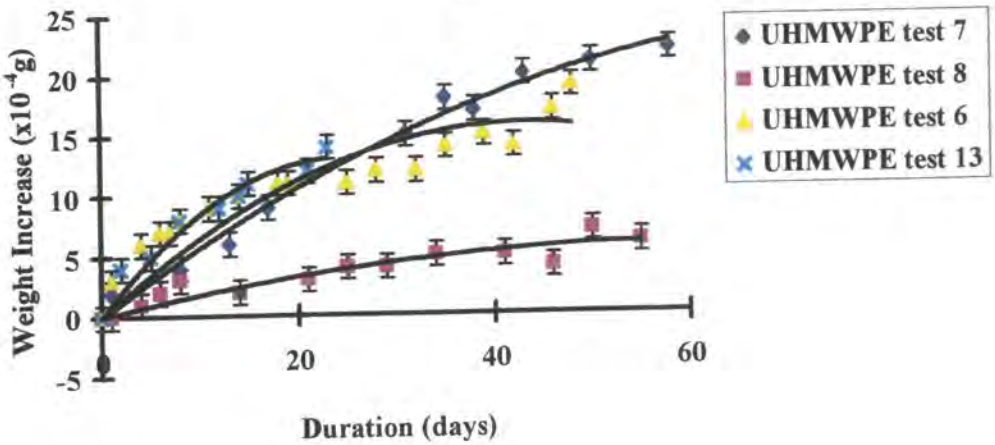

Table A6.5 Absorption of Distilled Water by UHMWPE Control Plates

Test Duration km/(days)	Initial Weight	Test No.	Weight Increase (g)	% Weight Increase (WI)	%WI per 100km
154km (48)	5.0874g	6	+0.0019	0.037	0.024
153km (58)	4.4146g	7	+0.0022	0.050	0.033
156km (55)	4.6762g	8	+ 0.0006	0.013	0.008
106km (23)	4.3436g	14	+ 0.0014	0.032	0.030

6.3 Comparison of Absorption of Distilled Water by the Two Types of Polyethylene

The results of water absorption by the control pins imply that no fluid uptake by XLPE had occurred, therefore it was necessary to look at changes in weight of the control plates. Furthermore, as the plates were much heavier than the pins and fully immersed in distilled water, then weight change due to lubricant absorption should be easier to detect in their case. If test 14 is considered, than a direct comparison of XLPE with UHMWPE is available. Although this test was of a relatively short duration, Figure A6.4 again indicates that the trend of the XLPE water absorption curve was downward, while that of the UHMWPE was upward and then levelling out. The actual increases in weight for the XLPE and UHMWPE control plates, which were within 3.3% of each other's initial weight, in test 14, are given in table A6.6. At the cessation of the test, after 23 days

(106km) the UHMWPE control plate had absorbed twice the amount of distilled water as had the XLPE control plate.

Figure A6.4 - Uptake of Distilled Water by XLPE & UHMWPE Control Plates (test 14)

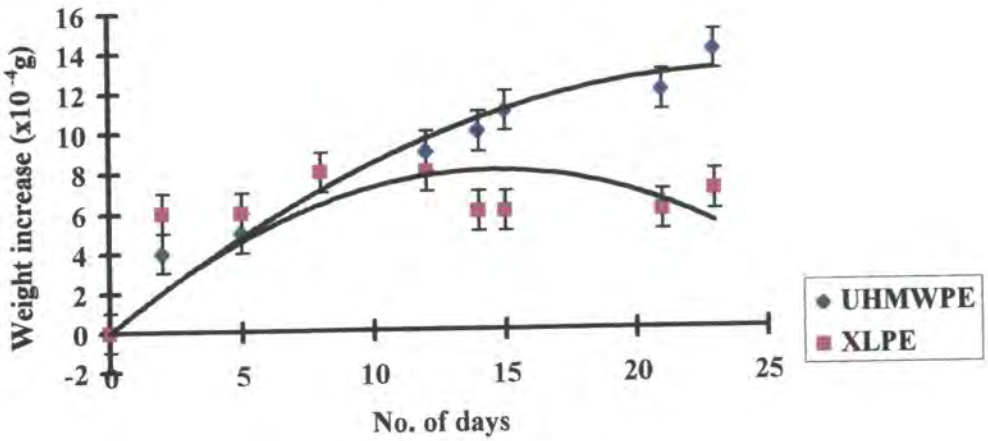

Table A6.6 Absorption of Distilled Water by UHMWPE and XLPE Control Plates in Test 14.

Duration (km)	UHMWPE Control Plate	XLPE Control Plate
0	4.3436g	4.4852g
9.4	+0.0004g	+0.0006g
23.4	+0.0005g	+0.0006g
36.9	+0.0008g	+0.0008g
54.7	+0.0009g	+0.0008g
64.3	+0.0010g	+0.0006g
87.4	+0.0011g	+0.0006g
96.9	+0.0012g	+0.0006g
106.1	+0.0014g	+0.0007g
% Weight Increase (WI)	0.032	0.016
%WI per 100km	0.030	0.015

Appendix 7

Absorption of Oil by XLPE and UHMWPE

While the results of all polyethylene wear tests showed that little water absorption by the two types of polyethylene occurred, less than 0.5% by XLPE after 600km or some 300 days (finger simulator test 3) the situation with regard to mineral oil was much different. Offcuts of XLPE and UHMWPE were taken, weighed, then immersed in mineral oil. On regular occasions, the offcuts were removed, cleaned in acetone, weighed, then replaced in the oil. The results obtained are shown in table A7.1 below and in figure A7.1.

Figure A7.1 - Absorption of Oil by Polyethylene

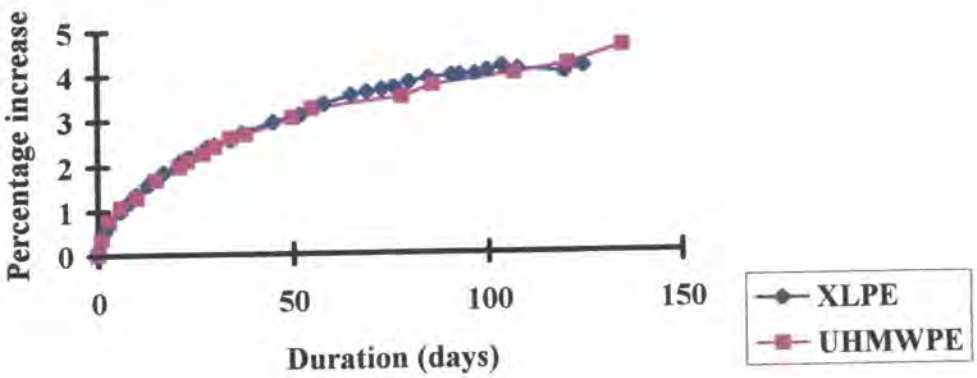

The coefficient of friction for XLPE against itself has been measured to be 0.14 (Sibly and Unsworth, 1991). There may be potential for an oil soaked bearing, injection mouldable to fine tolerances. Checks on changes in hardness and dimension would need to be undertaken.

Table A7.1 Absorption of Oil by XLPE and UHMWPE

XLPE			UHMWPE		
Time Immersed	**Wt. Inc. ($x10^{-3}g$)**	**Wt. Inc. %**	**Time Immersed**	**Wt. Inc. ($x10^{-3}g$)**	**Wt. Inc. %**
3 hours	0.9	0.11	1 day	3.1	0.35
1 day	3.1	0.38	3 days	7.1	0.80
2 days	4.5	0.55	6 days	9.5	1.07
3 days	5.6	0.69	10 days	11.5	1.29
6 days	8.1	1.00	15 days	14.9	1.67
8 days	9.6	1.18	21 days	17.5	1.97
9 days	10.3	1.27	23 days	18.7	2.10
10 days	11.0	1.35	27 days	20.1	2.26
13 days	12.8	1.57	30 days	21.5	2.41
14 days	13.6	1.67	34 days	23.1	2.59
17 days	15.0	1.84	38 days	23.9	2.68
21 days	16.9	2.08	50 days	27.1	3.04
22 days	17.2	2.12	55 days	28.9	3.25
23 days	17.6	2.16	78 days	31.1	3.49
24 days	17.8	2.19	86 days	33.4	3.75
28 days	19.5	2.40	107 days	35.8	4.02
30 days	20.0	2.46	121 days	37.4	4.20
34 days	20.9	2.57	135 days	41.0	4.60
37 days	22.1	2.72			
45 days	24.1	2.96			
52 days	25.4	3.12			
58 days	27.4	3.36			
69 days	29.4	3.62			
76 days	30.2	3.71			
80 days	31.1	3.82			
85 days	31.9	3.92			
93 days	32.4	3.98			
97 days	32.6	4.01			
100 days	33.1	4.07			
108 days	33.4	4.11			
120 days	32.8	4.03			
125 days	33.8	4.16			

Appendix 8

Determination of Position of Components to Mimic MCP Joint

The load across the test prosthesis was provided by the tension in the two 'tendons', the flexor and the extensor. Leijnse et al (1993) gave the physical positions of the extensor and flexor tendons as 9 and 11mm respectively from the centre of rotation of the MCP joint (an extensor to flexor ratio of 9:11 or 0.82). However, the simulator must be capable of testing all sizes of the Durham MCP prosthesis and the largest of these is R9.5mm, giving a 19mm outer diameter. Therefore the 9mm dimension given by Leijnse et al (1993) cannot be employed. Despite this, the design aimed to keep as near as possible to the dimensions of the natural MCP joint and therefore to maintain the same 0.82 extensor to flexor ratio of Leijnse et al (1993).

The closest position of an extensor pulley was at 45° to centre of rotation of the MCP joint. Allowance for a pulley diameter of 4mm gave an extensor tendon position of 11.5mm from the centre of rotation of the MCP joint. Then, using the 0.82 extensor to flexor ratio, gave the position of the flexor tendon as 14mm from the centre of rotation of the MCP joint.

The position of the offset of the ligament attachment from the MCP joint centre of rotation is given by Minami et al (1984) for an index finger, as 4.2mm and 5.0mm in the proximal and dorsal directions respectively. These 2 values, plus the calculated flexor and extensor tendon positions were used to locate the position of a 'metacarpoglenoidal' pulley, such that the natural situation of the ligaments being taught in flexion and slack in extension (Minami et al, 1984; Smith and Kaplan, 1967) was achieved.

Table A8.1 Simulator geometry compared with that of the natural joint

Dimension	Joyce	Leijnse et al (1993)
a	11.5	9
b	14	11
c	5.0#	----
d	4.2#	----
e	24	----
a:b	0.82	0.82

\# from Minami et al (1984).

x centre of rotation of MCP joint

\+ centre of rotation of metacarpoglenoidal pulley

ET extensor tendon FT flexor tendon

Figure A8.1 Geometry to mimic MCP joint in simulator

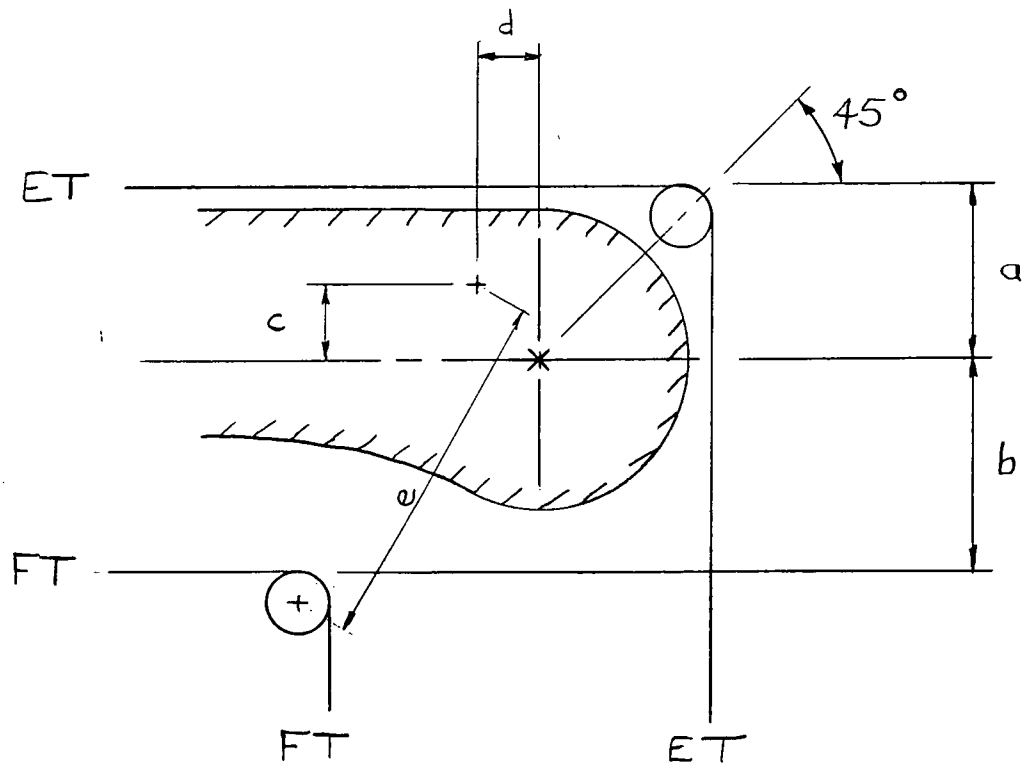

Appendix 9

New Finger Function Simulator
General Arrangement Drawings
and List of Major Components

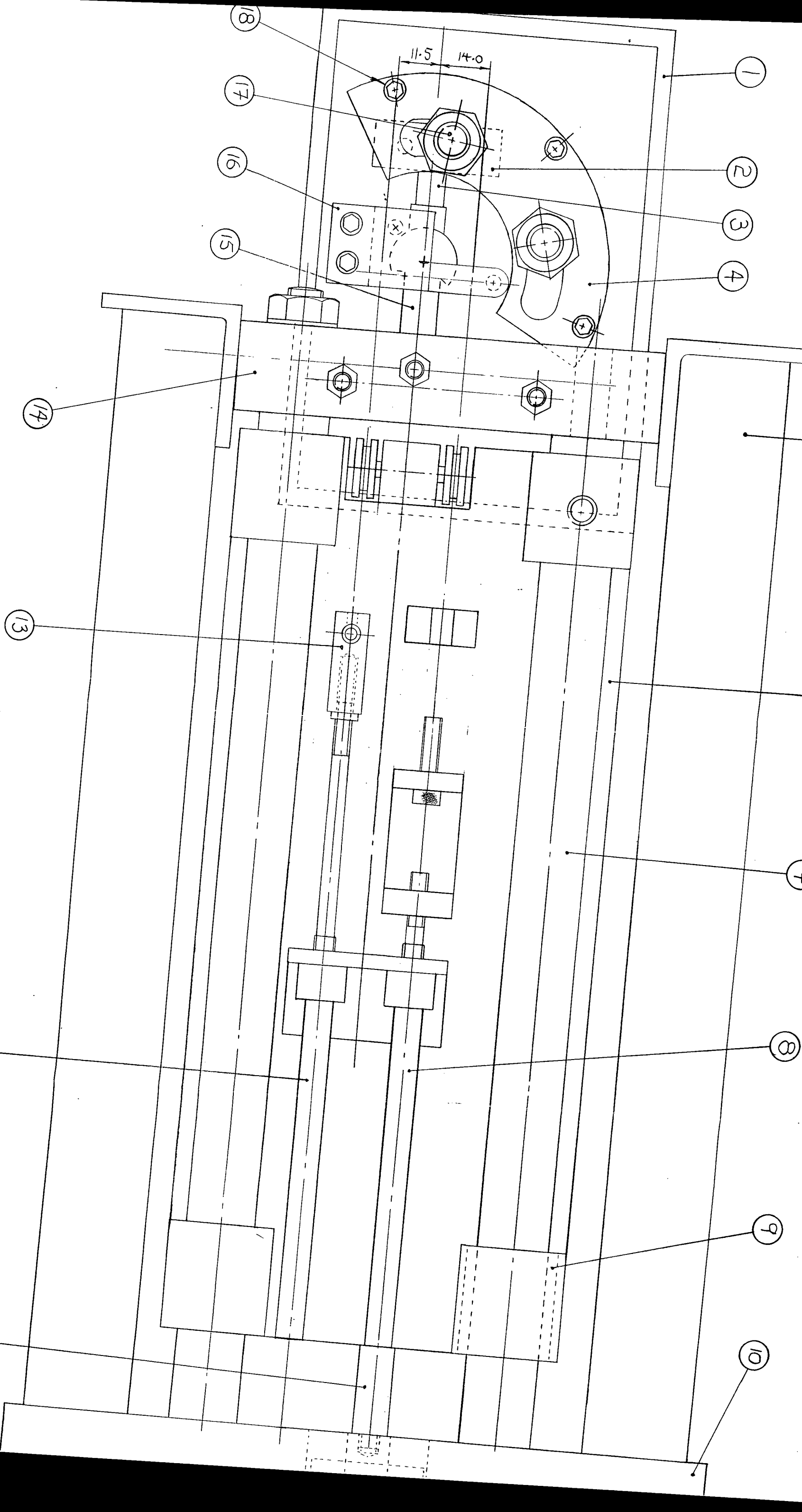
11·5
14·0
18
17
16
15
14
13
12
1
2
3
4
8
9
10

15
25
108
360
40
5
25
10
20
40
14
30
140
R25
13
R52
24
23
22
21
25
26
20
19
27
28
31
30

REAR VIEW

105

57

24

135

200

FRONT VIEW

50

50

33

35

20

30

118

133

5

100

15

32

List of Major Components

1 Bath
2 Phalangeal clamp (nylon)
3 Phalangeal component holder (nylon)
4 Phalangeal arc (UHMWPE)
5 Side framework (30 x 30 mild steel)
6 Aluminium slider (tooling plate)
7 Stub steel rod (Ø20mm)
8 Flexor pneumatic cylinder (PDA Ø10 x 60-A)
9 Oil lite phosphor bronze bush
10 Back plate (mild steel)
11 Universal coupling
12 Extensor pneumatic cylinder (PDA Ø10 x 60-A)
13 Extensor adjuster
14 Bridge (20 x 20 mild steel)
15 Metacarpal component holder
16 'Metacarpoglenoidal' mobile pulley (stainless steel)
17 Arc magnet (1 of 2)
18 Column (1 of 3)
19 Upper pulley
20 Tendon
21 Flexor adjuster
22 Throttle
23 Restrictor
24 Heavy load cylinder (Ø32 x 50)
25 Flexor stop fork
26 Fork cylinder (Ø25 x 15)
27 Lower pulley
28 Base plate (stainless steel)
29 Phalangeal clamp magnets
30 Cantilever (stainless steel)
31 'Thumb' solenoid
32 Support column (stainless steel)
33 'Pinch' guide bar
34 'Slider stop' bolts

Appendix 10

Pneumatic Circuit Diagram

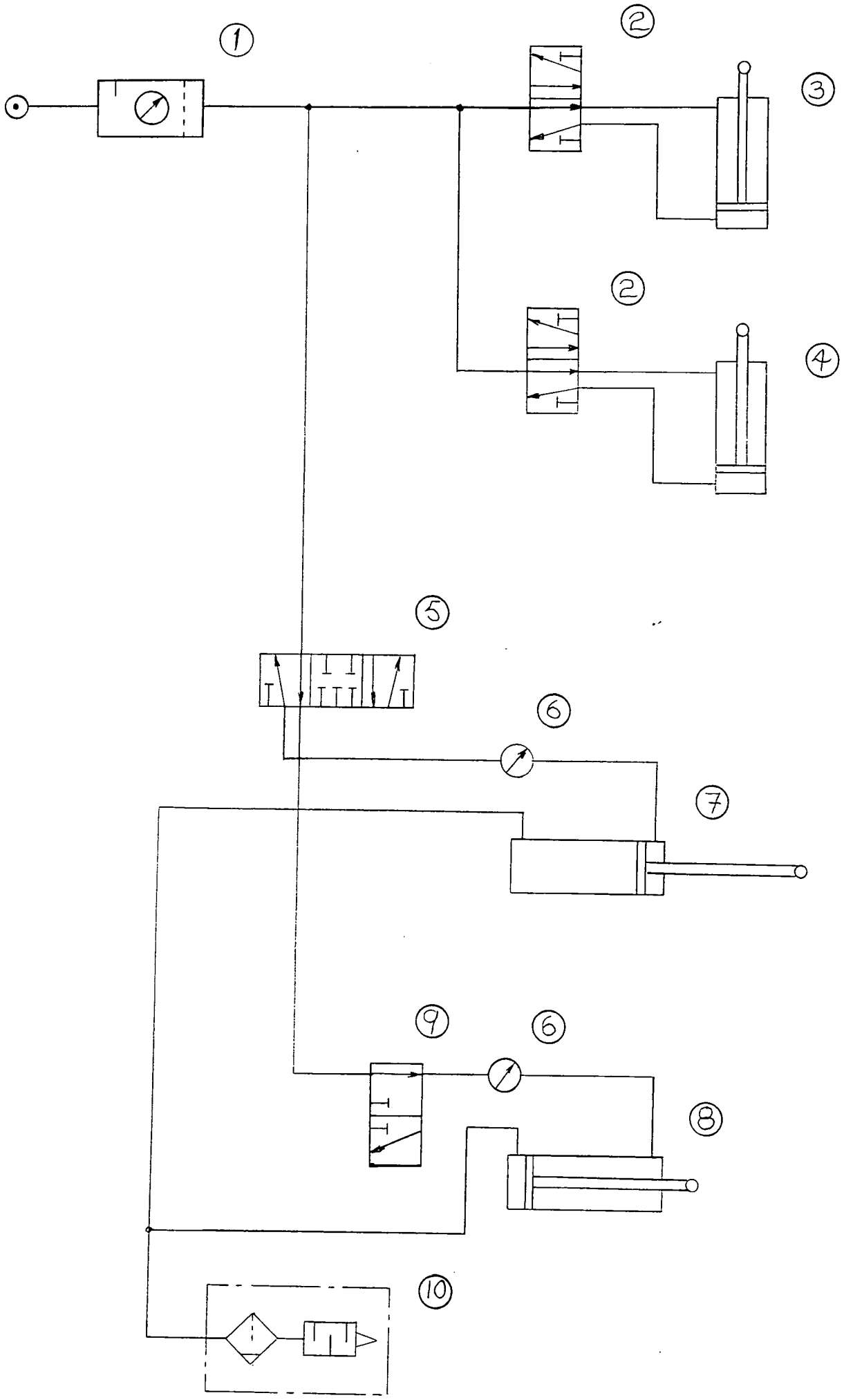
①
②
③
②
④
⑤
⑥
⑦
⑨
⑥
⑧
⑩

Table A10.1 - List of Major Pneumatic Components:

Item	Qty	Bosch Part No.	Description
1	1	0821 300 300	Filter/Regulator
2	2	0820 022 026	5/2 Directional Control Valve
3	1	0822 010 033	Fork Cylinder Ø25 x 15
4	1	0822 010 247	Heavy Load Cylinder Ø32 x 50
5	1	0820 034 993	5/3 Directional Control Valve
6	2	0821 302 720	Precision Regulator
7	1	PDA 10 x 60-A	Lateral Port Cylinder (Extensor)
8	1	PDA 10 x 60-A	Lateral Port Cylinder (Flexor)
9	1	0820 005 101	3/2 Directional Control Valve (Dump)
10	1	0821 303 050	Reclassifier

Purchased from:

Durham Fluid Power Limited, 5 Brighouse Court, Burtree Road, Aycliffe Industrial Estate, Newton Aycliffe, DL5 6HZ. Tel: 01325 312760 Fax: 01325 300693

Appendix 11

Computer Program for New Finger Function Simulator

```
/*
** Program Name :          MEAS.C
** Purpose     : Measurement and Control program for new simulator
** Date        : 17/04/96
*/

#include <stdio.h>
#include <string.h>
#include <conio.h>
#include <graph.h>
#include <stdlib.h>                 /* from control program */
#include "alpha.h"
#include <math.h>

void autotare(void);                /* function prototype */

int Ad = 0x0601;                    /* Alpha card + module address */
int D[8];                          /* data array */
int Num = 0;                        /* Number of readings */
int St = 0;                        /* Alpha card status */
char Cmd[80];                       /* commands */
int tare_val[4];                   /* tare values */

float A, B, x = 0.0;
double L;
int port = 0x1B0;                   /* from control program */

void initialise (void);             /* from control program */
void leave (void);                  /* from control program */
void valves (void);
void pause (void);
void longpaws (void);
void thumbon (void);
void dumpon (void);
void forkon (void);
void loadon (void);
void thumboff (void);
void dumpoff (void);
```

```
void forkoff (void);
void loadoff (void);


void main(void)
{

  int porta = 0xff;                    /* from control program */
  int i;
  initialise();                        /* from control program */

  _clearscreen(_GCLEARSCREEN);
  _settextposition(1,7);
  printf("Finger Function Simulator.");
  _settextposition(2,7);
  printf("Press ESC Key to Quit any other to Start Flexion-Extension.");
  _settextposition(3,7);
  printf("Channel I0 gives lateral load.");
  _settextposition(4,7);
  printf("Channel I1 gives forward load.");

  for (i = 0; i < 4; i++)                          /* init tare values */
    tare_val[i] = 0;

  while(1)                                       /* load measurement loop   */
    {
        while (!kbhit())

                {
                x = x + 1.0;
                _settextposition(5,40);
                printf("Count %4.1f\n",x);
                sprintf(Cmd, "%s,T%d,%s,T%d,%s,T%d,%s,T%d,%s",
                                "G,F50,B10000,G2,K2085,P1000",
                 tare_val[0],
                 "I0",
                 tare_val[1],
                 "I1",
```

```
 tare_val[2],
 "I2",
 tare_val[3],
 "I3"
);
Num = 4;
alpha(Ad, Cmd, D, Num, &St);              /*  transfer data */
for (i = 0; i < 2; i++)
        {
        _settextposition(7 + i, 10);        /* print lateral result */
        printf("I%d = %7d", i, D[i]);
        A = fabs ((D[0] - 54) * 0.1063);
        _settextposition(7, 52);          /* print forward result */
        printf("a = %4.1f", A);
        B = fabs ((D[1] - 50) * 0.1067);
        _settextposition(7, 32);              /* print result */
        printf("b = %4.1f", B);
        _settextposition(8, 32);              /* print result */
         L = sqrt (A*A + B*B);
         _settextposition(9, 46);
         printf("Load is %5.2f Newtons", L);
        }

if (x >= 80.0)                          /* time while f-e occurs */
    {
    outp(port,255);
    _settextposition(10,7);
    printf("Flexion-extension has stopped.");
    pause();
    dumpon();
    pause();
    forkon();
    pause();
    thumbon();
    pause();
    loadon();
    longpaws();
    loadoff();
```

```
                    pause();
                    thumboff();
                    pause();
                    forkoff();
                    pause();
                    dumpoff();
                    pause();
                    leave();
                    break;
                    }
                }

        if(getch() == 27)                   /* if key pressed is ESC quit */
                {
                    leave();
                    break;
                }

        else
                {
                autotare();                 /*  autotare is a GO signal  */
                x = 1.0;
                outp(port,porta &= 0xef);   /*  239  or 11101111 */
                }
        }
}


void autotare()                     /*  autotare() - performs an autotare scan  */
{
 int i;
 strcpy(Cmd, "G,F50,B10000,G2,K2085,P1000,I0,A,I1,A,I2,A,I3,A");
 Num = 8;
 alpha(Ad, Cmd, D, Num, &St);
 for (i = 0; i < 4; i++)
  tare_val[i] = (D[(i * 2) + 1] & 4095);          /* get tare value from string */
}
```

```
void initialise (void)                                  /* from control program */
{
 outp(port+3,0x80);                    /* control word sets port A to outputs */
 outp(port,0xff);
}


void leave (void)                      /* from control program */
 {
 outp(port,0xff);                      /* sets all outputs high and exits */
 exit;
 _settextposition(20,7);
 printf(" Test complete so far!  Press ESCAPE key");
 }

void valves (void)
 {
  _settextposition(21,7);
  printf(" valves works!  Press escape key");
  _settextposition(22,7);
  printf("       ");
 }


void pause (void)
 {
  int j, k, l = 0x0;
  for ( j = 1; j < 32000; j = j + 1)
   for ( k = 1; k < 40; k = k + 1)
    while ( l != 0xff )
    l = l + 0x1;
  /*   _settextposition(16,7);                          */
  /*   printf("First part is complete, it took 5.5 seconds\n");  */
 }


void longpaws (void)
```

```
{
 int i, j, k, l = 0x0;
 for ( j = 1; j < 2200; j = j + 1)
  for ( k = 1; k < 800; k = k + 1)
   while ( l != 0xff )
          l = l + 0x1;
   _settextposition(8,34);
/*  printf("longpaws complete\n");      */
/*  printf("2nd part is complete, it took 4 minutes, 50 seconds\n"); */
}


void thumbon (void)
{
  int porta = 0xff;
  outp(port,porta &= 0xf8);       /* thumb solenoid (fork & dump) activated  */
  _settextposition(13,7);
  printf("Thumb solenoid has been activated.");
}


void dumpon (void)
{
   int porta = 0xff;
   outp(port,porta &= 0xfe);                  /*  dump valve 254 activated    */
   _settextposition(11,7);
   printf("Dump valve has been activated.");
}


void forkon (void)
{
   int porta = 0xff;
   outp(port,porta &= 0xfa);             /*  fork valve 251 (& dump) activated  */
   _settextposition(12,7);
   printf("Fork has been activated.");
}
```

```
void loadon (void)
{
        int porta = 0xff;
        outp(port,porta &= 0xf0);          /* heavy load cylinder et al activated */
        _settextposition(14,7);
        printf("Pinch Load is being applied.");
}


void loadoff (void)
{
        int porta = 0xff;
        outp(port,porta &= 0xf8);          /* heavy load cylinder de-activated */
        _settextposition(15,7);
        printf("Pinch Load is released.");
}


void thumboff (void)
{
  int porta = 0xff;
  outp(port,porta &= 0xfa);                /* thumb solenoid de-activated  */
  _settextposition(16,7);
  printf("Thumb solenoid has been de-activated.");
}


void forkoff (void)
{
   int porta = 0xff;
   outp(port,porta &= 0xfe);               /*  fork valve (251) de-activated  */
   _settextposition(17,7);
   printf("Fork has been de-activated.");
}
```

```
void dumpoff (void)
{
   int porta = 0xff;
   outp(port,porta &= 0xff);                    /*  dump valve (254) de-activated  */
   _settextposition(18,7);
   printf("Dump valve has been de-activated.");
}
```

Appendix 12

Protocol

Protocol for a Pilot Study of a Clinical Trial of the Durham Surface Replacement Metacarpophalangeal Prosthesis

Protocol - DF/95/01

Principal Investigator: Mr C Viva

Principal Investigator's signature: Date:

Principal Investigator's address: Middlesbrough General Hospital
Ayresome Green Lane
Middlesbrough
Cleveland
TS5 5AZ

Sponsor: Dr P McCullagh
Research and Development Director
DePuy International Limited

Sponsor's signature: Date:

Sponsor's address: DePuy International Limited
St Anthony's Road
Leeds
LS11 8DT
UK

Contents

1 Summary

Title: Protocol for a Pilot Study of a Clinical Trial of the Durham Surface Replacement Metacarpophalangeal Prosthesis.

Study No.: DF/95/01

Objective: To evaluate the safety of the Durham Surface Replacement Metacarpophalangeal Prosthesis operation and, during the duration of this study, to evaluate the amount of pain relief provided by the prosthesis.

Secondary Objective: To measure the grip and pinch strength; metacarpophalangeal joint stiffness and range of motion; and obtain a subjective, patient-provided comment on the clinical results given by the Durham Surface Replacement Metacarpophalangeal Prosthesis.

Design: Open, single-centre, prospective investigation. 40 joints in 10 hands are required.

Assessments: Radiological Evaluation
Clinical Questionnaire
Adverse Event Reporting

Secondary Assessments: Hand strength
Finger strength
Metacarpophalangeal joint range of motion
Metacarpophalangeal joint stiffness
Patient satisfaction questionnaire

Assessments: Pre-op, 3 months, 6 months, 9 months, and 12 months post operatively.

Investigators: Mr C Viva, Middlesbrough General Hospital
(Principal Investigator)
Prof. I Haslock, South Cleveland Hospital (Co-Investigator)
Prof. A Unsworth, University of Durham (Co-Investigator)
Mr T Joyce, University of Durham (Monitor)
Ms H Ash, University of Durham (Monitor)

Investigation Centre: Middlesbrough General Hospital
Ayresome Green Lane
Middlesbrough
Cleveland
TS5 5AZ
Tel. 01642 850222 xtn. 5816

2 Study Contacts

Mr C Viva FRCS FRCSE DL Principal Investigator
Senior Consultant Plastic Aesthetic and Hand Surgeon
Middlesbrough General Hospital
Ayresome Green Lane
Middlesbrough
Cleveland
TS5 5AZ

Tel. 01642 850222 xtn. 5816
Co-Investigator: Professor I Haslock, Consultant Rheumatologist,
South Cleveland Hospital.

Professor A Unsworth, MSc, PhD, DEng, FIMechE Co-Investigator
Centre for Biomedical Engineering
School of Engineering
University of Durham
Durham
DH1 3LE

Tel 0191 374 3932
Fax 0191 374 2550
Monitors: Mr T Joyce, BEng, MSc, Research Assistant
Ms H Ash, BSc MSc Research Student

Dr P McCullagh Sponsor
Research and Development Director
DePuy International Limited
St Anthony's Road
Leeds
LS11 8DT

Tel. 01132 700461
Fax. 01132 724198

3 Introduction

Rheumatoid arthritis, one of the most common and debilitating forms of arthritis, frequently affects the joints of the hands, in particular the metacarpophalangeal joints. Sufferers face pain, a loss of strength and mobility which may in turn lead to a loss of independence and income, together with cosmetically upsetting changes to their hands.

Surgical treatment of rheumatoid arthritis at Middlesbrough General Hospital involves the diseased bones being cut away and a silicone spacer, known as the Swanson prosthesis, being inserted. However, the success of this procedure is limited as the prosthesis often breaks and deformity gradually returns (1). Further, there is no increase in grip strength, little improvement in range of motion (1) and there are concerns over silicone synovitis (2). For these reasons, the operation is not popular and it is generally undertaken when little can be salvaged from the joint.

At the University of Durham, a new artificial joint has been designed, based on a fresh approach, and manufactured from a unique material, called cross-linked polyethylene (XLPE). This new artificial joint, the Durham Surface Replacement Prosthesis, is shaped to match the ends of the natural finger bones so that a normal joint can be recreated. It is inexpensive, easy to fit, has a projected long life and, unlike the Swanson prosthesis, requires only a minimal amount of bone removal. Experimental work indicates a life in excess of 25 years for the Durham Prosthesis (3), unlike the Swanson which shows a 26% breakage rate after 2.5 years (4).

The Durham Prosthesis will now be implanted into a small number of patients, and its success evaluated by clinical and radiological outcomes. It is hoped that the results will be equivalent to those given by the Swanson. Grip and pinch strength, metacarpophalangeal joint range of motion and stiffness, together with patient satisfaction will be recorded, and these results compared with the published results given by the Swanson prosthesis.

This study will be conducted in accordance with the World Medical Declaration of Helsinki (Appendix 1) and the British Standard on the Clinical Investigation of Medical Devices for Human Subjects BS EN 540 (Appendix 2).

4 Risk Benefit Analysis

4.1 Design of the Durham Prosthesis

The current most popular metacarpophalangeal joint prosthesis in use in the United Kingdom is the Swanson. This prosthesis is a single flexible piece of silicone rubber which acts only as a spacer and does little to restore the original joint dynamics. The Durham Prosthesis offers a new approach to metacarpophalangeal joint replacement. Its concept is that of a surface replacement joint in which the two separate surfaces slide over one another, as occurs in the natural joint. Therefore the original joint dynamics can be restored, and the ligaments which naturally stabilise the joint can be maintained. Trial fitting of the new prostheses into cadaveric hands has been successfully undertaken and a full set of surgical instruments manufactured. Surgical

risks are the same as those existing if a Swanson prosthesis was to be fitted. Should the Durham prosthesis not be successful, then a Swanson prosthesis can still be fitted as an alternative. Such an operation would constitute a satisfactory rescue procedure.

4.2 Durham Prosthesis Material

Cross linked polyethylene (XLPE) the material from which the prosthesis is manufactured, has been successfully used in prosthetic implants for a number of years. This use has mainly been in a non-wearing situation, for instance the DePuy Ogee flange of the acetabular component of a total hip replacement joint. However, trial acetabular cups manufactured entirely from XLPE have been implanted for eight years and have shown success (5). This use has been in a wearing situation, as will be the case with the Durham Prosthesis. Further, XLPE debris has been shown to be no worse to the body than debris from the most common type of polymeric material used in the body, ultra high molecular weight polyethylene (6). Therefore, XLPE is considered to be a suitable material from which to manufacture prosthetic components.

5 Study Design

This will be an open, single centre, prospective investigation in 40 joints of 10 hands.

6 Patient Selection

The suitability of each patient for inclusion in the study will be reviewed pre-operatively according to the criteria in sections 6.1 and 6.2 and the results recorded in the Case Report Form (appendix 5).

6.1 Inclusion Criteria

Patients will be considered for participation in the study according to the following criteria:

1 Rheumatoid arthritis of the four metacarpophalangeal joints of one hand requiring joint replacement as the treatment of choice.
2 Patients who have sufficient bone to stock to seat the Durham Prosthesis.
3 Patients who are able to understand the study, co-operate with the study procedures and who are will to return for all required post operative assessments.
4 Patients who are skeletally mature.

6.2 Exclusion Criteria

Patients with any of the following conditions will be excluded from participating in the study:

1 Patients who have a concomitant infection at the time of surgery.
2 Patients with a documented history of drug or alcohol abuse.
3 Patients with infectious, highly communicable diseases, e.g. AIDS, active tuberculosis, venereal disease or hepatitis.
4 Patients with a previous prosthetic metacarpophalangeal replacement device in the operative hand.
5 Patients for whom the correct size of Durham Prosthesis can not be provided. Should this be the case then Swanson prostheses will be fitted in all joints requiring replacement. Therefore it will not be possible to have a patient's hand having both Swanson and Durham prostheses fitted at the same time.
6 Patients who have had recent high doses of systemic corticosteroids.
7 Patients who, in the opinion of the Principal Investigator will be unable to complete the study.
8 Patients who have evidence of primary or secondary cancer.

7 Study Procedures

7.1 Study Device

The study device is the Durham Surface Replacement Metacarpophalangeal Prosthesis. This is a new design of prosthesis which has not before been inserted into human patients. The Durham prosthesis is designed to replace the damaged articular cartilage of the MCP joint and in addition act as a low friction shield to the undamaged bone beneath. As such, prosthesis shape and dimensions are closely related to those of the natural joint, imitating it as closely as possible, and therefore permitting the same range of motion. In turn, loads and stresses will be transmitted to the same bearing area as in the natural joint. The prosthesis is therefore two piece, having a metacarpal and a phalangeal component. Being two piece the problem of fracture associated with single piece prostheses such as the Swanson prosthesis is eliminated. The two components have conforming spherical surfaces so that, not only are torsion and shear forces across the MCP joint allowed for, but contact stresses are minimised. The metacarpal component has a volar lip to counter any coronal plane rotation and an offset stem to match the natural cross section of the metacarpal bone. Another advantage of the Durham design is that bone removal is minimised. Then, since bone stock is preserved, future surgery is still feasible. To counter any rotational forces, both components have square section stems. Additionally the phalangeal component has an elliptical face, so that it sits firmly in the concavity of the base of the proximal phalanx. Both components are injection moulded and made from XLPE. The prosthesis comes in three sizes, based on the radius of the metacarpal head. These sizes are radius 6.5mm, 7.5mm and 8.5mm. A sketch of the Durham MCP prosthesis is shown below.

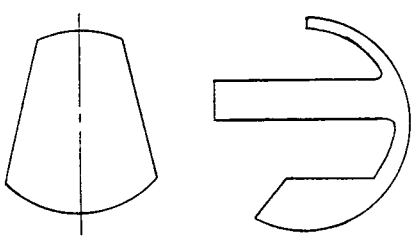

Metacarpal Component
Front and Side Views

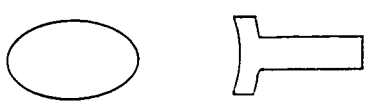

Phalangeal Component
Front and Side Views

7.2 Informed Patient Consent

The study will be conducted in accordance with the Declaration of Helsinki (Appendix 1). Patients will be informed of the nature and purpose of the study and be given an opportunity to ask questions regarding the study before they are enrolled into the study. Patients will be given information concerning the study to read and to keep. They will also be given sufficient time to allow them to decide whether or not they wish to participate in the study. All patients must sign an Informed Patient Consent Form prior to entry into the study (Appendix 4). All patients who are enrolled in the study, will have their GP informed.

7.3 Patient Management

Patients will be evaluated pre-operatively by the Principal Investigator and the results recorded on the Case Report Form (Appendix 5). Surgical technique will be standardised, and all surgery will be undertaken by the Principal Investigator only. Under a tourniquet, a longitudinal skin incision will be made on the dorsum of the hand, over the metacarpal necks. A longitudinal incision will be made in the extensor hood, parallel to the extensor tendon on the ulnar aspect. The ulnar intrinsic tendons, including the abductor digiti minimi, will be released. The extensor hood will be retracted radially, a longitudinal incision made in the mid-portion of the capsule, and the metacarpophalangeal joint will be exposed subperiosteally. A complete synovectomy will be performed. The metacarpal head will be measured using a template, then the appropriate size of cutter used to produce a part-sphere on the metacarpal head. A palmar flat will be made on the metacarpal head with a power saw, an offset hole drilled in the head and a metacarpal component of the appropriate size will be inserted. The cartilage on the proximal phalanx will be cleaned away, then a hole reamed in medullary canal of the proximal phalanx and the phalangeal component of the prosthesis will be push fitted. The capsule will be repaired, the collateral ligaments released or re-tensioned as appropriate and the extensor tendons reefed back to the radial side of the joint. The skin will be sutured either with or without a drain, after releasing the tourniquet, and a sulphur compression bandage will be fitted. After surgery the arm will be elevated and movement encouraged. After three days the bandages will be removed and replaced with a lighter bandage, so that increased mobility will be permitted. After three or four nights, the patient will be discharged. Alternative sutures will be removed after one week, the remainder after two weeks. Peri-operative management will be standard. Post-operative rehabilitation will be as quick as possible and adapted, to a certain extent, to the individual requirements of each patient. Concomitant medication will be recorded.

7.4 Clinical Evaluation

Clinical evaluation of the metacarpophalangeal joints fitted with the Durham Prosthesis will be completed by the Principal Investigator pre-operatively, at three, six, nine and twelve months post-operatively. The results will be recorded on the Case Report Form (Appendix 5).

7.5 Radiographic evaluation

Radiographic evaluation of the metacarpophalangeal joint will be completed by the Principal Investigator pre-operatively, at three, six, nine and twelve months post-operatively. As a minimum requirement, a single dorsal X-ray of the hand will be taken on each of these occasions. Any bone resorption, radiolucent lines or evidence of prosthesis migration will be recorded on the Case Report Form (Appendix 5).

7.6 Adverse Event Reporting

The only currently anticipated adverse events likely to be associated with the devices in this study are infrequent occurrences of infection. A record of all adverse events including description, details of duration, severity, relationship to study device and outcome will be made using the Case Report Form (appendix 5). All adverse events will be reported to DePuy International in writing. Any adverse event which:

1 is fatal or life threatening;
2 requires or prolongs in patient hospitalisation;
3 is permanently incapacitating or debilitating;
4 causes a congenital anomaly, foetal distress or foetal death, or malignancy results;

is regarded as severe. Upon discovery of a severe adverse event, the Principal Investigator must report it immediately to DePuy International (telephone 0113 2700461, fax 0113 2724198). A full written report will be sent to DePuy International and the ethics committee who approved the protocol, within ten working days of the discovery of the adverse event. In the case that any adverse event is found to be device related, DePuy International will also inform the relevant competent authority. If an unexpected device related adverse event (e.g. breakage of one or more of the components) occurs, it shall be recorded on the Complication Form and the Principle Investigator shall submit a written report to DePuy International Limited and the respective Ethics Committee within ten working days after the problem is discovered using the complication form in the CRF (Appendix 5).

7.6.1 Lost to follow up reports

If for any reason a patient is lost to follow up, the Complication Form must be completed. The reasons for lost to follow up may include, but is not limited to:

1 death not related to the study device
2 arthrodesis
3 amputation

These conditions represent known outcomes whereby a study device implanted patient has been lost to continued follow up.

7.7 Secondary Objective

The metacarpophalangeal joints fitted with the Durham Prosthesis will have their function evaluated. This work will be done at pre-surgery and at three, six, nine and twelve months after surgery. The relevant documents are included in Appendix 3.

7.7.1 Finger and Hand Strength

Grip and pinch strength of rheumatoid patients is known to be approximately one third that of normal subjects (7). The fitting of a metacarpophalangeal prosthesis may lead to an increase in grip and pinch strength. Therefore, this theory will be investigated. Mr T Joyce will be responsible for the required measurements. The equipment used will be the Durham grip and pinch strength units (7).

7.7.2 Metacarpophalangeal Joint Range of Motion

Range of motion of metacarpophalangeal joints is often reduced in rheumatoid patients (1). Therefore any improvements due to the fitting of a new metacarpophalangeal prosthesis will be measured. Range of motion will be defined as flexion-extension and ulnar deviation, and measured using a goniometer. These measurements will be undertaken by Mr T Joyce.

7.7.3 Metacarpophalangeal Joint Stiffness

Rheumatoid patients often complain of stiff joints (8). The fitting of a metacarpophalangeal prosthesis may alleviate this complaint, therefore joint stiffness will be measured by Ms H Ash using the Durham arthrograph (9).

7.7.4 Patient Satisfaction Questionnaire

Even with limited objective results, patient satisfaction can still be high if pain is alleviated and the appearance of the hand is improved (1). Therefore subjective measurements of criteria which together give an indication of patient satisfaction will be recorded using a questionnaire which will be completed by the patient.

7.8 Approval of Study

The study will not commence until approval from both the South Durham Lead Research Ethics Committee and the Medical Devices Agency has been received.

8 Protocol deviations and revisions

If the Investigator deviates from the Protocol to protect the well-being of a patient in an emergency, he should report the deviation to the Ethics Committee within five working days.

If the Ethics Committee withdraws its approval for the Investigator's participation in the study, the Investigator must notify DePuy International within five working days of the Ethics Committee's action.

Ethics Committee approval must be obtained prior to the implementation of any change in the Protocol that may effect the scientific credibility of the investigation or the rights, safety, or welfare of patients involved in the study.

9 Statistical Design

As this is a pilot study to evaluate a new design of finger prosthesis, no formal power calculation has been prepared. It is felt that a sample size of 40 devices in 10 hands is appropriate for a limited but informative evaluation of this investigational device. The results of the data from the 40 joints involved in this study will be analysed by descriptive statistics. All results will be reported in full, twelve months after the tenth hand has been fitted with Durham Prostheses.

10 Data Collection

The Principal Investigator will be responsible for the completion of the radiographic assessment form and the complication/lost to follow up form, should the latter be required.

The Principal Investigator will examine each patient pre-operatively, at three months, six months, and twelve months post-operatively, and thereafter as required. The results of these examinations will be recorded in the patient's notes and on the case report form (appendix 5). At the same intervals Mr T Joyce and Ms H Ash will undertake measurements of hand and finger strength, metacarpophalangeal joint range of motion and stiffness, and ensure the completion of a questionnaire by the patient.

There may be study patients who will not, or can not return for follow up examinations, yet who still have the devices implanted. These individuals will be considered as non-compliant within the follow up protocol, thus entering a missing data category. This may include patients who refuse to return for follow up, re-locate without notifying the Principal Investigator, or can not receive adequate clinical evaluation for medical reasons (i.e. confined to bed or wheel chair following stroke, etc.).

The Principal Investigator will have the responsibility for maintaining a record of his communications with and attempts of his communications with patients who do not return for follow up examinations. This record will be kept in the Principal Investigator's office and reviewed on monitoring visits. In this manner, the Principal Investigator can determine the conditions leading to such follow up violations and attempt to obtain and document at least the current status of the study device (i.e. still in place and functioning satisfactorily, painful, revised, etc.). During the monitoring visits, the Principal Investigator will also check that the data in the case report form conforms with that in the patient's file.

Lost to follow up patients will be replaced. All patient information will be treated as confidential and kept in locked cabinets.

11 Duration and Termination of Study

The study will run for a minimum of one year after the last patient has been fitted with Durham Prostheses.

12 Reporting

A complete final study report, detailing the findings of the study, will be prepared by the University of Durham at the end of the study and signed by the Principal Investigator on approval.

13 Archive

A copy of the questionnaire together with strength, stiffness and range of motion measurements and the case report form for each patient must be stored by the Principal Investigator for a minimum of five years after the end of the study.

Appendix 1

World Medical Association Declaration of Helsinki

September 1989 Original: English

WORLD MEDICAL ASSOCIATION DECLARATION OF HELSINKI

Recommendations guiding physicians
in biomedical research involving human subjects

Adopted by the 18th World Medical Assembly
Helsinki, Finland, June 1964

and amended by the
29th World Medical Assembly
Tokyo, Japan, October 1975
35th World Medical Assembly
Venice, Italy, October 1983
and the
41st World Medical Assembly
Hong Kong, September 1989

INTRODUCTION

It is the mission of the physician to safeguard the health of the people. His or her knowledge and conscience are dedicated to the fulfillment of this mission.

The Declaration of Geneva of the World Medical Association binds the physician with the words, "The health of my patient will be my first consideration", and the International Code of Medical Ethics declares that, "A physician shall act only in the patient's interest when providing medical care which might have the effect of weakening the physical and mental condition of the patient".

The purpose of biomedical research involving human subjects must be to improve diagnostic, therapeutic and prophylactic procedures and the understanding of the aetiology and pathogenesis of disease.

In current medical practice most diagnostic, therapeutic or prophylactic procedures involve hazards. This applies especially to biomedical research.

Medical progress is based on research which ultimately must rest in part on experimentation involving human subjects.

In the field of biomedical research a fundamental distinction must be recognized between medical research in which the aim is essentially diagnostic or therapeutic for a patient, and medical research, the essential object of which is purely scientific and without implying direct diagnostic or therapeutic value to the person subjected to the research. Special caution must be exercised in the conduct of research which may affect the environment, and the welfare of animals used for research must be respected.

Because it is essential that the results of laboratory experiments be applied to human beings to further scientific knowledge and to help suffering humanity, the World Medical Association has prepared the following recommendations as a guide to every physician in biomedical research involving human subjects. They should be kept under review in the future. It must be stressed that the standards as drafted are only a guide to physicians all over the world. Physicians are not relieved from criminal, civil and ethical responsibilities under the laws of their own countries.

I. BASIC PRINCIPLES

1. Biomedical research involving human subjects must conform to generally accepted scientific principles and should be based on adequately performed laboratory and animal experimentation and on a thorough knowledge of the scientific literature.

2. The design and performance of each experimental procedure involving human subjects should be clearly formulated in an experimental protocol which should be transmitted for consideration, comment and guidance to a specially appointed committee independent of the investigator and the sponsor provided that this independent committee is in conformity with the laws and regulations of the country in which the research experiment is performed.

3. Biomedical research involving human subjects should be conducted only by scientifically qualified persons and under the supervision of a clinically competent medical person. The responsibility for the human subject must always rest with a medically qualified person and never rest on the subject of the research, even though the subject has given his or her consent.

4. Biomedical research involving human subjects cannot legitimately be carried out unless the importance of the objective is in proportion to the inherent risk to the subject.

5. Every biomedical research project involving human subjects should be preceded by careful assessment of predictable risks in comparison with foreseeable benefits to the subject or to others. Concern for the interests of the subject must always prevail over the interests of science and society.

6. The right of the research subject to safeguard his or her integrity must always be respected. Every precaution should be taken to respect the privacy of the subject and to minimize the impact of the study on the subject's physical and mental integrity and on the personality of the subject.

7. Physicians should abstain from engaging in research projects involving human subjects unless they are satisfied that the hazards involved are believed to be predicable. Physicians should cease any investigation if the hazards are found to outweigh the potential benefits.

8. In publication of the results of his or her research, the physician is obliged to preserve the accuracy of the results. Reports of experimentation not in accordance with the principles laid down in this Declaration should not be accepted for publication.

9. In any research on human beings, each potential subject must be adequately informed of the aims, methods, anticipated benefits and potential hazards of the study and the discomfort it may entail. He or she should be informed that he or she is at liberty to abstain from participation in the study and that he or she is free to withdraw his or her consent to participation at any time. The physician should then obtain the subject's freely-given informed consent, preferably in writing.

10. When obtaining informed consent for the research project the physician should be particularly cautious if the subject is in a dependent relationship to him or her or may consent under duress. In that case the informed consent should be obtained by a physician who is not engaged in the investigation and who is completely independent of this official relationship.

11. In case of legal incompetence, informed consent should be obtained from the legal guardian in accordance with national legislation. Where physical or mental incapacity makes it impossible to obtain informed consent, or when the subject is a minor, permission from the responsible relative replaces that of the subject in accordance with national legislation.

Whenever the minor child is in fact able to give a consent, the minor's consent must be obtained in addition to the consent of the minor's legal guardian.

12. The research protocol should always contain a statement of the ethical considerations involved and should indicate that the principles enunciated in the present Declaration are complied with.

II. MEDICAL RESEARCH COMBINED WITH PROFESSIONAL CARE (Clinical research)

1. In the treatment of the sick person, the physician must be free to use a new diagnostic and therapeutic measure, if in his or her judgement it offers hope of saving life, reestablishing health or alleviating suffering.

2. The potential benefits, hazards and discomfort of a new method should be weighed against the advantages of the best current diagnostic and therapeutic methods.

3. In any medical study, every patient - including those of a control group, if any - should be assured of the best proven diagnostic and therapeutic method.

4. The refusal of the patient to participate in a study must never interfere with the physician-patient relationship.

5. If the physician considers it essential not to obtain informed consent, the specific reasons for this proposal should be stated in the experimental protocol for transmission to the independent committee (1,2).

6. The physician can combine medical research with professional care, the objective being the acquisition of new medical knowledge, only to the extent that medical research is justified by its potential diagnostic or therapeutic value for the patient.

III. NON-THERAPEUTIC BIOMEDICAL RESEARCH INVOLVING HUMAN SUBJECTS (Non-clinical biomedical research)

1. In the purely scientific application of medical research carried out on a human being, it is the duty of the physician to remain the protector of the life and health of that person on whom biomedical research is being carried out.

2. The subjects should be volunteers - either healthy persons or patients for whom the experimental design is not related to the patient's illness.

3. The investigator or the investigating team should discontinue the research if in his/her or their judgement it may, if continued, be harmful to the individual.

4. In research on man, the interest of science and society should never take precedence over considerations related to the wellbeing of the subject.

Appendix 2

BS EN 540 Clinical Investigation of Medical Devices for Human Subjects

Section 5.6 Role of the Clinical Investigator

The Role of the Clinical Investigator(s) from The British Standard EN 540 - Clinical Investigation of Medical Devices for Human Subjects

NATIONAL FOREWORD

This British Standard has been prepared under the direction of the Health Care Standards Policy Committee and is the English language version of EN 540 : 1993 *Clinical investigation of medical devices for human subjects*, published by the European Committee for Standardization (CEN).

EN 540 was produced as a result of international discussions in which the United Kingdom took an active part.

Compliance with a British Standard does not of itself confer immunity from legal obligations.

5.6 Role of the CLINICAL INVESTIGATOR(S)

5.6.1 The CLINICAL INVESTIGATOR(S) shall ask the SPONSOR for information as described in the CLINICAL INVESTIGATOR'S BROCHURE and any other information he judges essential for the conduct of the CLINICAL INVESTIGATION. He shall be well acquainted with the use of the DEVICE.

5.6.2 The CLINICAL INVESTIGATOR(S) shall be well acquainted with the CLINICAL INVESTIGATION PLAN before signing it.

5.6.3 The CLINICAL INVESTIGATOR(S) shall ensure that he and his team will be available to conduct and complete the CLINICAL INVESTIGATION.

Any other concurrent CLINICAL INVESTIGATION conducted by him shall not give rise to a conflict of interest or interfere with the specific CLINICAL INVESTIGATION in hand.

5.6.4 As far as the CLINICAL INVESTIGATION is concerned, the CLINICAL INVESTIGATOR(S) shall be responsible for the personal safety, and well being of SUBJECTS.

5.6.5 The CLINICAL INVESTIGATOR(S) shall make the necessary arrangements, including emergency treatment, to ensure the proper conduct of the CLINICAL INVESTIGATION.

5.6.6 The CLINICAL INVESTIGATOR(S) shall endeavour to ensure an adequate recruitment rate of SUBJECTS during the CLINICAL INVESTIGATION.

5.6.7 If appropriate, SUBJECTS enroled in a CLINICAL INVESTIGATION shall be provided with some means of identification that they are taking part. Contact address/telephone numbers shall be given and the medical records shall be clearly marked.

Note: The SUBJECT's physician should, with the SUBJECT's agreement, be informed.

5.6.8 SUBJECTS who cannot be expected to derive any direct therapeutic benefit shall be examined to ascertain their state of health before entering the CLINICAL INVESTIGATION.

SUBJECTS shall be invited to confirm by a signed declaration that they have disclosed all matters concerning their health and any current medication shall be recorded.

5.6.9 The CLINICAL INVESTIGATOR(S) shall ensure that adequate information is given to the SUBJECT (or his guardian or legal representatives) both in oral and written form, on the nature of the CLINICAL INVESTIGATION.

This information shall be easily understandable by the SUBJECT.

This information shall include the aims, expected benefits for him and/or others, risks and inconveniences and an explanation of any alternative methods, and of possible consequences of any withdrawal from the CLINICAL INVESTIGATION.

Payment or any other form of inducement to SUBJECTS who cannot be expected to derive any direct therapeutic benefit, shall only be for expense, time and inconvenience.

The SUBJECT shall be made aware that there are procedures for compensation and treatment if he is injured/disabled by participating in the CLINICAL INVESTIGATION.

SUBJECTS shall be given the opportunity to enquire about the details of the CLINICAL INVESTIGATION. The information shall make clear to the SUBJECT that he remains free to refuse to participate or to withdraw from the CLINICAL INVESTIGATION at any stage without any sanction (see 5.6.10).

SUBJECTS shall be allowed sufficient time to decide whether or not they wish to participate.

The SUBJECT shall be informed that his participation in the CLINICAL INVESTIGATION is confidential. He shall be made aware that the data relating to the study may be made available to third parties while maintaining anonymity.

5.6.10 A SUBJECT who wishes to withdraw from the CLINICAL INVESTIGATION shall be informed of the possible consequences of this withdrawal, by the CLINICAL INVESTIGATOR.

5.6.11 The CLINICAL INVESTIGATOR(S) shall obtain INFORMED CONSENT preferably in writing.

Following national policy, INFORMED CONSENT shall be documented either by the SUBJECT's dated signature or by the signature of

an independent witness (see also 5.6.12) who records the SUBJECT's assent.

Note: Obtaining INFORMED CONSENT from some categories of SUBJECTS raises particular ethical and legal issues which need special consideration (see the Declaration of Helsinki).

5.6.12 The CLINICAL INVESTIGATOR(S) shall document how INFORMED CONSENT will be obtained and recorded in emergency circumstances where the SUBJECT is unable to give it.

In the exceptional case when neither signed INFORMED CONSENT nor witnessed signed oral consent are possible, each case shall be documented and reported to the ETHICS COMMITTEE and the SPONSOR with the reasons, by the CLINICAL INVESTIGATOR(S).

5.6.13 The CLINICAL INVESTIGATOR(S) shall be responsible for submitting the CLINICAL INVESTIGATION PLAN for opinion or approval to an appropriate ETHICS COMMITTEE and shall transmit the results to the SPONSOR.

If not already included in the CLINICAL INVESTIGATION PLAN, the CLINICAL INVESTIGATOR(S) shall also provide the ETHICS COMMITTEE with at least information on the following:-

a) an assessment of the scientific merit of the proposal, taking into account the preclinical data (see 5.2.1);

b) possible effects on the health of the SUBJECTS;

c) possible hazards and the facilities available to deal with them;

d) the degree of discomfort or distress foreseen;

e) proposed method of supervision of the CLINICAL INVESTIGATION and the responsibilities of the CLINICAL INVESTIGATOR(S);

f) any monetary or other inducements, to be offered to the SUBJECTS;

g) arrangements to be made between the SPONSOR and the CLINICAL INVESTIGATOR(S);

h) the procedures for obtaining CONSENT from the SUBJECT or, where appropriate, their guardians or legal representatives;

i) provisions for compensation in the event of injury or death arising from participation in a CLINICAL INVESTIGATION and any insurance or indemnity to cover the liability of the CLINICAL INVESTIGATOR(S) and SPONSOR;

j) the methods of maintaining SUBJECT's confidentiality.

5.6.14 The CLINICAL INVESTIGATOR(S) shall inform the ETHICS COMMITTEE and ask for its opinion or approval regarding any significant change in the CLINICAL INVESTIGATION PLAN that has been approved by the SPONSOR, and the reasons for the change. The CLINICAL INVESTIGATOR(S) shall inform the ETHICS COMMITTEE of any severe ADVERSE DEVICE EFFECT.

5.6.15 The CLINICAL INVESTIGATOR(S) shall inform without undue delay the SPONSOR and the MONITOR (if applicable) about any severe ADVERSE EVENT, about all ADVERSE DEVICE EFFECTS, and provisions made.

5.6.16 The CLINICAL INVESTIGATOR(S) shall have primary responsibility for the accuracy, legibility and security of all CLINICAL INVESTIGATION data, documents and patient records both during and after the CLINICAL INVESTIGATION. The CASE REPORT FORM shall be signed by the CLINICAL INVESTIGATOR(S). Any alteration of the raw data shall be signed and dated, the original entry being retained for comparison.

5.6.17 The CLINICAL INVESTIGATOR(S) shall discuss with the SPONSOR any question of modification of the CLINICAL INVESTIGATION PLAN and shall obtain his written agreement (see 5.6.18).

5.6.18 In any emergency situation the CLINICAL INVESTIGATOR(S) shall exercise his judgement to safeguard the SUBJECT's interests. In that case deviations from the CLINICAL INVESTIGATION PLAN shall not require the prior approval of the SPONSOR or the ETHICS COMMITTEE. Such deviations shall not be considered as a breach of agreement and shall be reported to the SPONSOR.

5.6.19 The CLINICAL INVESTIGATOR(S) shall make sure that the CLINICAL INVESTIGATION PLAN is followed by all members of the investigation team, and by other parties involved in the execution of the CLINICAL INVESTIGATION. Any significant deviation shall be recorded.

5.6.20 The CLINICAL INVESTIGATOR(S) shall specify and document a procedure for recording ADVERSE EVENTS and ADVERSE DEVICE EFFECTS and reporting severe ADVERSE EFFECTS and all ADVERSE DEVICE EFFECTS to the SPONSOR.

5.6.21 The CLINICAL INVESTIGATOR(S) shall be responsible for the supervision and assignment of duties to the members of the CLINICAL INVESTIGATION team.

He shall be responsible for the measures needed to maintain confidentiality.

5.6.22 After the CLINICAL INVESTIGATION, the clinical records and investigation data shall be kept by the CLINICAL INVESTIGATOR(S) for an appropriate time and the SUBJECT's identity shall not be released to third parties without the SUBJECT's prior consent.

Appendix 3

Secondary Objective Supportive Documents

Assessment of Grip and Pinch Strength

All patients will be given a brief introduction to the equipment and an opportunity to try all the devices before the test is started. For each strength test the scores of three successive trials will be noted. Patient's name, age, sex, and hand dominance will be recorded. Hand domination will be determined by asking 'are you right handed or left handed?' The dominant hand will be tested first. Tests should be undertaken at the same hour of each day.

A standard position for the strength tests is to be maintained in which the patient is seated upright with their forearm horizontal, and the elbow at 110° of flexion. The wrist is to be maintained close to the neutral position. Grip strength will be tested first, followed by lateral pinch and finally pulp pinch.

The grip strength device is to be held vertically, with the wires trailing beneath. For the lateral pinch test, the two platens are to be set vertically. Lateral pinch is defined as the pad of the thumb pressing against the side of the middle phalanx of the index finger, all other fingers being clenched in support. For the pulp pinch tests, the platens are to be set horizontally. Pulp pinch is defined as the pad of the thumb pressing against the distal phalangeal pad of the finger.

The following verbal instructions will be given:

Verbal Instructions

Grip strength. 'I want you to hold the gripper like this and squeeze as hard as you can'. The examiner demonstrates and then gives the gripper to the patient. After the patient is positioned appropriately, the examiner says 'Are you ready? Squeeze as hard as you can'. The test is repeated with the same instructions for a second and third time.

Lateral pinch. 'I want you to place your thumb on this side and your index finger on the other side as I'm doing and pinch as hard as you can. See how the other fingers are in support'. The examiner demonstrates the position and then gives the pinch unit to the patient. After the patient is positioned appropriately, the examiner repeats the series of questions and tests a further two times.

Pulp Pinch. 'I want you to place the tip of your thumb on this side and the tip of each of your fingers in turn on top as I'm doing, as if to make an 'O' and pinch as hard as you can'. The examiner demonstrates the position and then gives the pinch unit to the patient. After the patient is positioned appropriately, the examiner repeats the series of questions and tests a further two times.

Final - 10/5/96

DF/95/01

Durham Metacarpophalangeal Prosthesis Pilot Study

HAND STRENGTH REPORT FORM

Patient's Initials _____ **Hospital ID** _____

Patient's Age _____ Patient's Sex M/F Patient's Dominant Hand L/R
Date _____ Time of test _____am/pm

Visit pre-op / 3 months / 6 months / 9 months / 12 months (please ring)

Durham MCP Prostheses fitted Left Hand Right Hand (please ring)

---

1 Grip Strength - Dominant Hand

Test Number	1	2	3
Total			
Index Finger			
Middle Finger			
Ring Finger			
Little Finger			

---

2 Lateral Pinch Strength - Dominant Hand

Test Number	1	2	3
Total Lateral Pinch			

---

3 Pulp Pinch Strength - Dominant Hand

Test Number	1	2	3
Index Finger			
Middle Finger			
Ring Finger			
Little Finger			

Comments: _____

Strength Values Recorded By _____

Final - 10/5/96 DF/95/01

Durham Metacarpophalangeal Prosthesis Pilot Study

HAND STRENGTH REPORT FORM

Visit pre-op / 3 months / 6 months / 9 months / 12 months (please ring)

1 Grip Strength - Non-dominant Hand

Test Number	1	2	3
Total			
Index Finger			
Middle Finger			
Ring Finger			
Little Finger			

---

2 Lateral Pinch Strength - Non-dominant Hand

Test Number	1	2	3
Total Lateral Pinch			

---

3 Pulp Pinch Strength - Non-dominant Hand

Test Number	1	2	3
Index Finger			
Middle Finger			
Ring Finger			
Little Finger			

Comments: _____

Strength Values Recorded By _____

Section 3 Activities of Daily Living (ADL)
Strength, range of movement and joint stiffness are all important factors to consider when assessing the performance of a prosthesis and all of these criteria will be assessed either objectively, subjectively or both. Objective assessment of these is especially important when comparing the performance of different individuals and of patients with normals. However pain relief and overall functional capacity are equally as important, if not more so, as far as a patient is concerned. Hence overall functional capacity is assessed in section 3. The difficulty in performing selected activities of daily living is assessed using descriptive scales. The activities and scales have been used in previous questionnaires and have been shown to be valid, reliable and repeatable (10, 15-17). Patients are also asked to indicate the reasons for any difficulty that they have with the activities.

POST-OPERATIVE QUESTIONNAIRE

Section 1 Pain and Stiffness Assessment
Pain and joint stiffness are rated on horizontal visual analogue identical to those in section 2 of the pre-operative questionnaire for a comparison between the pre and post-operative joint condition.

Section 2 Pre-Operative and Post-Operative Joint Comparison
The aim of joint replacement is obviously to improve overall hand function and alleviate pain. This section rates pain, stiffness, range of movement, overall hand function, appearance and strength as a direct comparison of the pre-operative and post-operative condition of the joints. The categories are rated on horizontal visual analogue scales indicating whether the patient feels his/her joints are much better, much worse or the same. These scales have been used in previous clinical trials and are validated, reliable and repeatable (10-14).

Section 3 Activities of Daily Living
This section is identical to section 3 on the pre-operative assessment questionnaire in order to directly compare overall hand function pre-operatively and post-operatively.

The Development of the Durham MCP Finger Joint Prosthesis
Centre for Biomedical Engineering, University of Durham

Patient Assessment Questionnaire

Introduction

A new artificial joint is being designed at the University of Durham to replace finger joints badly affected by arthritis. We are interested in looking at arthritis from the patient's view, hence the following questionnaire will ask you about your arthritis and how it affects you and your daily activities. For those people who are going to have their finger joints replaced you will be asked to fill in a second questionnaire about a month after your operation to find out how your new joints are doing. We would like to thank you for your help with this project which is very much appreciated.

If you do not know the answer to a question, do not understand what a question is asking, do not wish to answer a question, or think that a question is not applicable then please leave the answer blank.

Section 1) Patient Details

Surname Initials

Date and Time of Assessment

Dominant Hand RIGHT / LEFT

Occupation/Hobbies

Section 2) About Your Arthritis

1) How long have you had arthritis in your hands or wrists? _____ YEARS

2) Please mark with crosses on Figure 1 which of your joints are affected by arthritis, and circle the joints that are affected the worst.

3) Do any of the following describe your hand/wrist joints? Please tick.

Unstable		Swollen		Weak	
Tender to touch		Stiff		Painful	
Reduced range of movement					

4) Do you experience morning stiffness in your hands/wrists? YES / NO

If yes, on average for how long after you get up in the morning? _____ HOURS

5) Please rate your finger joints **over the past week** for the following categories by marking the scales.

Pain with Resisted Motion

Pain with Non-Resisted Motion

Joint Stiffness

Section 3) Daily Activities

On the following page there is a list of possible daily activities. Please rate how difficult the following have been for you to do **over the past week** without help from another person, and also indicate any specific reasons for the difficulty because of the condition of your hands from the following lists. Please tick as many reasons as are applicable. **If you do not usually perform any of the activities then please state this but putting NA (not applicable) by the activity.**

Difficulty	**Reasons for difficulty**
No difficulty in performing this activity	1 = weakness
Slight difficulty in performing this activity	2 = pain
Moderate difficulty in performing this activity	3 = lack of range of movement
Severe difficulty in performing this activity	4 = sensory problems
Impossible to do this activity	5 = other reasons

	Difficulty					Reasons				
	None	Slight	Mod.	Severe	Impos.	1	2	3	4	5
Dressing Activities										
Buttons										
Zips										
Shoelaces										
Socks/stockings/tights										
Shaving/make up										
Hygiene Activities										
Taps										
Washing/brushing hair										
Cleaning teeth										
Wash and dry body										
Eating and Cooking										
Using knife and fork										
Drinking from cup										
Opening cartons										
Lifting jug, teapot, kettle										
Pouring jug, teapot, kettle										
Unscrewing lids										
Using a tin-opener										
Preparing vegetable										
Housework										
Vacuuming										
Using a broom										
Hand washing										
Ironing										
Others										
Carrying bags/boxes										
Handling money										
Writing										
Sewing or knitting										
Using door key										
Driving										

THANK YOU FOR SPENDING THE TIME TO FILL IN THIS QUESTIONNAIRE

The Development of the Durham MCP Finger Joint Prosthesis
Centre for Biomedical Engineering, University of Durham

Post-operative Patient Assessment Questionnaire

Introduction

Before you had some of your finger joints replaced you may have been asked to complete a questionnaire on the severity and extent of your arthritis and how it affected daily activities. In order to assess the performance of your new finger joints we are asking you to complete this follow up questionnaire. Once again we thank you for your help with this project.

Section 1

Please rate your finger joints from **over the past week** for the following categories by marking the scales.

Pain with Resisted Motion

Pain with Non-Resisted Motion

Joint Stiffness

Section 2

Please rate the following categories comparing your replaced finger joints with your joints before they were replaced, by marking the scales.

Joint Pain

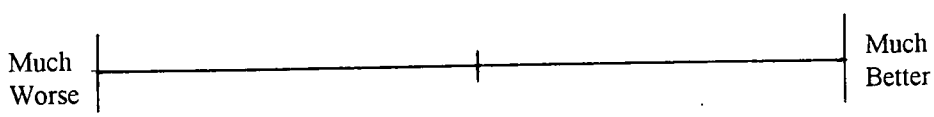

Joint Stiffness

Range of Movement

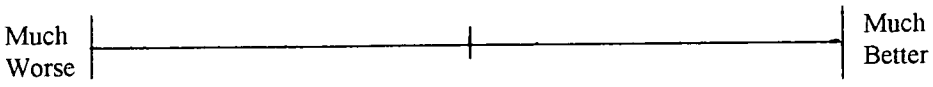

Overall Hand Function

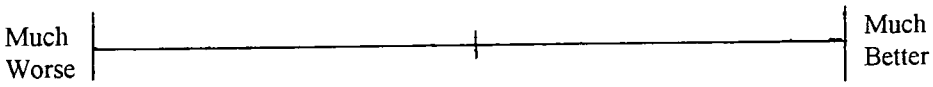

Appearance

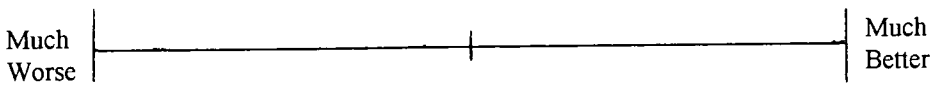

Overall Hand Strength

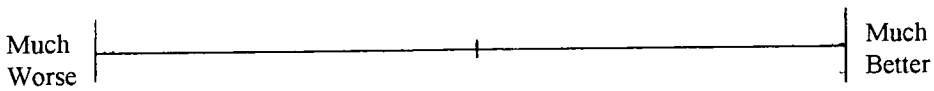

Section 3) Activities of Daily Living

On the following page there is a list of possible daily activities. Please rate how difficult the following are for you to do without help from another person, and also indicate any specific reason for the difficulty because of the condition of your hands from the following lists. Please tick as many reasons as are applicable. **If you do not usually perform any of the activities then please state this but putting NA (not applicable) by the activity.**

Difficulty	Reasons for difficulty
No difficulty in performing this activity	1 = weakness
Slight difficulty in performing this activity	2 = pain
Moderate difficulty in performing this activity	3 = lack of range of movement
Severe difficulty in performing this activity	4 = sensory problems
Impossible to do this activity	5 = other reasons

	Difficulty					Reasons				
	None	Slight	Mod.	Severe	Impos.	1	2	3	4	5
Dressing Activities										
Buttons										
Zips										
Shoelaces										
Socks/stockings/tights										
Shaving/make up										
Hygiene Activities										
Taps										
Washing/brushing hair										
Cleaning teeth										
Wash and dry body										
Eating and Cooking										
Using knife and fork										
Drinking from cup										
Opening cartons										
Lifting jug, teapot, kettle										
Pouring jug, teapot, kettle										
Unscrewing lids										
Using a tin-opener										
Preparing vegetable										
Housework										
Vacuuming										
Using a broom										
Hand washing										
Ironing										
Others										
Carrying bags/boxes										
Handling money										
Writing										
Sewing or knitting										
Using door key										
Driving										

THANK YOU FOR SPENDING THE TIME TO FILL IN THIS QUESTIONNAIRE

OBJECTIVE JOINT STIFFNESS ASSESSMENT

Objective and subjective methods can be used to measure joint stiffness. However in previous clinical trials there have been differences in objectively measured stiffness and subjective stiffness rated by patients on scales such as visual analogue scales (18-21). Objective joint stiffness has been defined as the passive resistance to motion of the joint, whereas stiffness measured subjectively has shown a that patient's perception of joint stiffness relates to factors such as joint pain and range of movement. Both objective and subjective methods of measuring joint stiffness are to be included in the pilot study.

Objective stiffness measurements pre-operatively and post-operatively will give an indication of how the joint replacement surgery affected the overall stiffness of joint which will be dependent not only on the prosthesis but also on the initial condition of the soft tissues and the surgical technique used. A comparison will also be able to be made between the subjective and objective stiffness measurements.

An arthrograph, (stiffness measuring machine), designed in Durham and used in previous clinical work, will be used to measure stiffness of the index finger metacarpo-phalangeal joint of the right hand. The arthrograph consists of a strain gauge system to measure the resistance to motion of the joint (torque reading) and a rotary potentiometer to measure the angular displacement of the joint. The torque and displacement readings are read into a computer where several parameters are calculated from the acquired data and a graph plotted.

At least two sets of data are required to acquire valid joint stiffness readings. The first set of data will be collected with the joint oscillating about a mid-position 20°. From this set of data the mean equilibrium position of the joint can be calculated. The torque and displacement data form a hysteresis loop, (Figure 2). The mean equilibrium position (EQP) is the average of the two positions in the loop where the torque is zero, (EQP1, EQP2). For valid stiffness readings the joint must oscillate about this position hence a second set of data will be taken with the joint oscillating about the calculated mean equilibrium position.

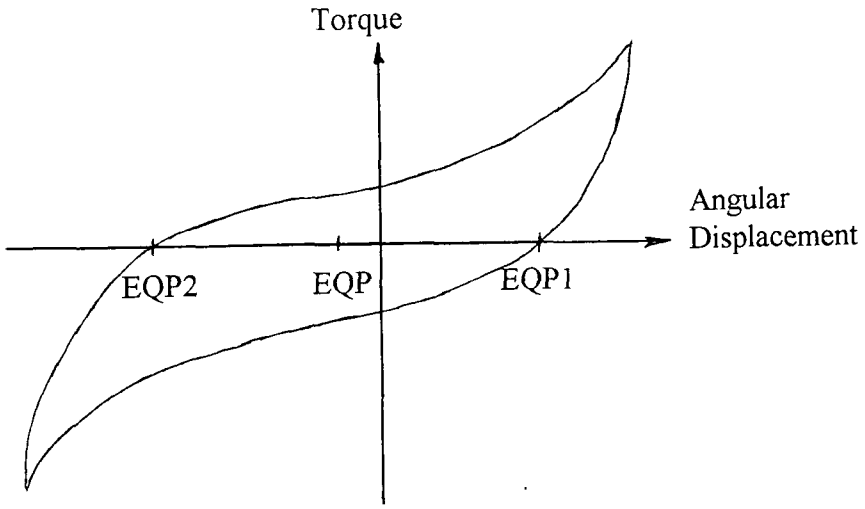

FIGURE 2 : JOINT STIFFNESS HYSTERESIS LOOP

OPERATIONAL PROCEDURE

1) The range of movement of the patient's index finger will be checked to make sure that the oscillation performed to measure joint stiffness will not be uncomfortable for the patient. If it would be then no stiffness assessment will be undertaken.

2) Before the patient's hand is positioned in the carriage the assessor will switch the motor on and let the carriage rotate until it is at full flexion. The motor will then be turned off and a zero force reading taken.

3) The assessor will correctly locate the right hand index finger in the correct position on the arthrograph with the patient's forearm resting on the board, the middle, ring and little fingers curled around the cylinder for support and the thumb held in its support sling. The centre of rotation of the index finger MCPJ will be correctly aligned with the centre of rotation of the carriage and the finger strapped to the carriage to keep it located in the correct position.

4) The patient will be asked to relax and not to actively resist the motion of his/her finger so that the force measured by the arthrograph is purely passive measuring no active muscle force.

5) The assessor will manually rotate the carriage holding the index finger to 40° or to a position comfortable for the patient. The carriage will be set to oscillate with an amplitude of 20° if this is comfortable for the patient, and hence will initially be set to oscillate about a mid-position of 20° flexion, (a good estimate for the equilibrium position of the MCPJ).

6) The motor will be switched on so that the finger oscillates around the set centre of rotation and a cycle of torque/displacement readings will be taken when the computer is prompted by the assessor.

7) When the readings have been taken the motor will then be switched off.

8) After calculation of the equilibrium position of the finger joint the carriage will be manually realigned so that oscillation now occurs about the equilibrium position. The motor will then be switched on again and a second set of readings will be taken when the computer is prompted by the assessor.

9) Finally the motor will be switched off and the hand removed from the arthrograph.

10) The computer can then be prompted for further analysis of the collected data and it can be saved on floppy disk.

Appendix 4

Patient Explanation Leaflet and Consent Form

Patient Explanation Leaflet

Introduction

This leaflet aims to describe the design and advantages of a new type of artificial finger joint, which you have agreed to have fitted. The years of laboratory and background work undertaken on the new design will then be outlined. Finally, a description of the regular assessments to be undertaken after your surgery will be given, and a summary of the risks and benefits associated with this project.

The Durham Artificial Finger Joint

At the Centre for Biomedical Engineering, within the University of Durham, a new artificial finger joint has been designed, based on an original approach, and manufactured from a unique material, called cross-linked polyethylene. Cross-linked polyethylene is currently used in other artificial joints and has been seen to be a material which can safely be inserted into the body. The new artificial joint is shaped to match the ends of the natural finger bones, so that a normal joint can be recreated. The artificial joint will replace only the diseased articular cartilage which is found on the ends of the finger bones, and will then act as a shield to the bone beneath. Furthermore, the artificial joint is easy to fit so that the duration of surgery is minimised.

Laboratory Testing

Comprehensive experimental work at Durham, which began in 1985, indicates a life in excess of 25 years for the new artificial joint. This is greater than for the existing artificial joints. All of the pre-clinical work has revealed no significant problem with either the artificial joint or the material from which it is made. This experimental work has been carried out in conjunction with Mr Charles Viva, the consultant hand surgeon, Professor Ian Haslock, the consultant rheumatologist, and one of the world's major manufacturers of artificial joints.

After Surgery

Following the surgery to fit the new artificial finger joint, regular assessments will be made to assess its success. This assessment will occur at 3, 6, 9 and 12 months post-operatively. There will also be a pre-operative assessment. The range of motion of your joints, together with their stiffness and strength will all be measured. You will also be requested to complete a questionnaire concerning your feelings on the results of your hand operation and an X-ray of your hands will be taken. The entire evaluation will take place at South Cleveland Hospital, at those times when you are seen by Professor Ian Haslock, so there will be no need to attend any additional appointments.

Patient Explanation Leaflet (continued)

Risks and Benefits

There are no additional risks involved in this surgery, other than those which would be associated with any operation, such as sepsis, embolism, haemorrhage, haematoma and bruising. It is expected that the pain from your fingers will be removed and that the cosmetic appearance of your hands improved. Because of the design of the prosthesis there is the chance that an increased range of finger motion could be restored. If something does go wrong, then another type of artificial finger joint can be inserted instead. Liability rests with the manufacturers of the new artificial joint, the address to contact, should it be required for a claim of compensation, is the Department of Clinical Research, DePuy International Limited, St Anthony's Road, Leeds, LS11 8DT.

Statutory Regulations

Approval for this trial has been obtained both from the Ethics Committee of the South Durham Health Authority, in whose district you reside. If you wish, you can withdraw from the trial without prejudice. Finally, all information gained during the course of this trial will be treated in the strictest confidence.

Standard Consent Form

LOCAL RESEARCH ETHICS COMMITTEE

CONSENT FORM FOR AN ADULT TO TAKE PART IN RESEARCH

Name of Research Project: .....

Name of Researcher: .....

Name of Participant: .....

I consent to take part in this research project.

I understand that the research is designed to add to medical knowledge.

I have read the note of explanation about the study. This attached and I have had time to think about it.

I have had the study explained to me by .....

I have been told that I can withdraw my consent at any stage without giving reason, and without prejudice to my treatment.

I have been given a copy of this Consent Form.

Signed ..... Date .....

I can confirm that I have explained to the participant the nature of this study, and have given adequate time to answer any questions concerning it.

Signed: ..... Date .....

Name (in capitals): .....

Post: .....

Appendix 5

Complication and Case Report Form

Durham Metacarpophalangeal Prosthesis Pilot Study

CASE REPORT FORM

1 Patient History

Patient ID _____

Patient's initials _____

Date of Birth _____ Sex M/F

Condition of other joints:

elbow _____

wrists _____

thumb _____

PIP _____

DIP _____

Concomitant medical problems _____

Concomitant medication type/dose/reason _____

MCP joints involved _____

Signed informed patient consent received: Yes/No

Patient inclusion/exclusion criteria reviewed: Acceptable/Unacceptable

---

2 Operative Details

Date of surgery _____

Durham MCP Prostheses fitted Left I, M, R, L Right I, M, R, L

Operative Complications: _____

---

3 Pre-Operative Radiographic Evaluation

Date

Hand	Left				Right			
Finger	I	M	R	L	I	M	R	L
Bone Erosion (yes/no)								
Ulnar Drift (yes/no)								
Volar Subluxation (yes/no)								

Comments: _____

---

4 Pre-Operative Patient Comments

Date

Hand	Left				Right			
Finger	I	M	R	L	I	M	R	L
Pain (yes/no)								
Content with Range of Movement (yes/no)								
Happy with Cosmetic Appearance (yes/no)								

Comments: _____

Signed by Principal Investigator Date

Patient ID _____

9 Nine month Post-operative Radiographic Evaluation **Date**

Hand	Left				Right			
Finger	I	M	R	L	I	M	R	L
Bone Resorption (yes/no)								
Radiolucent Line (yes/no)								
Prosthesis Migration (yes/no)								

Comments: _____

10 Nine month Post-operative Patient Satisfaction **Date**

Hand	Left				Right			
Finger	I	M	R	L	I	M	R	L
Pain (reduced/increased)								
Range of Movement (reduced/increased)								
Cosmetic appearance (improved/no change)								

Comments: _____

Specify any changes in concomitant medication _____

Signed by Principal Investigator Date

---

11 Twelve month Post-operative Radiographic Evaluation **Date**

Hand	Left				Right			
Finger	I	M	R	L	I	M	R	L
Bone Resorption (yes/no)								
Radiolucent Line (yes/no)								
Prosthesis Migration (yes/no)								

Comments: _____

12 Twelve month Post-operative Patient Satisfaction **Date**

Hand	Left				Right			
Finger	I	M	R	L	I	M	R	L
Pain (reduced/increased)								
Range of Movement (reduced/increased)								
Cosmetic appearance (improved/no change)								

Comments: _____

Specify any changes in concomitant medication _____

Signed by Principal Investigator Date

Durham Metacarpophalangeal Prosthesis Pilot Study

COMPLICATION FORM

Patient's initials _____ Date of surgery _____

MCP joints involved _____

---

1 Adverse Event

1.1 Post-operative Complication (circle)

Metacarpal Component Failure
Metacarpal Component Loosened
Phalangeal Component Failure
Phalangeal Component Loosened
Infection
Other (specify)

1.2 Date of Onset _____

1.3 Status of Complication Improving/Deteriorating/No change

1.4 Re-operation Date (if applicable) _____

1.5 Describe Treatment _____

1.6 Was the complication related to the joint replacement procedure? _____

1.7 Was the complication related to the prosthesis? _____

1.8 If no to 1.6 and 1.7, what then was the complication was related to? _____

1.9 Describe any changes in indication, contraindication, method of use, or concurrent treatments that this incident suggests _____

_____

---

2 Lost to Follow Up

Date lost to follow up

Death - cause _____
Amputation cause _____
Arthrodesis _____
Consent withdrawn
Cannot locate patient
Attempts to contact (attach details or copies of correspondence)

Signed by Principal Investigator Date

Appendix 6

References

References

1 Blair, W. F., Shurr, D. G. and Backwalter, J. A. Metacarpophalangeal joint implant arthroplasty with a silastic spacer. Journal of Bone and Joint Surgery, 66-A, 365-370, 1984.

2 Khoo, C. T. K. Silicone synovitis. Journal of Hand Surgery, 18B, 679-686, 1993.

3 Sibly and Unsworth. 'Wear of cross-linked polyethylene against itself: a material suitable for surface replacement of the finger joint'. Journal of Biomedical Engineering, 13, 217-20 1991.

4 Beckenbaugh et al. 'Review and analysis of silicone-rubber metacarpo-phalangeal implants'. Journal of Bone & Joint Surgery, 58-A, 483-487, 1976.

5 Wroblewski, B. M. 22.25mm ceramic head articulating with cross linked polyethylene - a prospective study. Biomechanics of joints and joint replacements, University of Leeds, 1993.

6 Rae, T., Rushton, N. Thomson, L., Lardner, A. and Martin, S. Biocompatability studies of cross linked polyethylene. Journal of Bone and Joint Surgery, 70-B, 5, 852, 1988.

7 Jones, A R, Unsworth A and Haslock I. A microcomputer controlled hand assessment system used for clinical measurement. Engineering in Medicine, 14, 4, 191-198, 1985.

8 Helliwell P S in Mechanics of Human Joints, eds Wright and Radin, Marcel Dekker, Inc. New York, 1993.

9 Unsworth, A, Yung, P and Haslock I. Measurement of stiffness in the metacarpophalangeal joint: the arthrograph. Clinical Physics and Physiological Measurement, 3, 4, 273-281, 1982.

10 Health Assessment Questionnaire

11 B Dellhag, I Wollersjo and A Bjelle. 'Effect of Active Hand Exercise and Wax Bath Treatment in Rheumatoid Arthritis Patients'. Arthritis Care and Research, 1992, 5, 2, 87-92.

12 B Dellhag and CS Burckhardt. 'Predictors of Hand Function in Patients with Rheumatoid Arthritis'. Arthritis Care and Research, 1995, 8, 1, 16-20.

13 K Lorig, RL Chastin, E Ung, S Shoor and H Holman. 'Development and Evaluation of a Scale Measure Perceived Self-Efficacy in People with Arthritis'. J. Arth. Rheum., 1989, 32, 1, 37-44.

14 J Scott and EC Huskisson. 'Accuracy of Subjective Measurements Made With or Without Previous Scores: An Imporant Source of Error in Serial Measurement of Subjective States.' Ann. Rheum. Dis., 1979, 38, 558-559.

15 JF Fries, P Spitz, RG Kraines and HR Holman. 'Measurement of Patient Outcome in Arthritis'. J. Arth. Rheum., 1980, 23, 2, 137-145.

16 RJ McGuire and V Wright. 'Statistical Approach to Indicies of Disease Activity in Rheumatoid Arthritis, with Reference to a Trial on Indomenthacin'. Ann. Rheum. Dis., 1971, 30, 574-580.

17 P Tugwell, C Bombardier, WW Buchanan, CH Goldsmith, E Grace and B Hanna. 'The MACTAR Patient Preference Disability Questionnaire - An Individualised Functional Priority Approach for Assessing Improvement in Physical Disability in Clinical Trials in Rheumatoid Arthritis. J. Rheumatol., 1987, 14, 3, 446-451.

18 V Wright. 'Some Observations on Diurnal Variation of Grip'. Clin. Sci., 1959, 18, 17-23.

19 V Wright and RJ Johns. 'Observations on the Measurement of Joint Stiffness'. 1960, 328-340.

20 DT Thompson, V Wright and D Dowson. 'A New Form of Knee Arthrograph for the Study of Stiffness'. Eng. Med., 1978, 7, 2, 84-92.

21 VM Rhind, A Unsworth and I Haslock. 'Assessment of Stiffness in Rheumatology: The Use of Ratings Scales'. Br. J. Rheumatol., 1987, 26, 126 130.

Appendix 13

Published Papers

The wear of cross-linked polyethylene against itself

T J Joyce, BEng, MSc, **H E Ash,** BSc, MSc and **A Unsworth,** MSc, PhD, DEng, FIMechE
Centre for Biomedical Engineering, School of Engineering, University of Durham

Cross-linked polyethylene (XLPE) may have an application as a material for an all-plastic surface replacement finger joint. It is inexpensive, biocompatible and can be injection-moulded into the complex shapes that are found on the ends of the finger bones. Further, the cross-linking of polyethylene has significantly improved its mechanical properties. Therefore, the opportunity exists for an all-XLPE joint, and so the wear characteristics of XLPE sliding against itself have been investigated. Wear tests were carried out on both reciprocating pin-on-plate machines and a finger function simulator.

The reciprocating pin-on-plate machines had pins loaded at 10 N and 40 N. All pin-on-plate tests show wear factors from the plates very much greater than those of the pins. After 349 km of sliding, a mean wear factor of 0.46 × 10^{-6} mm^3/N m was found for the plates compared with 0.021 × 10^{-6} mm^3/N m for the pins. A fatigue mechanism may be causing this phenomenon of greater plate wear. Tests using the finger function simulator give an average wear rate of 0.22 × 10^{-6} mm^3/N m after 368 km. This sliding distance is equivalent to 12.5 years of use in vivo. *The wear factors found were comparable with those of ultra-high molecular weight polyethylene (UHMWPE) against a metallic counterface and, therefore, as the loads across the finger joint are much less than those across the knee or the hip, it is probable that an all-XLPE finger joint will be viable from a wear point of view.*

Key words: finger prosthesis, cross-linked polyethylene, wear

1 INTRODUCTION

Currently, the most popular finger prosthesis in use in the United Kingdom is the Swanson prosthesis. This prosthesis is a single piece of silicone rubber which acts as both a flexible hinge and a spacer, around which encapsulation occurs. Surgery is straightforward, pain relief is achieved and deformity corrected (**1**). Despite this success, the prosthesis has several disadvantages. Clinical deformity gradually returns after surgery (**1**), there are concerns over synovitis due to the silicone material (**2**), and the prostheses often snap (**1**, **3**). Such breakage is thought to be due to the prosthesis flexing at the stem rather than the hinge, in combination with lacerations on the surface of the prosthesis (**4**). These lacerations, which may be produced by bony spurs, become surface cracks which then propagate through the prosthesis under the cyclic loading of finger flexion–extension. Therefore, an improved design of finger prosthesis has been sought.

By moving from the principles of the flexing hinge encompassed by the Swanson prosthesis, to the concept of a surface replacement joint in which the two separate surfaces slide over one another, several benefits can be achieved. The original joint dynamics can be restored, the ligaments which stabilize the joint can be maintained and, being two pieces, the prosthesis cannot snap. Instead wear between the articulating surfaces becomes of concern.

The metal/polymer combination widely used in knee and hip prostheses has also been applied to finger prostheses, but with varying degrees of success (**5**). As an alternative arrangement, as the loads across the finger joint are relatively low, a two-piece, all-polymer prosthesis has been considered. A polymeric prosthesis has the additional advantage of having material properties closer to those of rheumatoid bones than either metal or ceramic would have. Also, should it be necessary, such a prosthesis could be modified in theatre to suit the individual patient by simply trimming away small amounts of material from the edge (being careful not to damage the articular surface).

Polyethylene, in the form of UHMWPE, is the most widely used polymeric prosthetic material in a sliding joint. Ultra-high molecular weight polyethylene has been tested against itself on pin-on-plate rigs, but a combination of adhesive, abrasive and fatigue wear was found to occur leading to a large amount of polyethylene debris production, together with wear factors of the order of 2 × 10^{-5} mm^3/N m for the pins (**6**, **7**). Indeed, the wear factors were found to increase with the applied load. Polyethylene wear debris is to be avoided in the body as it can become deposited in surrounding tissues (**8**), leading to inflammation and bone resorption (**9**), and causing eventual loosening of the prosthesis, possibly with associated pain for the patient (**10**). Such high wear rates make an all-UHMWPE finger prosthesis unacceptable.

However, the cross-linking of polyethylene has improved the material's mechanical properties. Cross-linking has the additional advantage of permitting a lower molecular weight base material to be used, so that components can be injection-moulded rather than machined. Injection-moulding offers the opportunity of mass-producing complex three-dimensional shapes, such as those found on the end of the finger bones, to repeatable, close tolerances. Cross-linked polyethylene has been used in experimental hip implants for several years and has shown no adverse biological reaction (M. Wroblewski, 1995, personal communication). Therefore, in view of this blend of biocompatibility, low cost, ease of manufacture and appropriate mechanical properties, XLPE has been considered as a potential material for use as a surface replacement prosthesis for the finger joints, and its wear properties have been investigated and are reported here.

Cross-linked polyethylene pins and plates together with a prototype XLPE surface replacement metacarpophalangeal (MCP) prosthesis were tested. A prototype

This paper was presented at the Leeds Annual Day Conference on 'Biomechanics of upper limb joints and their replacements' held in Leeds on 6 January 1995. The MS was received on 6 February 1995 and was accepted for publication on 12 October 1995.

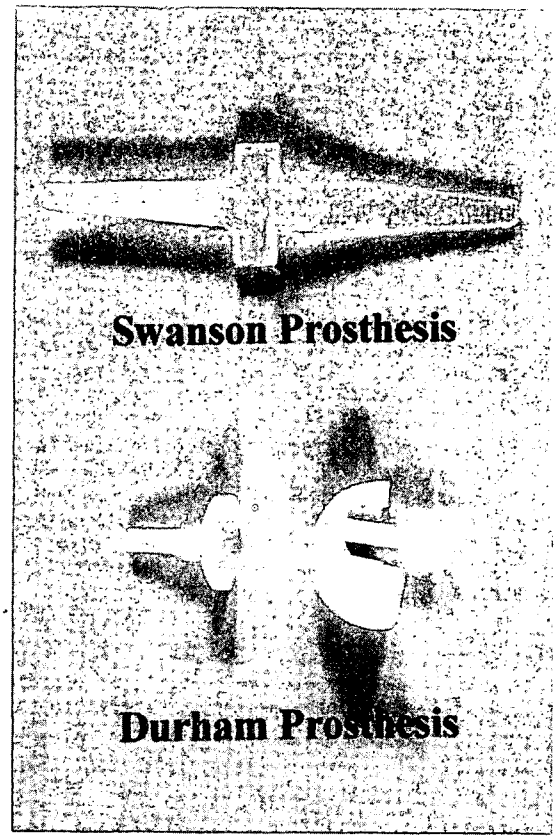

Fig. 1 Swanson prosthesis and Durham prosthesis

Durham prosthesis, with a Swanson for comparison, is shown in Fig. 1. The XLPE test samples were manufactured from powdered polyethylene which was mixed with liquid silane. This mixture was then extrusion injection-moulded. The cross-linking process between the polyethylene molecules occurred by placing the samples in a steam autoclave. Finally, the samples were sterilized by irradiation. The degree of cross-linking was measured from a number of sacrificial samples by boiling away in xylene the non-cross-linked material. Therefore, the weight of the material remaining after this process, divided by the original weight, gave the percentage of cross-linking. The percentage of cross-linking measured in all sacrificial samples was identical in each case to within measurement error of 2 per cent.

2 APPARATUS AND METHOD

2.1 Finger function simulator

The finger function simulator has been described elsewhere and shown to be a device which effectively simulates the loads and motions encountered by a finger prosthesis *in vivo* (**11**). The simulator flexed a test XLPE prosthesis cyclically over a 90° range of motion to represent the light loading found during normal flexion–extension. It then applied a heavy static load to imitate pinch grip. Motion was uni-planar as flexion–extension is the predominant action of the finger. The light loading simulated those situations where loads were small (10–15 N) (**12**) but the finger was moving quickly. In contrast, situations such as turning a key or holding a handle show minimal motion but large joint forces. These situations are therefore mimicked by the pinch grip action of the simulator, which occurred once every 30 min. During this part of the cycle, the compressive force across the test prosthesis was increased to 100 N, and held at this level for 45 s. During light loading, the simulator ran at 112 r/min, equivalent to a sliding speed of 0.055 m/s, at an excursion of 14.7 mm. The test prosthesis was immersed in a bath containing distilled water at a temperature of 37 °C. A control XLPE prosthesis was also included to take account of any lubricant absorption. At regular intervals, the simulator was stopped and the XLPE prosthetic components, both test and control, were cleaned and weighed. Two tests were undertaken. The first test used prostheses which had a low percentage of cross-linking, the metacarpal component being 36 per cent cross-linked and the phalangeal component 66 per cent cross-linked. The second test used prostheses made with a high percentage of cross-linking, 87 per cent. The new XLPE finger prosthesis is designed to have conforming spherical surfaces, and all test prostheses had articulating surfaces of radius 9.5 mm, giving a nominal stress value of 0.08 MPa during flexion–extension.

2.2 Pin-on-plate test rig

Pin-on-plate machines are widely used as screening devices in wear studies (**13**, **14**). The pin-on-plate machine employed a reciprocating motion which mimicked the natural flexion–extension of the finger. Load, speed and stroke could all be varied as appropriate. The rig consisted of a sledge reciprocating along two fixed parallel bars. On this sledge was positioned a heated bed and a stainless steel bath. The sledge was driven by a 125 W d.c. shunt motor. Motor speed was controlled using a variable voltage supply and the stroke could be altered by adjusting the crank radius of the drive shaft. Heating of the distilled water, which acted as a lubricant, was provided by resistors positioned within the heated bed. These resistors, together with a thermocouple, were connected to a controller which maintained the lubricant at a constant, pre-set temperature of 37 °C. Four XLPE test plates were located in the stainless steel bath using a plastic frame into which suitable location slots had been milled. Each XLPE test pin was held within a holder and in turn each holder fitted within a machined arm. Each pin was notched at its upper end to provide good location and hence to prevent rotation. It also ensured that the pin was replaced in its original position after removal for weighing. On the top of each holder rested a cantilevered bar to which weights were added to provide an applied load. An automatic lubricant level controller was fitted, such that the fluid was maintained between pre-set maximum and minimum levels which prevented the rig from operating without any lubricant. Finally, an electronic counter was connected to the sledge and a glass cover fitted to minimize any contamination from the atmosphere.

Prior to the commencement of a test, the XLPE test plates and XLPE pins were carefully weighed, and the roughness of the plates measured using a Taylor Hobson Talysurf 4. In each test, an XLPE control pin was included to take account of any lubricant absorption. This pin was unloaded and kept with its unnotched end in the same distilled water as the test pins at 37 °C. At regular intervals, the test was stopped, all of

the pins and plates were removed, cleaned with acetone, weighed, visually inspected and the roughness of the wear track on each of the test plates was measured. Pins and plates were weighed to the nearest 0.1 mg using a Mettler AE200 balance. Wear of the test pin was defined as the weight loss with respect to the initial weight, to which was added any weight gain of the control pin. Therefore, the weight gain of the control and test pins was assumed to be equal. The wear factors (k, units mm^3/N m) were calculated from the equation

$$k = \frac{V}{LD}$$

where

V = volume lost (mm^3)
L = load (N)
D = sliding distance (m)

but volume = mass/density, therefore

$$k = m/\rho LD \qquad \rho \text{ (XLPE)} = 949 \text{ kg/m}^3$$

Three pin-on-plate tests, each exceeding 300 km, were undertaken. All used XLPE with 86 per cent cross-linking after irradiation as material for pins and plates. Loads of 10 N and 40 N were employed. The 10 N load provided a 'normal' load for the MCP joint during motion, while the 40 N supplied a greater load to give a factor of safety and to provide the opportunity of discovering whether wear factors changed with load. The pins were turned to form flat-ended, circular cylinders, 20 mm long and of diameter 4 and 5 mm. The pin-on-plate machine employed a stroke of 20 mm and velocities of 0.037 m/s and 0.035 m/s. Test 3 employed a longer stroke to give a greater velocity (see Table 1).

3 RESULTS

3.1 Finger function simulator

Two tests were conducted, using prostheses with different percentages of cross-linking, and the results are shown in Fig. 2. As can be seen, the degree of cross-linking has a significant effect on the wear of XLPE. After 190 km, the prostheses with a low percentage of cross-linking had wear factors of 6.0×10^{-6} mm^3/N m for the metacarpal and 2.2×10^{-6} mm^3/N m for the phalangeal component. In contrast, after 368 km the prostheses with a high (87) percentage of cross-linking had wear factors of 0.25×10^{-6} mm^3/N m for the metacarpal and 0.16×10^{-6} mm^3/N m for the phalangeal component.

3.2 Pin-on-plate machine

Each of the XLPE tests summarized in Table 1 revealed similar characteristics, therefore test 1 has been reported

Table 1 Summary of XLPE pin-on-plate wear factors

Test number	1		2		3
Load (N)	10	40	10	40	40
Stress (MPa)	0.51	2.04	0.80	3.18	2.04
Pin diameter (mm)	5	5	4	4	5
Number of pins	2	2	2	2	2
Distance (km)	349	349	359	359	332
Cycles ($\times 10^6$)	8.73	8.73	8.98	8.98	4.88
Average velocity (mm/s)	35.3	35.3	37.3	37.3	47.6
Mean k plate ($\times 10^{-6}$ mm^3/N m)	0.50	0.42	0.68	0.48	0.58
Mean k pin ($\times 10^{-6}$ mm^3/N m)	0.030	0.012	0.014	0.014	0.065

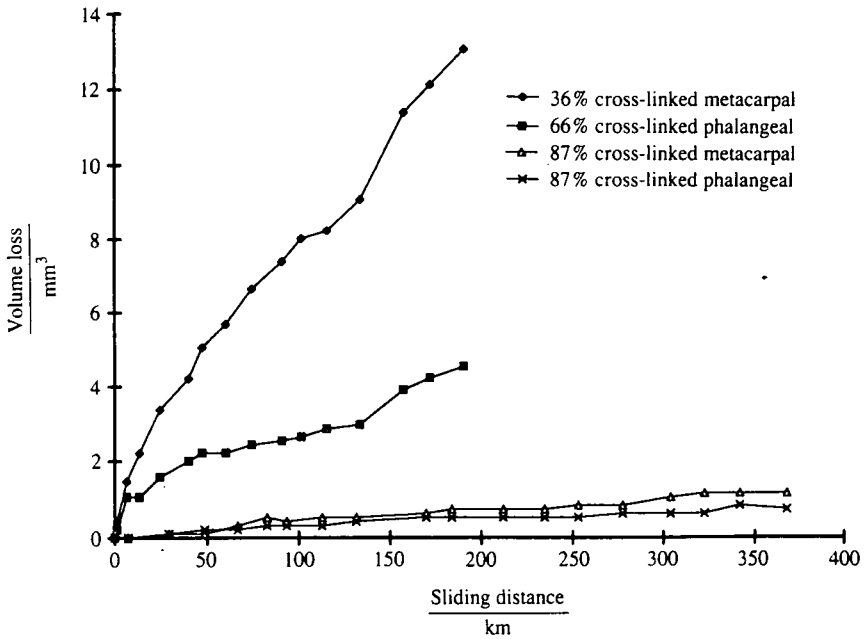

Fig. 2 Wear of metacarpal and phalangeal components in the finger function simulator

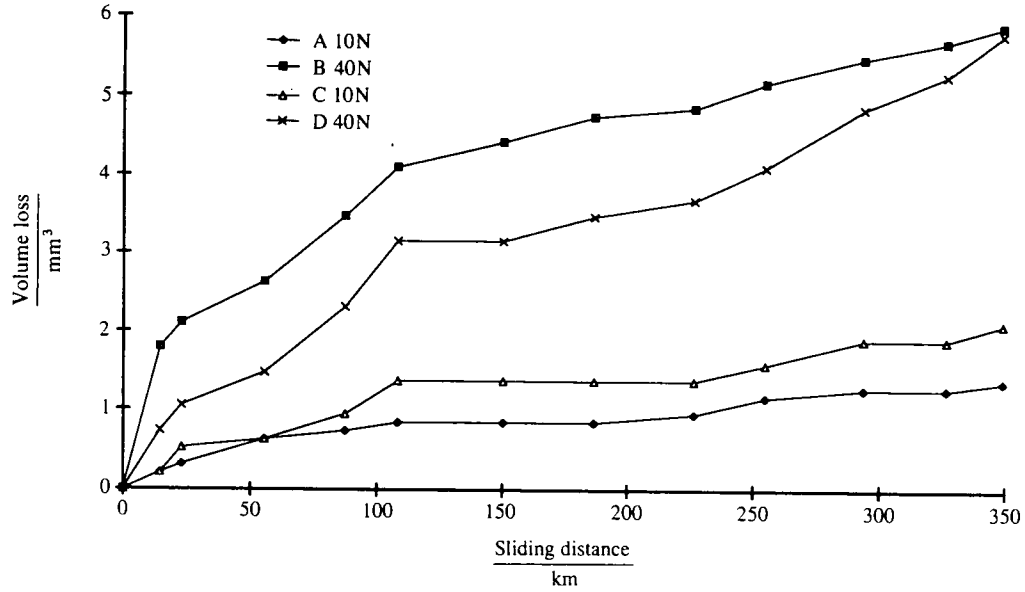

Fig. 3 Wear of XLPE plates loaded at 10 N and 40 N in the reciprocating pin-on-plate machine

in detail as this was illustrative of all three tests. Figure 3 shows XLPE plate wear at 10 N and 40 N from test 1. From this figure it can be seen that XLPE plate wear is related to load, as expected. There is an initial bedding-in period, after which the slope of the wear curve becomes relatively constant with increased sliding distance. Figure 4 shows a graph of the wear of corresponding XLPE pins and plates under 40 N loads. The XLPE test pins show virtually no wear. For reference, the XLPE control pin of test 1 showed no fluid absorption after 349 km. The roughness values of the wear tracks on the XLPE plates were measured throughout the test, and are shown in Fig. 5. The longitudinal values, in the direction of sliding, fell rapidly from a mean of 1.5 μm *Ra* to 0.05 μm *Ra* in the 40 N case. Transverse roughness values also fell from a similar start value to around 0.6 μm *Ra*.

4 DISCUSSION

Figure 2 clearly indicates the decrease in wear found with an increase in the percentage of cross-linking. That the metacarpal components showed higher wear factors than those of their respective phalangeal components can be explained by their geometrical differences, as it is known that convex surfaces tend to wear more than concave surfaces. Additionally, the XLPE prostheses have a wear curve which has a constant gradient, indicating that a period of fatigue wear seems not to have occurred. This conclusion is supported by visual inspection which revealed neither pitting nor delamination.

If a normal MCP joint is considered to perform one million cycles per year, then the 368 km (or 12.5 million cycles) achieved from the second test in the finger function simulator is equivalent to 12.5 years. At this point, the XLPE prostheses with a high percentage of cross-linking showed no cuts, no fractures and low wear. Further, the wear factors were calculated to be 0.25×10^{-6} mm^3/N m for the metacarpal and 0.16×10^{-6} mm^3/N m for the phalangeal component. These values correspond to wear volumes of 1.16 mm^3 and 0.74 mm^3 respectively. In turn, this total wear volume of 1.9 mm^3 can be interpreted as a wear rate of 0.15 mm^3 per million cycles, or per annum. Dowson (**14**) states that, for an artificial hip joint, a wear rate of 38 mm^3 per annum is considered acceptable. However, a hip joint of radius 20 mm will have a capsule volume 23 times greater than that of a finger joint of radius

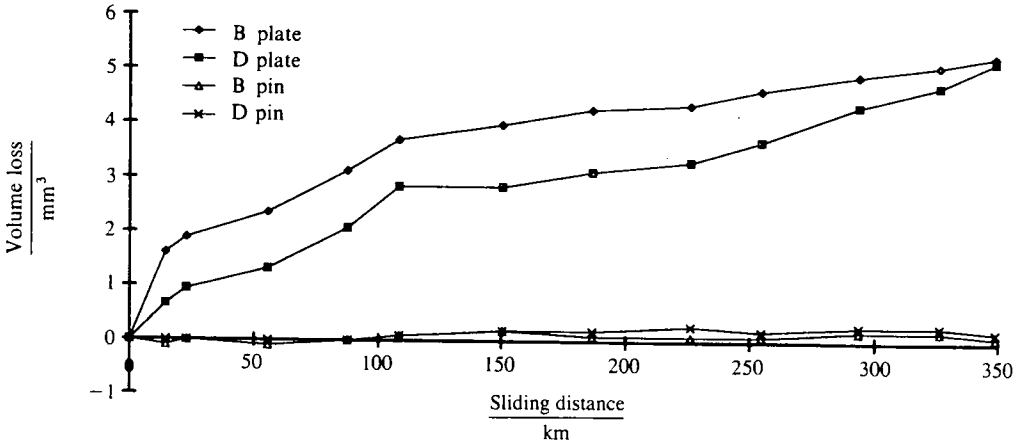

Fig. 4 Wear of XLPE pins and corresponding XLPE plates loaded at 40 N in the reciprocating pin-on-plate machine

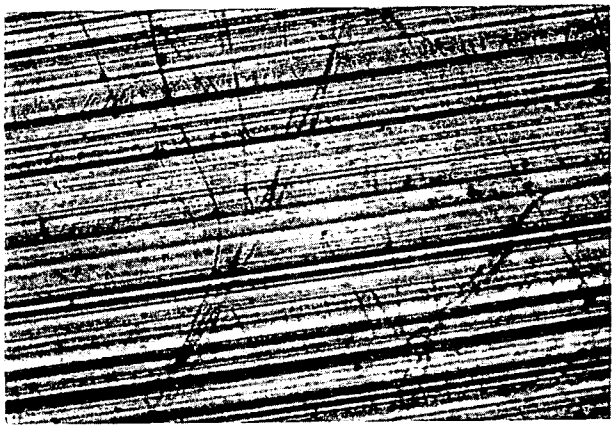

(a)

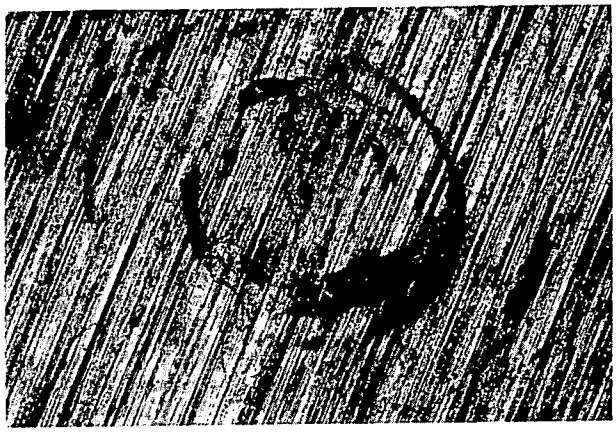

(b)

Fig. 5 (a) Plate after 350 km at 40 N
(b) Pin after 350 km at 40 N

7 mm. Therefore, for a finger joint, a wear rate of 1.65 mm^3 per annum should be acceptable. Consequently, the 0.15 mm^3 wear rate per million cycles reported here suggests that an all-XLPE finger prosthesis will be acceptable from a wear point of view.

Regarding the XLPE pin-on-plate tests, it should be asked why so little pin wear occurred compared with plate wear. The XLPE material used in each test was identical, originating from the same moulding. The pins were constantly loaded whereas the individual parts of the wear track on the plates undergo a cyclic load. Therefore, it is possible that there may be a fatigue element—but not in a gross sense of delamination or pitting (as is sometimes seen in the tibial components of knee prostheses for example) which is associated with a sudden increase in the amount of wear. It should also be noted that this is the first time that plate wear from an all-XLPE pin-on-plate test has been measured (**15**). Additionally, the plate wear of UHMWPE in a UHMWPE against UHMWPE pin-on-plate test has not been measured in previous studies (**6**, **7**). Atkinson (**7**) assumed that during such a UHMWPE test, plate wear equalled pin wear. The results reported here show this assumption to be incorrect for XLPE pins and plates. Indeed, a mean wear factor of 12×10^{-9} $mm^3/N\ m$ for the XLPE pins under 40 N load was found from test 1. This value approaches that of UHMWPE pins against ceramic plates (**13**). Although significant differences in wear factors between XLPE pins and XLPE plates were measured, the XLPE plate wear factors were still of the order of those of the high percentage cross-linked prostheses. Further, pin-on-plate results allow comparison with other material combinations (**13**, **14**, **16**).

With both XLPE pins and XLPE plates, the dominant feature of the wearing surfaces was parallel grooves in the direction of sliding (Fig. 5) giving the appearance of abrasive wear. Once this surface finish was achieved, there was very little change (Fig. 6). The constant values of roughness which were measured imply no evidence of a transfer film. It has been suggested that serum would be a more appropriate medium in which to run pin-on-plate tests involving potential biomaterials (**17**). The reason being that, unlike distilled water, serum prevents the formation of a transfer film between UHMWPE and stainless steel and a transfer film is not found *in vivo*. Cooper *et al.* (**17**) indicated the presence of a transfer film by increased plate roughness at the cessation of a test. However, the XLPE pin-on-plate results reported here show no increase in the surface roughness of the plates and therefore indicate no evidence of a transfer film. Further, tests employing distilled water permit a fuller comparison with other

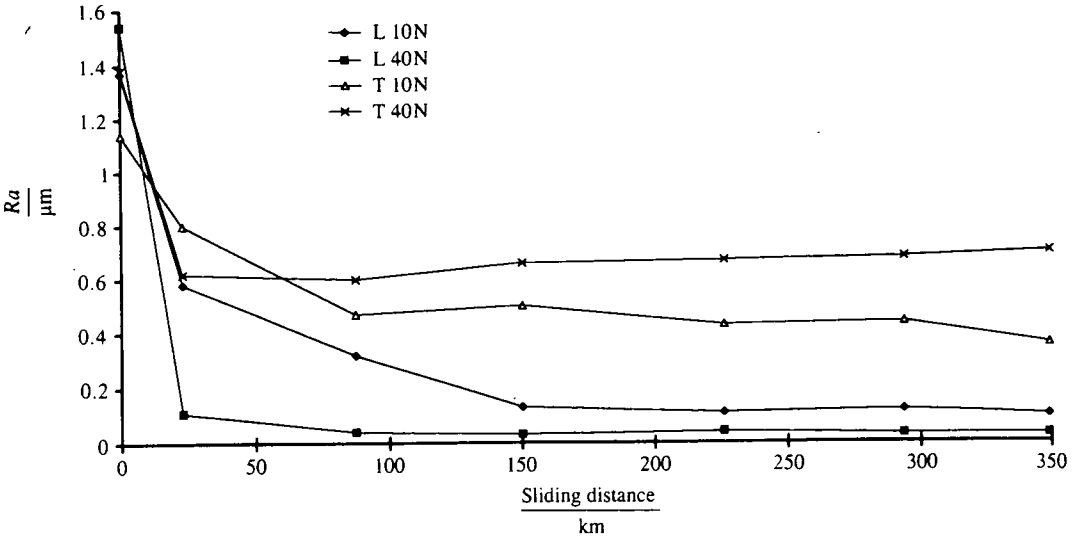

Fig. 6 Mean roughness of XLPE plates loaded at 10 N and 40 N in the transverse (*T*) and longitudinal (*L*) directions

researchers (**13**, **14**, **16**). Visual inspection of XLPE pins and plates revealed little evidence of adhesive or fatigue wear. In the case of the XLPE pin shown in Fig. 5, the original concentric machining marks are still visible, indicating that the pins have experienced little wear, even after 349 km. There appears to be little correlation between roughness and wear, except perhaps in the initial stages.

If a comparison of wear factors is made between XLPE against itself, and UHMWPE against a metallic counterface, then a similarity is seen. Cooper *et al.* (**16**), also employing reciprocating rigs, de-ionized water and a test distance of 350 km (as was the case in this study), obtained wear factors from 0.18 to 1.3×10^{-6} mm^3/N m for UHMWPE pins rubbing against a metallic counterface. However, Saikko (**13**) obtained a wear factor of 0.1×10^{-6} mm^3/N m for UHMWPE pins rubbing against Co–Cr–Mo plates. These values compare with 0.42 to 0.68×10^{-6} mm^3/N m for XLPE plates from the reciprocating tests found in this study. Further, if coefficients of friction are considered, similarity is again seen. Tests using reciprocating pin-on-plate rigs gave a coefficient of friction of 0.14 for XLPE against itself (**15**). This value compares with a figure of 0.10 for UHMWPE against Co–Cr–Mo (**13**).

5 CONCLUSIONS

Wear factors of XLPE rubbing against itself have been found to be comparable with those of UHMWPE rubbing against a metallic counterface. Additionally, the coefficient of friction of XLPE against itself has been measured to be similar to that of UHMWPE against Co–Cr–Mo. Therefore, as the loads across the finger joints are so much smaller than those across the knee or the hip, and the total wear volume is directly proportional to load, it is felt that an all-XLPE finger prosthesis will be viable from a wear point of view.

ACKNOWLEDGEMENTS

The authors would like to thank Action Research (grant reference A/F/0475) for providing financial support. De Puy International Limited supplied the XLPE material and moulded the XLPE prostheses.

REFERENCES

1 **Blair, W. F., Shurr, D. G.** and **Backwalter, J. A.** Metacarpophalangeal joint implant arthroplasty with a silastic spacer. *J. Bone Jt Surg.*, 1984, **66A**, 365–370.
2 **Khoo, C. T. K.** Silicone synovitis. *J. Hand Surg.*, 1993, **18B**, 679–686.
3 **Beckenbaugh, R. D., Dobyns, J. H., Linscheid, R. L.** and **Bryan, R. S.** Review and analysis of silicone rubber metacarpophalangeal implants. *J. Bone Jt Surg.*, 1976, **58A**, 483–487.
4 **Swanson, A. B.** and **de Groot Swanson, G.** Flexible implant arthroplasty in the rheumatoid metacarpophalangeal joint. *Clin. Rheum. Dis.*, 1984, **10**(3), 609–629.
5 **Beevers, D. J.** and **Seedhom, B. B.** Metacarpophalangeal joint prostheses. a review of past and current designs. *Proc. Instn Mech. Engrs, Part H*, 1993, **207**(H4), 195–206.
6 **Stokoe, S. M.** A finger function simulator and surface replacement prosthesis for the metacarpophalangeal joint. PhD thesis, University of Durham, 1990.
7 **Atkinson, J. R.** An investigation into the wear of ultra-high molecular weight polyethylene when a polyethylene wear pin is loaded against a reciprocating polyethylene counterface lubricated by bovine synovial fluid at ambient temperature. Report, Department of Metallurgy, Leeds University, 1976, pp. 1–12.
8 **Malcolm, A. J.** Pathology of longstanding cemented total hip replacements in Charnley's cases. *J. Bone Jt Surg.*, 1988, **70B**, 153.
9 **Howie, D. W., Vernon-Roberts, B., Oakeshott, R.** and **Manthey, B.** A rat model of resorption of bone at the cement–bone interface in the presence of polyethylene wear particles. *J. Bone Jt Surg.*, 1988, **70A**, 257–263.
10 **Mirra, J. M., Marder, R. A.** and **Amstutz, H. C.** The pathology of failed total joint arthroplasty. *Clin. Orthop. Rel. Res.*, 1982, **170**, 175–183.
11 **Stokoe, S. M., Unsworth, A., Viva, C.** and **Haslock, I.** A finger function simulator and the laboratory testing of joint replacements. *Proc. Instn Mech. Engrs, Part H*, 1990, **204**(H4), 233–240.
12 **Tamai, K., Ryu, J., An, K. N., Linscheid, R. L., Cooney, W. P.** and **Chao, Y. S.** Three-dimensional geometric analysis of the metacarpophalangeal joint. *J. Hand Surg.*, 1988, **13A**, 521–529.
13 **Saikko, V.** Wear and friction properties of joint materials evaluated on a reciprocating pin-on-plate apparatus. *Wear*, 1993, **166**, 169–178.
14 **Dowson, D.** A comparative study of the performance of metallic and ceramic femoral head components in total replacement hip joints. Proceedings of *Austrib '94*, pp. 59–73.
15 **Sibly, T. F.** and **Unsworth, A.** Wear of cross-linked polyethylene against itself: a material suitable for surface replacement of the finger joint. *J. Biomed. Engng*, 1991, **13**, 217–220.
16 **Cooper, J. R., Dowson, D.** and **Fisher, J.** Macroscopic and microscopic wear mechanisms in ultra-high molecular weight polyethylene. *Wear*, 1993, **162–164**, 378–384.
17 **Cooper, J. R., Dowson, D,** and **Fisher, J.** The effect of transfer film and surface roughness on the wear of lubricated ultra-high molecular weight polyethylene. *Clin. Mater.*, 1993, **14**, 295–302.

Typically over 30% of the equilibrium deformation ular cartilage takes place within 20 milliseconds of d being applied. Cartilage deformation does not increase over a matter of minutes compared with olved response.

BILITY OF ARTICULAR CARTILAGE TO LISE STRESS DUCED BY SUSTAINED LOADING.

dams, L.S. Bhatia, P. Dolan.
nent of Anatomy, University of Bristol.

tion: Little is known about the ability of cartilage ise contact stresses between adjacent bones. Varia- tissue composition, or irregularities in the sub- l bone, may lead to localised stress concentrations rtilage, especially after its water content has been by sustained loading. We investigated this possi- sing a miniature pressure transducer to measure the distribution of compressive stress within articu- age.

: Tibial plateaux were obtained from patients ng knee replacement for osteoarthritis. In most rtilage from the lateral compartment appeared nd of full thickness. Plugs of tissue, 11mm × were removed from this region, with 1-2mm of dral bone being retained. Each plug was set in one and a compressive force applied to its surface s of a 10mm plane-ended metal indentor attached erials testing machine. The distribution of com- stress within the cartilage matrix was measured by gauged pressure transducer mounted in the side of diameter needle. The transducer was pulled rough the cartilage while its output and position pled at 17Hz. Stress profiles were obtained with ducer orientated vertically and horizontally, and ous loads applied to the specimen. Tests were after the cartilage had been creep loaded at or one hour, and again after the cartilage had been by compressive overload. Ten plugs have been date.

Validation tests suggested that measurement arti- e not great provided cartilage thickness exceeded Transducer output within cartilage increased lin- applied load, from a mean intrinsic pressure of (vertical) and 0.07MPa (horizontal). Stress pro- ted at higher load showed similar features "scaled en stress was averaged across the profile and by the plug's surface area, the calculated com- orce was usually within 15% of the actual applied rtical and horizontal profiles often differed mark- p loading increased the number of stress peaks in ens. The average number of peaks increased to 2.75 after creep (vertical orientation, 2MPa ess). Stress peaks were reduced or lost following amage.

n: The validation tests suggest that the transduc- ilage, measures the average compressive stress its membrane to an accuracy of 15%. The of these measurements with position and ori- demonstrates that cartilage does not behave cally". Evidently, chondrocytes are *deformed* as mpressed when cartilage is loaded. The stress follow creep loading should make cartilage owever, in another experiment we have shown makes cartilage stronger. This paradox can be s follows: before creep, tensile forces cause) failure in the surface zone of cartilage, whereas , failure occurs by compression or shear in the , or in the subchondral bone.

F FORCE DURING LIMB ENING

T Gardner, M Evans, J Kenwright, AHRW

ffield Orthopaedic Centre, Headington, Oxford

n: Limb lengthening operations are now done hore frequently. Early reports of limb lengthen- he early part of the century indicate that soft ses were perfomed prior to limb lengthening as to overcome the resistance of the soft tissues. Since the Ilizarov technique became well known soft tissue releases have been done less frequently. Soft tissue complications however are still very common and pose a difficult problem while lengthening any limb.

Aims and objectives: The hypothesis was that soft tissues provide the maximum resistance to the distraction. It was decided to find out the focus of force which develops during limb lengthening. The effect of the force developed on the range of joint movements and also the effect of physiotherapy on these forces was studied.

Material and methods: A force measuring system was developed to monitor the soft tissue forces during limb lengthening. This system comprised of four transducers which could be fitted on the four columns on the ilizarov fixator. These transducers were then connected to a 486 DX computer via a six channel amplifier. The computer was given the exact location of the transducers on the frame and it then calculated the resultant focus of force before and after each distraction. During the consolidation phase the patients had a CT scan to assess the regenerate. This CT scan also provided the bone position with respect to the frame. This bone position was then plotted on the computer which gave the focus of force for that particular patient. A simple hand held device was also given to the patient which the patients used at home to take readings before and after five minutes of each distraction.

Five patients and six bony segments were studied. Three tibiae and three femora underwent lengthening using circular frames. One patient had fibrous dysplasia, one suffered from Ollier's disease. The other three had congenital causes of limb length discrepancy. Three patients also had angular deformity correction.

Results: The focus of force during limb lengthening is located in the soft tissues. During femoral lengthening, the focus is located in the vastus lateralis and during tibial lengthening the focus is located in the lateral head of gastrocsoleus. Forces rose during the first three weeks and then tended to plateau off. In all five patients the forces rose to a very high level just before they developed a joint contracture. Forces fell after stopping the distraction. Physiotherapy had a beneficial effect; it reduced the forces. Large amount of forces also were associated with pain which localised to the focus of force.

Conclusion: The focus of the resultant force during limb lengthening lies within the soft tissues and can indicate when angular deformity is likely to occur.

DESIGN OF A SURFACE REPLACEMENT METACARPOPHALANGEAL PROSTHESIS.

T J Joyce and A Unsworth
Centre for Biomedical Engineering, School of Engineering,
University of Durham, Durham, DH1 3LE.

Despite a multitude of designs, the most commonly implanted metacarpophalangeal (MCP) prosthesis remains the Swanson, a single flexible piece of silicone rubber which acts only as a spacer and does little to restore the original dynamics of the joint. Surgical results can be disappointing due to prosthesis breakage, a lack of increase in grip strength and the recurrence of deformity.

To overcome these problems, a two piece surface replacement MCP prosthesis has been designed, based on the dimensions of the natural joint. This new prosthesis is unconstrained and will rely on the natural ligaments of the joint for stability, so that the original dynamics of the joint can be restored. The prosthesis employs cementless fixation, and is designed to replace only the diseased articular cartilage found in rheumatoid cases. This means that bone removal is minimised so that future surgery remains an option. The metacarpal component has an offset stem to match the natural section of the metacarpal bones, together with a flat on the inner palmar aspect of the bearing surface to resist coronal plane rotation. Both the metacarpal and phalangeal components are designed to have conforming spherical surfaces and a fixed centre of rotation. In this way contact stresses are minimised and prosthesis life maximised. A range of five sizes of prosthesis have been designed which will cover all sizes of the MCP joint.

Cross linked polyethylene (XLPE) has been chosen as the biomaterial as it permits the complex shape of the prosthesis to be manufactured by the inexpensive and rapid process of injection moulding. Additionally, tests on XLPE reveal low friction together with low wear under the loads experienced by the MCP joint. New prostheses, manufactured from XLPE, have been tested on a finger simulator and sample XLPE material has been wear tested using pin on plate machines. The finger simulator has previously reproduced failures of Swanson prostheses in a manner and time comparable with surgical experience. Using this simulator, wear factors for the metacarpal and phalangeal components of the new XLPE prosthesis have been found to be $0.26 \times 10^{-6} mm^3/Nm$ and $0.15 \times 10^{-6} mm^3/Nm$ respectively. These were measured over 600km, equivalent to more than 20 years in vivo. Pin on plate tests of XLPE rubbing against itself, in excess of 1500km, gave consistent results as well as wear factors comparable to those obtained from the simulator.

This work has been supported by Action Research.

WEAR AND IMPINGEMENT FOUND IN UHMWPE ACETABULAR SOCKETS RETRIEVED AT REVISION SURGERY

R M Hall, P Siney*, A Unsworth and B M Wroblewski*
Centre for Biomedical Engineering, University of Durham, Durham, DH1 3LE.
*Centre for Hip Surgery, Wrightington Hospital, Appley Bridge, Wigan, WN6 9EP.

One hundred and twenty six Charnley hip prostheses were retrieved at the time of revision surgery of which 89% were found to be loose. For each, an inspection was undertaken especially with reference to any evidence for impingement in the form of damage to the socket rim. The penetration depth and direction for each of the acetabular components was determined using a shadowgraph technique. The wear volume was calculated using the modified version of the formula presented by Kabo *et al* (1,2). The number of cycles undergone by each of the joints *in vivo* was estimated using the implant period and the patient age at the time of primary surgery (3). A mean clinical wear factor, $k_{clinical}$, was calculated and was found to have a value of 1.3 (±0.2) 10-6 mm3/N m. One possible reason for the differences in the wear factor for each of the sockets may be due to the variations in the topography of the femoral head. The surface roughness, *Ra*, was measured for 35 of the femoral heads. A significant association was found to exist between the clinical wear factor and the surface roughness such that:

$$k_{clinical} = 9.7 \times 10^{-6} (R_a)^{0.5}$$

The wear volumes at the time of revision showed a wide variation and would indicate that other factors may contribute to the loosening process. In this type of prostheses, impingement of the stem against the rim of the socket has often been considered to be a contributory factor in the loosening process. The percentage of sockets with rim wear increased as the penetration depth increased. It should, however, be noted that rim damage occurred in explanted sockets for which there was minimal wear. Sockets which articulated against heads with the reduced neck diameter showed marginally reduced occurrence of rim damage at lower penetration depths where numbers were sufficient to allow comparison. However, difficulties arise in formulating conclusions about the effects of impingement between normal and reduced neck stems in that there is no information on the frequency of impingement only on its occurrence. Rim damage only indicates the impingement at each extent of the patients activity.

References
1. J M Kabo *et al*; *JBJS* 75-B (1993) 254.
2. R M Hall *et al; submitted to the Proc. Instn. Mech. Engrs.*.
3. J R Atkinson *et al*; *Wear* 104 (1985) 225.

The work undertaken has been funded by the Arthritis and Rheumatism Council.

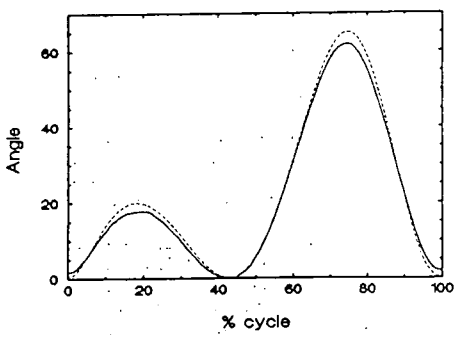

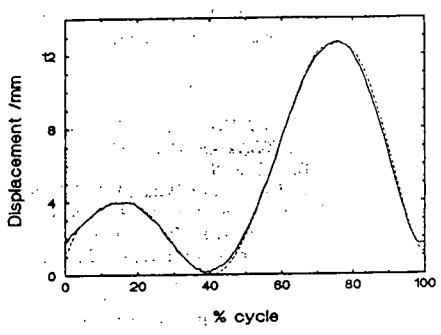

Preliminary wear test: the femoral component of a Kinemax Total Knee (Howmedica) was mounted with the centre of rotation of the posterior condyles incident with the centre of rotation of the simulator. The test was conducted in 30% bovine serum with 0.2% sodium azide added to slow down micro biological degradation and reduce frothing. A control UHMWPE tibial sample was kept under similar conditions. The lubricant was changed every 48 hours, at which time the bearing surfaces were examined, and the UHMWPE tibial components were weighed. Over 5 million cycles, a tibial wear rate of 2.5×10^6 cycles was measured. The appearance of the surface and the wear rates were in general agreement with other in vitro studies.

WEAR OF CROSS-LINKED POLYETHYLENE AGAINST ITSELF: A MATERIAL SUITABLE FOR A SURFACE REPLACEMENT FINGER JOINT

TJ Joyce, HE Ash, A Unsworth Centre for biomedical engineering, Durham University, Durham

Cross linked polyethylene (XLPE) may have an application as a material for replacement finger joints. It is inexpensive, biocompatible and can be injection moulded into the complex shapes that are found on the ends of the finger bones. However, the use of any plastic against itself in a bearing situation is not good engineering practice as it tends to leadto high wear rates. Despite this, the cross linking of polyethylene has significantly improved both its mechanical properties and its wear characteristics. Therefore, wear tests of XLPE against itself have been carried out on both pin on plate machines and a finger functin simulator and the results are summarised here:

The pin on plate machines employ a reciprocating motion which simulates the natural flexion- extension of the finger. These machines had pins loaded at 10N and 40N and employed distilled water as a lubricant. Control pins were included to take account of any lubricant adsorption, although adsorption was found to be negligible. All tests showed wear factors from plates very much greater than those of the pins, and it should also be noted that plate wear has been ignored in previous studies. After 350km, the wear factors were found to be $0.46 \times 10^{-6} mm^3 N^{-1} m^{-1}$ for the plates and $0.036 \times 10^{-6} mm^3 N^{-1} m^{-1}$ for the pins, the latter figure compares with 0.1×10^{-6} mm^3/Nm for UHMWPE pins against Co.Cr plates. A fatigue mechanism may be causing this phenomenon of greater plate wear - but not in the conventional sense of fatigue, where pitting or delamination is seen, together with a corresponding sudden increase in the amount of wear. Visual inspection implied that abrasive wear was the dominant factor, with no sign of significant adhesive or fatigue wear. Visual inspection together with roughness measurements suggested no evidence of a transfer film.

The finger function simulator flexes a test prosthesis cyclically over a 90° range of motion to represent light loading (10-15N) during flexion-extension, then applies a heavy static load (100N) to imitate pinch grip. During light loading, the simulator ran at 112 rpm, equivalent to a sliding speed of 0.055m/s, and again employed distilled water at a temperative of 37°C as a lubricant. Gel content; or the degree of cross linking, was found to be crucial, low gel content prostheses having wear factors an order of magnitude greater than approved gel content prostheses. The shape of the wear graph of the normal gel content prostheses was again seen to be flat, indicating that fatigue wear has not occured, even after 368km, or 12.5 million cycles. At this point, the wear factors were calculated to be $0.25 \times 10^{-6} mm^3 N^{-1} m^{-1}$ for the metacarpal and $0.16 \times 10^{-6} mm^3 N^{-1} m^{-1}$ for the phalangeal component. In turn, these wear factors can be interpreted as a wear rate of 0.09mg and 0.06mg per million cycles, while Saikko obtained a wear rate for UHMWPE v Co.Cr. of 1.05mg per million cycles. The prostheses showed no cuts, no fractures and low wear.

Conclusion: wear factors and friction coefficients of XLPE against itself have been found to be comparable with those of metal against UHMWPE. Therefore, as the loads in the finger are much lower than in the knee or hip, an all XLPE finger prosthesis will be viable from a wear point of view.

BIOMATERIAL WEAR-INDUCED FOREIGN BODY MACROPHAGES ARE CAPABLE OF BONE RESORPTION *IN VITRO*

Pandey R, Quinn J, Sabokbar A, Athanasou NA NDOS, Nuffield Orthopaedic Centre, Headington, Oxford, OX3 7LD

Introduction: Aseptic loosening of biomaterial implant components is the commonest cause of failure of both cemented and uncemented joint replacements[1]. All implant biomaterials produce wear particles which evoke a pronounced mononuclear phagocyte (MP) foreign body response in the fibrous membrane surrounding prosthetic implant components[2,3]. The clinical severity and rapidity of onset of aseptic loosening can be correlated with both the amount of wear particles and the number of MPs present in the membrane; in turn this is reflected in the degree of pathological bone resorption occurring around the prosthesis in aseptic loosening[1,4]. Using an *in vitro* model we investigated the effect of various orthopaedic wear particles on the differentiation of monocytes into bone resorbing cells.

Experimental Procedure: Murine monocytes were co-cultured with UMR106 osteoblastic cells and 1,25 dihydroxyvitamin D_3 $\{1,25(OH)_2D_3\}$ on bone slices and coverslips in the presence and absence particles of biomaterials commonly used in joint arthroplasties (PMMA, PE, Co-Cr and Ti; all at <80μm). After 14 days in culture, the bone slices were examined using scanning electron microscopy whilst the characteristic of the adherent cells on the coverslips were determined by various histochemical techniques.

Results and Discussion: Foreign body MPs avidly phagocytosed the various wear particles and differentiated into tartrate resistant acid phosphatase positive cells capable of forming extensive resorption lacunae. The presence of UMR106 and $1,25(OH)_2D_3$ was necessary for the development of both these cytochemical and functional features of osteoclast differentiation. Addition of all the above biomaterials to the MP/stromal co-cultures was associated with bone resorption. However, the greatest amount of resorption was observed in co-cultures with PMMA and PE particles. These findings emphasise the importance of biomaterial wear particle generation and the mononuclear phagocyte response to wear particles in the pathogenesis of aseptic loosening.

References
1. Harris WH. *Acta Orthop Scand*1994;65(1):113.
2. Revell PA. *Current Trends in Path*, Berlin, etc: Springer-Verlag,.1982:73.
3. Lennox DW *et al. Clin Orthop*1987;225:171.
4. Horikoshi M *et al.Trans Orthop Soc* 1994;19:34.

QUANTIFICATION OF UHMWPE WEAR IN EXPLANTED ACETABULAR COMPONENTS

I.D. Learmonth, A. Spirakis, A. Breckon Dept of Orthopaedic Surgery, Bristol Royal Infirmary, Bristol

Wear of plastic acetabular components may predispose to implant failure. Analysis of wear patterns and wear rates are therefore important. A variety of different techniques have been used to assess plastic wear, including shadowgraphs, prolifometry, radiographs, CMM, etc. These methods have different strengths and weaknesses, but none cater for the confounding influence of cold flow and creep. The authors present a biostereometric method (stereophotogrammetric analysis) for the quantification of UHMWPE in explanted cups, using the reflex microscope. The inner surface of the cup was appropriately marked to allow systematic measuring. The reflex microscope allowed three-dimensional measurements to be made, and the x, y and z co-ordinates were recorded. The results were then processed using specialised software (SCALANT). An unused cup was measured as a control. It was possible to produce a topographical map of surface irregularities and a 3-D representation of volume difference.

Eleven Charnley 22 mm cups and 6 Muller 32 mm cups were examined in this preliminary study:

Results	22 mm	32 mm
Volumetric wear	61 mm^3/year	137 mm^3/year
Penetration wear	.23 mm/1 year	.11 mm/year

These results correlate well with those reported in the literature.

Stereophotogrammetry using the reflex microscope is a sensitive, reproduceable method of analysing plastic wear which allows distinction between displacement and true wear.

RESEARCH AND REGULATION - WHAT IS THE LINK?

G A Crosbie Medical Devices Agency, Department of Health

From January 1995, a European Directive requires that medical devices (including orthopaedic implants) placed on the market in Europe should be labelled with a CE mark, to indicate that they comply with appropriate safety requirements (the Essential Requirements). The Directive will be implemented by independent third parties (notified bodies) who will be overseen by Competent Authorities (in the UK the Medical Devices Agency of the Department of Health).

Technical requirements for orthopaedic implants will be defined via new harmonised European standards, which will in turn make reference to existing/new International standards covering specific technical aspects of implant design or performance.

Standard methods of laboratory testing need to be developed before *in vitro* performance requirements can be established and used as criteria for regulatory approval of new implants. The development of test methods (and associated performance requirements) for measuring wear of joint replacement implants is particularly important, since wear debris is now widely recognised to play a major role in causing arthroplasties to fail by aseptic loosening. Further work on the development of fatigue tests for joint replacement implant components is also required.

Looking ahead, it may be possible to predict the long term outcome of arthroplasty procedures from clinical data obtained during early stages of implantation. Techniques which measure early migration of joint replacement components *in vivo* look particularly promising, and equipment which measures bone density changes around implants may also prove useful. Much experimentation and validation and will be required before data obtained using such techniques can be used reliably in the implant approval process.

Technical Note

A comparison of the wear of cross-linked polyethylene against itself with the wear of ultra-high molecular weight polyethylene against itself

T J Joyce, BEng, MSc and **A Unsworth,** MSc, PhD, FEng, FIMechE
Centre for Biomedical Engineering, School of Engineering, University of Durham

Wear tests were carried out on reciprocating pin-on-plate machines which had pins loaded at 10 N and 40 N. The materials tested were irradiated cross-linked polyethylene sliding against itself, irradiated ultra-high molecular weight polyethylene sliding against itself and non-irradiated ultra-high molecular weight polyethylene sliding against itself. After 153.5 km of sliding, the non-irradiated ultra-high molecular weight polyethylene plates and pins showed mean wear factors under 10 N loads, or a nominal contact stress of 0.51 MPa, of 84.0 × 10^{-6} mm^3/N m for the plates and 81.3 × 10^{-6} mm^3/N m for the pins. Under 40 N loads, or a nominal contact stress of 2.04 MPa, the non-irradiated ultra-high molecular weight polyethylene pins sheared at 22.3 km. At the last measurement point prior to this failure, 19.1 km, wear factors of 158 × 10^{-6} mm^3/N m for the plates and 85.0 × 10^{-6} mm^3/N m for the pins had been measured. After 152.8 km, the irradiated ultra-high molecular weight polyethylene plates and pins showed mean wear factors under 10 N loads of 59.8 × 10^{-6} mm^3/N m for the plates and 31.1 × 10^{-6} mm^3/N m for the pins. In contrast, after 150.2 km, a mean wear factor of 0.72 × 10^{-6} mm^3/N m was found for the irradiated cross-linked polyethylene plates compared with 0.053 × 10^{-6} mm^3/N m for the irradiated cross-linked polyethylene pins.

Key words: wear, ultra-high molecular weight polyethylene, cross-linked polyethylene

NOTATION

- D distance (m)
- k wear factor (mm^3/N m)
- L load (N)
- m mass (kg)
- V wear volume (mm^3)
- ρ density (kg/m^3)

1 INTRODUCTION

Most artificial joints currently in use in joints such as the hip or knee have one component made from ultra-high molecular weight polyethylene (UHMWPE) and the other from either metal or ceramic. These combinations have been found to be acceptable in the body, though recently worries have been raised about the effects of plastic wear particles on local joint reaction and ultimately bone resorption (**1**). In extreme cases bone resorption can lead to the prosthesis becoming loose and the patient requiring revision surgery (**2**).

In the case of finger joint replacements, the most successful prosthesis at present is the Swanson integral hinge prosthesis which works by flexing an elastomeric single component (silicone rubber) and thereby avoids having an articulating surface. However, 'pistoning' of the prosthesis within the medullary cavity still produces some wear debris. More importantly though, the point about which the integral hinge flexes tends to become abraded by the bone ends, which produces a notch and hence a stress concentration. This, together with the normal fatigue process associated with cyclical stress applications, causes the joint to fail by fracturing (**3**).

Recently (**4**, **5**) it has been proposed that an articulating, two piece finger joint of the surface replacement type might prove to be better in the long term than the Swanson joint. While it is perfectly possible to produce a metal-on-plastic finger joint, there are some advantages to producing an all-plastic joint. These largely revolve around the closer modulus match between plastic and bone, giving a better stress distribution to the somewhat softer rheumatoid bone into which most finger prostheses are fitted. As there is a large amount of experience with UHMWPE, it was thought sensible to evaluate the wear rate of such a combination of two similar UHMWPE surfaces to see if the wear rate would be acceptable. It should be said that work from 20 years ago (**6**) showed that this combination produced very high wear rates which were unacceptable, but the materials have developed since then. Also, a new cross linked polyethylene (XLPE) is now being used largely in low load bearing situations (Ogee flange etc.) but not exclusively so. Cross-linked polyethylene has been successfully used as an acetabular cup material in combination with a ceramic femoral head (**7**). Since this material has potentially better mechanical properties than UHMWPE it is possible that its wear rate against itself in a finger joint application might give low enough wear for the plastic-on-plastic combination to be a realistic proposal.

Thus, this paper describes the direct comparison of wear tests conducted on UHMWPE (irradiated and non-irradiated) against itself and of XLPE (irradiated only) against itself.

2 METHOD

The tests were conducted on a pin-on-plate wear rig (Fig. 1) which employed a reciprocating motion that mimicked the natural flexion–extension of the finger. Load, speed and stroke could all be varied as appropriate. The rig consisted of a sledge reciprocating along two fixed parallel bars. On this sledge was positioned a heated bed and a stainless steel bath. The sledge was driven by a 125 W d.c. shunt motor. Motor speed was controlled using a variable voltage supply and the stroke could be altered by adjusting the crank radius of the drive shaft. Heating of the distilled water, which

The MS was received on 6 September 1995 and was accepted for publication on 19 March 1996.

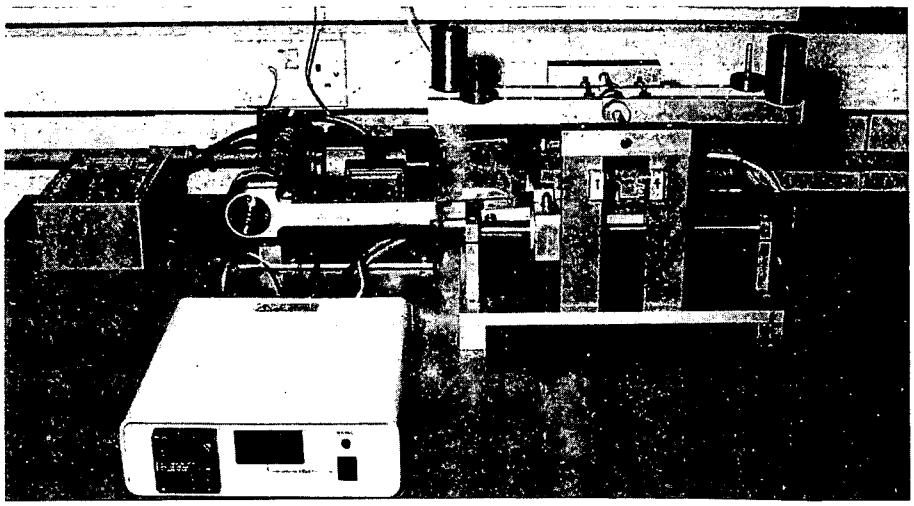

Figure 1 Reciprocating pin-on-plate rig

acted as a lubricant, was provided by resistors positioned within the heated bed. These resistors, together with a thermocouple, were connected to a controller which maintained the lubricant at a constant, pre-set temperature of 37 °C. Four test plates were located in the stainless steel bath using a plastic frame into which suitable location slots had been milled. The test plates were a tight fit in these slots. Therefore the plates were held rigidly during testing but could be replaced in exactly the same position as before after they had been removed for weighing. Each test pin was held within a holder and in turn each holder fitted within a machined arm. Each pin was notched at the upper end to provide good location in the pin holder, and also to prevent rotation. It also ensured that the pin was replaced in its original position after removal for weighing. On the top of each holder rested a cantilevered bar to which weights were added to provide an applied load. An automatic lubricant level controller was fitted, such that the fluid was maintained between pre-set maximum and minimum levels and to prevent the rig from operating without lubricant. Finally, an electronic counter was connected to the sledge, and a glass cover fitted to minimize any contamination from the atmosphere.

Prior to the commencement of a test, the polyethylene test plates and pins were carefully weighed. Both a control pin and a control plate were included to take account of any lubricant absorption. These control specimens were unloaded and kept in the same distilled water as the test specimens at 37 °C. At regular intervals, the test was stopped, pins and plates were removed, cleaned with acetone, weighed and visually inspected. Pins and plates were weighed to the nearest 0.1 mg using a Mettler AE200 balance. Wear of a test pin, or plate, was defined as the weight loss with respect to the initial weight, to which was added any weight gain of the control pin, or plate. Therefore the weight gain of the control and test pins was assumed to be equal, as was that of the control and test plates. The wear factors k (mm^3/N m) were calculated from the equation:

$$k = \frac{V}{LD}$$

but $V = m/\rho$, therefore

$$k = \frac{m}{\rho LD}$$

$$\rho(\text{XLPE}) = 949 \text{ kg/m}^3$$

$$\rho(\text{UHMWPE}) = 953 \text{ kg/m}^3$$

Three tests were undertaken. The first employed irradiated XLPE pins and plates, the second used non-irradiated UHMWPE pins and plates, and the third used irradiated UHMWPE pins and plates. Loads of 10 N and 40 N were employed in the first two tests; two pins being loaded at 10 N, the other two pins at 40 N. In the third test, all four pins were loaded at 10 N. The 10 N load is regarded as a 'normal' load for the metacarpophalangeal joint during motion (**8**), while the 40 N load was for scientific interest and to provide the opportunity of discovering if wear factors changed with load. The pins were 'turned' to form flat-ended, circular cylinders, 20 mm long and 5 mm in diameter. The nominal stress values were therefore 0.51 MPa for the 10 N load and 2.04 MPa for the 40 N load. The pin-on-plate rig employed a stroke of 20 mm and an average velocity of 0.037 m/s.

3 RESULTS

Test results are summarized in Table 1. Figure 2 shows a graph of the wear of XLPE and UHMWPE pins and plates under 10 N loads. The XLPE test continued to 349 km.

4 DISCUSSION

Regarding the irradiated XLPE test, the lack of pin wear compared with plate wear is difficult to explain. It is speculated that, as the pins were constantly loaded whereas the individual parts of the wear track on the plates underwent a cyclic load, there may be a fatigue element producing the higher XLPE plate wear in contrast to the lower XLPE pin wear. In comparison, UHMWPE pins showed wear factors much closer to those of their respective plates. For the non-irradiated pins and plates, the values of wear factor were almost identical for the test under 10 N loads. For the irradi-

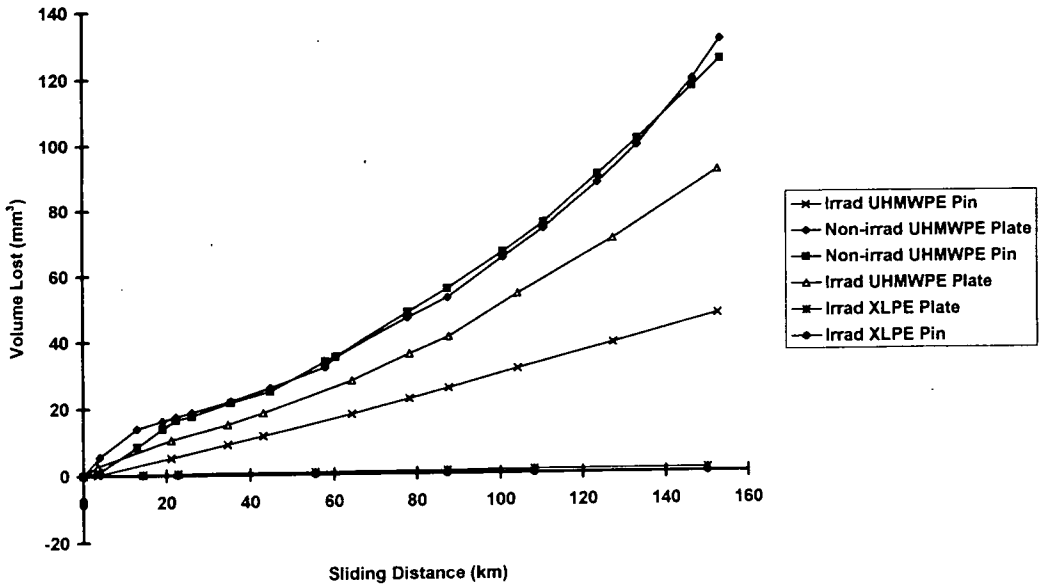

Figure 2 Mean wear of XLPE and UHMWPE pins and plates under 10 N loads

Table 1 Summary of pin and plate wear factors

Test	Load (N)	Distance (km)	Mean k plate (10^{-6} mm^3/N m)	Mean k pin (10^{-6} mm^3/N m)
Irradiated XLPE	10	150.2	0.78	0.070
	40	150.2	0.67	0.035
Non-irradiated UHMWPE	10	153.5	84.0	81.3
	40	19.1	158	85.0
Irradiated UHMWPE	10	152.8	59.8	31.1

ated material, the pin wear factors were approximately half those of the plates. Perhaps then, while the irradiation of UHMWPE improves the material's mechanical properties, the fatigue element causing greater plate wear than pin wear becomes more noticeable. It should also be noted that previous work has not included measurement of plate wear in such a UHMWPE against UHMWPE test (**6**, **9**).

The XLPE control pin showed no fluid absorption after 150 km. Similarly the weight of the XLPE control plate was the same as it was at the commencement of the test. In contrast the UHMWPE control pins and plates did show a slight increase in weight. However, this weight increase was small in comparison with the weight loss due to wear. In the duration of a test, the UHMWPE control pin increased in weight by 0.1 mg (the accuracy of the Mettler balance) while the minimum weight loss by a UHMWPE test pin was 43.7 mg. The maximum weight increase by a UHMWPE control plate was 2.2 mg, while the minimum weight loss by a UHMWPE test plate was 54.8 mg. The weight of each of the polyethylene plates was of the order of 5.0 g, while that of the pins was of the order of 0.36 g.

The non-irradiated UHMWPE pins under 40 N loads sheared at 22.3 km, and wear factors under 40 N loads were found to be greater than those at 10 N indicating that, for non-irradiated UHMWPE, wear factors increase with load. As would be expected by the difference in wear factors, a lot of wear debris was visible to the eye during the UHMWPE tests, whereas none was seen during the XLPE test.

From Table 1, overall wear factors for irradiated XLPE and irradiated UHMWPE can be taken as 0.85×10^{-6} mm^3/N m and 90.9×10^{-6} mm^3/N m respectively. If a finger joint is assumed to perform 1 million cycles per annum, in this case equivalent to 40 km, then these wear factors can be interpreted as wear rates of 0.32 mm^3 per annum for irradiated XLPE and 36.4 mm^3 per annum for irradiated UHMWPE. Dowson (**10**) quotes a wear rate of 38 mm^3 per annum as acceptable for an artificial hip joint. However, a hip joint of radius 20 mm will have a capsule volume 23 times greater than that of a finger joint of radius 7 mm. Therefore, for a finger joint, a wear rate of 1.65 mm^3 per annum should be acceptable. Consequently, based on the results reported here, an all-XLPE finger prosthesis would be acceptable from a wear point of view, while an all-UHMWPE finger prosthesis would not.

5 CONCLUSION

Wear factors of non-irradiated UHMWPE against itself have been found to be over 100 times higher than those of irradiated XLPE against itself. The irradiation of UHMWPE was found to decrease its wear rate under the above test conditions, but wear factors were still approximately 75 times greater than those of irradiated XLPE against itself.

ACKNOWLEDGEMENTS

The authors would like to thank Action Research, grant reference A/F/0475, for providing financial support. De

Puy International Limited supplied all of the polyethylene material.

REFERENCES

1 **Howie, D. W., Vernon-Roberts, B., Oakeshott, R.** and **Manthey, B.** A rat model of resorption of bone at the cement–bone interface in the presence of polyethylene wear particles. *J. Bone Jt Surg.*, 1988, **70A**, 257–263.

2 **Mirra, J. M., Marder, R. A.** and **Amstutz, H. C.** The pathology of failed total joint arthroplasty. *Clin. Orthop. Rel. Res.*, 1982, **170**, 175–183.

3 **Swanson, A. B.** and **de Groot Swanson, G.** Flexible implant arthroplasty in the rheumatoid metacarpophalangeal joint. *Clin. Rheum. Dis.*, 1984, **10**(3), 609–629.

4 **Joyce, T. J.** and **Unsworth, A.** The wear of cross-linked polyethylene against itself. *Proc. Instn Mech. Engrs, Part H*, 1996, **210** (H1), 11–16.

5 **Sibly, T. F.** and **Unsworth, A.** Wear of cross-linked polyethylene against itself: a material suitable for surface replacement of the finger joint. *J. Biomed. Engng*, 1991, **13**, 217–220.

6 **Atkinson, J. R.** An investigation into the wear of ultra high molecular weight polyethylene when a polyethylene wear pin is loaded against a reciprocating polyethylene counterface lubricated by bovine synovial fluid at ambient temperature. Report, Department of Metallurgy, Leeds University, 1976, pp. 1–12.

7 **Wroblewski, B. M., Siney, P. D., Dowson, D.** and **Collins, S. N.** Prospective clinical and joint simulator studies of a new total hip arthroplasty using alumina ceramic heads and cross-linked polyethylene cups. *J. Bone Jt Surg.*, 1996, **78B**, 280–285.

8 **Tamai, K., Ryu, J., An, K. N., Linscheid, R. L., Cooney, W. P.** and **Chao, Y. S.** Three dimensional geometric analysis of the metacarpophalangeal joint. *J. Hand Surg.*, 1988, **13A**, 521–529.

9 **Stokoe, S. M.** A finger function simulator and surface replacement prosthesis for the metacarpophalangeal joint. PhD thesis, University of Durham, 1990.

10 **Dowson, D.** A comparative study of the performance of metallic and ceramic femoral head components in total replacement hip joints. Proceedings of *Austrib '94*, pp. 59–73.

Biomechanics of the distal upper limb

H. E. Ash, T. J. Joyce, A. Unsworth

INTRODUCTION

The hand is not only a crucial tool for everyday life and work, but a means of conveying and receiving information. It is a mechanism of great complexity and intricacy. This paper will discuss the forces acting on, and movement of, the joints of the distal upper limb, the metacarpo-phalangeal, proximal interphalangeal and the distal interphalangeal joints together with the joints of the thumb and the wrist.

FORCES IN THE JOINTS OF THE DISTAL UPPER LIMB

In-vivo joint, tendon and muscle forces are difficult to measure directly, and the large number of muscles and ligaments involved make the task of modelling, and then calculating these forces equally as difficult. The positions of the joint and its surrounding joints must be specified as these will directly affect the forces acting on it. Due to this complexity, models have to be simplified.

Experimental measurements of forces

Value of measurements

The clinical measurement of hand strength allows pathological conditions and their response to treatment to be assessed, feasible treatment goals to be set, and the effectiveness of different surgical procedures to be compared. Measurement must be reliable and valid, necessitating the use of standardized equipment, procedures and positioning of the hand.

Definitions of hand and finger strength

Tip, pulp, lateral and three-point pinch, grip strength, long finger flexion force and thumb force have all been extensively measured.[1–24] However, the definitions of the type of forces being measured have often been contradictory and vague. The following pinches and grips are defined in order to compare experimental results and to apply this information to the various theoretical models reviewed, (Fig. 1).

Grip strength-power grip. The fingers and thumb gripping an object, producing maximum hand grip strength.

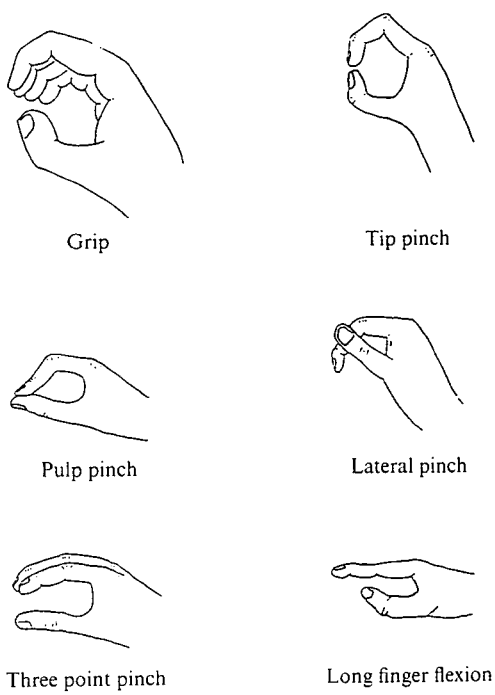

Fig. 1—Definitions of hand and finger strength.

H. A. Ash BSc MSc, **T. J. Joyce** BEng MSc, **A. Unsworth** MSc PhD DEng FIMechE, School of Engineering, University of Durham, Science Laboratories, South Road, Durham DH1 3LE, UK.

Tip pinch. The tip of the index, middle, ring or little finger against the tip of the thumb, with the interphalangeal joint (IPJ) flexed.

Pulp pinch. The distal phalangeal pad of the index, middle, ring or little finger against the distal phalangeal pad of the thumb, (the IPJs are more extended than in tip pinch).

Lateral radial pinch. The distal phalangeal pad of the thumb against the lateral or radial side of the middle phalanx of the index finger, the other fingers being clenched in support.

Three point palmar pinch. The index and middle fingers reacting against the thumb. Pinching with the pads or tips is not always defined. However, Kellor[1] defined palmar pinch using the pads of the fingers and thumb and three-point pinch using the tips.

Long finger flexion. The pad of the distal phalanx of the finger exerting a force in a neutral, cantilever position.

Thumb force. The pad of the distal phalanx of the thumb exerting force, with the angles of joints defined.

Equipment used

A popular method of measuring grip strength is to squeeze an inflated bag connected to a manometer and to note the increase in pressure. However, different techniques of squeezing give different results, as indeed will different original bag volumes or pressures.[25] Additionally, the contribution of individual fingers cannot be determined.[2] Strain-gauged devices, however, offer the ability to measure the force of a grip, rather than the pressure indicated by an inflated bag. With certain strain-gauged devices, the magnitude and contribution of the individual fingers, and finger segments, to the grip strength can also be determined.

Influential factors

It has been found that the forces acting on and around the joints of the hand depend on environmental, mechanical and human factors, the latter including the patient's cooperation. From past investigations, comparison between different authors' results show that these factors include age,[1,3–7] sex,[1,3–10] pathological condition,[11–16,26] bilateral hand function,[1,4,6,8,9,14,15,17,18] occupation and exercise,[6,17,18] measuring device or size of object being grasped,[2,19,25] technique of grasp,[25] difference in hand function,[1,6–9,17] temperature,[18,27] diurnal or circadian effects,[11,13,18] and drugs.[4,13] In addition, the orientation of other joints in the upper limb may influence joint forces.

Grip strength

The grip strength of subjects and patients has been measured and shows total grip strength ranging from a minimum of 80N in normal women to a maximum of 520N in normal men (Table 1). Arthritic patients were only one-third as strong. The range of grip-strength data shows that either the equipment itself influences the values recorded[19] or that there is a large subject to subject variation which is also influenced by the variation of the position of the finger joints.

The distal phalangeal force component of the total grip strength was found to be the largest, followed by the proximal then the middle phalanx (Table 2).[7,19] The mean contributions of the fingers to grip strength were found to be 30% index, 30% middle, 22% ring and 18% little.[19]

Table 1 Hand grip strength (N)

Reference	Sex	Hand	No.	Mean force or range of means	Maximum or range of force
Mathiowetz et al[8]	M	R	310		142–783
	M	L	310		138–712
	F	R	328		111–610
	F	L	328		102–512
Reikeras[9]	M	D	30	186	
	M	ND	30	182	
	F	D	30	105	
	F	ND	30	106	
Swanson et al[6]	M	D	50	467	
	M	ND	50	441	
	F	D	50	241	
	F	ND	50	220	

Table 2 Individual finger grip strength (N)

Reference	Finger	No.	Total finger	Distal phalanx	Middle phalanx	Proximal phalanx
Amis[19]	I	17	150	80	30	45
	M	17	160	70	40	50
	R	17	125	55	30	35
	L	17	105	50	25	30

Table 3 Additional factors affecting grip strength (N)

Factor	Reference	Normal/RA	No.	Hand	Force	Force
Diurnal	Pearson et al[18]	Normal	10	D	am 65	pm 68
		Normal	10	ND	am 65	pm 67
Temp.	Pearson et al[18]	Normal	13	D	10°C 48	40°C 49
		Normal	13	ND	10°C 50	40°C 49
		RA	11	D	10°C 18	40°C 18
		RA	11	ND	10°C 18	40°C 17
Exercise	Pearson et al[18]	Normal	13	D	pre 50	post 50
		Normal	13	ND	pre 51	post 50
		RA	11	D	pre 17	post 18
		RA	11	ND	pre 17	post 17
Sports	Cutts and Bollen[17]	Climbers	13	R	507	
		Climbers	13	L	532	
		Normal	12	R	445	
		Normal	12	L	412	

Males were found to be stronger than females in grip strength, female grip strength being approximately 50–80% that of males.[1,3,4,6–9] Pathological conditions such as rheumatoid arthritis and osteoarthritis also severely reduce grip strength. Grip-strength values are greater than tip and pulp pinch. The influence of additional factors is shown in Table 3.

Pinch forces

Pinch strength depends on the type of pinch and the finger–thumb combination, i.e. tip, pulp, three point or lateral. The experimental data show that males have greater pinch strengths than females. Tip, pulp and long finger flexion all seem to produce similar force ranges. Lateral and three-point pinch in general have a greater upper value of force than tip and pulp pinch possibly because more than one finger is involved either in pinch or in support. For tip and pulp pinch, the index finger is approximately equal in strength to the middle finger, with the ring finger next and then the little finger, (Tables 2, 4–6).

Table 4 Tip pinch force (N)

Reference	Finger	Sex	No.	Maximum force	Range of force
An et al[7]	I	M	18	63	
		F	22	47	
	M	M	18	63	
		F	22	46	
Cantrell[16]	I				34–49
	M				34–49
	R				22–49
	L				20–39

Table 6 Lateral pinch force (N)

Reference	Finger	Sex	No.	Mean force
An et al[7]	I	M	18	75
		F	20	59
	M	M	18	68
		F	20	51

BIOMECHANICS OF THE FINGERS

Joint anatomy

The metacarpo-phalangeal joint (MCPJ) is a complex joint, with local soft tissue structures making important contributions to both joint function and stability. It consists of the convex metacarpal head and the concave base of the proximal phalanx, forming a condylar joint stabilized by the metacarpo-phalangeal and metacarpo-glenoidal ligaments, volar plate and joint capsule.

The metacarpo-phalangeal (or collateral) ligaments arise from each side of the metacarpal head and are the primary link between the metacarpal and proximal phalanx. These ligaments run obliquely, so the tension in the ligaments increases as the joint moves from 0° to 90°. Quantitative results exist to show that the collateral ligaments are the primary means of stabilizing the MCPJ. In addition the flexor tendon sheath is supported by the metacarpo-glenoidal ligaments.[29]

The IPJ which consist of the proximal interphalangeal joint (PIPJ) and the distal interphalangeal joint (DIPJ), are bicondylar with 1° of freedom. They have no muscular support in abduction and adduction

Table 5 Pulp pinch force (N)

Reference	Finger	Sex	No.	Maximum force	Sex	No.	Maximum force
An et al[7]	I	M	18	66	F	22	45
	M	M	18	62	F	22	45
Swanson et al[6]	I	M	50	52D 47ND	F		35D 32ND
	M	M	50	55D 56ND	F		35D 33ND
	R	M	50	37D 35ND	F		25D 24ND
	L	M	50	23D 22ND	F		17D 16ND

hence the fibrous capsule, volar plate, and palmar and collateral ligaments provide joint stability.

Range of motion

The MCPJ has 2° of freedom, allowing active motion in flexion, extension, abduction and adduction, and a small amount of passive motion in axial rotation. The range of motion in flexion is typically 0–100°, in extension 0–45°, and in abduction–adduction, 0–60°. Passive movement is greater than active in both the flexion–extension plane and the radio-ulnar plane.[21,29] There is little difference in motion between men and women and between different age groups; although there is a decline in manipulative ability with age.[21] The IPJ have 1° of freedom, allowing active motion in flexion and extension, and a small amount of passive axial rotation and lateral movement to accommodate externally applied forces. The range of movement in flexion is typically 0–90° and 0–100° for the DIPJ and PIPJ respectively.

Centre of rotation

The centre of rotation of the MCPJ lies within the head of the metacarpal, although its exact location is open to debate. Flatt and Fischer[30] found that in the sagittal plane, the MCPJ has a fixed centre of rotation. Their work was done with living hands rather than cadavers and joint motion was studied rather than simply the geometry of the joint itself. This is important because the centre of rotation depends not only on the geometry of the joint surfaces, but on the ligaments too, which have an offset attachment relative to any centre of the metacarpal head. Other work examining only the dimensions of the MCPJ has of necessity involved the removal of the ligaments surrounding these joints but has agreed with their findings.[31]

Youm et al[29] using an X-ray technique, also found the centre of rotation of the MCPJ to be constant in both the sagittal and transverse planes. Additionally, using an analytical method, and taking into account possible errors, they concluded that the centre of rotation was fixed within a 1.5 mm sphere. This result was also found by Unsworth & Alexander[31] who showed that the MCPJ has a single centre of rotation in both sagittal and transverse planes.

However, other researchers disagree with the concept of a fixed centre of rotation. Pagowski & Piekarski[32] using measurements from cadavers, calculated the centre of rotation to travel on an arc of radius 1.5 mm. One aspect of their argument against a fixed centre of rotation was that a point load would result, leading to localized wear. Obviously, this localized wear does not occur. However, the lack of wear is due to the cartilage forming a compliant surface, and has little to do with the position of the centre of rotation. An additional assumption was that the collateral ligaments are always taut. However, the tension in the ligaments varies with flexion, so that at maximum flexion, tension in the ligaments is such that abduction–adduction is eliminated.

Walker & Erkman[33] again using cadavers, fixed the phalanx and moved the metacarpal bones, then graphically determined the position of the centre of rotation. Results gave its position as within 3 mm of the centre of the metacarpal head; much greater than that found by any other researchers. Tamai et al[34] attached springs to the tendons and muscles of cadavers to simulate normal loading, then analysed the MCPJ. They concluded that a fixed centre of rotation did not exist but did not give the dimensional variance.

If a fixed centre of rotation is assumed, then a pin jointed model can be employed. Most theoretical models are based on a pin-jointed structure, assuming a constant centre of rotation.[22,23,35–41]

Inter-relationships between the finger joints

The PIPJ and DIPJ are tightly restrained, moving synchronously in flexion and extension.[42] The DIPJ angle is also dependent on the PIPJ angle.[30] Retinacular ligaments encourage synchronous motion between the PIPJ and the DIPJ, with the amount of flexion supposedly in a ratio of 2:1 respectively.[43] The retinacular ligaments run from the flexor tendon sheaths on the proximal phalanx to the terminal tendon on the distal phalanx linking movement of the DIPJ and the PIPJ.

Reciprocal and synchronous angular movement between IPJ and MCPJ is possible.[43] The range of movement of the MCPJ and PIPJ are interrelated. With a more flexed MCPJ the PIPJ range of movement increases. This inter-relationship is influenced by the centres of rotation of the joints and the anatomy of the tendon systems that couple the two joints.[30]

Finger tendons and muscles

There are two main groups of muscles and associated tendons that act on the fingers, the extrinsics and the intrinsics.

Extrinsics

The extensor digitorum communis (EDC) inserts on the distal phalanx via the terminal extensor, on the middle phalanx via the central slip, and on the proximal phalanx via the extensor slip, extending the MCPJ and the IPJ. The flexor digitorum profundus (FDP) inserts on base of the distal phalanx flexing the MCPJ and the IPJ. The flexor digitorum superficialis (FDS) inserts on the middle phalanx flexing the MCPJ and PIPJ.

Intrinsics

The lumbricals (L) originate from the FDP tendon and insert on the EDC tendon extending the IPJ. The

interossei originate from the sides of the metacarpals and insert on the proximal phalanges abducting and adducting the MCPJ and extending the IPJ. The lumbricals and interossei muscles extend the IPJ due to their partial attachment to the EDC.

Finger tendon and muscles roles in hand function

Effective hand function requires stability and strength from the balanced action of the extrinsic tendons, intrinsic muscles, constraining forces and joint contact forces.[35] Extrinsic tendons transmit the force for 'power' grip and exert compressive and subluxing forces on the IPJ. Intrinsic muscles allow fine positioning of the fingers and thumb and contribute to the strength of the hand. Interossei muscles position the pulps of the fingers and the lumbricals modify the relative tensions between flexors and extensors about the IPJ acting as a feedback system.[43]

Antagonists and synergists stiffen the joint for control purposes increasing joint stability and also increasing the joint contact force.[44] Antagonists produce counterbalancing moments, reduce subluxation forces and increase axial compressive forces. The extensor mechanism probably acts passively as an antagonist and stabilizer to increase joint stability, other tendon forces and the joint contact forces.

Tendons have primary and secondary functions. Secondary contributions vary greatly throughout the population. Variation of joint orientation varies the contributions of the tendons, giving the fingers different functional capacities in different positions with optimum configurations.[36] The maximum grip strength also changes with joint angle.[37]

THEORETICAL MODELS

Smith et al[38] developed a two-dimensional index finger pulp-pinch model for analysis of tendon and joint forces from simplified planar analysis. Since then many three-dimensional models have been developed[35,36,37,39] to analyse static isometric functions using forces and moments to determine the resultant forces on the load bearing structures of the finger joints.

Weightman & Amis[22] after reviewing previous models, suggested that one of the most important factors influencing discrepancies between previous finger joint models was the differences in postures adopted in the different models. They found that the joint contact forces increased as the pinching position moved from tip to pulp.

Berme et al[23] and Purves et al[44] developed three-dimensional models of an isometric moment on a water tap and the cap of a jar. The externally applied forces, when applying a maximum clockwise moment, were measured on a six component strain gauged load transducer. Variance in measurements was thought to be due to habitual and anatomical differences. They found that joint contact forces during twist were greater than those during pinch grip.

Storace & Wolf[40,41] applied the principle of virtual work and kinematic analysis to a simple pin-jointed model producing indeterminate equilibrium equations without constraining forces, for the MCPJ and the PIPJ. Relationships of displacement of working tendons with respect to joint angles were calculated and thought to be more accurate than the determination of moment arms. Actual tendon forces could not be calculated but the model was used to predict conditions of instability of joints for abnormal anatomy such as volar subluxation of the extensor tendon.

Tamai et al[34] have also offered some figures for MCPJ forces. Though not providing a model, they calculated forces from contact area and contact pressure. Such a method gave a force of 14N for a static MCPJ in the 'neutral' position due to the balance of muscle forces alone.

Model assumptions

Due to the complexity of hand functions, the involvement of many tendons, and the additional involvement of the soft tissue structures of the joints, theoretical models produced to analyse the roles of the load-bearing structures of the finger and thumb joints were statically indeterminate. This meant that assumptions had to be made in order to obtain solutions which were thought most closely to match the forces encountered in normal hand function.

In most models frictional, inertial and viscoelastic effects of the soft tissues were neglected, and the tendons and tendon sheaths were modelled as frictionless cables and pulleys. The joint contact forces were constrained to act through the bearing surface for joint stability, and models where this was not the case were modified with additional antagonistic stabilisers to increase the joint stability. Joint forces were required to be compressive, and tendon forces tensile. Centres of rotation of the joints were commonly assumed to be constant producing pin-jointed models, and intrinsic forces were assumed to have a single line of action even though they have a broad base of insertion.

Relationships between tendons

Assumptions have been made about the relationships between the interossei, the lumbricals, and the bands of the EDC in order to reduce the numbers of unknowns in the analysis of different hand functions.[22,35,37,39] The relationships were derived from information of the anatomy of the hand and the insertion and orientation of the tendons. Weightman & Amis[22] believed these to be dependent on the angle of flexion of the joints, although all of the authors used set relationships regardless of joint flexion.

Extensor action

In their analysis of the different hand functions An et al[35] and Chao & An[37] assumed the extensor tendon to play an active role. However, Chao et al[39] assumed the extensors had an antagonistic stabilizing role and solutions and results where extensor forces were large enough to imply active and not passive involvement were eliminated. Purves et al[44] introduced extensor or collateral ligament activity only in unstable joints to modify the line of action of joint contact forces to bring them within the bearing surface, stabilizing the joint.

Several models[22,38] have neglected to include the extensor tendon involvement during pinch or grip analysis because EMG results have shown them to be inactive. However, Linscheid & Chao[43] assumed the extensor to assume a passive role during pinch activities providing another joint constraint acting as an antagonist and stabilizer. Passive muscle activity is not always detected by EMG because the thresholds for certain muscles under various levels of activities are too low to detect.[36] Hence, in some models EMG results may have caused the passive stabilizing role of the extensors to be overlooked.

Physiological cross-sectional area

The strength of a muscle was thought to be proportional to the number of sarcomeres firing simultaneously, which in turn was thought to be proportional to the physiological cross-sectional area (PCSA) of the muscle. Estimations of the PCSA of each muscle have been used to predict the maximum strength of individual muscles. Hence, upper strength limits can be imposed on individual muscles in the analysis of hand function. An et al,[35] Chao & An[37] and Chao & An[36] utilized this method estimating the PCSA for muscles of the hand. Results where muscles exerted a force greater than the upper strength limit of the muscle were modified or eliminated. Weightman & Amis[22] also used this theory to develop inter-relationships between the lumbrical and interossei muscles in the ratios of radial interrosei (RI): ulnar interrosei (UI): L = 4.3:1.45:0.52.

Two- and three-dimensional models

The majority of authors have modelled pinch and grip activities in three dimensions,[35,36,39,43] apart from Smith et al[38] and Weightman & Amis[22] who assumed pinching to be simply two-dimensional. However, from three-dimensional models it can be seen that pinch and grip activities have lumbrical and interossei active involvement as well as the flexor and extensor systems. Hence the two-dimensional analyses without lumbrical and interossei involvement produce oversimplified models of the true pinch and grip activities. Joint contact forces are the resultant of the axial compressive force and the volar and lateral shear forces. However, neglecting the lumbrical and interossei involvement in two-dimensional models eliminates the lateral shear force component.[22,38]

Moment arms

Flatt & Fischer[30] suggest that extensor moment arms decrease slightly and flexor moment arms increase with increasing flexion of the finger joints. However, Linscheid et al[42] believed that the flexor sheaths kept the flexor moment arms virtually constant during flexion with respect to the centre of rotation of the joints. Youm et al[29] found that the extensor moment arm was almost constant during flexion, although the flexor moment arms increased by 50% at full flexion. The palmar aspect of the phalangeal base also increased the flexor moment arm during flexion, increasing its mechanical advantage. However, although the flexor moment arm appears to change significantly during flexion of the finger joints, it has been neglected in most models.

Joint surface load sharing

Most models appear to assume that the bearing surfaces of the joints share the joint contact force. However, Purves et al[44] investigated the possibility that either both PIPJ condyles support the joint contact force with both the collateral ligaments and the extensors slack, or only one condyle supports the joint contact force with the opposite collateral ligament in tension. They surprisingly found that the PIPJ radial ligament was load bearing and joint loading was exclusively in the ulnar compartment.

The effects of these assumptions have in some cases been analysed to investigate their effects on the resulting force distribution between the load bearing structures of the hand during upper limb functions. In some cases they have made little difference, although they must account for some of the discrepancies between the models. However, such assumptions are needed in some cases to simplify the force analysis of a joint and produce a determinate model.

Theoretical forces

The forces from the theoretical models were calculated in terms of unit force applied to the distal phalanx in tip and pulp pinch and unit force applied to the radial side of the middle phalanx in lateral pinch. Three forces were applied normal to the long shaft of the proximal, middle and distal phalanges for grip hand functions. Chao & An[36] and Chao et al[39] applied three unit forces; however, An et al[35] determined the ratios experimentally and applied forces in the ratios of DP:MP:PP = 1:0.34:0.66, compared with 1:0.52:0.77[7] and 1:0.375:0.56.[19]

Conclusions

Difficulties occur in the comparison of the different theoretical models and in combining experimentally measured forces with the theoretical models in order to calculate joint contact forces. Confusion in the definition of the different hand functions has occurred, and forces have been applied to the models in different positions, directions and distributions. Differences occur within the joint angles used during specific hand functions and with those encountered when experimentally measuring the forces during the different activities.

Joint angle

Differences in joint angles during pinch and grip hand functions are responsible for some discepancy between the calculated forces. For example, for a constant pinch force with increased joint flexion the FDP force decreased, FDS force and shear components increased, and the intrinsic tension remained constant. The joint force decreased due to the reduction of moment arm of the external force from pulp to tip, and its direction of action changed.[22]

Joint contact forces

The maximum forces being applied to the fingers during grip hand functions are greater than in pinch functions (Tables 1, 4–6). This would possibly imply that joint contact forces during gripping would be larger than those during pinching. However, in some models this is not so.[36,39] This is possibly due to assumptions in the distribution of forces. Chao & An[36] and Chao et al[39] applied unit forces at each of the phalanges and found the joint contact forces in tip pinch to be greater than in grip. However, An et al[35] experimentally measured the distribution of forces between the three phalanges in grip and used a unit ratio of these forces in their model and found the joint contact forces of grip to be greater than tip pinch which would be expected.

To make a fair comparison between the joint contact forces between pinch-and-grip hand functions realistic forces must be used. For instance, the maximum measured forces in grip, (Table 2), are far greater than those of pinch, (Table 4), hence comparing models using unit forces for both is totally unjustifiable. If unit forces are applied to both pinch and grip functions, tip pinch joint contact forces may well come out larger than those of grip due to the increased distance of the force from the joints.

By matching experimental hand function positions with the theoretical models as far as possible it was found that grip joint contact forces are greater than pinch joint contact forces. For grip function, inserting 80N DP component[19] into An's model[35] gives maximum joint contact forces of 279N, 437N, 387N for the DIPJ, PIPJ, and MCPJ respectively. For tip pinch function inserting 66N[7] gives maximum joint contact forces of 180N, 331N, 299N. (Results from Amis[19] were used and not An et al[7] as the distribution of forces is closer to that of the theoretical model). In all hand activities it has also been shown that in general, joint contact forces increase with more proximal joints, possibly due to the increase in the moment arm of the externally applied force.

Comparison between pinch and grip hand functions

There is some discrepancy in the comparison of muscle forces between grip and pinch activities. Chao & An[36] found that flexor forces were slightly greater in gripping but intrinsic forces (lumbricals and interossei) were less because they are more important for stability in pinch which is a more unstable position. In pinching flexor forces were still greater than intrinsic forces.

However, Chao et al[39] found that the FDP force was greater in pinch than grip, but the FDS force and the intrinsic forces were less. In grip the intrinsic muscles provided greater forces than flexor tendons, but in pinch the flexor tendons produced greater forces than the intrinsic muscles. An et al[35] found that flexor forces were in general greater in grip than in tip or pulp pinch, but intrinsic forces were about the same. Flexor forces were greater than intrinsic forces.

In general it seems that the flexors contribute greatly to hand strength in all hand functions. The intrinsic muscle forces seem to be smaller than the flexor forces in the majority of cases but still contribute appreciably to hand strength and stability of the joints. Muscle contributions vary with position of grip.

Stability

The finger joints rely on soft tissues and tendons around the joints for joint stability. Muscles are recruited to increase joint stability and can act as antagonists to other muscles such as the flexors, whose forces increase to overcome the effects of the antagonists. This increase in muscle forces in turn increases the joint contact forces. The majority of models ignore the involvement of the fibrous joint capsule, joint ligaments, and volar plate in force analyses of the finger joints due to their complexity. However, it is generally recognized that these structures play an important role in resisting the shear forces of the joints and towards increasing joint stability. The collateral ligaments decreased the volar shear component of the joint force and increased the axial compressive component, resulting in a slight increase in the joint contact force.[22,38]

The EDC has also been ignored in the majority of models, even though it probably exerts a passive tension across the joints, and consequently increases joint stability.[44] Muscle forces in tip and pulp pinch cover

similar ranges, however, lateral pinch has increased EDC and radial interossei forces to resist the greater shear forces which then stabilises the joint. Storace & Wolf[40,41] showed that intrinsic interossei muscles were required in addition to extrinsic FDP and EDC tendons for stability in hand function.

Pathological condition

Rheumatoid arthritic joints show gross deformity due to a loss of the balance of tendon forces, constraining ligaments and joint architecture. The radial interossei tend to have a larger force than the ulnar interossei showing that the proximal phalanx has a tendency to try to move in an ulnar direction. Volar and ulnar forces are usually resisted by the collateral ligaments and joint capsule; however, a loss of integrity in the supporting structures allows ulnar drift and subluxation to occur.

The paths of the tendons and muscles also affect the balance of joints.[42] A small disturbance in their position will upset the balance of forces around a joint resulting in deformation of the fingers. Storace & Wolf[40,41] found that volar relocation of the long extensor produced an unstable finger, that is one where the line of action of the joint contact force acted outside the articular surface of the joint. Rheumatoid arthritic patients often have better 'power' grip function than precision handling due to the increased stability of their hand function.[36]

BIOMECHANICS OF THE THUMB

The thumb provides strength, stability, and increased manipulation of the hand in its various activities. In precision pinch it acts as a pillar for the fingers to act against, and in 'power' grip it reacts directly against the object being held. Strength in hand functions relies heavily on the stability of the thumb which in turn depends on the configuration of the articulating surfaces and the surrounding soft tissues. Antagonist muscles also help to stabilise the joint. If the ligaments or tendons of the thumb are damaged, such as in rheumatoid arthritis, then the strength of the hand is significantly reduced.

Joint anatomy and range of movement

The IPJ is bicondylar with 1° of freedom allowing active movement in flexion and extension and a small amount of passive axial rotation and lateral movement. The range of movement is typically 0–90° of flexion and 0–20° of extension. The collateral ligaments, volar plate, joint capsule, and supporting soft tissues provide joint stability.

The MCPJ is condylar with 2° of freedom allowing active movement in flexion, extension, abduction and adduction, and a small amount of passive axial rotation. The range of movement is typically 0–60° of flexion and 0–10° of extension. The collateral ligaments and volar plate-sesamoid bones complex limit abduction, adduction and axial rotation. The fibrous capsule, collateral ligaments, and volar plate with sesamoid bones provide joint stability.

The carpo metacarpal joint CMCJ or trapezium-metacarpal joint, is a biconcave saddle joint with 2° of freedom allowing active movement in flexion, extension, abduction and adduction, and a small amount of passive axial rotation depending on the congruity of the articulating surfaces maintained by the ligaments. The range of movement is typically 0–15° of flexion, 0–20° of extension, and 0–70° abduction/adduction. The CMCJ of the fingers allow little movement and contribute little to the manipulation of the hand. However, the thumb CMCJ has a wide range of movement, allowing the hand to manipulate a wide range of objects.

Tendons and muscles

The main load-bearing structures of the thumb are the flexor, extensor, adductor and abductor muscles and associated ligaments, the joint constraining ligaments and the articular surfaces. The main load-bearing muscles are the flexors and adductors. The abductors, extensors and constraining ligaments act mainly as antagonists or stabilizers, increasing the stability of the joints. There are two main groups of muscles acting on the thumb, the extrinsics and the intrinsics (Fig. 2)

Extrinsics

The extensor pollicis brevis (EPB), the extensor pollicis longus (EPL), the abductor pollicis longus (APL), the flexor pollicis brevis (FPB), and the flexor pollicis longus (FPL).

Intrinsics

The abductor pollicis brevis (APB), the adductor pollicis (ADD), and the opponens pollicis (OPP).

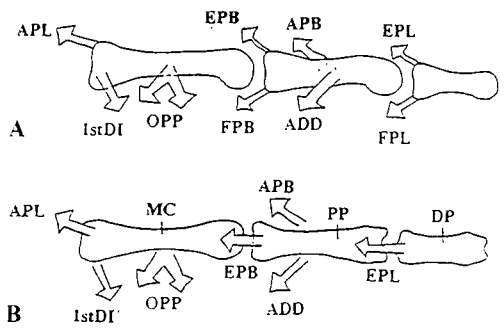

Fig. 2—Muscles and tendons of the thumb: (A) sagittal plane, (B) posterior frontal plane.

Theoretical models

Three theoretical models of the thumb have been considered for this paper. The first was developed by Hirsch[45] who modelled the thumb MCPJ producing two-dimensional lateral and pulp pinch models with point forces applied perpendicular to the long axis of the bones. The location and orientation of the load-bearing structures were estimated from cadaveric samples, although it was found that varying the angles of the tendons did not affect the results significantly. The forces exerted on the thumb in lateral and pulp pinch were measured in 70 males and seven females. These were found to be 89N for pinch force and 42N for lateral force and were used to estimate joint contact forces.

The second model considered was developed by Cooney & Chao[46] who produced three-dimensional finger force models for pinch and grip actions. A two-dimensional model was developed but this proved inadequate in calculating the joint and tendon forces. Joint and tendon locations and orientations were obtained from biplanar roentgenograms of cadaveric specimens. Forces in the relevant tendons and joint contact forces were calculated from equilibrium equations using assumed loads applied to the tip of the thumb in tip, lateral and pulp pinch. The orientations of each segment were defined by Eulerian angles. No attempt to calculate the forces in the individual joint ligaments was made.

The final model to be considered was developed by Toft & Berme[47] who produced a three-dimensional model of the CMCJ, the MCPJ and the IPJ of the thumb. Position and orientation of load-bearing structures were observed from cadavers, and spatial configuration of the hand functions from cine cameras and skin markers. Force readings were taken from four female subjects applying isometric twist and squeeze grips to a 45 mm diameter strain gauged cylindrical force transducer. The grip positions varied between lateral, pulp and grip.

Assumptions

Assumptions were required in all cases to solve the statically indeterminate models. Simplification of the hand functions is required in order to produce statically determinate models due to the complexity of the thumb and the number of muscles involved for different hand functions and stability.

Tendons and tendon sheaths were modelled as inextensible cables running on frictionless pulley systems. Tendon moment arms were assumed to be constant about the centres of rotation of the joints, due to the tendons being constrained within their sheaths.[46] Deformation of the bones, and frictional, viscoelastic and mass effects were also neglected.[46]

Joint motion

The IPJ was modelled as a hinge joint allowing movement in flexion and extension only, with axial rotation and lateral bending neglected. The MCPJ and the CMCJ were modelled in three dimensions as universal joints allowing movement in flexion, extension, abduction and adduction only, with no axial movement. Two-dimensional models neglect abduction and adduction movement as well, allowing only flexion and extension movement.

Cooney & Chao[46] assumed that all the joint articular surfaces shared the loads. However, the possibility of either both condyles of the IPJ sharing the load with lax collateral ligaments, or one condyle taking the load and the opposite collateral ligament being active was investigated by Toft & Berme[47]. Joint forces were assumed to act through the joint surface contact area for stability, with antagonists and/or ligament forces incorporated to modify the line of the joint force if necessary.

Tendon involvement

Cooney & Chao[46] assumed that the extensor tendons, had a passive role only to enhance the stability of the joints. Their contribution to the joint contact forces and other tendon forces was investigated. The FPB and OPP were assumed to act as one combined force at the CMCJ. The shear forces were assumed to be resisted by the collateral ligaments, capsule, volar plate and bone architecture although this was not investigated further.

Hirsch[45] neglected all antagonists and stabilizing ligaments when determining the joint forces, assuming their contribution to the joint force to be small. All muscles were assumed to have a single line of action even though anatomically they have broad insertions. The transverse and oblique heads of the ADD were assumed to act as one. Toft and Berme[47] neglected the extensors and the constraining ligaments although their roles as stabilisers were investigated. The contributions of the antagonists and the adductors were included. Tendon and ligament forces had to be tensile and joint reaction forces compressive.

Calculated forces

The different models assumed different loads or forces to be acting on the thumb in the different positions assumed. Cooney & Chao[46] applied pinch forces of 9.8N (normal 9.8–98N), and grip forces of 98N (normal 49–196N) to the thumb. Hirsch[45] applied a pinch force of 89N and a lateral force of 42N to the thumb. Toft & Berme[47] applied an average force of 74N, with no significant difference between the squeeze and twist, due to the difference in grip positions and direction of applied force.

Joint contact force

No significant difference between the joint contact forces in different types of pinch was found; however, there was a significant increase with grip. In grip the thumb exerts much greater forces than in pinch in

order to resist the forces of all four of the fingers, rather than just one as in pinch functions. The joint contact force increases from the IPJ to the CMCJ showing that the more proximal the joint, the higher the joint contact force, as with the finger joints.

Flexor and adductor forces

No significant difference between the forces of the FPL, FPB or ADD in different types of pinch was found. However, there was a significant increase with grip. The separate adductor forces contribute to the joint contact force but do not alter its line of action significantly.[47]

Antagonists and stabilisers

EPL and EPB contributions to the joint contact forces and other tendon forces are insignificant, increasing them only slightly, but enhancing joint stability.[46] The extensors and collateral ligaments also increase joint stability by modifying the line of action of the joint contact force to within the bearing surface, increasing the flexor tension and the joint force slightly.[47] Stability was possible without the APB, which acted as an antagonist to the adductors and a synergist to the flexors, minimally increasing the joint contact force.[47]

Finally, it was found that axial rotation moments at all joints and lateral bending moment at the IPJ occurred during pinch functions showing that three-dimensional analysis of pinch functions is necessary for valid hand function analysis.[46]

Summary

The intrinsic muscles are important joint stabilisers and transmit active forces across the MCPJ and the CMCJ. Large intrinsic forces occur due to need of the thumb for stability and strength in pinch and grip.[46] A combination of antagonists and collateral ligaments are necessary to stabilise the joints,[47] especially in pinch which adopts a more unstable configuration than grip. Flexor, adductor and joint contact forces are much greater in grip than pinch due to the thumbs resisting the forces of all four fingers in grip which increases the required counterbalancing forces in muscles and hence increases the joint contact force. Lateral shear force and bending moment are restrained by the collateral ligaments, volar plate, fibrous capsule, and bone architecture, providing the necessary stability for the joints.[45–47]

BIOMECHANICS OF THE WRIST

The wrist joint is a complex linkage of bones and ligaments between the forearm and the hand which, while offering an impressive arc of motion, retains a remarkable degree of stability.

Anatomy of the wrist

The wrist consists of the radio-carpal, ulnar-carpal, inter-carpal and the carpo-metacarpal joints. The inter-carpal joint is complex, consisting of two transverse rows of four carpal bones each, together with ligaments.

These bones are interconnected by a network of ligaments, which are divided into two general classes, intrinsic and extrinsic. The intrinsic ligaments interconnect the carpal bones, while the extrinsic ligaments connect the carpal bones to either the metacarpals, radius or ulna. Of particular interest is the triangular fibrocartilage complex, the ligamentous and cartilaginous structure that suspends the distal radius and ulnar carpus from the distal ulna.[48]

Range of motion

Normal subjects have an average of 133° of maximum flexion–extension and 40–50° of maximum radio-ulnar deviation.[49,50] In full extension or flexion, abduction–adduction is eliminated.

Normal use

The normal functional range of wrist motion has been found to consist of 5–10° of flexion, 30–35° of extension, 10° of radial deviation and 15° of ulnar deviation, i.e. the majority of tasks require little wrist motion, but it is necessary to be three-dimensional.[49]

Palmer et al[49] undertook a number of of standardized tasks on volunteers and found that, of 24 tasks, 21 were performed with the wrist in extension and 15 with the wrist in ulnar deviation. These 24 tasks were divided into three groups: personal hygiene tasks such as 'comb hair' and 'tie shoe'; culinary tasks such as 'eat with fork' and 'drink from cup'; and other activities of daily living such as 'put phone to ear' and 'turn key'.

A similar experiment was carried out in which the loss of wrist motion was simulated by volunteers wearing splints, the volunteers then performing 10 standardized activities of daily living.[50] The splints provided for four different positions of wrist immobilization; 15° of palmar flexion, neutral, 15° of palmar extension and 20° of ulnar deviation. Results disclosed that the least compromised hand function was with wrists immobilized in 15° of extension, while wrists placed in 20° of ulnar deviation exhibited the greatest degree of disability.

Rotation and bone movement

The wrist joint has 3° of freedom, these being flexion–extension, radioulnar deviation and rotation.[50] However, rotation of the hand results from motion arising at the proximal and distal radial ulnar joints; it does not occur through the carpal complex.

The radius and hand move in relation to, and function about, the distal ulna.[48] Forearm rotation of up

to 150° occurs at the distal radioulnar joint, with the distal radius and its fixed distal member (the hand) rotating about the ulnar head. However, the ulnar head itself is not immobile during rotation of the forearm, but moves slightly dorsally in pronation and slightly toward the palm in supination.[48] The centre of rotation of the wrist is located in the head of the Capitate.

Forces in the wrist

The loads transmitted by the wrist joint during normal activities are not precisely known but are thought to be great. Observations of the articular surfaces of the bones of the wrist suggest that significant compressive loads are dealt with in a static fashion.[50] For example, the opposing joint surfaces of the mid-carpal articulation have a close conformity, and depressions exist for the scaphoid and lunate on the articulating surface of the distal radius.

By applying compressive loads across the proximal carpal articulation with the wrist in a neutral position, it was found that these loads have a resultant line of action which passes through the head of the capitate to the scapho-lunate junction, and then to the distal radial and ulnar surfaces.[50] When the forearm of cadavers, including the elbow, were loaded in a neutral position it was found that the radius, through its articulation with the lateral carpus, carried approximately 80% of the axial load of the forearm, and the ulna, through its articulation with the medial carpus via the triangular fibrocartilage complex, 20%.[48] The same experiment revealed peak pressure across the articulations of the wrist to have a maximum value in the order of 4MPa.

Effect of wrist position on grip strength

No significant difference in grip strength with the wrist positioned at 0° and 15° ulnar deviation and 0° and 15° extension, or any combination of these, has been found[51,52] However, both studies did find grip strength to be significantly less at 15° of palmar flexion.

REFERENCES

1 Kellor M, Frost J, Silberberg N, Iverson I, Cummings R. Hand strength and dexterity. Am J Occup Ther 1971; 25: 77–83
2 Jones AR, Unsworth A, Haslock I. A microcomputer controlled hand assessment system used for clinical measurement. Engng Med 1985; 14: 191–198
3 Agnew J, Maas F. Hand function related to age and sex. Arch Phys Med Rehabil 1982; 63: 269–271
4 Smith HB. Smith hand function evaluation. Am J Occup Ther 1983; 27: 244–251
5 Sperling L. Evaluation of upper extremity function in 70-year-old men and women. Scand J Rehabil Med 1980; 12: 139–144
6 Swanson AB, Matev IB, De Groot G. The strength of the hand. NY University Medical School Interclinical Information Bulletin 1974; 13, 1: 1–8
7 An KN, Cooney III WP, Chao EYS, Linscheid RL. Functional strength measurement of normal fingers. Orthopaedic Biomechanics Laboratory, Mayo Clinic 1978
8 Mathiowetz V, Kashman N, Volland G, Weber K, Dowe M, Rogers D. Grip and pinch strength: normative data for adults. Arch Phys Med Rehabil 1985; 66: 69–74
9 Reikeras O. Bilateral differences of normal hand strength. Arch Orthop Trauma Surg 1983; 101: 223–224
10 Ellison MR, Kelly JK, Flatt AE. The results of surgical synovectomy of the digital joints in rheumatoid disease. J Bone Joint Surg 1971; 53-A: 1041–1060
11 Harkness JAL, Richter MB, Panayi GS, Van de Pette K, Unger A, Pownall R. Circadian variation in disease activity in rheumatoid arthritis. BMJ 1982; 284: 551–554
12 Clawson DK, Souter WA, Carthum CJ, Hymen ML. Functional assessment of the rheumatoid hand. Clinical Orthopaedics and Related Research 1971; 77: 203–210
13 Kowanko IC, Pownall R, Knapp MS, Swannell AJ, Mahoney PGC. Circadian variations in the signs and symptoms of rheumatoid arthritis and in the therapeutic effectiveness of flurobiprofen at different times of day. J Clin Phar 1981; 11: 477–484
14 Myers DB, Grennan DM, Palmer DG. Hand grip function in patients with rheumatoid arthritis. Arch Phys Med Rehabil 1980; 61: 369–373
15 Labi MLC, Gresham GE. Hand function in osteoarthritis. Arch Phys Med Rehabil 1982; 63: 438–440
16 Cantrel T. Measurement of weakness and dysfunction in the rheumatoid hand. Rheumatol Rehabil 1976; 15: 182–184
17 Cutts A, Bollen SR. Grip strength and endurance in rock climbers. Proc Instn Mech Engrs 1993; 207: 87–92
18 Pearson R, MacKinnon MJ, Meek AP. Diurnal and sequential grip function in normal subjects and effects of temperature change and exercise of the forearm on grip function in patients with rheumatoid arthritis and in normal controls. Scand J Rheumatol 1982; 11: 113–118
19 Amis AA. Variation of finger forces in maximal isometric grasp tests on a range of cylinder diameters. J Biomed Eng 1987; 9: 313–320
20 Kroemer KHE, Gienapp EM. Hand-held device to measure finger (thumb) strength. J Appl Physiol 1970; 29, 4: 526–527
21 Walker PS, Davidson W, Erkman MJ. An apparatus to assess function of the hand. J Hand Surg 1978, 3, 2
22 Weightman B, Amis AA. Finger joint force predictions related to design of joint replacements. J Biomed Eng 1982; 4: 197–205
23 Berme N, Paul JP, Purves WK. A biomechanical analysis of the metacarpo-phalangeal joint. J Biomech 1977; 10: 409–412
24 Dickson RA, Petrie A, Nicolle FV, Calnan JS. A device for measuring the force of the digits of the hand. Biomed Eng 1972; 270–273
25 Unsworth A, Haslock I, Vasandakumar V, Stamp J. A laboratory and clinical study of pneumatic 'grip strength' devices. Br J Rheumatol 1990; 29: 440–444
26 Baron M, Dutil E, Berkson L, Lander P, Becker R. Hand function in the elderly: relation to osteoarthritis. J Rheumatol 1987; 14: 815–819
27 Laws CA, Myers BD, Palmer DG. The effect of temperature on work and power output during hand grip assessment of rheumatoid patients and controls. Wellcome Medical Research Institute Department of Medicine 1979: 45–46
28 Ohtsuki T. Inhibition of individual fingers during grip strength exertion. ERGOA 1981; 24: 21–36
29 Youm Y, Gillespie TE, Flatt AE, Sprague BL. Kinematic investigation of normal MCP joint. J Biomech 1978; 11: 109–118
30 Flatt AE, Fischer GW. Biomechanical factors in the replacement of rheumatoid finger joints. Ann Rheum Dis 1969; 28: Supp 36–41
31 Unsworth A, Alexander WJ. Dimensions of the metacarpo-phalangeal joint with particular reference to joint prostheses. Engng Med 1979; 8: 75–80
32 Pagowski S, Piekarski K. Biomechanics of the metacarpo-phalangeal joint. J Biomech 1977; 10: 205–209
33 Walker PS, Erkman MJ. Laboratory evaluation of a metal plastic type of metacarpo-phalangeal joint prosthesis. Clin Orthop 1975; 112: 349–356
34 Tamai K, Ryu J, An KN, Linscheid RL, Cooney WP, Chao EYS. Three dimensional geometric analysis of the metacarpo-phalangeal joint. J Hand Surg 1988; 13-A, 4

35 An KN, Chao EYS, Cooney WP, Linscheid RL. Forces in the normal and abnormal hand. J Orthop Res 1985; 3, 2: 202–211
36 Chao EY, An KN. Determination of the internal forces in human hand. J Engng Mech Div Proc ASCE 1978: 255–272
37 Chao EY, An KN. Graphical interpretation of the solution to the redundant problem in biomechanics. J Biomechan Eng 1978: 100: 159–167
38 Smith EM, Juvinall RC, Bender LF, Pearson JR. Role of the finger flexors in rheumatoid deformities of the metacarpo-phalangeal joints. Arth Rheum 1964; 7, 5: 467–480
39 Chao EY, Opgrande JD, Axmear FE. Three dimensional force analysis of finger joints in selected isometric hand functions. J Biomech 1976; 9: 387–396
40 Storace A, Wolf B. Functional analysis of the role of the finger Tendons. J Biomech 1979; 12: 575–578
41 Storace A, Wolf B. Kinematic analysis of the role of the finger tendons. J Biomech 1982; 15, 5: 391–393
42 Lincheid RL, Dobyns JH. Total joint arthroplasty, the hand. Mayo Clin Proc 1979; 54: 516–526
43 Linscheid RL, Chao EYS. Biomechanical assessment of finger function in prosthetic joint design. Orthop Clin North Am 1973; 4, 2: 317–330
44 Purves WK, Berme N, Paul JP. Finger joint biomechanics. Disability – Proc Seminar Rehab (RM Kenedi, JP Paul, J Hughes eds). Macmillan: London 1979: 318–332
45 Hirsch D, Page D, Miller D, Dumbleton JH, Miller EH. A biomechanical analysis of the metacarpo-phalangeal joint of the thumb. J Biomech 1974; 7: 343–348
46 Cooney WP, Chao EYS. Biomechanical analysis of static forces in the thumb during hand function. J Bone Joint Surg 1977; 59-A: 27–36
47 Toft R Berme N. A biomechanical analysis of the joints of the thumb. J Biomech 1980; 13: 353–360
48 Palmer AK, Werner FW. Biomechanics of the distal radioulnar joint. Clin Orthop Relat Res 1984; 187: 26–35
49 Palmer AK, Werner FW, Murphy BS, Glisson R. Functional wrist motion: a Biomechanical study. J Hand Surg 1985; 10-A: 39–46
50 Volz RG, Leib M, Benjamin J. Biomechanics of the wrist. Clin Orthop Relat Res 1980; 149: 112–117
51 Kraft GH, Detels PE. Position of function of the wrist. Arch Phys Med Rehabil 1972; 53: 272–275
52 Pryce JC. The wrist position between neutral and ulnar deviation that facilitates the maximum power grip strength. J Biomech 1980; 13: 505–511